Optimization of membrane process architecture

Marjan Bozorg

Doctoral Thesis

in order to obtain the Ph.D. degrees of

Université de Lorraine
Laboratoire de Réactions et Génie des procédés
Process and Products Engineering
Génie des Procédés et des Produits et des Molécules

Università degli Studi di Roma Tor Vergata
Dipartimento di Ingegneria Civile e Ingegneria Informatica
Computer Science, Control and GeoInformation
Informatica, Controllo e Geoinformazione

Optimization of membrane process architecture

by:
Marjan Bozorg

Supervisor:
Christophe Castel

Co-Supervisors:
Veronica Piccialli, Bernardetta Addis

Thesis defended on December 6th, 2019, in Nancy, France

Jury:

Supervisors:	Christophe Castel	Professor at University of Lorraine
	Veronica Piccialli	Professor at University of Rome "Tor Vergata"
Reviewers:	Marco Locatelli	Professor at University of Parma
	Adele Brunetti	Researcher at Italian National Research Council
President:	Jean-Yves Marion	Director of LORIA
Examiners:	Andrea Pacifici	Associate professor at University of Rome "Tor Vergata"
	Thibaut Neveux	Research Engineer at EDF
Invited:	Eric Favre	Professor at University of Lorraine
	Bernardetta Addis	Associate professor at University of Lorraine

Acknowledgments

The research included in this dissertation could not have been performed if not for the assistance, patience, and support of many individuals. I would like to express my greatest appreciation to my thesis supervisors, Eric, Christophe, Veronica, and Bernardetta, for supervising my thesis through these three years, for your patience, for your enthusiastic encouragement, and for the precious discussions and advise all along my doctoral study.

In particular, I would like to extend my gratitude to Álvaro, for sharing with me a lot of knowledge in doing my research associated with membrane gas separation.

Also, I want to thank Roda, for his time, assistance and support in using of COCO simulator and simulation of optimal membrane process configurations.

I would additionally like to thank my friends in EMSP: Simon, Ridha, Zoulfida, Laetitia, and Mahbub, for all the interesting time and discussion we had together. For my friends in LORIA: Meihui, Tayeb, Valia, and Iordan, thanks for your accompany and friendly manner through this time. I want to thank my friends in Rome: Chiara, Anastasiia, and Matteo, for interesting discussions we had and a warm and friendly environment that you made.

I want to thank my parents and my siblings, Davood, Maryam, and Mehrdad, for their endless love, support and encouragement through all my life.

Finally, I would like to thank Hamed, my love, who always guides me when I was lost, encourages me when I was down, supports and motivates me to go further and stands next to me. Thank you for your endless help and great advice for working and writing my thesis. I love you and I cannot wait to start new adventures of my life with you.

Contents

List of Figures

List of Tables

Introduction

Different separation technologies have been used in chemical processing through years, such as Distillation concepts, Absorption, Adsorption, Extraction, and Drying. The limitations of these technologies (i.e. performance, compacity, flexibility, energy consumption) yield to search for alternative methods [1]. This search for differentiation has led to the introduction of separation processes based on membranes. Membrane technologies became increasingly important in industrial applications throughout the last decades. They became a reference process in the food industry, water treatment, and desalination; and they are taking a higher place and role in other sectors such as health care, medicine and pharmacy, energy, gas treatment, and petrochemical industry.

Membrane processes can also be found in other industrial fields such as purification and recovery of substrates, recovery, and recycling of catalysts and solvents, the concentration of solutions, crystal cleaning, filtration, clarification of process streams, and purification of waste streams, etc.

Membrane units have usually relatively small footprints with an interesting reduction in energy consumption and use of chemicals, (i.e. gas treatment by gas permeation is solvent-free). The simplicity of operation and installation of membrane systems with their modularity allows an easy numbering-up and results in significant flexibility. Operation under continuous steady-state conditions with partial or complete recycle of retentate/permeate stream is another advantage of membrane systems [2], [3].

Different kind of membrane processes exist, depending on the targeted applications, operating conditions and phases (principally gas or liquid): gas permeation, pervaporation, membrane distillation, reverse osmosis, ultrafiltration, microfiltration, dialysis, and electrodialysis. Also, various hybrid processes exist because of the coupling of membrane processes with other separation processes including adsorption, absorption, evaporation, cryogenic and distillation. [4].

Also, the membrane separation process can be applied in different separation fields such as particle–liquid separation, liquid-liquid separation as well as gas separation. This dissertation will focus on the synthesis of membrane gas separation process.

Although more than one century passed from the time that gas diffusion and mass transport principles through polymer films, only 30 years passed from the membrane applications on an industrial scale in gas separation [2].

The first scientific observation about membrane gas separation was made by John Kears-

ley Mitchell ([5]) in 1831. He investigated the diffusion of gas through the wall of balloons that are made of India rubber(natural rubber). After that, in 1866, Thomas Graham proposed the solution-diffusion model [6]. In 1980, the first large industrial application of membrane-based gas separation was launched by Permea for hydrogen separation from the purge gas stream of ammonia plants with Prism membrane. Since then, the membrane gas separation has grown exponentially [2], [7]. Figure 0.1 presents the history and development of membrane gas separation since 1850 based on the displaying in [7].

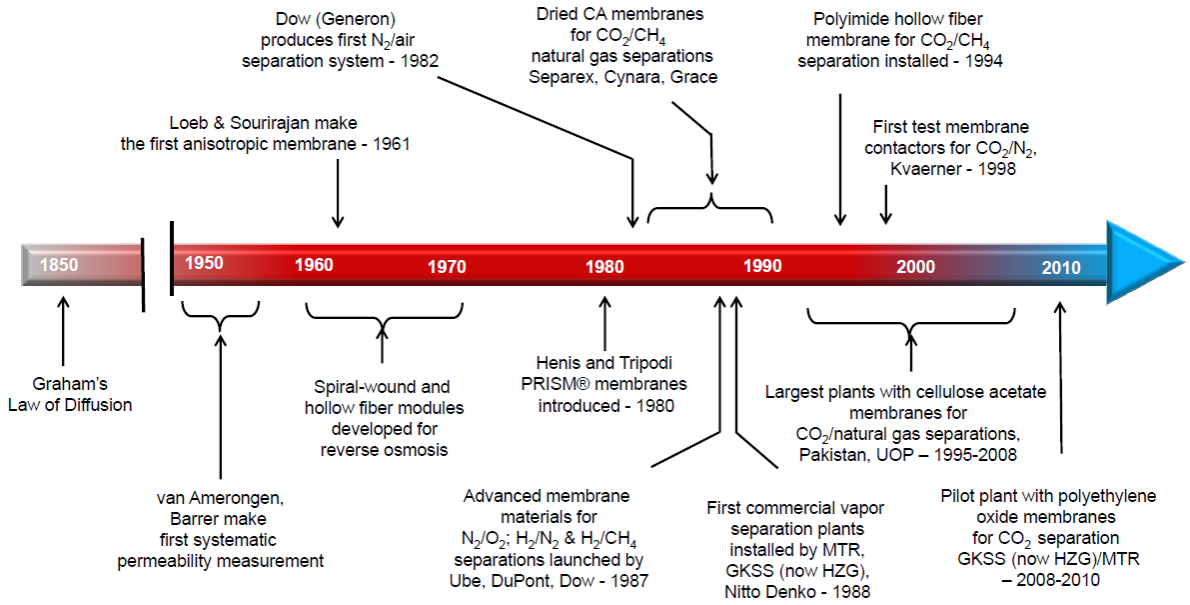

Figure 0.1: Milestones of gas separation development [2], [3], [7]

Nowadays, due to increasing applications of membrane gas separation technology in the industry, the development of accurate, efficient and reliable design strategy is essential. To design an efficient membrane gas separation system, different aspects of it must be investigated. Most of the recently published membrane gas separation literature has focused on a range of different approaches for promoting the design of a membrane separation system (i.e. membrane material, membrane module design and design of membrane gas separation processes). Besides the improvement in the materials as well as in membrane module design, the efficient designing of membrane gas separation processes have great importance in the industry.

Figure 0.2: Membrane gas separation system

Most of the industrial applications utilizing membrane gas separation processes are confined to a single-stage operation. However, because of the inherent limitations of the solution-diffusion separation mechanism in polymeric membranes, several separation stages are often necessary when applications demand high levels of recovery and purity of one or several components, or when the feed is poor in the component(s) to be recovered or both. Also, strict environmental legislation and capital cost constraints demand the utilization of membrane networks in many applications where the partial or complete processing of retentate or permeate streams is subjected to multiple stages [8].

Multiple process configurations are possible when considering a multi-stage membrane separation (i.e. the number of membrane stages, performance (permeability-selectivity) and the surface of each stage, upstream and downstream pressure of each stage and stream connections among stages). Apart from membranes, choosing the proper options as the driving force selection (i.e Vacuum pumps, Compressors, Expander, Valve, etc) lead to more and more complex membrane systems. Different combinations of these modules yield different results in the percentage of separated gases. This task becomes more and more complex as the number of separation stages increases [9]. Thus finding the optimal design for the gas separation process system becomes the main aim of the process design.

There are several simulation-based software for membrane gas separation process design. They often lead to the evaluation of a limited number of process configurations based on heuristics and experience. Thus, covering all possibilities of gas separation process configuration especially in multi-stage membrane process is tedious and time-consuming

by these software. Therefore, an accurate, efficient and reliable approach to optimize the design of membrane gas separation process architecture is imperative.

The optimization approach aims to explore and obtain the optimal process configuration with the most efficient conditions (i.e. obtain the desired percentage of separated gases and minimize the cost of the process); this thesis proceeds in this direction.

A rigorous model would allow to exploit the full potential of a membrane system. Nevertheless, the more rigorous models incorporate accurate local mass flux are utilized, the more inaccuracies incorporate into the results of design studies. In other words, inaccuracies in the modeling of the membrane process will lead to the development of sub-optimal plant designs with the possible over (or under) prediction of plant performance and a lack of generality due to implicit assumptions.

To the best of our knowledge, very few optimization approaches able to successfully design the membrane-based gas separation process have been developed until now. In fact, due to the complex nature of flow through membrane modules, the existing unit models depend on several fixed assumptions. Consequently, the existing numerical tools often rely on their process and are only valid within a limited operating range. Therefore, the main objective of this work is to develop a detailed model of a generic membrane gas separation process for the optimal design of membrane systems. A global optimization algorithm is then described to solve the optimization problem heuristically. The proposed method will be validated and applied to four important gas separation markets. The work which is presented in this dissertation is organized as follows:

Chapter 1 introduces a brief review of different gas separation methods. A clear focus will be on a membrane gas separation process. A summary of important and essential explanations of membrane physical phenomena (i.e. different membrane materials, membrane modules, and considered mass transfer mechanism in a membrane) will be presented. It will explain about the design of a membrane system and its issues and challenges. In addition, it will quickly describe the different applications of membrane processes in the industry.

Chapter 2 addresses the membrane process synthesis as a Non-linear Programming (NLP) optimization model according to a superstructure which includes a wide range of possible configurations. A heuristic continuous global optimization approach will be proposed to solve the optimization model. Membrane area, the pressure ratio of the system and process design are considered as the main variables of the optimization model. In addition, it will discuss the simulating of the optimization results to validate their concordance with reality. Finally, the optimization approach will be validated by comparing its results with a reference case in the domain [10].

Chapter 3 is dedicated to the application of the optimization approach to CO_2 recovery from blast furnace gas with up to four membrane stages. The optimal process configuration and main process variables, upstream and downstream pressure and membrane area will be determined for processes with CO_2 recoveries of 90, 95 and 99 % and N_2 residual contents of 1, 0.5 and 0.1 %.

Chapter 4 represents the synthesis of the process of nitrogen enrichment from the air which is the first commercial market of gas separation. Firstly, the impact of two commercial membranes (PPO and PSf) in terms of nitrogen production cost and associated process configurations will be discussed at four different levels of N_2 purity (90, 95, 99, 99.9%). Latter, instead of commercial membranes, the same strategy will be used to discuss the impact of optimal membrane performances.

Chapter 5 will express an exhaustive comparison between polymeric and high-performance membranes to identify the most cost-effective membrane in CO_2/CH_4 separation. This chapter is dedicated to two case studies, biogas and natural gas upgrading. The inlet pressure in the natural gas case will consider 60 times more than biogas case study. In biogas upgrading, besides the membrane material, the impact of three levels of outlet pressures will be investigated.

Finally, we close up with the Conclusion chapter that gives a full summary of the work with the conclusions drawn and future perspectives.

Part I

A process synthesis strategy for membrane gas separation process

Chapter 1

Generalities on membrane gas separation

This chapter briefly presents the main gas separation technologies. Among those technologies membrane processes will be presented in detail through the description of the

main occurring physical phenomena. A review of the main membrane and module types will be proposed. Emphasize is done on parameters and equipment which are the cornerstone of the gas separation in a membrane and have an important role in design of the membrane system. A list of applications of membrane process in gas separation is presented which will be explained extensively in chapters three to five.

1.1 Different gas separation techniques

Gas separation has a broad range of applications. It becomes a crucial technique for several industrial processes such as reducing the greenhouse effect by removing of CO_2, separation and purification of commercially important gases such as H_2, CH_4 and O_2 from natural gas, biogas or flue gases .... Cryogenic distillation, Pressure swing adsorption (PSA), Chemical absorption process (CAP) and membrane techniques are the most well-known and industrially implemented gas separation processes.

1.1.1 Cryogenic distillation

Such as classical distillation, Cryogenic distillation is a low-temperature process that operates at different boiling temperatures (relative volatilities) of the feed components. It is widely used to reach high purity (typically $> 90\%$) of desired component. In addition, it enables to produce liquid gas directly, which is very useful for shipping. It however needs a high amount of energy for refrigeration and is usually not an appropriate method for a diluted feed gases. It is one of the main disadvantages of Cryogenic method [11], [12].

Figure 1.1: Cryogenic distillation industrial plant (Linde company)

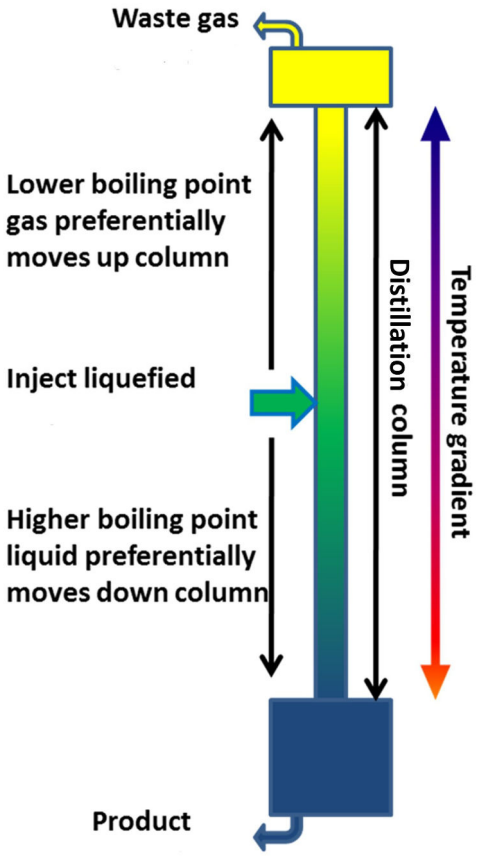

Figure 1.2: Cryogenic distillation column

1.1.2 Pressure swing adsorption(PSA)

Pressure swing adsorption (PSA) is a technology used to separate some gas species from a mixture of gases under pressure according to the species' molecular characteristics and affinity for an adsorbent material (e.g. zeolites, activated carbon, silica, alumina). Species are preferentially adsorbed at high pressure. The process then swings to low pressure to desorb and regenerate (even partially) the adsorbed material [13].

1.1.3 Physical and chemical absorption process

Absorption is a process that relies on a solvent's chemical affinity with a solute to preferably dissolve one species over another. A long list of available solvents is existing from aqueous to organic ones. In a chemical absorption process (CAP), a chemical reaction takes place between the solute and the solvent (absorbent). Chemical reactions increase the rate of absorption, the absorption capacity of the solvent and usually increase selectivity through the specificity of the reaction [14], [15].

Figure 1.3: PSA industrial plant (Linde company)

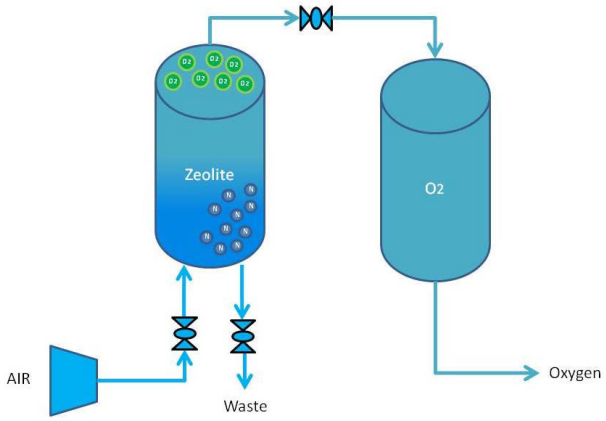

Figure 1.4: Flow sheet of PSA unit

1.2 Membrane gas separation process

Membranes have been defined in various ways; Mulder [16] has defined it as "a selective barrier between two phases", whereas Ho and Sirkar [17] describe it as an "inter-phase between two bulk phases". Membrane-based gas separation is a pressure driven process. When a membrane module is fed with a gas mixture, the more permeable components will preferentially permeate through the membrane as permeate stream because of their partial pressure difference between the feed and permeate sides of the membrane. The less permeable components exit from the membrane as retentate stream.

The separation's level is achieved by imposing a pressure ratio between the feed and permeate sides. Figure 1.5 illustrates the basic process of a membrane. Depending on the application, either the permeate or retentate could be the final product.

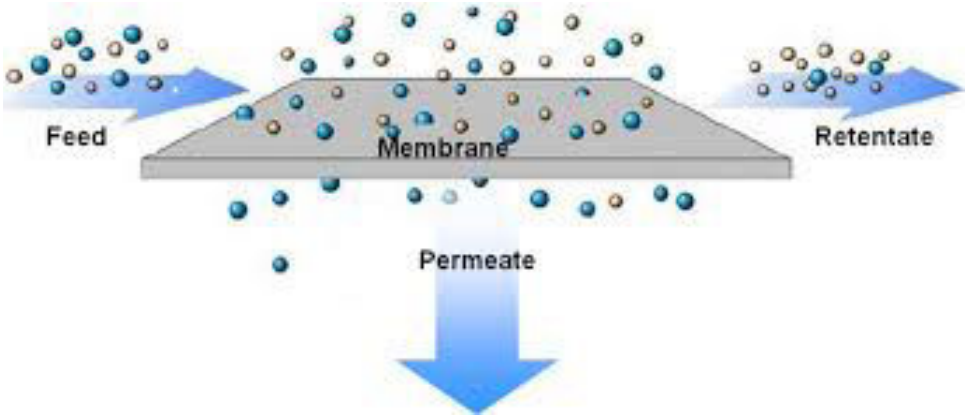

Figure 1.5: Basic membrane gas separation process

1.3 Membrane materials in gas separation

A proper selection of the membrane material is extremely important in determining the performance of the gas separation module. For each gas separation process, there are two possibilities to select the proper membrane:

- Select a proper membrane with determined characteristics (e.g. permeability, selectivity and thickness).
- Find the best membrane, with the optimal characteristics by using the optimization strategy that computes together membrane material, process architecture, and operating conditions.

Membranes are generally classified into three main categories of polymeric, inorganic, and mixed matrix membranes. Currently, most of the industrial processes are based on polymeric materials. Membranes can also be synthesized from non-polymeric (inorganic) materials like metal, ceramic, carbon, zeolites, and liquid membranes. Polymeric and inorganic materials can be used together to form hybrid membranes called mix matrix membranes (MMM) consisting of a molecular sieving or adsorbing materials (inorganic) dispersed in a polymer matrix. The mixed matrix membranes are aimed to combine the advantages of both: high separation capabilities of the molecular sieving materials with the desirable mechanical properties and economical processing capabilities of polymers.

1.3.1 Polymeric membranes

The main characteristics of a polymeric membrane for its selection in a gas separation process are based on their chemical resistance, sorption and diffusion capacity, good mechanical properties, relatively low price, and stability at moderate temperatures.

PS (polysulfone and polyethersulfone), PVDF (polyvinylidenedifluoride), PE (polyethylene), PP (polypropylene), PI (polyimide) and natural membrane such as CA (Cellulose acetate) are widely used for several commercial applications. Polymers with Microporosity (PIM) are innovative polymers firstly synthesized ten years ago. Their exceptional

transport properties introduced significant novelty in polymer science. The polymer membrane materials are now growing. They will be able to go beyond the current upper-bound for different gas pair separations [18].

Polymeric membrane materials will probably continue to dominate the market thanks to their relatively low initial costs and their ability to be used in a variety of applications [19]. Two different kinds of polymeric membranes have to be carefully distinguished because their transfer mechanisms are intrinsically different : porous and dense polymer.

Porous membranes

Porous membranes are composed of a solid matrix with determined pores, which diameter varies between 2 nm to 20 μm. The selectivity depends on the pores diameter and the dimension of the molecule to be separated.

Transport mechanism in porous membranes is driven by viscous flow or diffusion. In gas separation, the separation is principally done by the diffusion of species through the pores. A good separation is achieved when the molecular size distribution of the compounds to be separated is broad enough.

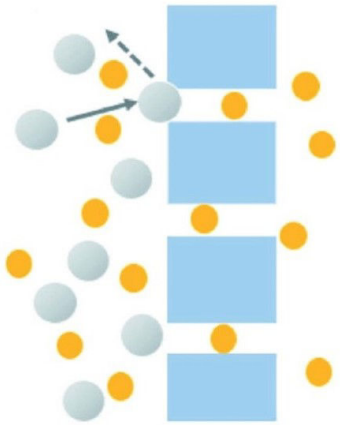

Figure 1.6: Porous polymer membrane

Porous membranes are the most permeable membranes, leading to high permeation fluxes at low energy expenditure.

Dense membranes

A dense membrane is a membrane without pores or with very small (0.2 nm) pore size. The transport mechanism in the dense membrane is based on the well-known solution-diffusion mechanism. The membrane material and its interactions with permeate species characterize the permeability and selectivity of a membrane. These membranes are con-

siderably selective. Dense membranes are widely applied in gas permeation for their good compromise between relatively high permeation rates and good selectivities.

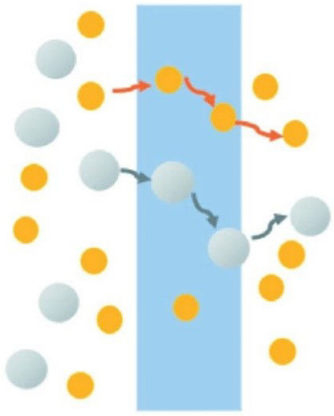

Figure 1.7: Dense polymer membrane

Dense polymeric membrane are usually composite membrane where a thin dense layer is deposited on a porous structure, which functions as a support.

The dense layer regulates the separation. The porous structure is added to the dense layer to provide mechanical support. In the dense layer, the transport mechanism is governed by the solution-diffusion model which represents the highest mass transfer resistance. In the porous network, the transport is convective and very fast compared to the dense layer. These membranes combine the selectivity of a dense membrane with the very fast transport rate of a thin layer and the mechanical strength of a porous network.

1.3.2 Inorganic membranes

Inorganic membranes made of materials such as amorphous silica, various oxides (alumina, titania, zirconia), carbon and zeolite. They are classified into two major categories based on their structure, porous inorganic membranes, and dense (non-porous) inorganic membranes. Table 1.1 presents some of the advantages and disadvantages of using inorganic membranes.

Amorphous silica membranes

Amorphous silica membranes are prepared by sol-gel processing and consist in a three-layer system (i.e. support prepared from α-alumina powder, γ-alumina intermediate layer, and a molecular sieving silica top layer). They can be applied in gas separation. Alumina, zirconia or titania may be added to silica to increase the stability of the composite in high humidity environment. The stability of the silica layer should be increased towards hot steam.

Table 1.1: Advantages and disadvantages of inorganic membranes

Advantages of inorganic membranes	Disadvantages of inorganic membranes
Long-term stability at high temperature	High capital costs
Resistance to harsh environments	Brittleness
Resistance to high pressure drops	Low membrane surface per module volume
Inertness to microbiological degradation	Difficulty in achieving high selectivities in large scale microporous membranes
Easy cleanability after fouling	Generally low permeability of the highly selective (dense) membranes at medium temperature
Easy catalytic activation	Difficult membrane to module sealing at high temperature

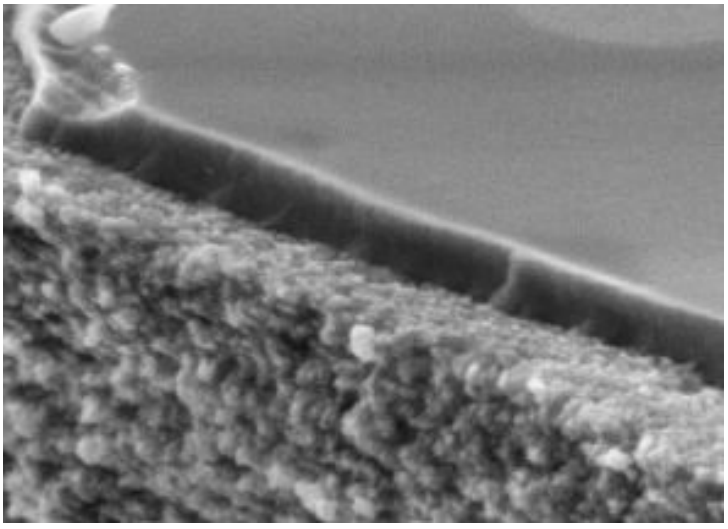

Figure 1.8: Microporous silica membrane in top layer with intermediate ceramic layer

Carbon membranes

Carbon Membranes are produced by pyrolysis (temperature - 500-900 °C) of polymeric precursor films on a macroporous carbon substrate or an alumina support tube. Carbon molecular sieve (CMS) is a promising candidate for gas separation in terms of separation and stability [20].

Zeolite membranes

Zeolite is a Microporous crystalline alumina-silicate membrane with uniform pore size. It is formed on porous support by hydrothermal synthesis. It can separate molecules based on size, shape, polarity, and degree of unsaturation. The majority of zeolite membranes are of MFI-type (ZSM-5-type) and FAU-type.

Inorganic membranes have an important role in gas separation but their extremely expensive cost limits their applications on a very small scale. Zeolites and carbon belong

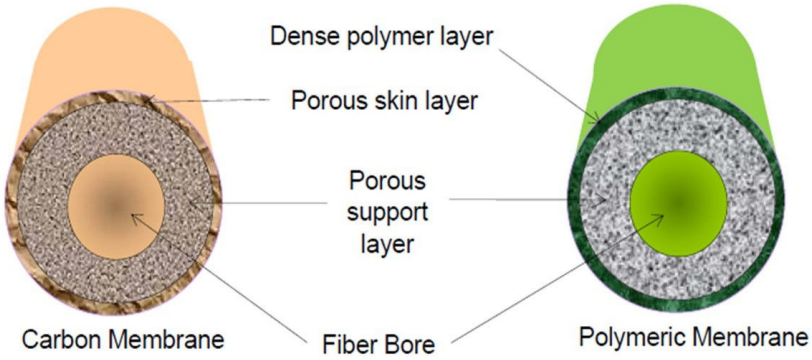

Figure 1.9: Comparison between carbon and polymeric membrane materials

to molecular sieves and are more selective than polymers for specific gas components due to the important contribution of entropic selectivity to the global selectivity. However, some of the considerable limitations of inorganic membranes are the difficulty to produce defect-free thin films and manufacturing cost for the former, poor resistance to poisoning and stability for the latter.

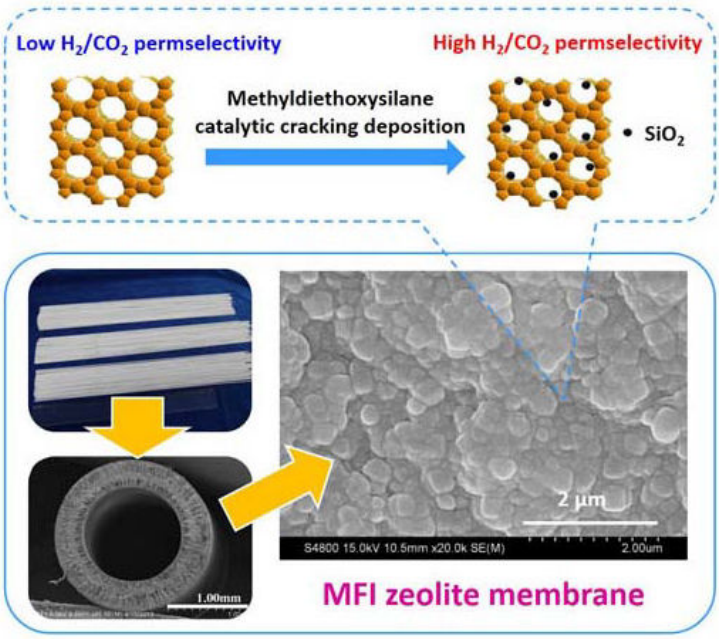

Figure 1.10: Improvement of hydrogen-separating performance by on-stream catalytic cracking of silane over hollow fiber MFI zeolite membrane [21]

1.4 Membrane modules

There are different ways to develop membrane materials into membrane modules: Tubular, Plate-and-frame, Spiral-wound and Hollow-fibre modules [1] for the main ones. Gas separation membranes modules are mainly formed into spiral-wound and hollow fiber modules.

1.4.1 Spiral wound modules

Spiral wound modules consist of numerous plate-and-frame membranes, separated by a thin meshed spacer material, in wrapped around a central perforated tube and fitted into a tubular vessel [3] .

The Feed stream passes through the membrane surfaces and the permeate stream spirals, it finally collected in the central collection tube. The Feed flows through the membrane in the axial direction while the permeate flows in a radial direction towards the center. Figure 1.11 presents a Spiral wound module.

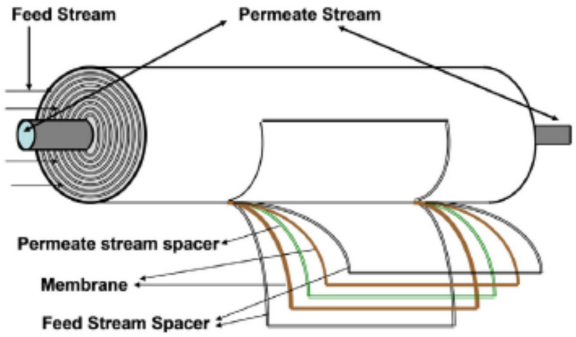

Figure 1.11: Spiral wound module

1.4.2 Hollow fiber modules

Hollow fiber modules typically contain numerous fibers which are grouped together to form a hollow fiber bundle. Each bundle is packed into a larger tube shell, forming a shell-and-tube structure. Feed enters at one end of the module and retentate leaves at the other end. A pair of permeate exit ports, one at each end of the module, allows the unit to be operated using either co-current or counter-current retentate and permeate flows. Figure 1.12 illustrates how the hollow fiber module work [22]–[24].

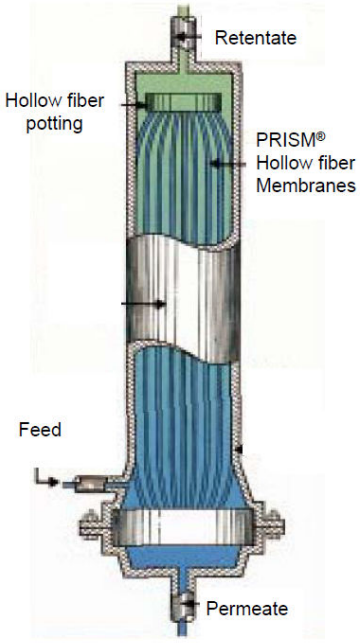

Figure 1.12: Hollow fiber module

1.5 Mass transfer through a membrane: the permeability approach.

Selection of the correct membrane is imperative as both the transfer and specific of flux are functions of the membrane structure. In 1855, Adolf Fick presented the diffusion concept concerning mass transport through diffusive means which is now well-known as Fick's first law. The transfer flux depends upon the physical properties of the permeating components such as its molecular size. Thus the introduction of a membrane between two phases permits the selective transfer of components and their separation.

The solution-diffusion mechanism describes the permeation mechanism in dense membranes. Generally, the solution-diffusion mechanism consists of the following steps:

- Sorption of the permeate stream or solubility at the upstream surface of the membrane
- Diffusion through the membrane
- Desorption at the downstream surface of the membrane

Figure 1.13 illustrates the solution-diffussion mechanism in a dense membrane [25].

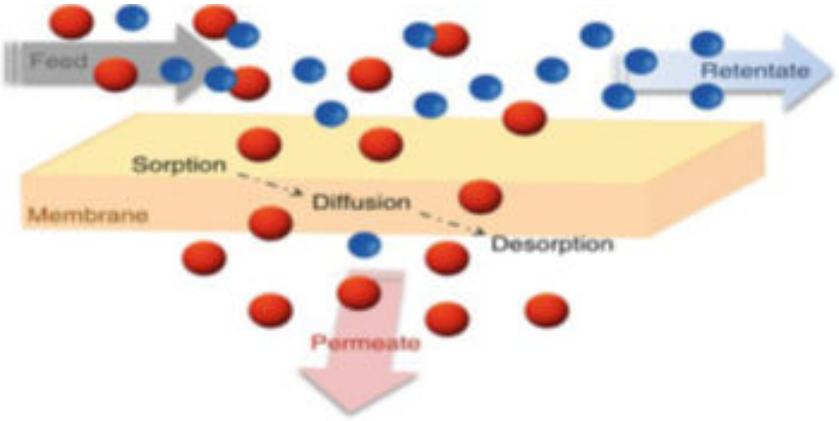

Figure 1.13: Steps of solution-diffusion mechanism in a non-porous membrane

Permeability and permeance are the two parameters usually used to describe the ability of a component to traverse a membrane. Permeability is expressed in units of component rate per surface, per thickness of the membrane, per unit of pressure difference (e.g. mol.m/m^2.s.Pa), while permeance does not include membrane thickness (e.g. mol/m^2.s.Pa). They were derived from the empirical observation of thickness and pressure dependence of the steady-state permeation of gases through membranes, leading to the following expression:

$$J = P(\Delta p_i / L) \tag{1.1}$$

Where J is the measured flux, Δp_i is the partial pressure difference across the membrane, and L is the membrane thickness.

$$J_i = -D_i \cdot (\frac{dC_i}{dl}) \tag{1.2}$$

Where $\frac{dC_i}{dl}$ is the concentration gradient of the component i across the membrane.

Integrating Equation 1.1 for a membrane of thickness l gives:

$$J_i = -D_i \cdot (\frac{C_{iRet} - C_{iPerm}}{L}) \tag{1.3}$$

where C_{iRet} and C_{iPerm} are the concentrations of component i at the high-pressure membrane interface (Ret) and the low-pressure membrane interface (Perm) respectively.

In gas membrane separation, we are interested in describing transport in terms of the pressure at each side of the membrane since the process is performed by imposing such pressure difference. Concentration at each side of the interface for the gas components will be proportional to their partial pressure as expressed by the following general expression:

$$C_i = S_i \, p_i \tag{1.4}$$

where S_i is the solubility coefficient, which can be constant or a function of p_i. This behavior will depend on the sorption thermodynamic model chosen for the gas components at the polymer interface.

Considering the case of a constant sorption coefficient from Equation 1.4 and re-expressing Equation 1.3 for a pure gas we get:

$$J = D\ S\frac{(p_i^{up} - p_i^{down})}{l} \tag{1.5}$$

when compared with Equation 1.1 it becomes clear that:

$$P = D \cdot S \tag{1.6}$$

The permeability coefficient is thus expressed as a product of both a kinetic mobility term, D, a measure of the ability of gas molecules to diffuse in the polymer, and a thermodynamic term, S, a measure of the quantity of molecules that can be sorbed into and onto the polymer. Equation 1.6 emphasizes that high permeability can result from high D values, high S values or both. Permeability is an intrinsic property of a gas-polymer system [26].

The second notion used to describe gas separation membranes is membrane selectivity. It is defined based on the notion of permeability and it is defined as the ratio of permeabilities of two components i and j according to:

$$\alpha_{ij} = \frac{P_i}{P_j} = \frac{D_i \cdot S_i}{D_j \cdot S_j} \tag{1.7}$$

where the most permeable gas is taken as i. Selectivity can thus only be calculated for gas pairs and expresses the ability to separate component i from a mixture of i and j. When pure gas permeabilities are used, it is called the ideal selectivity, often noted as α_{ij}^*.

Permeability and selectivity are two main factors of performance of a membrane material. They directly effects on the purity and the application of a gas separation process. Membrane materials suffer from a trade-off between high selectivity and high permeability. Highly permeable membranes will offer lower selectivities than less permeable membranes.

The trade-off between permeability and selectivity in polymer membrane for separation of some of gas pairs ($O_2/N_2, CO_2/CH_4, CO_2/N_2, H_2/CH_4$ and etc) was firstly presented by Robeson in 1991 [27] and then updated in 2008 [28]. Figure 1.14 illustrates this type of plot for the CO_2/CH_4 couple. The line traced upon the edge of the data is known as the "upper bound" and it represents an empirical limit for the separation of polymer membranes.

The modifications on the upper bound accrues slightly in the past years, evidencing a shift in the upper bound [2] thanks to development in novel polymeric membranes. The

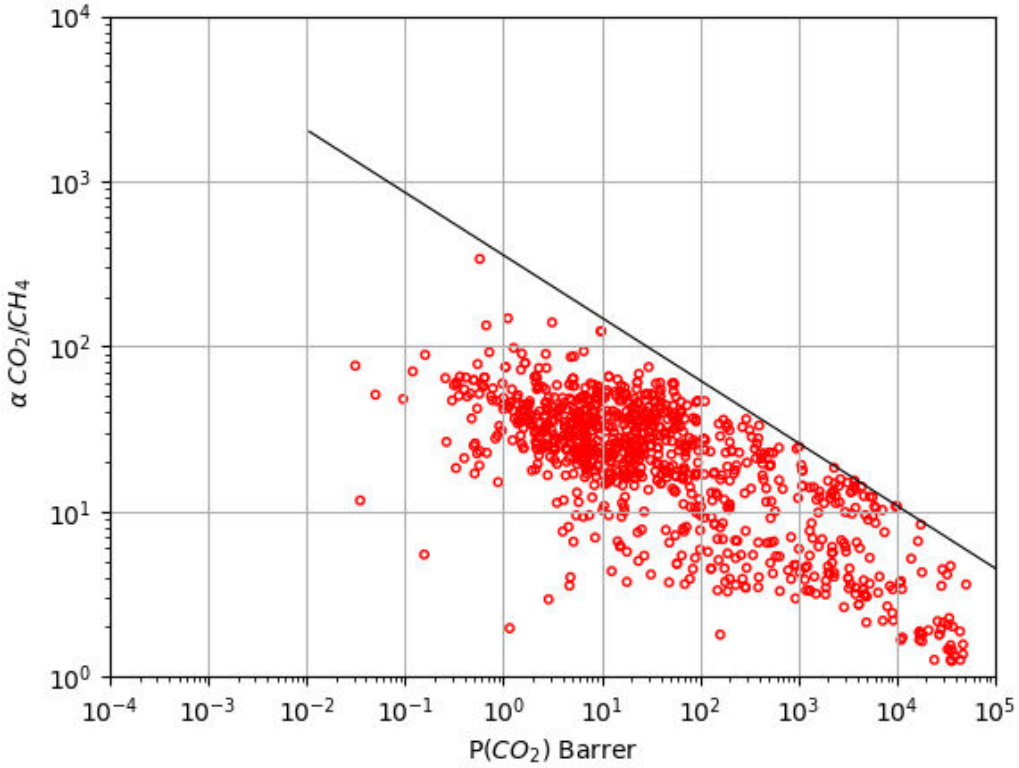

Figure 1.14: CO_2/CH_4 trade-off curve [28].

upper bound represents then the maximum achievable selectivity for a given permeability or vice versa, the maximum achievable permeability for a given selectivity of the specific gas pair. Figure 1.15 represents the permselectivity trade-off in terms of CO_2/CH_4 gas pair separation for two polymers (Polyimide and Cellulose acetate) and an inorganic (Zeolite) membrane. We will discuss more on choosing a proper membrane in terms of permselectivity concerning separation of two gas pairs O_2/N_2 and CO_2/CH_4 in chapters 4 and 5.

1.6 Design of membrane gas separation process

1.6.1 Mass transfer in a membrane

Section 1.5 explained how gradients in chemical potential, and ultimately gradients in concentration, are the driving force for gas permeation in polymeric dense membranes. These gradients are the product of pressure differences imposed between the high-pressure side or feed side, and the low-pressure side or permeate side. In practice, this pressure difference is achieved either by compression of the feed gas in mechanical compressors or by vacuum pump on the permeate side or by a combination of both. Industrial gas separation of permanent gases, however, continues to rely on compression-vacuum operation modes. A schematic representation of a gas separation module in operation is

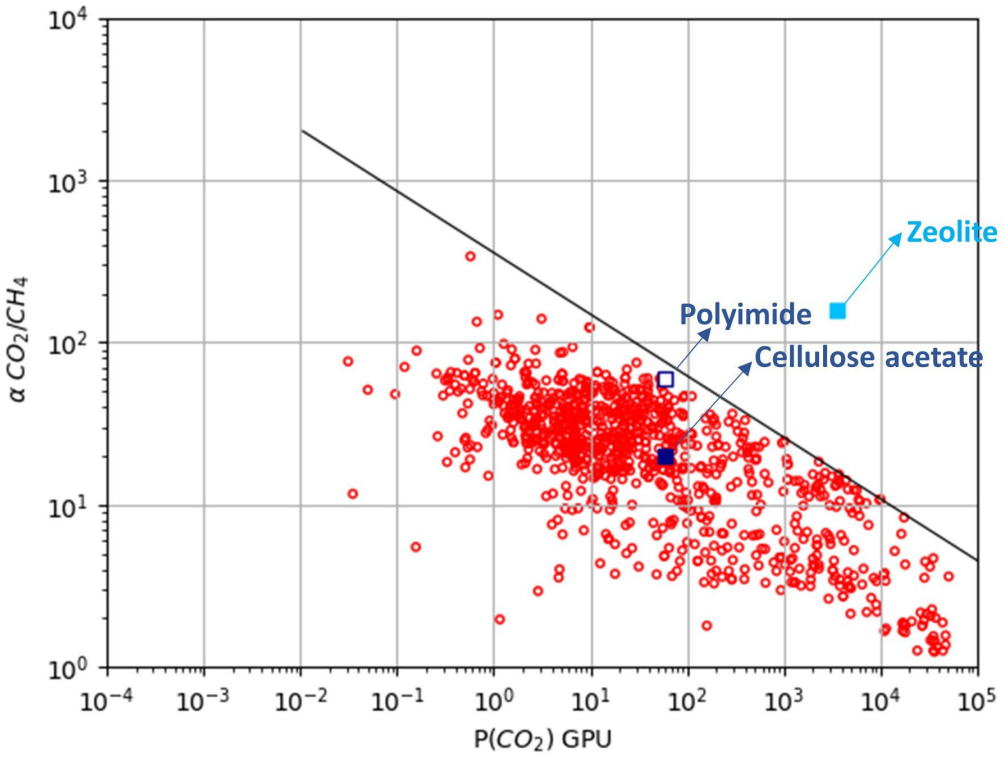

Figure 1.15: CO_2/CH_4 trade-off curve and performances of two polymers (Polyimide and Cellulose acetate) and an inorganic (Zeolite) membrane materials[28].

presented in Figure 1.16.

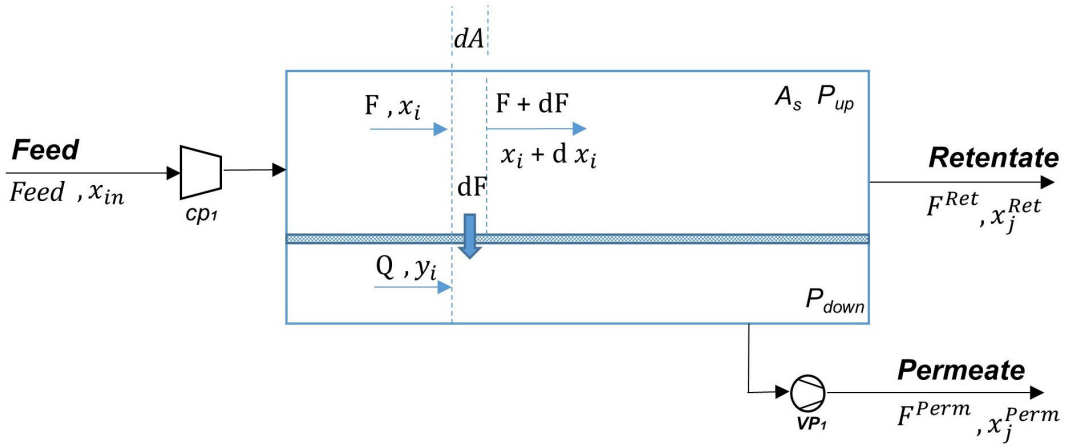

Figure 1.16: Schematic representation of a gas separation membrane module. A pressure difference is applied by a compressor on the feed stream and/or a vacuum pump on the permeate stream [29].

Hydrodynamic conditions inside both sides of the membrane module must be considered to evaluate the permeation process. Four hydrodynamic configurations cover well operation cases found in commercial modules, these are illustrated in Figure 1.17. The cross-plug-flow model, which remains the corner-stone when it comes to models in this field [29], will be taken here to illustrate the mathematical development of membrane module design.

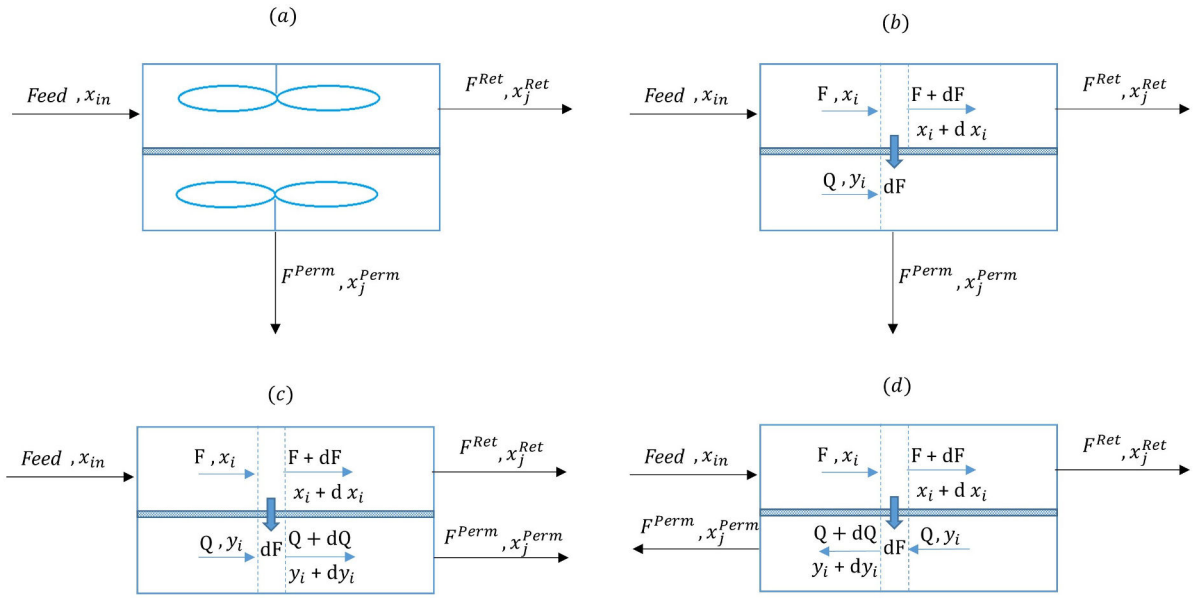

Figure 1.17: Representation of the four main flow configurations in gas permeation: (a) perfect mixing: both high and low-pressure sides of the module have a different uniform concentration; (b) cross plug flow: high pressure is considered to flow in plug-flow mode, while the low-pressure side is considered to have uniform concentration; (c) cocurrent flow: both sides are consider to flow in the same direction in plug-flow; and (d) counter-current flow: both sides flow in plug-flow mode in opposite directions.

Classical design of membrane module for separation of multicomponent mixtures considers the following assumptions related to transport conditions as presented by Shindo et al. [30]:

- The rates of permeation obey Fick's law
- The permeability/permeance of each gas component is the same as that of the pure gas, and is independent of pressure
- The effective membrane thickness is constant along the length of the permeator
- Concentration gradients in the permeation direction are negligible
- Pressure drops of the feed and permeate gas streams are negligible

1.6.2 Main parameters of the process performances

Three parameters determine the membrane gas separation system performances, pressure ratio, membrane selectivity and the stage cut. The membrane selectivity is defined in 1.7. The ratio of the Feed pressure to the permeate pressure across the membrane is called the pressure ratio, ρ , which is defined as:

$$\psi = \frac{p^{up}}{p^{down}} \tag{1.8}$$

The stage cut is the fraction of the Feed stream that permeates the membrane. It is defined as:

$$\theta = \frac{F^{Perm}}{Feed} \tag{1.9}$$

The usual target of a gas separation system is to produce a residue stream essentially stripped of the permeable component and a small, highly concentrated permeate stream [31]. However, these two requirements cannot be met simultaneously. The stage cut shows a trade-off between the recovery of a component (i.e. fraction extracted into permeate) and its purity: at high recovery the purity will be low, and vice versa.
The membrane system can be described by the permeation equations that express:

- trans membrane fluxes
- mass balance equations

Equations 1.10 and 1.11 represent the material balances through the differential area, dA, overlay and for a component j respectively. Equations 1.12 and 1.13 express that the sum of the molar fractions in each phase is equal to unity.

$$dF^{Perm} = dA \quad \sum_{j=1}^{n} \frac{P_j}{\delta} \left(p^{up} X_j^{Ret} - p^{down} X_j^{Perm}\right) \tag{1.10}$$

$$d(X_j^{Perm} F^{Perm}) = dA \quad \frac{P_j}{\delta} \left(p^{up} X_j^{Ret} - p^{down} X_j^{Perm}\right) \tag{1.11}$$

$$\sum_{j \in C} X_j^{Ret} = 1 \tag{1.12}$$

$$\sum_{j \in C} X_j^{Perm} = 1 \tag{1.13}$$

This system is solved within the frame of this thesis by an optimization strategy, which will be explained extensively in chapter 2.

1.6.3 Pressure driven process

Apart from the membranes, there can be distinguished other driven equipment such as Compressors, Expander, Vacuum pumps, and Valve that can be used in a gas separation process. They can effect on the driving force of a system. One of the aim of the process design is to select the most efficient driving force strategy. In fact, Molecules are driven across a membrane due to the driving force that is subjected to a gradient in chemical or electrical potential. This is often the result of a concentration or pressure difference between the two phases. All of these modules are schematically presented and explained below:

- **Compressor:** is a mechanical device that increases the pressure of a gas by reducing its volume. Gas compression is generally performed in multi-staged devices with usually the same compression ratio for each. Coolers between each stage allow to decrease temperature and lead to less adiabatic and more isothermal process. Figure 1.18 shows a schematic of a compressor module.

Figure 1.18: Compressor module

- **Vacuum pump:** is a device that remove air, gases and vapour from a confined space and create a vacuum in that given space. Different types of vacuum pump exist that allow to reach different levels of vacuum.Figure 1.19 shows a schematic of a Vacuum pump module.

  There are some difficulties in using of vacuum pump in a separation process in comparison with compressor:

  - It is hard to achieve vacuum at an industrial scale.
  - The compressor is more energy efficient than vacuum pump.
  - Larger foot-prints of vacuum pump in comparison with compressor.

- **Expander:** It is used on the retentate side in order to recover part of the compression energy by expands the gas stream.

Figure 1.19: Vacuum pump module

- **Valve:** The valve is used in order to decrease the pressure of a stream to give it the possibility to mix with another stream with a lower pressure.

1.6.4 Design of a membrane system

Designing a membrane separation process means selecting the elements, which are included in the system (e.g. membranes, compressors, vacuum pumps, expander, and other necessary equipment), their operating conditions, and their connections (including partial or total recycles, streams mixers and splitters). Generally, there is no difficulty in designing a single stage membrane process; however, high separation performances can generally not be achieved with a single stage process. A multi-stage process is then proposed to improve the separation.

The number of possible process configurations increased exponentially, by considering a multi-stage membrane process. So finding the best configuration design becomes tedious and time-consuming. Therefore, the development of an accurate and reliable design strategy is essential to obtain the best process configuration and optimize the performances and the global costs of the process simultaneously. To this aim, an optimization strategy is proposed in this work, that firstly expresses the membrane process synthesis as a mathematical optimization model and then solve it by applying an optimization algorithm. We will discuss in details about the proposed optimization methodology in chapter 2.

1.7 Membrane-based gas separation applications

Membrane-based gas separation industrial applications have achieved significant improvement recently due to their advantages such as low energy consumption, lower operation and maintenance costs.

Membrane process is applied in a very broad domain of gas treatment: air separation, CO_2 capture and H_2 or CH_4 purification are among the most popular ones.

1.7.1 Air separation

Currently, the most commercialized application of gas separation process is the production of nitrogen from the essentially free air [31]. Today, not only N_2 enrichment from the air is a well-known market in the air separation applications but also, the O_2 enriched air has been well-known in industrial fields [17]. The main reason of interest in producing purified O_2 and N_2 is the fact that these are the third and fifth largest bulk gases produced worldwide. N_2 is produced by membrane process for inert gas blanketing besides storing and shipping of flammable liquids, fresh fruits and vegetables. Although today there is limited utility of membranes for commercial-scale production of O_2, it is primarily for medical purposes and industrial combustion. Oxygen-enriched air improves combustion efficiency of coal. Also it is a desirable feedstock for gasifiers. Despite the commercial membranes show low permeability and selectivity in O_2 production, membrane materials with high permeability of 250 Barrer and O_2 separation factor ≥ 10 are desirable to enhance feasibility of industrial oxygen production [3]. We will discuss extensively about the overall energy savings and economic benefits which can be obtained regards to nitrogen-enriched process based on optimal membranes performance/selectivity and processes design thanks to the optimization method in the chapter 4.

1.7.2 CO_2 Capture

Capture and storage of CO_2 has been recognized as an effective way to tackle the problem of greenhouse emissions from fossil fuel utilization. Studies have indicated that increasing of atmospheric CO_2 concentration has severe effects on climate, contributing to global warming. Therefore, it is essential to investigate and find a suitable way to reduce CO_2 emissions of coal-fired power plants or flue gases which are followed by underground sequestration. The flue gas refers to the combustion of exhaust gas which is produced at power plants. The exhaust gas is usually consist of N_2, CO_2 and water vapor as well as excess O_2 that are derived from the combustion air.

Today, membrane-based separation processes are considered to be a viable and attractive option for CO_2 capture that can potentially compete with some traditional separation methods (e.g. reversible solvent absorption) in terms of energy requirements and costs, because of their low total cost and high energy efficiency.

1.7.3 Separation of acid gases from natural gas

The latest natural gas separation purification in a worldwide market is estimated at approximately US$ 5 billion/year. Membrane-based separation is considered as a promising technology for natural gas upgrading by removing of water and acid gases (H_2S and CO_2).

Membranes can be used for bulk removal of acid gases from natural gas followed by amine absorption method to decrease the economical and energy consumption of the integrated process.

1.7.4 Biogas upgrading

Biogas is considered as an important renewable and sustainable energy which is produced from anaerobic digestion of organic wastes in digesters or landfills, manure or municipal waste. It consists methane as main component and some impurities such as CO_2, O_2, and N_2. The purification of biogas is essential to make the methane commercially viable. The purified methane is used in generating heat and power(co-generation of electricity), compressing to power vehicle or entering directly into the natural gas grid for resale.

Among variety of separation techniques that have been used for biogas upgrading (e.g. physical and chemical absorption, pressure swing adsorption, water scrubber, chemical scrubber) membrane separation technology attracts lots of interests thanks to its advantages such as ease of operation and maintenance, no chemical disposal, modularity for easy scale up, mobility for transportation to areas, and potentially high energy efficiency and low cost.

1.8 Summary and conclusion

Gas separation has become a major industrial application of membrane technology through recent decades [31]. The search for a proper membrane material, module configuration and process design constitutes the key factors for continuously improving and enlarging membrane technology applications.

Membrane materials play the most important role in membrane technology. The research in membrane material has left to more permeable, selective, mechanically and chemically resistant membranes. There are variety of polymer and inorganic membranes that can be used in gas separation. Dense polymeric and inorganic (Zeolite) membranes are used through this thesis based on the targeted applications.

The main challenge of membrane process design is to obtain the best compromise between the highest separation performances and the lowest process cost. Numerous configurations are possible by considering a multi-stage membrane process. Exploring through them and obtaining the optimum one by simulation and traditional methods is tedious and time consuming. Applying optimization strategies in designing membrane system leads to the best process configuration heuristically. It can determine the most efficient equipment, their connections and performances in a process while minimizing the process separation cost. Furthermore, It gives the possibility of achieving the optimal membrane performance/selectivity based on each case study. We will discuss about optimization methodologies for process design in chapter 2.

Membranes have a wide variety of gas separation applications, ranging from removing acid gas from natural gas to nitrogen enrichment from air. Application of the membrane technology is expanding rapidly and further growth is likely to continue for the next 10 years or so. We will consider and study some of the most important membrane markets in chapter 3 to 5.

Chapter 2

Optimization and simulation of membrane-based gas separation process

Membrane separation process design consists of determining the equipment of a system, their performances, and also connect them in such a way to minimize the separation cost while obtaining the optimal production target. A membrane process involves lots of elements such as membranes, compressors, vacuum pumps, expanders, etc. Also, different factors affect the performance of a membrane and consequently the process production. The production target is mostly high purity, recovery or both of a special component of a flux gas.

Most of the process design strategies are based on experimental and trial methods. So they are often time-consuming, tedious and it is not possible to cover and investigate all the possibilities in a process design especially for the multi-stage membrane process. For this reason, a systematic method is essential to cover and synthesis all the possibilities in order to achieve the best process design.

The importance of an optimization strategy for designing the membrane process was acknowledged in the early 90s. Since then, lots of different optimization methods have been proposed. However, each of them has some limitations because of the complexity of designing the system. A generic, rigorous and systematic optimization strategy to achieve a good approximation of the optimal process design will be presented in this chapter.

This chapter starts with a literature review on different methods for optimizing a membrane gas separation process. Then the optimization method used in this thesis is described. A superstructure is used to represent the search space for designing the membrane process. The process synthesis is expressed by means of an optimization model. To solve this optimization model, a heuristic global optimization strategy is described. Finally, the obtained results are validate by means of a suitable simulator.

Parts of this chapter have been published in: A. A. Ramirez-Santos, M. Bozorg, B. Addis, V. Piccialli, C. Castel, and E. Favre, "Optimization of multistage membrane gas separation processes. example of application to CO_2 capture from blast furnace gas", Journal of Membrane Science, 566 (2018) 346–366 [32].

2.1 Literature review on optimization of membrane gas separation processes

Because of the inherent limitations of the solution-diffusion separation mechanism in polymeric membranes, several separation stages are often necessary when applications demand high levels of recovery and purity of one or several components, or when the feed is poor in the component(s) to be recovered, or both. Multiple process configurations are possible when considering a multi-stage membrane separation (i.e. number of membrane stages, membrane surface of each stage, upstream and downstream pressure of each stage and stream connections among stages). Thus finding the optimal design for the selected membrane(s) becomes the main objective of process design. This task becomes more and more complex as the number of separation stages increases[9], making the traditional simulation-based approach for process design tedious and time-consuming and often leading to the evaluation of a limited number of process configurations based on heuristics and experience. The optimization approach for process design aims to explore the set of meaningful configurations in order to ensure that the process operates under the most favorable conditions. The objective function used for the optimization is typically expressed in terms of the total process costs after accounting for the main cost elements of the process, or as specific costs when the total costs are expressed by unit of the recovered component, or as a revenue function when a market price is attributed to the recovered gas. Depending on the specific separation conditions, adding an additional separation stage can be cost-effective, however the general trend is an increase in total process costs as the number of stages increases. This is mainly because of the costs arising from the need of additional compression/vacuum equipment for each new membrane stage. The

cost of an eventual increase in total membrane surface must also not be neglected. For most of the gas separations of industrial relevance reported in the literature, the number of stages typically varies between one and three [8], [33]–[37], and in some cases up to four stages are considered [10], [38], [39].

Optimization approaches for multi-stage membrane separations have been reported in scientific literature mainly for natural gas and biogas applications[10], [34]–[36], [39], and for CO_2 capture applications [37], [38], [40]. Uppaluri et al.[8], [41] reported the application of an optimization approach to enriched oxygen production, nitrogen enriched air, and to hydrogen recovery from synthesis gas and refinery streams. Most of these works are based on the optimization of the mathematical model derived by a process superstructure. By superstructure it is denoted a general process configuration comprising all the possible process units and their connections that have to be evaluated and compared during process design. There is a trade-off between increasing the size and complexity of the superstructure, which allows for the evaluation of more process configurations, and dealing with more complex problems from a mathematical point of view. The specific approach to the superstructure design and derived mathematical model which is depended on the set of process units, interconnections and assumptions included in the superstructure for a given application and for defined separation goals as well as the use of appropriate optimization algorithms allowing to find ideally the global optimum within the feasible region. Varying process assumptions defining the possible configurations included in the superstructure as well as different optimization methods have been considered in previous works. Table 2.1 presents a non-exhaustive list of the most recent studies summarizing the main process assumptions of the system and modeling approach.

Qi et al.[10] proposed a membrane system configuration to separate multicomponent gas mixtures, based on an approximate permeator model and mixed-integer nonlinear programming (MINLP). A superstructure approach is presented, allowing the simultaneous optimization of the process configuration and operating conditions of a very large number of possible process alternatives. Different multi-stage membrane configurations were presented. Process layout and area are the main optimization variables. Feed side pressure, equal for all stages, was also considered as an optimization variable while permeate pressure was free to vary for each stage respecting a fixed value of the outlet CO_2-rich permeate of around 1 bar and restricted to pressures no lower than this value. Process layouts with variable feed-side pressure among membrane stages and vacuum operation on the permeate side were thus not included in the superstructure.

In the work by Uppaluri et al. [8], the cost minimization of the membrane separation problem is also modeled as a Mixed Integer Non-Linear Programming (MINLP) problem with a superstructure based approach. The optimization strategy is a simulated annealing algorithm with an exploration of the neighborhood based on structure and stream moves. The structure moves change the structure of the network (membrane areas, number of stages, flow configurations), while the stream moves only change the flow distribution. Therefore, the exploration is both in terms of continuous and discrete variables. For each new generated point, once integer variables are fixed, the nonlinear equations describing

the system behavior are imposed through a standard nonlinear equation solver. Then, this point is simulated, the cost function is computed, and the corresponding solution is accepted or rejected. Performance constraints are not directly inserted in the model, but enforced through a penalty term, therefore, solutions found by the optimization phase could be unfeasible. Upstream and downstream pressures are allowed to vary but are the same for each membrane stage. The use of vacuum pressure on the permeate side was considered in the evaluated configurations.

Yuan et al. [40], formulated a multi-objective optimization model to simultaneously minimize energy consumption and membrane area of six single and dual-stage membrane process designs for carbon capture from a CO_2-N_2 binary mixture. The optimization model is solved by means of a nondominated sorting genetic algorithm (NSGA-II) available in MATLAB's Global Optimization Toolbox. Operating upstream and downstream pressures, temperatures of inlet streams to compressors, vacuum pumps, and expanders, and intermediate composition have been considered as decision variables in the optimization which sought to minimize energy consumption and total membrane surface simultaneously. No cost modeling was performed for the process based on an ideal-N_2 selective metallic membrane.

Scholz et al. [35] presented a cost minimization for multi-stage configurations, modeled as a Mixed Integer Non-Linear Programming (MINLP) problem in a superstructure approach for biogas upgrading, and solved by means of the Branch-And-Reduce Optimization Navigator (BARON) solver. The feed was modeled as a CO_2-CH_4 binary mixture. A practical maximum number of three stages was defined for the study although the method presented is not limited to any number of stages. Upstream and downstream pressures are allowed to vary and can be different for each membrane stage. The use of compressors, vacuum pumps and pressure reduction valves were considered in the superstructure. The need to produce the upgraded gas at a pipeline pressure of 16 bar favored the use of feed compressing over permeate vacuum, and optimal process configuration remained the same for the required upgrading conditions when comparing membranes with a CO_2 permeance of 60 GPU and CO_2/CH_4 selectivities of 20 and 60. Interestingly, the resulting optimal configuration matches the configuration of a three stage process previously patented by Evonik industries [42]. Furthermore, the optimal CO_2/CH_4 selectivity for the process was also studied by considering the upper bound correlation of Robeson within the optimization problem. The optimized process configuration based on the optimal ideal membranes consisted of two stages, instead of the three necessary for the optimal configuration when commercial membranes are used, however the authors explain that the impact of the optimal membranes on overall profitability might not be enough to support the commercial development of new membranes for this application [35].

The same optimization approach was presented by Ohs et al. [36] for the removal of nitrogen from natural gas. The superstructure was limited to two stages and the effect of nitrogen selective vs. methane selective membranes on process configuration was evaluated. The use of both kinds of membranes in the same two-stage configuration led

to a lower process costs compared to the cost obtained by using only one kind of any of the two types of membranes. It was shown that new, more selective membranes would allow a noticeable reduction of process costs.

Arias et al.[38] presented recently a nonlinear programming (NLP) optimization approach of a superstructure of process configurations for CO_2 capture from coal-fired power plants at recovery-purity targets ranging from 90 to 98%. The feed was modeled as a binary CO_2-N_2 mixture. The process layout and operating variables are considered as decision variables, as well as the optimal number of stages. Upstream pressure is allowed to vary but is the same for each stage and downstream pressure is fixed for all stages. The use of vacuum pressure on the permeate side was not considered in the evaluated configurations. An analysis of the equations involved in their model, showed that they could get rid of the discrete variables describing the configuration, allowing thus a NLP formulation instead of a MINLP. The NLP problem has been solved by means of a local solver (CONOPT 3.0), using some heuristic to help generate a good starting solution with respect of feasibility. Results presented illustrate how the optimal number of stages, and process configuration, depend of the imposed purity-recovery constraints. The optimal two-stage configuration obtained agreed with that typically used in most capture studies while interesting configurations were proposed for processes with three and four membrane stages.

Gabrielli et al. [37], presented a multi-objective optimization model which was defined and solved by means of a genetic algorithm to minimize the specific energy consumption and required membrane area of CO_2 capture from a binary CO_2-N_2 flue gas mixture. Four fixed single and dual-stage process configurations were first analyzed by a parametric analysis and then the optimal configuration was evaluated for up to six membrane stages. Process layout, membrane selectivity according to Robeson's upper bound, and operating variables are considered as decision variables. Upstream pressure is fixed and equal to the feed pressure at atmospheric conditions, and permeate pressure is varied between 0.01 and 1 bar independently for each stage. A global minimum in terms of energy consumption was identified for the enricher configuration with recycle at three membrane stages, and across the selectivity range evaluated (20-60).

Aliaga-Vicente et al. [43] proposed a MINLP approach for two superstructures dealing with CO_2 separation from CO_2/CH_4 mixtures for natural gas sweetening and enhanced oil recovery. They employed the SBB algorithm which is a combination of the standard branch and bound method and CONOPT in the GAMS software. The superstructure approach is based on the evaluation of separation cascades as presented by Agrawal et al. [44] and included novel aspects such as the consideration of an expander for the exiting retentate stream, lateral extraction streams and the consideration of temperature changes during membrane separations and permeate compression by means of correlations obtained in Aspen Hysys. The process layout and operating variables are considered as decision variables, as well as the optimal number of stages. Upstream pressure is allowed to vary but the use of vacuum pressure on the permeate side was not considered in the evaluated configurations. It is explained by the authors that the approach presented

doesn't guarantee a global optimal solution because of the nonlinearity and non-convexity of the optimization problem.

Table 2.1: Summary of recent publications dealing with the optimization of multistage gas membrane separation processes.

Industrial application	Feed composition	Modeling approach	Assumptions on the system				Reference
			Upstream pressure	Downstream pressure	Max# stages	Permeability Selectivity	
N_2 removal from natural gas	Binary gas: CH_4 - N_2	Superstructure No self recycling	Fixed	Free and uniform	2-stages	Fixed permeance data Robeson's upper bound	[36]
Air separation H_2 recovery from synthesis gas and refinery streams	Binary gas: O_2 - N_2 H_2 - CH_4 - Ar - N_2	Superstructure	Free and uniform	Free and uniform	3-stages	Fixed permeance data	[41]
Biogas upgrading	Binary gas: CO_2 - CH_4	Superstructure No self recycling	Free and indep.	Free and indep.	3-stages	Fixed permeance data Robeson's upper bound indep. for each stage	[35]
CO_2 capture from coal-fired power plants	Binary gas: CO_2 - N_2	Superstructure with restricted interconnections No feed split	Free and uniform	Fixed	4-stages	Fixed permeance data	[38]
CO_2 capture from coal-fired power plants	Binary gas: CO_2 - N_2	Fixed configurations	Fixed	Free and uniform	6-stages	Fixed permeance data	[37]
CO_2 capture from coal-fired power plants	Binary gas: CO_2 - N_2	Fixed configurations	Free and indep.	Free and indep.	2-stages	Fixed permeance data	[40]
Natural gas sweetening and enhanced oil recovery	Binary gas: CO_2 - CH_4	2 superstructures with restricted interconnections no feed split	Free and uniform	Free and uniform	4-stages	Fixed permeance data	[43]
CO_2 capture from industrial gas	CO_2 - N_2- O_2- H_2O	Superstructures with restricted interconnections	Free and indep.	Free and indep.	3-stages	Fixed permeance data	[45]
CO_2 capture from coal-fired power plant	Binary gas: CO_2 - N_2	Superstructures with restricted interconnections	Free and indep.	Free and indep.	3-stages	Fixed permeance data	[46]
Natural gas sweetening and enhanced oil recovery	Binary gas: CO_2 - CH_4 CO_2 - H_2S - CH_4 - C+H CO_2 H_2S CH_4 C_2H_6 C+H	Superstructure	Free and uniform	Free and indep.	4-stages	Fixed permeance data	[10]
CO_2 capture from blast furnace gas	CO_2 - CO - N_2 - H_2	Superstructure	Free and uniform	Free and indep.	4-stages	Fixed permeance data	[32]

2.2 Superstructure design of a membrane process

To express process synthesis as an optimization problem, and solve it, the superstructure paradigm was introduced in the early 90s [47]. It exhaustively represents the allowed units and connections of a given process, on the basis of the assumptions made. In each work dealing with process synthesis [8], [35], [36], [39], [43], different assumptions have to be made on the superstructure, that exclude some configurations, both to neglect not meaningful configurations and to try to simplify the underlying optimization problem (see Table 2.1).

Starting from the superstructure, it is possible to derive a mathematical programming model of the system design process, that can in some cases involve discrete variables [10], or in some others lead to a continuous non-linear programming (NLP) (see Appendix A) problem [38]. Considering the number of membrane stages in the process as a parameter (fixed), only continuous variables will remain, allowing the mathematical problem to be considered as a NLP problem instead of a mixed integer non-linear (MINLP) (see Appendix A) problem. Similarly to [38], any connection involving a zero flow stream will be canceled. The resulting system leads to a highly non convex NLP problem allowing a very high number of degrees of freedom.

Figure 2.1 presents the proposed generic superstructure that will be used throughout the thesis for all case studies (It will be more enlarged to represent the possibility of applying compressor or expander on retentated stream, to obtain the expected outlet pressure for biogas upgrading in the chapter 5). It has to be noticed that this superstructure can consider the use of compressors, or vacuum pumps or both, as well as any recycling including self-recycling. In the next subsection, the assumptions are listed, the mathematical model is addressed, and the optimization problem is formally stated.

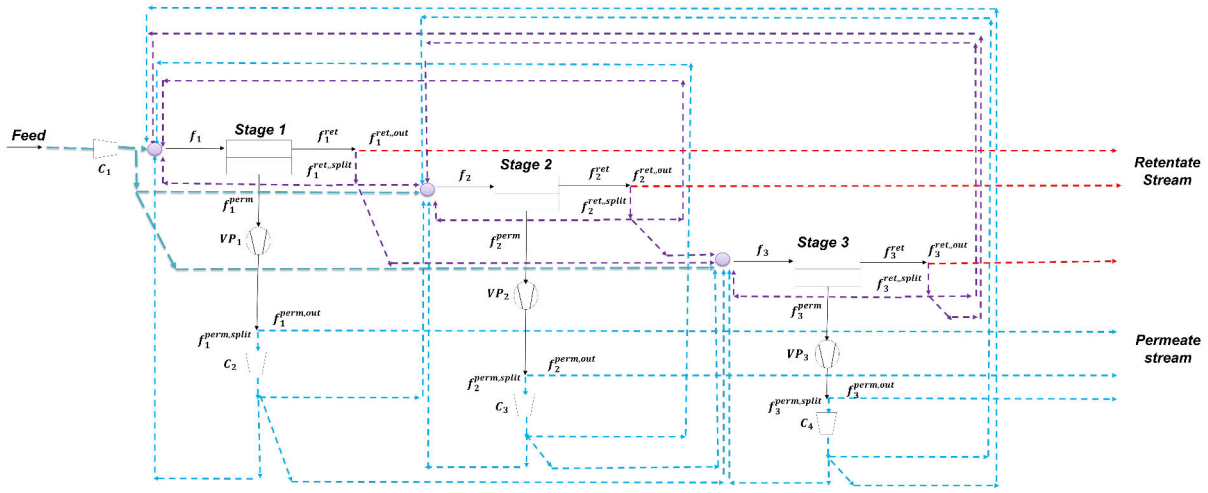

Figure 2.1: Superstructure

2.3 Mathematical Optimization model

The mathematical model refers to a generic number of gas components and number of stages defined by the following sets:

- $\mathcal{S}$: set of stages (membranes)
- $\mathcal{C}$: set of decomposition cells in a membrane
- C: set of gas components

Here are the parameters of the model:

- $maxArea$: Maximum allowed total area
- n_s: Number of cells in a membrane
- k_R: Front factor in the Robeson bound equation
- n_R: The slop of the log-log plot of the Robeson bound equation

The model is divided into three levels, with increasing level of details, which is presented in Figure 2.2.

- The overall system
- A single stage
- A single cell

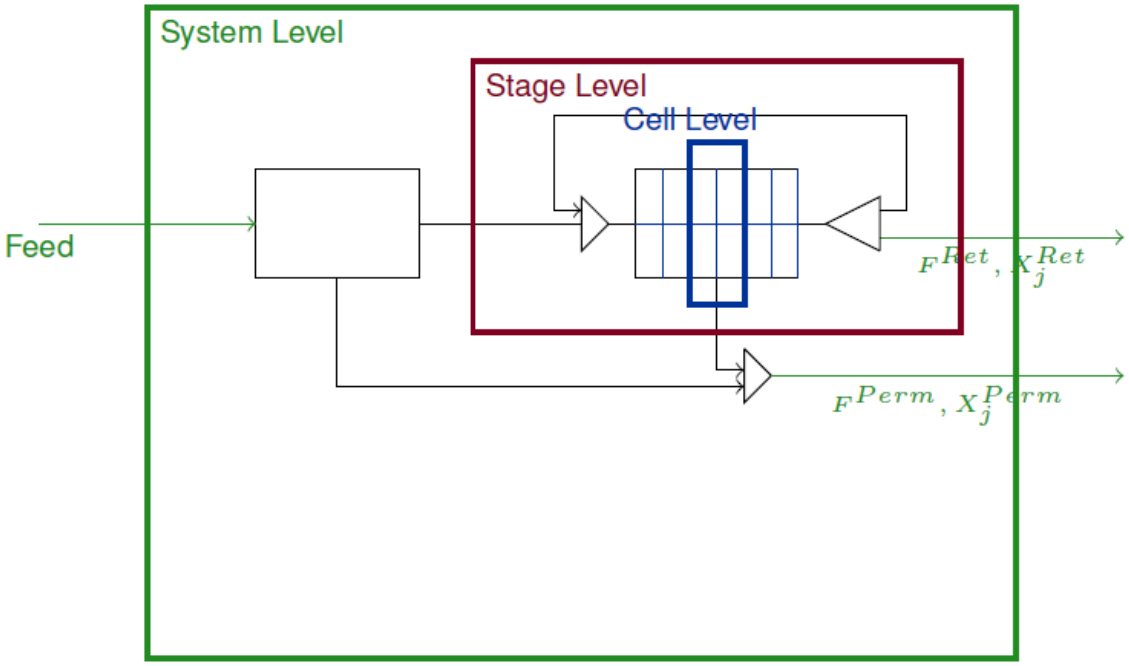

Figure 2.2: Level set of a membrane system

- **The overall system** has one given input, the feed, and two outputs, the retentate and the permeate streams as following:
  - Feed is the input flow to the system [mol/s]
  - F^{Ret} (and F^{Perm}) system retentated (and permeated) flow [mol/s]
  - X_j^{Ret} (and X_j^{Perm}) fraction of retentated (and permeated) flow of the system that is constituted by component j [dimensionless]

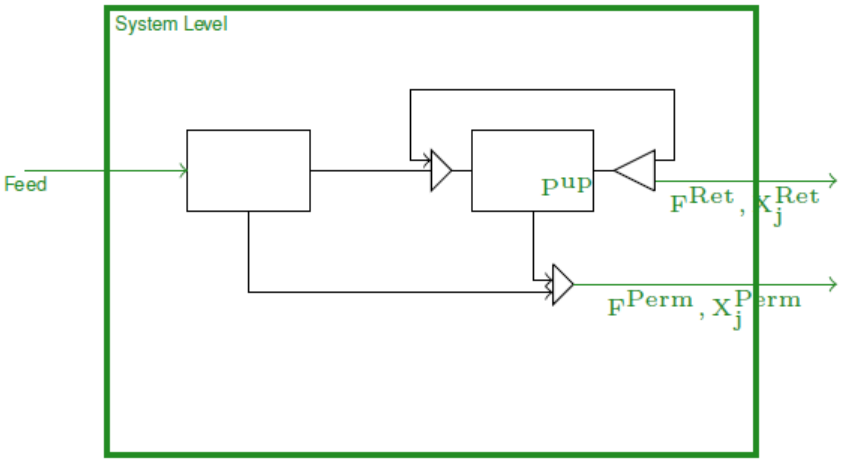

Figure 2.3: System level variables

- **The single stage** constitutes of a membrane $s \in \mathcal{S}$ with its input and output flows that can be split according to the superstructure
  - f_s is the input flow to the membrane s [mol/s]
  - f_s^{ret} (and f_s^{perm}) membrane s retentated (and permeated) flow [mol/s]
  - $x_{s,j}^{ret}$ fraction of retentated flow of membrane s that is constituted by component j [dimensionless]
  - $x_{s,j}^{perm}$ fraction of permeated flow of membrane s that is constituted by component j [dimensionless]

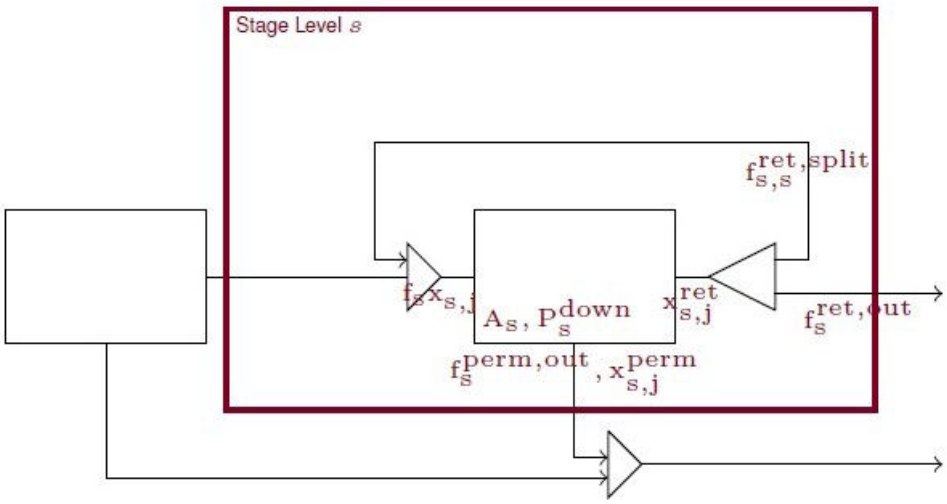

Figure 2.4: Stage level variables

- **The single cell** describes the behavior of the gas flow into a single cell $i \in \mathcal{C}$ of a given membrane.
  - $g_{s,i}$ is the input flow to the cell i of membrane s [mol/s]
  - $g_{s,i}^{ret}$ (and $g_{s,i}^{perm}$) cell i of membrane s retentated (and permeated) flow [mol/s]
  - $y_{s,j,i}$ fraction of the in flow of cell i of membrane s that is constituted by component j [dimensionless]
  - $y_{s,j,i}^{ret}$ fraction of retentated flow of cell i of membrane s that is constituted by component j [dimensionless]
  - $y_{s,j,i}^{perm}$ fraction of permeated flow of cell i of membrane s that is constituted by component j [dimensionless]

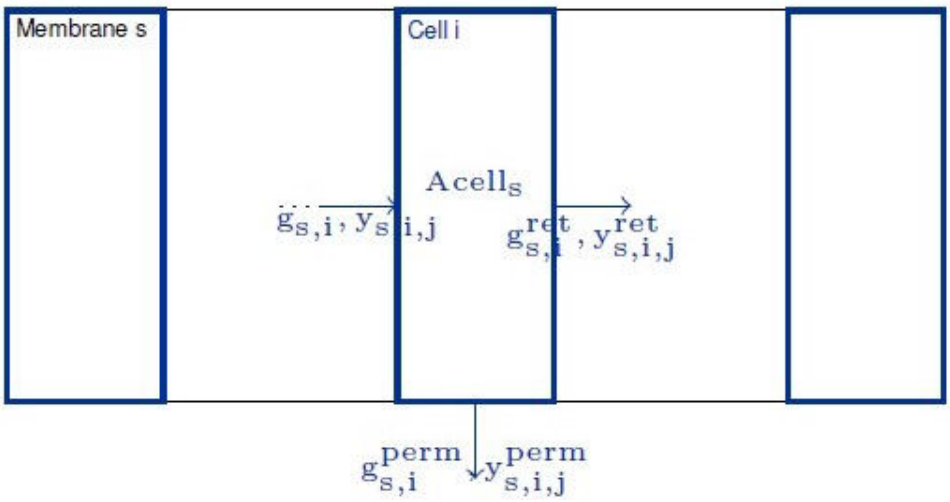

Figure 2.5: Cell level variables

The following variables are the main decision variables of the system:

- $Acell_s$ Area of the each cell of membrane s
- p_s^{up} Up stream pressure of membrane s
- p_s^{down} Down stream pressure of membrane s
- P_s^h High permeability of membrane s
- P_s^l Low permeability of membrane s

The flowrates in the proposed superstructure (Figure 2.1) are translated into the mathematical optimization model by using the following superscripts in the variables:

- split: it represents the flowrate that goes from one stage to another, e.g. $f_{s,s1}^{perm,split}$ represents the quantity of permeate flowrate of membrane s that is redirected to membrane s1.
- out: it expresses the flowrate that goes from one stage to the system output, e.g. $f_s^{perm,out}$ expresses the quantity of permeate flow rate of membrane s that is directed to the system output.

In the following the constraints included in the model are listed and described.

Flow conservation constraints at the level of the overall system:

$$Feed = F^{Ret} + F^{Perm} \tag{2.1}$$

$$F^{Ret} = \sum_{s \in \mathcal{S}} f_s^{ret,out} \tag{2.2}$$

$$F^{Perm} = \sum_{s \in \mathcal{S}} f_s^{perm,out} \tag{2.3}$$

Flow conservation constraints for each membrane s:

$$f_s = f_s^{ret} + f_s^{perm} \quad \forall s \in \mathcal{S} \tag{2.4}$$

and flow conservation constraints at the cell level (both for total flow and single component flow):

$$g_{s,i} = (g_{s,i}^{ret} + g_{s,i}^{perm}) \qquad \forall s \in \mathcal{S}, i \in \mathcal{C} \tag{2.5}$$

$$g_{s,i} y_{s,j,i} = (g_{s,i}^{ret} y_{s,j,i}^{ret} + g_{s,i}^{perm} y_{s,j,i}^{perm}) \quad \forall s \in \mathcal{S}, i \in \mathcal{C}, j \in C \tag{2.6}$$

$$g_{s,i+1} = g_{s,i}^{ret} \qquad \forall s \in \mathcal{S}, i \in \mathcal{C} \tag{2.7}$$

$$y_{s,j,i+1} = y_{s,j,i}^{ret} \quad \forall s \in \mathcal{S}, j \in C, i \in \mathcal{C} \tag{2.8}$$

The following equations describe the membrane behavior:

$$g_{s,i}^{perm} y_{s,j,i}^{perm} = Acell_s \frac{P_j}{\delta} (P^{up} y_{s,j,i}^{ret} - P_s^{down} y_{s,j,i}^{perm}) \quad \forall s \in \mathcal{S}, j \in C, i \in \mathcal{C} \tag{2.9}$$

The following equations model the correlation between the membrane level and the cell level:

$$f_s = g_{s,1} \qquad \forall s \in \mathcal{S} \tag{2.10}$$

$$x_{s,j} = y_{s,j,1} \quad \forall s \in \mathcal{S}, j \in C \tag{2.11}$$

$$f_s^{ret} = g_{s,n_s}^{ret} \qquad \forall s \in \mathcal{S} \tag{2.12}$$

$$x_{s,j}^{ret} = y_{s,j,n_s}^{ret} \quad \forall s \in S, j \in C \tag{2.13}$$

$$f_s^{perm} = (\sum_{i \in \mathcal{C}} g_{s,i}^{perm}) \qquad \forall s \in \mathcal{S} \tag{2.14}$$

$$x_{s,j}^{perm} f_s^{perm} = (\sum_{i \in \mathcal{C}} y_{s,j,i}^{perm} g_{s,i}^{perm}) \quad \forall s \in \mathcal{S}, j \in C \tag{2.15}$$

whereas the connection between the system level and the membrane level is regulated by:

$$F^{Ret} = \sum_{s \in \mathcal{S}} f_s^{ret,out} \tag{2.16}$$

$$X_j^{Ret} F^{Ret} = \sum_{s \in \mathcal{S}, j \in C} x_{s,j}^{ret} f_s^{out,ret} \quad \forall j \in C \tag{2.17}$$

$$F^{Perm} = \sum_{s \in \mathcal{S}} f_s^{perm,out} \tag{2.18}$$

$$X_j^{Perm} F^{Perm} = \sum_{s \in \mathcal{S}, j \in C} x_{s,j}^{perm} f_s^{out,perm} \quad \forall j \in C \tag{2.19}$$

At each level, it must be enforced that the fractions of the components sum up to one:

$$\sum_{j \in C} X_j^{Ret} = 1 \tag{2.20}$$

$$\sum_{j \in C} X_j^{Perm} = 1 \tag{2.21}$$

$$\sum_{s \in \mathcal{S}, j \in C} x_{s,j}^{ret} = 1 \tag{2.22}$$

$$\sum_{s \in \mathcal{S}, j \in C} x_{s,j}^{perm} = 1 \tag{2.23}$$

$$\sum_{s \in \mathcal{S}, j \in C, i \in \mathcal{C}} y_{s,j,i}^{ret} = 1 \tag{2.24}$$

$$\sum_{s \in \mathcal{S}, j \in C, i \in \mathcal{C}} y_{s,j,i}^{perm} = 1 \tag{2.25}$$

Finally, flow conservation constraints related to the superstructure are introduced:

$$f_s^{ret} = \sum_{s_1 \in \mathcal{S}} f_{s,s1}^{ret,split} + f_s^{ret,out} \qquad \forall s \in \mathcal{S} \tag{2.26}$$

$$x_{s,j}^{ret} f_s^{ret} = \sum_{s1 \in \mathcal{S}} x_{s,j}^{ret} f_{s,s1}^{split,ret} + x_{s,j}^{ret} f_s^{out,ret} \quad \forall s \in \mathcal{S}, j \in C \tag{2.27}$$

$$f_s^{perm} = \sum_{s_1 \in \mathcal{S}} f_{s,s1}^{split,perm} + f_s^{perm,out} \qquad \forall s \in \mathcal{S} \tag{2.28}$$

$$x_{s,j}^{perm} f_s^{perm} = \sum_{s1 \in \mathcal{S}} x_{s,j}^{perm} f_{s,s1}^{split,perm} + x_{s,j}^{perm} f_s^{out,perm} \quad \forall s \in \mathcal{S}, j \in C \tag{2.29}$$

$$f_s = \sum_{s1 \in \mathcal{S}} f_{s1,s}^{ret,split} + f_{s1,s}^{perm,split} + f_s^{split} \qquad \forall s \in \mathcal{S} \tag{2.30}$$

$$x_{s,j} f_s = \sum_{s1 \in \mathcal{S}} x_{s1,j}^{ret} f_{s1,s}^{split,ret} + x_{s1,j}^{perm} f_{s1,s}^{split,perm} + x_j f_s^{split,Feed} \quad \forall s \in \mathcal{S}, j \in C \tag{2.31}$$

$$Feed = \sum_{s \in \mathcal{S}} f_s^{split} \tag{2.32}$$

The expressed set of constraints describes the gas separation process. Depending on the case study, some performance constraints can be added on the percentage or on the recovery of some components.

We note that all the variables are bounded to be in a box where the lower bound is non-negative, and the upper bound can be derived by the physical meaning of the variable. Finally, a maximum recycling ratio of 0.9 is imposed on the splits of any stage towards itself (self-loops).

Optimizing the problem (even locally optimizing) is not an easy task. In the case of 3 stages and 20 cells for each stage, the total number of variables is 9116, and the number of constraints is 9754, of which 4845 linear equalities, 4880 nonlinear equalities, 28 linear inequalities. Also, the equality nonlinear constraints are numerically hard (the physical problem always admits a solution neglecting the performance constraints).

2.4 Global optimization strategy

We applied a continuous global optimization algorithm, that can be considered as the composition of two algorithms: Multistart and Monotonic Basin Hopping (MBH). Multistart and MBH can be considered as the basis of many other elaborated Global Optimization (GO) heuristics. Multistart is a modified version of the Monte-Carlo (MC) method: points are randomly sampled in the search space and then, differently from MC methods, a local optimization is performed on each point. This allows to combine a global

search (random sampling) to the power of standard local optimization (gradient-based, quasi-newton, etc.) in determining local optima. This key idea of combining global and local search is used by almost all successful GO stochastic algorithms. MBH combines the idea of using a standard local search with the idea that *near* a good local solution it could be possible to find some better local solution (as long as this is not the global optimum). Therefore, instead of restarting every time from a new different point like Multistart, MBH restricts its search in a neighborhood of the current local solution.
The scheme of MBH is reported in Algorithm 1. Note that in the algorithm $\mathcal{L}(x)$ denotes the point resulting from performing a local search starting from the point x. MBH starts randomly generating a point and applying a local optimization, then this first local solution is considered the center of search in a reduced space (the neighborhood of the current solution). Therefore, the current local optimum is perturbed and locally optimized. If the new solution is better then the previous one, this step is considered an improvement step, and the new local solution substitutes the previous one, otherwise another perturbation is applied to the old local solution. The algorithm continues until no improvement is found for a certain number of consecutive perturbations[1]. The whole procedure is repeated starting from different initial points of the search space, therefore we can consider our GO method as the composition of the function Multistart with the function MBH. In Algorithm 2 a very schematic representation of the overall GO method is reported.

Algorithm 1 `Monotonic Basin Hopping`

procedure MONOTONIC BASIN HOPPING(Δ,N,x_{start})
  $n = 0, k = 0$
  $x_0 = x^* = \mathcal{L}(x_{start})$
  while $n < N$ **do**
    y_k = random uniform point in $\mathcal{B}(x_k, \Delta)$
    if $C(\mathcal{L}(y_k)) < C(x^*)$ **then**
      $n = 0$
      $x^* = x_{k+1} = \mathcal{L}(y_k)$
    else
      $n = n + 1$
    $k = k + 1$
  return $x^*, C(x^*)$

MBH (as Multistart) is a meta-heuristic, and therefore must be adapted at the problem we want to solve. Furthermore, both MBH and Mulstistart are originally conceived for unconstrained or box constrained optimization. When the problem is highly constrained, even finding a feasible point could be challenging. Therefore the method must be tailored

[1]if an improvement is found, the number of unsuccessfully perturbation is re-set to zero

Algorithm 2 `Global Optimization Algorithm`

1: $t = 0$,x^{min}, $C^{min} = \infty$
2: **while** $t < maxT$ **do**
3: x_t^{start} = random uniform point in the feasible set
4: $x_t^*, C(x_t^*)$ =Monotonic Basin Hopping(Δ,N,x_t^{start})
5: **if** $C(x_t^*) < C^{min}$ **then**
6: $C^{min} = C(x_t^*)$
7: $x^{min} = x_t^*$
8: $t = t + 1$
return x^{min}, C^{min}

to the problem at hand.

We have adapted the algorithm working mainly on the random generation, both for the Multistart (full point generation, Algorithm 2-line 3) and for the MBH random perturbation (Algorithm 1-line 5), to allow the main constraints to be satisfied in the generated/perturbed points. In fact, if this part is not carefully done, the local search procedure could be not able to find a feasible point, or find a point *very far* from the original one, making the search "completely random" and therefore loosing the capacity to search in the neighborhood typical of MBH. Just to give some insight of the tailoring procedure, we explain some of the modification we made. We impose that the flow balance constraints are satisfied at the beginning and at the end of each membrane, and that the sum of the percentage of all the components is one. Therefore, in our modified version of MBH, the function $\mathcal{L}(x)$ can be considered as an operator that maps the point x to the "nearest" local minimum.

The best results produced for each configuration by our GO algorithm are then simulated in COFE in order to get the "real" values for each variable. Then, the objective function is calculated[2].We implemented our method in AMPL [48], and we chose (after extensive testing) KNITRO as local solver [49]. It performs better the other solvers in terms of numerical issues.

2.5 Simulation of membrane process

Efficient modelling simulation approaches are important to evaluate the potential of membrane gas separation processes. We used MEMSIC in order to simulate our optimal membrane process. MEMSIC is a compliant steady-state computer software with simulation environment including multicomponent mixtures computations and extendable to Process System Engineering (PSE) software through a CAPE-OPEN tool.

[2]from a practical point of view, and to reduce possible errors due to different ways to evaluate the cost, the objective is calculated by plugging the resulting point of the COFE simulation in the optimization code and just calling a routine to evaluate the cost without performing any optimization.

It can be used on a standalone basis for module performances simulations or integrated within any type of PSE software thanks to CAPE-OPEN standard. We used the CAPE-OPEN simulation module in order to simulate the optimal process configurations. A rigorous computation of transmembrane fluxes based on different solution-diffusion models (dual mode, Flory Huggins, ENSIC) for a set of absolute upstream and downstream pressure can be obtaine by using MEMSIC simulator.

MEMSIC is a very precise tool calculating all the outputs of the membranes system. All the data describing the system have to be precisely inserted before starting the simulation e.g. number of components into desired design, percentages of components, Feed flux, operating pressure and compounds permeability characteristics. There is no limitation to the number of compounds. In terms of geometric parameters, the model only requires the membrane surface area. The dense layer thickness can also be defined, or directly included in the gas permeance data. This allows the model to be used for any membrane module geometry.

Therefore, the user can create a system, combining whichever number of membranes, compressors, expander, valve and etc.Once all the values are correctly specified, the program calculates the behavior of fluxes into the system with its output flows and percentages of the components [50].

2.6 Validation of the optimization strategy

In order to validate the optimized configurations obtained by our GO algorithm, we applied it to a reference case for which an optimization approach was proposed by Qi et al. [10]. This choice is motivated by the detailed description of the applied model, optimization objective and optimal configurations, which allowed a clear and straightforward comparison. We focus on the case study of natural gas treatment with four component mixture with continuous membrane areas (Section 3.2 of [10]). We make the same assumptions, but we use our mathematical model as described in 2.3 for the membrane calculation. The superstructure in this case excludes the possibility of vacuum operation on the permeate side since this operation mode is not considered in the case studies in [10]. The same cost model used for the calculation of the annual process cost in [10] is used in this section.
Three sets of operating conditions were considered and evaluated during validation, with increasing degrees of freedom :

(i) both upstream and downstream pressures and membrane areas are fixed and only connections among membrane stages are allowed to change

(ii) upstream and downstream pressures are fixed but membrane area is free to vary among stages

(iii) both upstream and downstream pressures and membrane area are free to vary in a suitable range

For each of these three cases, the distribution of compressors can be determined a priori. Apart from these assumptions, we allow any connection between units (including self loops) and any split (number and fraction) of flows. Finally, each membrane process configuration resulting from the GO algorithm was compared (retentate and permeate fluxes and composition of each stage, objective function value) to simulations performed at the same conditions by means of a proprietary gas permeation calculation tool developed at the laboratory, MEMSIC 6.0 [50], implemented to the Aspen Plus V8.6 environment through the CAPE-OPEN standard, with the objective of evaluating the numerical difference between the optimization algorithm and our classical simulation approach.

2.6.1 Validation of the optimization approach with a reference case from the literature [10]

The first step is to compare the solutions offered by the optimization method from the reference case studies taken from [10] with our optimization method and verify that they produce comparable local solutions. To this aim, we consider the optimal configurations reported in Figure 2 and Figure 4 of [10] which are presented here as Figure 2.7a and Figure 2.8a respectively. These configurations and their corresponding objective values are considered as reference cases.

We perform two tests:

- Using the same conditions of the reference case on our AMPL implementation, obtained an optimum value. The value of the objective function calculated by the optimization algorithm is denoted as "GO".
- Simulating the same process conditions of the reference cases in Aspen Plus v8.6 and obtained the values. The objective value concerning the simulated values denoted as "ASPEN".

Through these validation test, the membranes types, Feed (flow and composition), presence of compressors, values of pressures, etc are completely fixed.

Table 2.2: Objective value comparison for model validation. Annual process cost expressed as USD/m^3. Values in parentheses taken from [10].

Case Name	2-stages	3-stages
Reference	11.422 (11.094)	11.236 (10.971)
ASPEN	11.660	11.807
GO	11.500	11.300

Table 2.2 presents the objective values of the References, GO, and ASPEN tests. Concerning the reference values, the original values presented in [10] are reported in parentheses while the recalculated values using the same cost equations are shown without

parentheses. The difference is likely due to some rounding up before computing the objective value. It can be seen that the differences between the three set of values are small, indicating that the difference in membrane modeling between the three approaches leads to small differences in the objective values (annual process cost) calculated in each case, and showing that our mathematical model is comparable with that of the reference case and with that of a classical process simulation.

2.6.2 Fixed pressures optimization

We performed a set of different tests (see Figure 2.6), adding step by step degrees of freedom. We have considered two different settings with respect to membrane areas:

- membrane areas are fixed to the values reported in [10]
- membrane areas are continuous variables, that is any area can be chosen in a given interval

and two different cases considering flows among membranes:

- the flow connections are kept fixed to the values reported in [10], meaning that we only allow nonzero flows on the connections reported in [10].
- flows are continuous variables, so we consider a general configuration where all mixers and splits can be used

We can observe, that the case with fixed areas and fixed flows is exactly the reference value, in fact in this case only one stationary point exists from the simulation point of view (and also from the optimization one). Therefore, at this step, we consider 3 global optimization problems for each case-study. In Figure 2.6, we report a schematic representation of the tests, from the reference configuration to the one with more degree of freedom.

$$
\begin{cases}
2-\text{stages} \begin{cases}
\text{Fixed Area} \begin{cases} \text{Fixed Flow} - \textbf{Reference} \\ \text{Free Flow} \end{cases} \\
\text{Free Area} \begin{cases} \text{Fixed Flow} \\ \text{Free Flow} \end{cases}
\end{cases} \\
3-\text{stages} \begin{cases}
\text{Fixed Area} \begin{cases} \text{Fixed Flow} - \textbf{Reference} \\ \text{Free Flow} \end{cases} \\
\text{Free Area} \begin{cases} \text{Fixed Flow} \\ \text{Free Flow} \end{cases}
\end{cases}
\end{cases}
$$

Figure 2.6: Summary of tests with fixed pressures

First of all we start keeping fixed the membrane areas and pressures as in [10], and we

allow the optimization algorithm to change the configuration of the system, that is to change the proportion in splits, the feed distribution and the layout of membranes stages. In Table 2.3, the best results found by our GO algorithm, and then simulated by ASPEN are reported. For comparison the reference values from [10] are reported.

Table 2.3: Annual process cost expressed as USD/m^3. Case with fixed membrane areas and pressures. Reference values recalculated from [10]

	2-stages		3-stages	
	Reference	This work	Reference	This work
GO	11.422	10.713	11.236	10.721
ASPEN	11.457	10.667	11.263	10.683

Even with the same pressures and the same membranes area, the global optimization performed here allows to achieve lower process costs when compared to the reference case, around 4 to 7%, showing its efficiency and ability to globally explore the search space. As areas are the same, the reduction in the objective is due to the reduction in the product loss term of the objective. Methane recovery is higher leading to reduced costs despite the increase in total power.

In the two stages case, the optimal configuration is similar to the reference one, except for the inclusion of a self-recycling loop of the retentate coming from the second stage. For the process with three membrane stages, the optimal configuration contains again a self-loop in the second stage, but other structural differences are present. Membrane area between the first and second stages is switched compared to the reference case, and it is the first stage that exhibits the larger membrane surface. Furthermore, the first stage takes as an input the permeate from the second stage. Finally, the third stage is fed by a fraction of the permeate of the first stage and not by the permeate of the second stage.

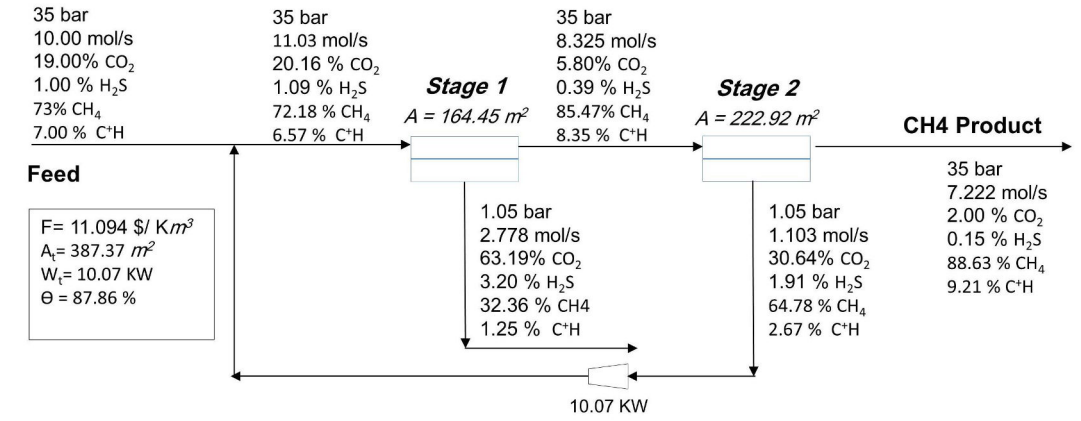

(a) Optimal 2-stage process from reference

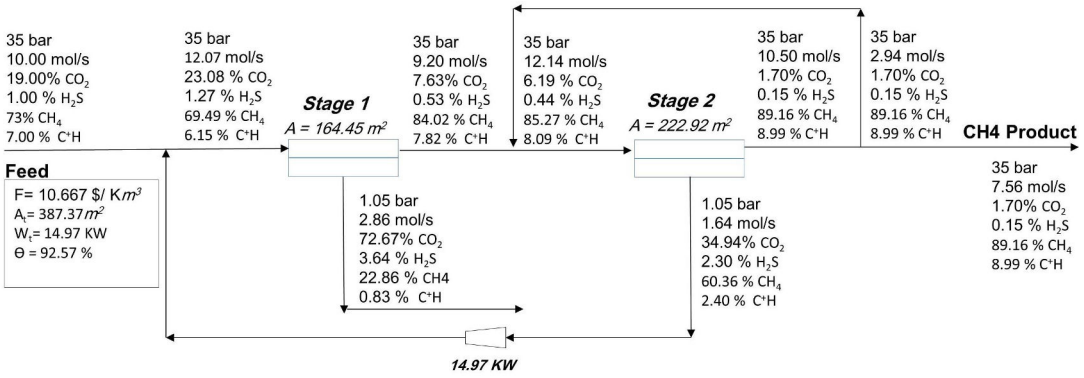

(b) Optimal 2-stage process obtained in this work

Figure 2.7: Comparison of optimization results for a two stage membrane process between the reference case [10] and the optimization approach developed in this work when both membrane area and pressure of each stage are fixed.

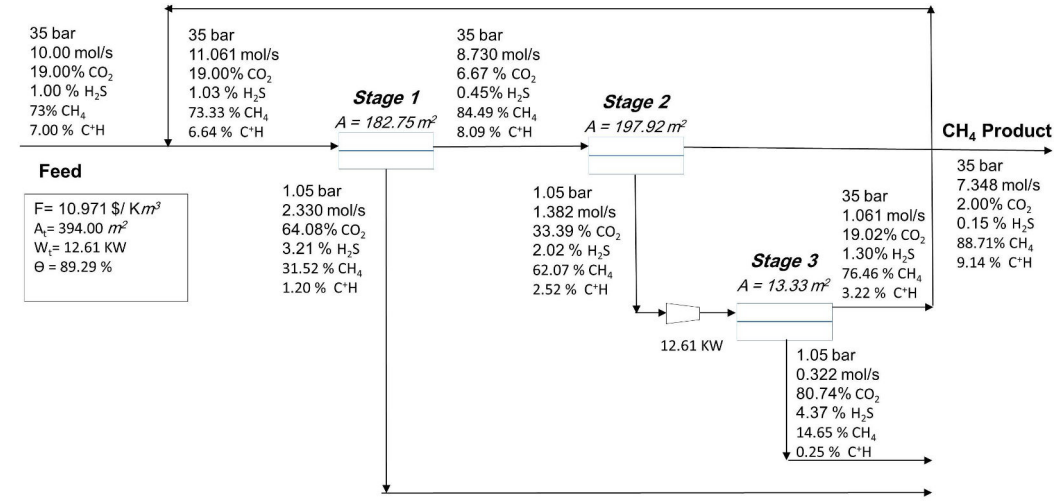

(a) Optimal 3-stage process from reference

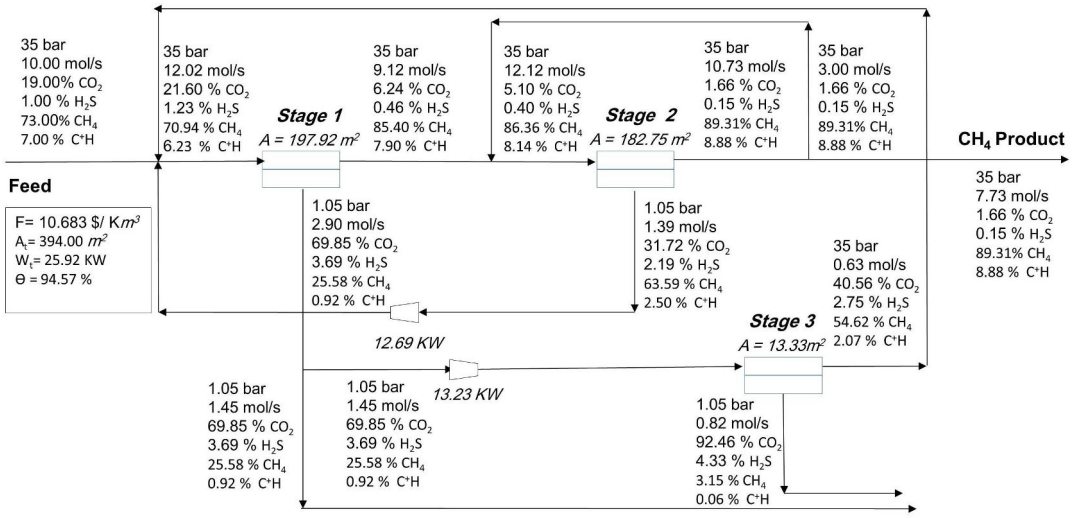

(b) Optimal 3-stage process obtained in this work

Figure 2.8: Comparison of optimization results for a three stage membrane process between the reference case [10] and the optimization approach developed in this work when both membrane area and pressure of each stage are fixed.

The next step is to allow the areas of the membranes to vary, having then both the connections among stages and the membrane areas as optimization variables. We present the results only for the three stage process for the sake of brevity and because they are better than the two stages ones. As expected, by increasing the degrees of freedom better solutions are obtained, whose objective function values are reported in Table 2.4. Once again, when compared to the optimal solution from the reference, the process configuration obtained with our approach leads to around 20% lower process cost. This is achieved by both a reduction of total membrane area and an increase in methane recovery. The optimal process calculated here and presented in Figure 2.9, has the same

general configuration that the reference case presented in Figure 2.8a. No self-recycling was included in the optimal configuration this time.

Table 2.4: Annual process cost expressed as USD/m^3. Case with fixed pressure and free area with three stages. Reference values recalculated from [10]

	Reference	This work
GO	11.236	9.115
ASPEN	11.263	9.095

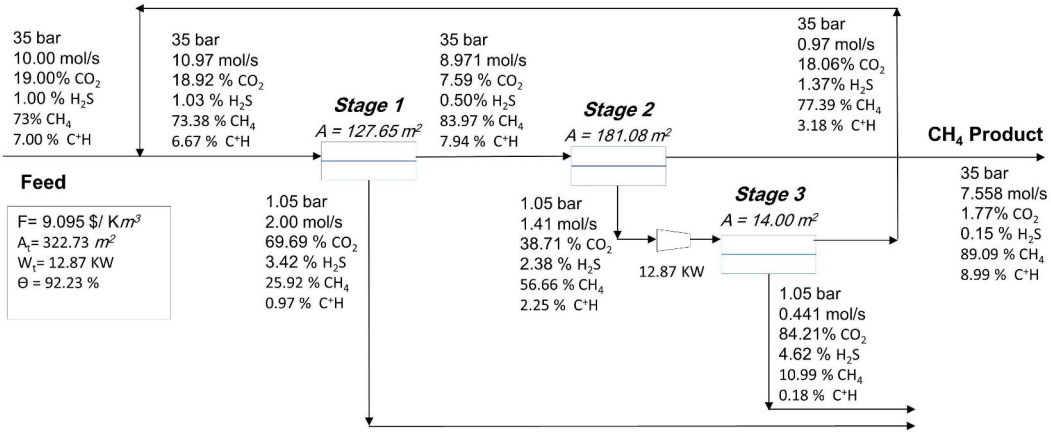

Figure 2.9: Optimal process for the case with fixed pressures and free area.

2.6.3 Free pressures optimization

As a further step, using the same feed conditions ($10 mol/s$ at $35 bar$), the degree of freedom of the system increased by considering the pressure as a variable. Indeed, the GO algorithm considered membrane areas, flux distribution (connection and value of flux and components) and also the pressures of the system as the decision variables of the system and determined them. Both upstream and downstream pressures to vary uniformly for all the membranes stages with an upper bound of 50 bar and lower bound of 1.05 bar for upstream and downstream pressures respectively. So, the following constraints were imposed to the system:

1. $P^{up} \leq 50$
2. $P^{down} \geq 1.05$
3. $P^{up} \geq P^{down} + 0.001$

The process cost reduces over 35% (Table 2.5) and the best configuration has only 2 stages (Figure 2.10) compared to the three stage process of the reference case. This

is explained in part by the structure of the objective function that privileges the use of compressors over the increase of the membrane areas (this was noted also in [10]). Indeed, the optimal solution has always the pressure at the upper bound, since the cost of the compressor is quite limited: according to the formulas used in [10] a compressor going from 35 to 50 bar only costs $0.074\$/Km^3$. This justifies the very low cost of the optimal configuration but at the same time shows the need of a more realistic objective function, further justifying our choice of a different objective function in the next subsection.

We stress that in Section 3.4 of [10] some experiments with different bounds on the feed side pressure and a different fresh feed pressure are reported. For the considered objective function, the different fresh feed pressure only implies a constant value added to the objective function due to the compressor on the inlet feed (from 1.05 to 35 this correspond to $0.736\$/Km^3$). Indeed, even adding this term our results outperform the results presented as the best in [10]. It is worth to notice that in their case the best solution reported is a 3-stage system, and not a 2-stage one, as in our case.

Table 2.5: Annual process cost expressed as USD/m^3. Case with free uniform pressures and free areas. Reference values recalculated from [10]. Case with fixed pressures is presented again for comparison.

	Reference	This work	
		Fixed pressures	Free pressures
GO	11.236 3 stages	9.115 3 stages	7.271 2 stages
ASPEN	11.660	9.095	7.262

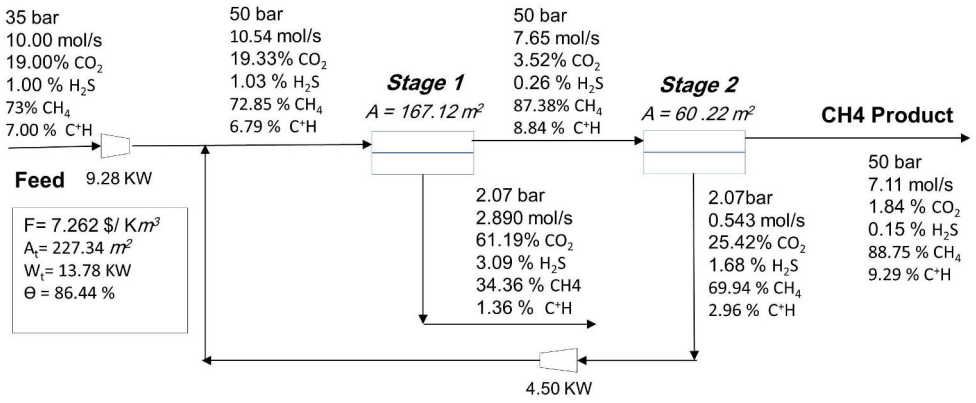

Figure 2.10: Optimal process for the case with free pressures and free area.

2.7 Summary and conclusions

This work presented the development and application of a Global Optimization approach for a Non Linear Programming formulation based on a superstructure for the design and optimization of multistage membrane separation processes.

General process superstructure with up to three stages is presented. Different auxiliary equipment such as compressor and vacuum pump on the permeate side, and mixed operation (using both) are included in it. Furthermore, interconnection possibilities among process units have been kept as numerous as possible to increase the number of possible process configurations. Upstream and downstream pressure, process layout and membrane surface of each stage are the decision variables. In addition, downstream pressure is allowed to vary independently for each membrane stage thus allowing an independent pressure ratio for each stage. To our knowledge, no superstructure-optimization approach for membrane separation has been presented in the scientific literature with these characteristics (multi component feed, exhaustive connection layout including recycling loops, variable pressure ratio for each stage with compression and/or vacuum possibilities).

The process synthesis is expressed as a mathematical optimization model. The mathematical problem is considered as a highly non-convex continuous NLP optimization problem. A global optimization approach is presented to solve the NLP formulation of the membrane architecture optimization problem.

The global optimization approach is based on a combination of two complementary algorithms, Multi-start and Monotonic Basin Hopping (MBH) which together allow the evaluation of a wide area of the feasible region during the global search phase and the exploration of potential better solutions near local optimums during the local search phase, thus improving the chances of finding optimal process configurations. The approach was validated by comparing its output with that of a reference work ([10]) from the literature dealing with the optimization of multistage processes for natural gas treatment. It was shown that it was possible to produce separation designs with lower objective values than the reference case, i.e. process configurations with a lower separation cost. Furthermore, the approach presented here allows for the use of vacuum pressure in the downstream side of the membrane which can be independently set for each membrane stage. This allows for the design and optimization of process configurations with independent pressure ratios among membrane stages.

Table 2.6: Summary of decision variables and auxiliary equipment which are considered for optimization of multistage gas separation processes of different case studies.

Industrial application	Feed compositions	Area	P_{up}	P_{down}	# of stages	PermSelectivity	Auxiliary equipment			
							C_p	Expander	V_p	Valve
Remove acid gases from crude natural gases	$CO_2 - H_2S$ $CH_4 - C + H$	Var	Var & Uniform	Var & Uniform	up to three	fixed	✓	✗	✗	✗
CO2 capture from BFG	$CO_2 - CO$ $N_2 - H_2$	Var	Var & Uniform	Var & Uniform	up to four	fixed	✓	✗	✗	✗
N2 enrichment from air	$O_2 - N_2$	Var	Var & Uniform	Var & Ind.	up to three	Var and Ind.	✓	✗	✓	✗
Biogas upgrading	$CO_2 - CH_4$	Var	Var & Uniform	Var & Ind.	up to three	fixed	✓	✓	✓	✓
Natural gas upgrading	$CO_2 - CH_4$	Var	Var & Ind.	Var & Ind.	up to three	Var and Ind.	✓	✗	✗	✓

Part II
Results

Chapter 3

Recovery of CO_2 from Blast Furnace Gas

In this chapter, the optimization approach which is described in the previous chapter, is applied to the optimization of CO_2 capture from blast furnace gas. We consider multistage processes with up to four membrane stages. The optimal process configuration and main process variables (upstream and downstream pressure and membrane area) are determined for different processes with respect of CO_2 recoveries (90, 95, and 99%) and N_2 residual contents (1, 0.5 and 0.1%). The objective function is based on NETL [51] type cost model.

The contents of this chapter have been published in: A. A. Ramirez-Santos, M. Bozorg, B. Addis, V. Piccialli, C. Castel, and E. Favre, "Optimization of multistage membrane gas separation processes. example of application to CO_2 capture from blast furnace gas", Journal of Membrane Science, 566 (2018) 346–366 [32].

3.1 Blast Furnace gas

Process optimization for multistage processes had been identified as one of the key research and development needs for the application of gas membrane separation for CO_2 recovery from Blast Furnace Gas (BFG) in previous studies[52], [53]. Here a flowrate of 1240 mol/s of blast furnace gas is considered, corresponding to around 100 000 Nm^3/h, representative of the order of magnitude of unused gas in a site producing over 6 million tons of steel per year. Gas pressure and temperature are 1 bar and 35°C respectively with the gas composition presented in Table 3.1. The gas is considered dry and free of impurities such as particles and minor components such as NO_X, SO_X and H_2S. Information on the separation cost and energy calculations are available in a section 3.2.

Gas permeances are those reported for MTR's Polaris© membrane, used here as a reference of the best performance offered by polymeric membranes currently available in the market for CO_2 capture applications [54], [55]. It should be noted that more permeable versions of the Polaris© membrane are currently under development at pilot and laboratory scales[56].

The effect of CO_2 recovery and residual N_2 constraints on optimal process configuration, operation parameters (upstream and downstream pressures, and membrane surface) and separation cost is studied for CO_2 recoveries of 90, 95 and 99% while N_2 content is varied between 0.1, 0.5 and 1%. Product purity is expressed in terms of residual N_2 since this would be the only inert component when considering the transformation of the recovered CO_2 by catalytic processes [52]. Luyben [57] reported the high sensitivity of transformation costs on feed inerts for a model reversible catalytic reaction in a gas-phase adiabatic tubular reactor. The presence of 2% inerts in the feed tripled the total annual costs and almost doubled the reactor size when compared to an inert-free feed [57].

Process configurations from 2 to 4 membrane stages were considered. The general superstructure for the case with 3 membrane stages, presented in Figure 2.1, is the same used for the validation with the reference case in the previous chapter. It includes the possibility to have vacuum downstream pressures independent for each membrane stage by including a vacuum pump on each permeate stream. Upstream pressure is allowed to vary between 1 and 100 bar and this pressure is the same for all membrane stages while downstream pressure is allowed to vary between 0.2 bar and 1 bar and is independent for each stage. The pressure limit of 0.2 bar has been suggested and used in previous works [40], [51], [54] and it is thus considered in the process configurations of this study.

The issue with the operation at higher vacuum levels (<0.2 bar) is not that this vacuum level is not achievable at industrial scale but that the permeate volumetric flows will exceed largely the capacity of most vacuum systems available [58]–[60]. Steam ejectors operate at the necessary capacities, however the use of steam introduces significant additional operational expenses that would make the separation not economically viable. For example, the steam consumption of a two-stage ejector operating at a suction pressure of 0.1 bar is 6.75 kg of steam (7bar) per kg of equivalent air at 20°C [61]. A one stage

separation of the BFG with the conditions from Table 3.1 operating with a downstream pressure of 0.1 bar and around 230 000 m^2 of membrane would allow for a 90% CO_2 recovery of a permeate stream with a mass flow of 52 065 Kg/h and 67% CO_2. With a conservative price of steam of 10 EUR/ton, only the steam cost would represent around 67 EUR/ton CO_2 under these operation conditions when considering the use of a steam ejector.

Finally, the effect of a uniform pressure ratio and a decrease of membrane permeance or membrane selectivity on optimal separation cost and process configuration were analyzed for one separation case with fixed purity and recovery constraints.

Table 3.1: Feed composition and gas permeance

Gas	Composition (%mol)	Pure gas permeance (GPU)
CO_2	23.2	1000
CO	22.6	20
N_2	50.3	15
H_2	3.9	85

3.2 Annual and specific separation costs

Separation cost used in the BFG case was based on a modified version of the model used in a previous work [52], following literature [62] and NETL[51] guidelines. Capital cost includes membrane area and membrane frame, compressors and vacuum pumps. Capital cost of compressors are taken from [61]. Heat exchangers represent a relatively small part of total final costs [52] and are not considered here for simplification purposes. Total capital investment (CAPEX) is calculated from the investment cost of the equipment supposing an indirect cost factor of 80%. This value is higher that the 31% used in the previous work, and is based on internal cost guideline recommendations within our project. This increase is notable on the final separation cost and it is meant to make up for the uncertainty of additional cost elements at this preliminary design stage. Operational costs include electricity costs related to compression and vacuum equipment, membrane replacement, and operation and maintenance cost. Operation and maintenance costs have been simplified and are estimated at 3% of capital expenditures plus membrane replacement costs. Membrane replacement costs have been set at 25 EUR/m^2, a more conservative value than the 10 EUR/m^2 used in the previous work and closer to the 40 EUR/m^2 used for capital cost estimation. Only one annualization factor is used for all equipment including membranes. The annualization factor was calculated considering a period of 23 years and an interest rate of 7.4%. Total annual costs are divided per unit of product gas per year to express final specific separation costs.
presents The cost equations and the cost parameters are presented in Table 3.2 and Table 3.3, respectively.

Table 3.2: Cost equations used to determine product gas separation cost

Equipment cost		
$I_{m_s} = A_{m_s} \cdot K_m$	(3.1)	Membrane cost
$I_{mf_s} = (A_{m_s}/2000)^{0.7} \cdot K_{mf} \cdot (p^{up}/55)^{0.875}$	(3.2)	Membrane frame cost
$I_{cc_s} = C_{cc} \cdot (W_{cp_s}/10^6)^{0.7} \cdot MF_{cc} \cdot MDF_{cc} \cdot UF_{2000}$	(3.3)	Stage compressor cost
$I_{cc_f} = C_{cc} \cdot (W_{cp_f}/10^6)^{0.7} \cdot MF_{cc} \cdot MDF_{cc} \cdot UF_{2000}$	(3.4)	Feed compressor cost
$I_{vp_s} = C_{vp} \cdot (W_{vp_s}/10^3)$	(3.5)	Vacuum pump cost
Capital expenditures		
$CAPEX = (I_{cc_f} + \sum_{s \in \mathcal{S}} (I_{m_s} + I_{mf_s} + I_{cc_s} + I_{vp_s})) \cdot ICF$	(3.6)	Total capital cost
Operational expenditures		
$C_{O\&M} = \sum_{s \in \mathcal{S}} A_{m_s} \cdot \nu \cdot K_{mr} + 0.03 \cdot CAPEX$	(3.7)	Operation and maintenance cost
$C_{en} = t_{op} \cdot W_{tot} \cdot K_{el}$	(3.8)	Energy cost
$OPEX = C_{en} + C_{O\&M}$	(3.9)	Total operational expeditures
Annual and specific separation costs		
$C_{cap} = CAPEX \cdot a$	(3.10)	Annual capital costs
$C_{tot} = C_{cap} + OPEX$	(3.11)	Total annual costs
$M_{CO_2 \text{ per year}} = F^{Perm} \cdot X_{CO_2}^{Perm} \cdot M_{CO_2} \cdot 10^{-6} \cdot 3600 \cdot t_{op}$	(3.12)	Annual separated CO_2
$SC_{CO_2} = C_{tot}/M_{CO_2 \text{ per year}}$	(3.13)	Specific CO_2 separation cost

Table 3.3: Cost parameters

Capital cost parameters		
C_{cc}	1×10^6	EUR_{2000}
C_{vp}	1500	EUR/KW
K_m	40	EUR/m^2
K_{mf}	286×10^3	EUR
MDF_{cc}	2.72	-
MF_{cc}	1.4	-
UF_{2000}	1.42	-
ICF	1.8	-
T	308.15	K
R	8.31446	$JK^{-1}mol^{-1}$
η	0.85	-
ϕ	0.95	-
γ	1.36	-
λ	0.85	-
Annual cost parameters		
ν	0.2	-
K_{mr}	25	EUR/m^2
t_{op}	8322	h/year
K_{el}	0.044	EUR/kWh
a	0.0854	-
M_{CO_2}	44.01	g/mol

The power W_{cp_f} required for compressing the fresh Feed is calculated by the following equation:

$$W_{cp_f} = \frac{Feed}{\eta} \cdot \frac{\gamma \cdot R \cdot T}{\gamma - 1}[(\frac{P^{up}}{P_{in}})^{\frac{(\gamma-1)}{\gamma}} - 1] \tag{3.14}$$

Note that if the Feed-side pressure is equal to the fresh Feed pressure, W_{cp_f} is zero.
The power W_{cp_s} required for compressing the permeate stream of stage s that does not go out of the system, is calculated by the following equation:

$$W_{cp_s} = \frac{f_s^{perm} - f_s^{perm,out}}{\eta} \cdot \frac{\gamma \cdot R \cdot T}{\gamma - 1}[(\frac{P^{up}}{P_{in}})^{\frac{(\gamma-1)}{\gamma}} - 1] \tag{3.15}$$

where P_{in} is equal to one, as we assumed that the compressor is preceded by a vacuum pump. The driving force is increased by utilizing the vacuum pump for the permeate-side of each stage. The power of vacuum pump is calculated by:

$$W_{vp_s} = \frac{f_s^{perm}}{\lambda} \cdot \frac{\gamma \cdot R \cdot T}{\gamma - 1}[(\frac{P_{in}}{P_s^{down}})^{\frac{(\gamma-1)}{\gamma}} - 1] \tag{3.16}$$

If the pressure down of the permeate equals the atmospheric pressure, then this term is zero.
Finally, the total consumption power of the system is the sum of the total compressing

power (W_{cp_s} for each stage and W_{cpf} for the feed) and the total vacuum pump power (W_{vp_s} for each stage) divided by the mechanical efficiency ϕ:

$$W_{tot} = \frac{W_{cp_f} + \sum_{s \in \mathcal{S}} (W_{cp_s} + W_{vp_s})}{\phi} \tag{3.17}$$

3.3 Mapping of two to four stage optimal configurations

3.3.1 Mapping of two stage configurations

First a mapping of the optimal process configurations under varying separation constraints for processes with fixed number of membrane stages is presented. Figure 3.1, presents these configurations when the number of membrane stages is fixed to two. Separation cost in this section corresponds to the values obtained using the global optimization algorithm. The difference between these values and the ones obtained by the simulation in Aspen Plus is quite small as shown in the previous chapter in section 2.6.1.

Separation costs vary from 29 to 75.7 EUR/ton CO_2 depending on the recovery-purity constraints imposed. Decreasing N_2 residual content of the CO_2 product stream at constant recovery almost doubles the separation cost when going from 1% to 0.1% N_2 at constant recoveries of 90, 95 and 99%. Increasing the recovery at constant product purity has a less pronounced effect, separation cost increases ∼1.4 times for the 1, 0.5 and 0.1% residual N_2 levels. CO_2 product purity is rather constant for the separation cases at equal N_2 residual levels despite varying recovery constraints, ∼96% CO_2 for 1% N_2, ∼98% CO_2 for 0.5% N_2, and ∼99.5% CO_2 for 0.1% N_2.

It can be seen that for all of the two stage separations in Figure 3.1, an enricher configuration with retentate recycle from the second stage to the first is the optimal configuration. This is a consequence of the separation problem, since the product is recovered in the permeate, and thus increasing of product purity, or decreasing of N_2 impurities in this case, exerced by the second stage must be done on the permeate of the first, leading to the enricher configuration when the number of membrane stages is set to two. The retentate recycling from the second to the first stage is present for all separation scenarios as well, indicating its necessity to achieve the separation goals for the gas-membrane system studied here, by increasing the recovery of CO_2 that otherwise would be lost if this stream would exit the system as does the retentate of the first stage.

Any kind of recycling must consider the eventual re-compression needs arising from the pressure difference between the streams to be mixed. This pressure difference will be much more important when recycling permeate streams for example, because of the inherent pressure difference between feed and permeate streams driving the separation at every membrane stage. Pressure differences between feed and retentate streams on the other hand are due to pressure drops arising from the flow of the gas in the upstream compartments of the membrane modules. Recycling of a permeate stream to a feed side of

one of the membrane stages would increase the capital and power related operational expenses because of the additional compression required. No permeate recycling is present in any of the optimal configurations independently of the number of membrane stages illustrating that these expenses overcome any process advantage that may arise from permeate recycling in a given configuration for CO_2 recovery as presented in this work. This agrees with optimal process configurations presented in other works dealing with CO_2 post-combustion capture [38], [51]. Note that for applications where the product is recovered on the retentate, and consequently some product is lost on the permeate side, permeate recycles are necessary to increase process recovery. CO_2 and N_2 removal from natural or biogas are some examples of this [10], [35], [36].

Pressure drop on the retentate side for gas separation in membrane modules is generally relatively small, and depends on module geometry so, most of the optimization and design approaches, such as those presented in Table 2.1 including this work, do not consider pressure drops in the retentate for simplification purposes. This leads to retentate recycling that does not consider additional compression when recycling to a feed stream with the same pressure. Configurations with recycling streams must be considered with care since additional costs are present depending on the recycled flowrate and pressure drop in the membrane. We consider here that this belongs to more detailed calculations that must take place in successive stages of process design. The idea of this work is to present a general screening of possible configurations before more detailed process design and economic assessment takes place. The cost-effectiveness of the suggested recycle streams, if present, can be better evaluated at these stages, based on custom pressure drop and cost parameters for the specific separation under design.

Interestingly, partial retentate self-recycles on the second stage are present in the process configurations for 95% CO_2 recovery and 0.1% N_2, Figure 3.1 (h), and the configurations at 99% CO_2 recovery and 1% and 0.5% N_2, Figures 3.1 (c) and (f). Self-recycles are often not considered in classic design of membrane gas separation processes, and also in several superstructure-based optimization approaches, self-recycling is not included in the superstructure to diminish the mathematical complexity or because it is considered not to contribute to the separation process [35], [36]. Other works [10], [39] have kept both retentate and permeate self-recycling within the process superstructures, with the purpose of offering more general solutions. This is also the spirit of this work.

From a technical economic point of view, the use of self-recycles offers to the optimization an easy method to increase recovery by increasing the membrane surface instead of the transmembrane pressure and thus reducing expenditures from compression and vacuum equipment. As it has been shown in previous studies [52], these expenditures typically have a greater impact on final cost than the membrane expenditures. So when separation is feasible by adding a self-recycle, most of the solutions of the optimization method converged to a configuration including a self-recycling. This is illustrated in Figure 3.2. The optimal solution included a self-loop where nearly half of the retentate from the second stage is recycled back to itself. Compared to the next best solution found during the optimization, which doesn't include a self-recycle, the optimal solution allowed for a

reduction of the upstream pressure at nearly equal downstream pressures. This reduction allows for savings in both CAPEX and OPEX related to the compressors and despite the cost increase in membrane area, the trade-off is positive and allows a reduction of the estimated separation cost from 65.1 to 58.8 EUR/ton CO_2. This analysis holds true for cases (h), (c) and (f) in Figure 3.1. However, for case (i) at a higher recovery of 99% the best configuration found by the optimization procedure does not include a self-loop while the second best does, as illustrated in Figure 3.3. For this case, the use of a self-loop does not allow to reduce the upstream pressure, but actually a higher pressure is needed in the case of the configuration including a self-loop. At this high purity-recovery conditions, no configuration with an upstream pressure lower than 7.28 bar was found, indicating the possible unfeasibility of the separation at lower pressures. Since the use of the recycle also increases the N_2 content, a higher upstream pressure is needed to reach the purity constraint at a 99% recovery for the configuration with the self-loop unlike for the case at 95% recovery. Because of this higher pressure the overall separation cost is higher. Other consequence of the higher pressure is the lower membrane surface even with a self-loop. This reduction in membrane surface is not enough to compensate the effect of the higher pressure on the costs because of its lower contribution to the final costs. This illustrates both the complex interaction between operation variables and the final recovery and purity targets, and the utility of a superstructure-based approach to screen and optimize multiple process configurations that would demand more effort compared to a classical process design methodology.

Separation cost quickly increases for the two-stage configurations as purity-recovery constraints become more demanding. Lower separation costs can be obtained in some cases by processes with higher number of membranes as presented in the following section.

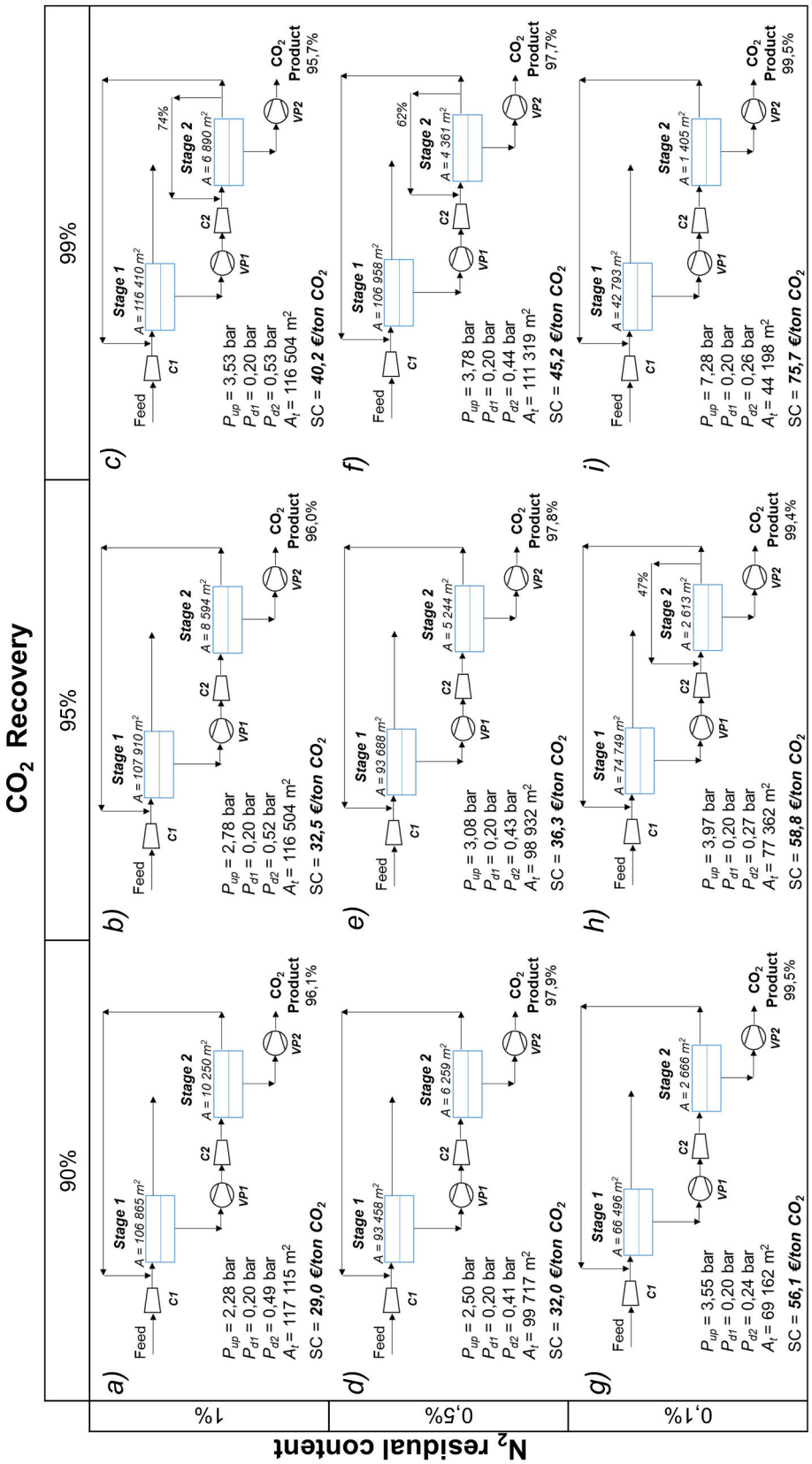

Figure 3.1: Best configurations when maximum number of stages is set to two. CO_2 recovery is set at 90, 95 and 99% while residual N_2 content is set at 0.1, 0.5 and 1%.

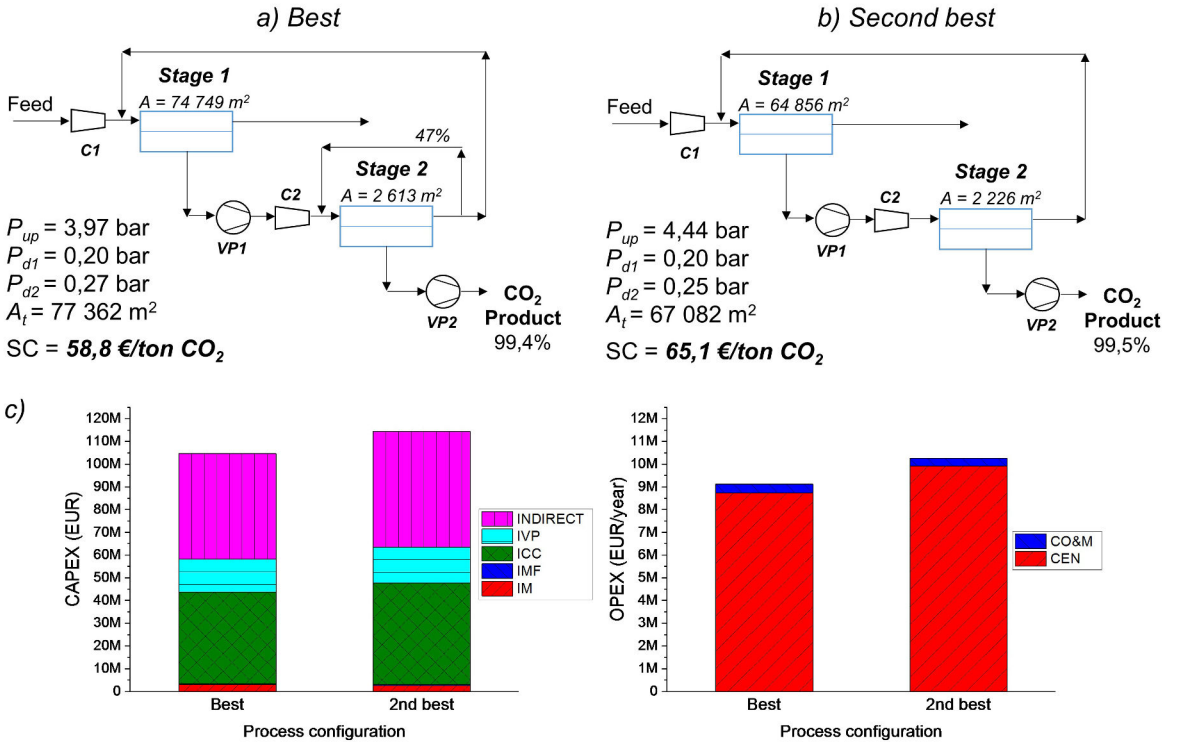

Figure 3.2: Best (a), second best (b) process configurations, and CAPEX and OPEX (c) when the number of membranes stages is set to two and separation constraints are 95% CO_2 recovery and 0.1 %N_2 content.

3.3.2 Mapping of three stage configurations

Figure 3.4 presents resulting process configurations when the number of membrane stages is fixed to three. Separation costs for the process configurations with three fixed membranes stages vary from 28.9 to 45.1 EUR/ton CO_2 depending on the recovery-purity constraints imposed. Decreasing N_2 residual content of the CO_2 product stream at constant recovery increases the separation cost when going from 1% to 0.1% N_2 albeit the increase is much less important than for the process configurations with two membrane stages, ∼1.1 to ∼1.3 times versus the ∼1.8-1.9 increase noted in the previous section. Increasing the recovery at constant product purity has a less pronounced effect as was seen for two stage processes, and separation cost increases ∼1.2 to ∼1.4 times for the 1, 0.5 and 0.1% residual N_2 levels, close to the increase noted for two stage processes. CO_2 product purity is somewhat lower than the purities obtained for the two stage processes especially for the configurations at 0.1% N_2 residual content, 98.3 to 98.7% vs. a more stable value of 99.5% for configurations with two stages.

Because the additional membrane stage allows for more interconnection possibilities, different process configurations are now possible compared to processes with only two

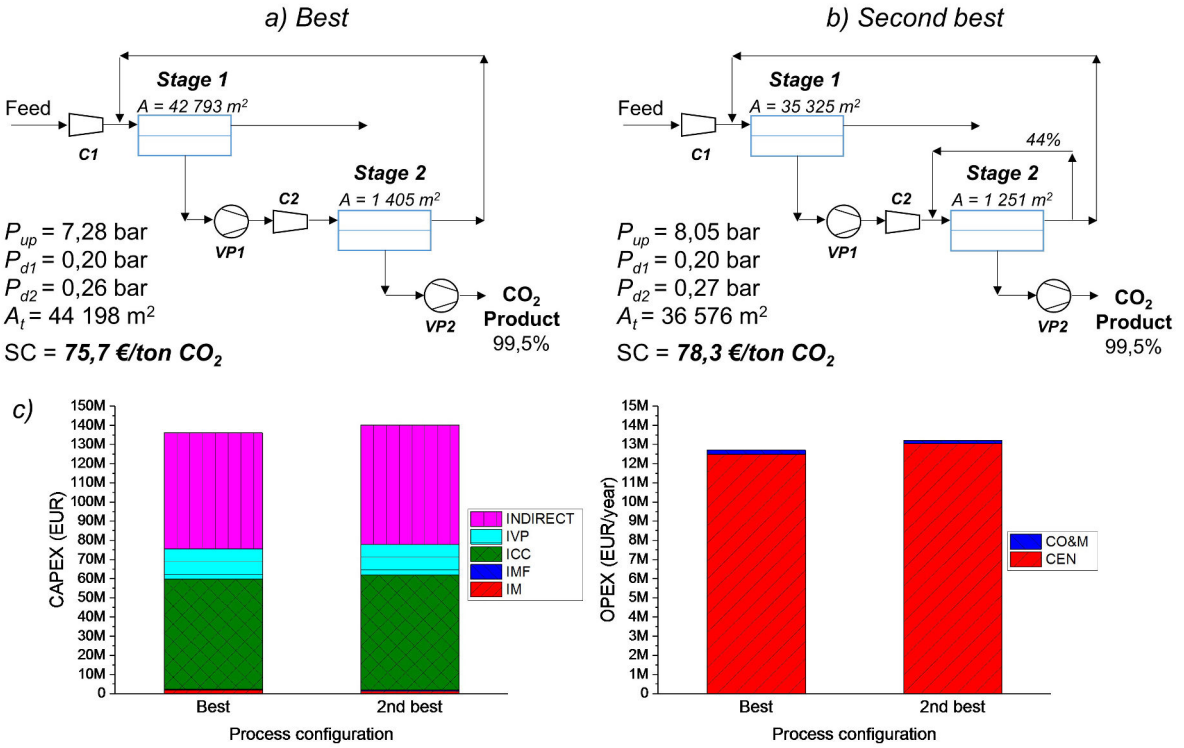

Figure 3.3: Best (a), second best (b) process configurations, and CAPEX and OPEX (c) when the number of membranes stages is set to two and separation constraints are 99% CO_2 recovery and 0.1 %N_2 content.

stages. Resulting configurations presented in Figure 3.4 can be grouped in three general configurations: a two stage cascade where the retentate of the second stage is sent to a third stage, comprising configurations a), b) and d); a two stage cascade where the retentate of the first stage is sent to a third stage, comprising configurations e), c) and f); a three stage cascade, comprising configurations g), h) and i).

The first configuration, in which the additional stage is applied on the retentate stream from the second stage, seems to be the optimal approach at "low" separation constraints, i.e. 1-0.5% N_2 at 90% recovery and 1% N_2 up to 95% recovery. However, separation costs are basically the same as for the two stage processes, indicating the sufficiency of two stage processes for separations under these conditions. For this configuration the full recycle towards the first stage is done from the third stage instead of the second. A ∼50% self-recycle of the retentate of the second stage is performed for cases a) and b), and the CO_2 product stream is obtained on both the permeates of stages 2 and 3. For configuration d) however, no self-recycling is performed and the CO_2 product is obtained from the permeate of the second stage only, since the permeate of the third stage is sent to feed the second stage.

The second configuration, in which the additional stage is applied on the retentate of the first stage, seems to be optimal for "intermediate" separation constraints, i.e. between

1-0.5% N_2 at 99% recovery and 0.5% N_2 at 95% recovery. Separation costs are lower than for two stage processes, from 3 to 11%. The retentate stream from the third stage exits the system while the permeate stream is fully recycled to the first stage, and the CO_2 product is always obtained in the permeate of the second stage.

The third configuration, the three stage cascade, seems to be the optimal for "high" separation constraints, i.e. 90-99% recovery and 0.1% N_2. Separation costs are noticeably lower than for two stage processes, 37 to 41% lower. Suboptimal solutions, i.e. more expensive, for these separation conditions included the use of self-loops and the use of the second and third configurations and some of their variations. This seems to indicate that the most cost effective process configuration for high-purity separations is the three stage cascade. The interest of four-stage processes is presented next.

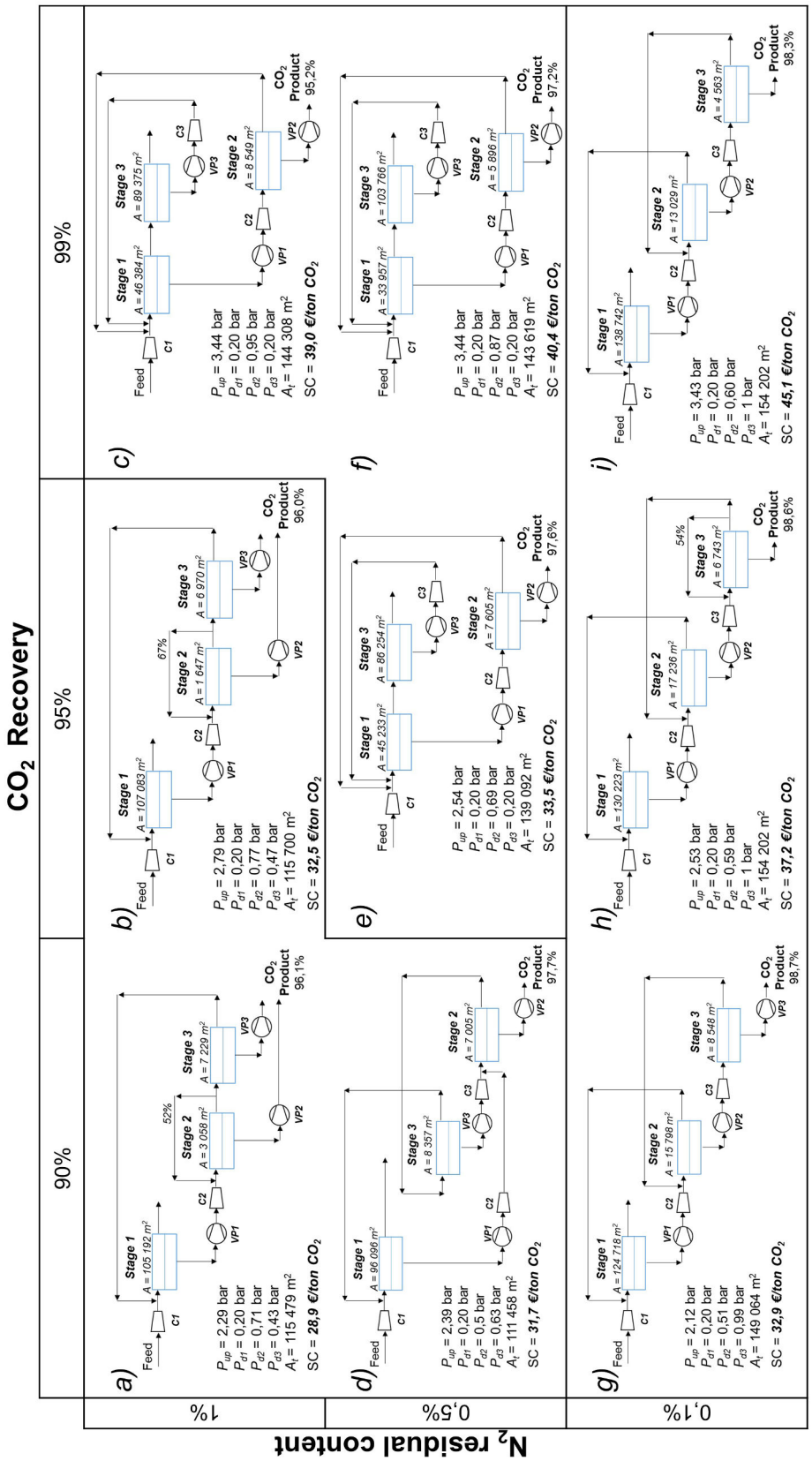

Figure 3.4: Best configurations when maximum number of stages is set to three. CO_2 recovery is set at 90, 95 and 99% while residual N_2 content is set at 0.1, 0.5 and 1%.

3.3.3 Mapping of four stage configurations

Process configurations when the number of membrane stages is fixed to four are presented in Figure 3.5. Separation costs vary from 28.9 to 45.4 EUR/ton CO_2 depending on the recovery-purity constraints imposed. In all cases separation cost is quite close to the corresponding three stage configurations from Figure 3.4. The effect of increasing the recovery-purity constraints on final separation cost, and the CO_2 product purity are also of the same order than for three stage configurations.

At four membrane stages even more interconnections are possible and many process configurations resulted from the optimization procedure. The classification of the configurations from Figure 3.5 into general configurations becomes more difficult. Five general configurations could be defined based on two and three cascades configurations as follows: A two stage cascade in which the retentate streams of both stages are sent independently to a third and fourth stages, comprising configurations a), d) and e); A two stage cascade in which the retentate of the second stage is sent to a third and four stages in series, comprising configuration b); A two stage cascade in which the retentate stream from the first stage is sent to a third and fourth stages in series, comprising configurations c) and f); A three stage cascade in which the retentate from the third stage is sent to a fourth stage, comprising configurations g) and h); And a three stage cascade in which the retentate from the first stage is sent to a fourth stage, comprising configuration i). The small recycle of 1% in configuration f) suggests that it can be probably ignored in this case which leads to the same configuration as in c). It is interesting to note that process configurations with four membranes stages follow the general cascade configurations obtained for processes at two and three stages. For N_2 concentrations above 0.1%, configurations are based on two stage cascades, while for a 0.1% concentration resulting configurations are based on three stage cascades.

3.3.4 Overall comparison of up to four stage configurations

The similarity of the separation cost between three and four stages processes along with the added complexity of the latter, indicate that for the separation scenarios presented in this work, there is no benefit for processes with more than three stages. This is the reason why Figure 3.6, presenting the optimal process configurations considering all the configurations at two, three and four stages, does not include any four stage configuration. Separation cost for four stage processes is lower than two or three stage process alternatives only for cases d) and h) in Figure 3.5, however the difference is inferior to 1 EUR/ton CO_2 which as explained above is not deemed to account for the multiple issues arising from a more complex configuration specially when considering more realistic scenarios where start up, operation, pressure drop and other real-life considerations escalate with the number of membrane stages. This is the same reasoning leading to select the two stage processes instead of the three stage alternatives for cases c) and d) in Figure 3.6.

Figure 3.7 illustrates the separation cost of the optimal configurations presented in Fig-

ures 3.1, 3.4 and 3.5 as a function of CO_2 purity for different recovery constraints. The cost reduction offered by three stage configurations increases for higher recoveries but the reduction is less dramatic than for higher purities i.e. CO_2 product streams with lower N_2 residual contents. All the configurations presented allow to reach the N_2 residual contents imposed as constraints during the optimization, however CO_2 concentration is higher for two stage configurations since more CO and H_2 are present in the product as the number of separation stages increases. This is not an issue under the chemical valorization scenario considered here, however for other applications such as CO_2 sequestration this is a limitation and optimization in that case should include a CO_2 purity constraint instead of the N_2 content used in this study.

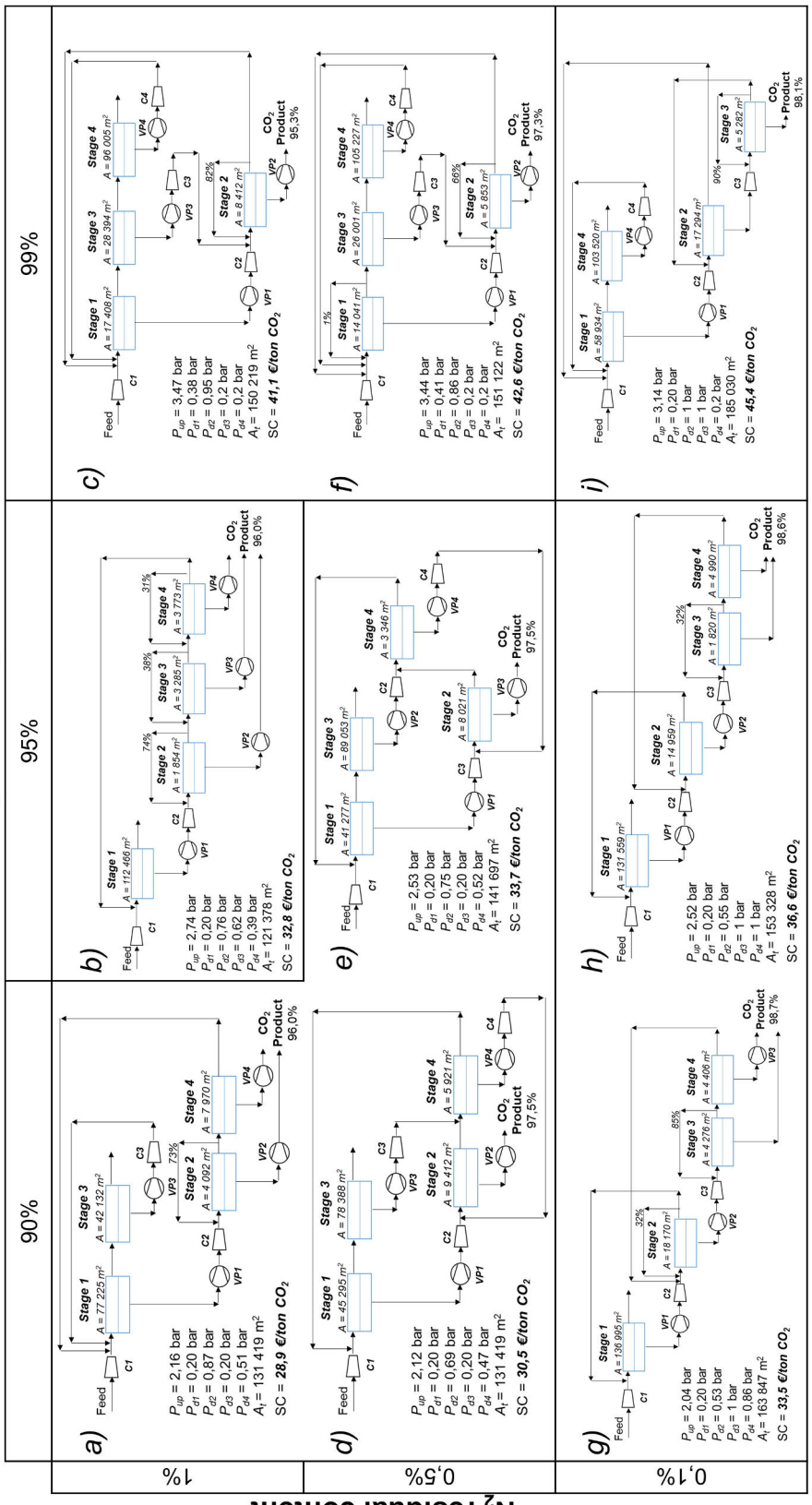

Figure 3.5: Best configurations when maximum number of stages is set to four. CO_2 recovery is set at 90, 95 and 99% while residual N_2 content is set at 0.1, 0.5 and 1%.

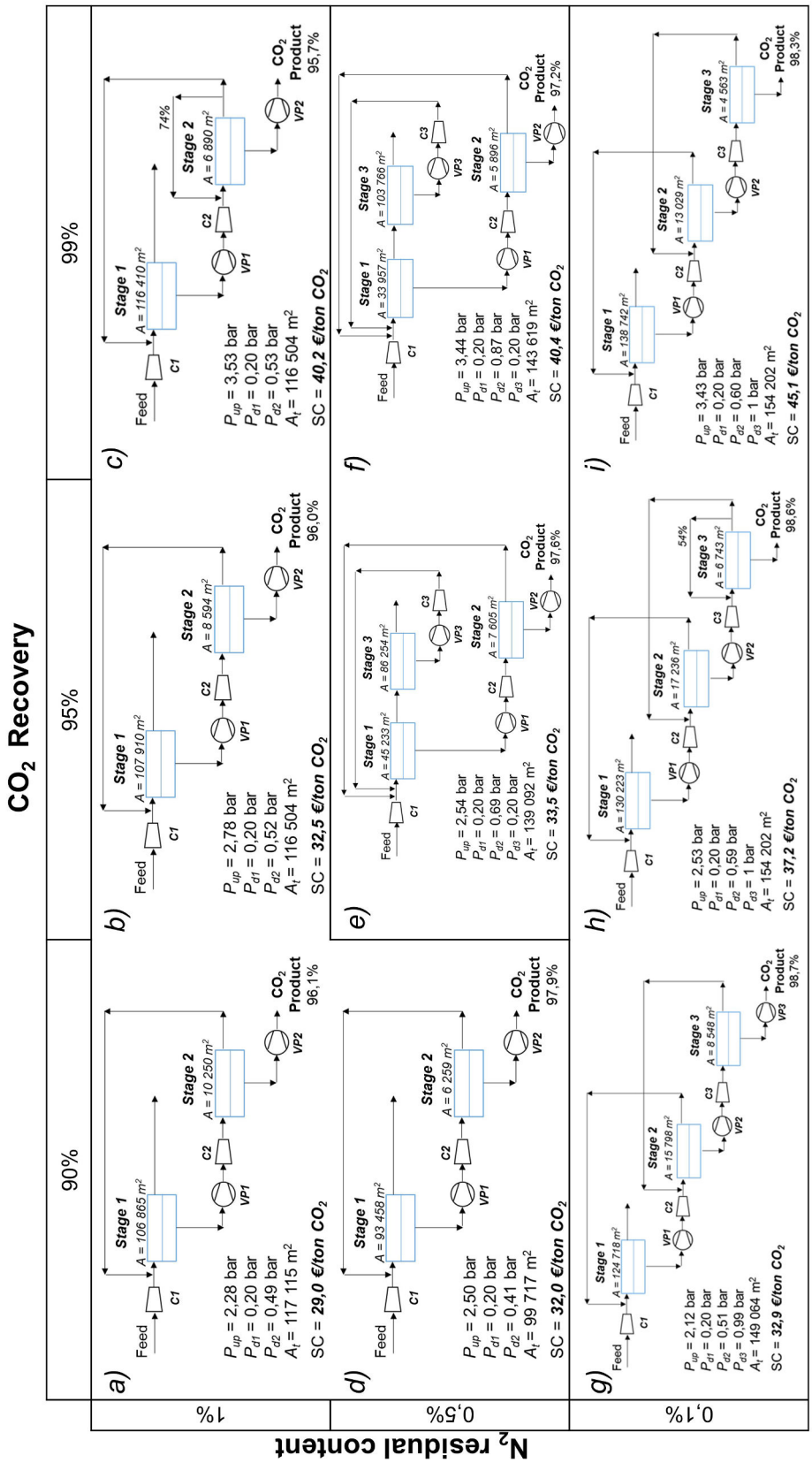

Figure 3.6: Overall best configurations when among processes with up to four membrane stages. CO_2 recovery is set at 90, 95 and 99% while residual N_2 content is set at 0.1, 0.5 and 1%.

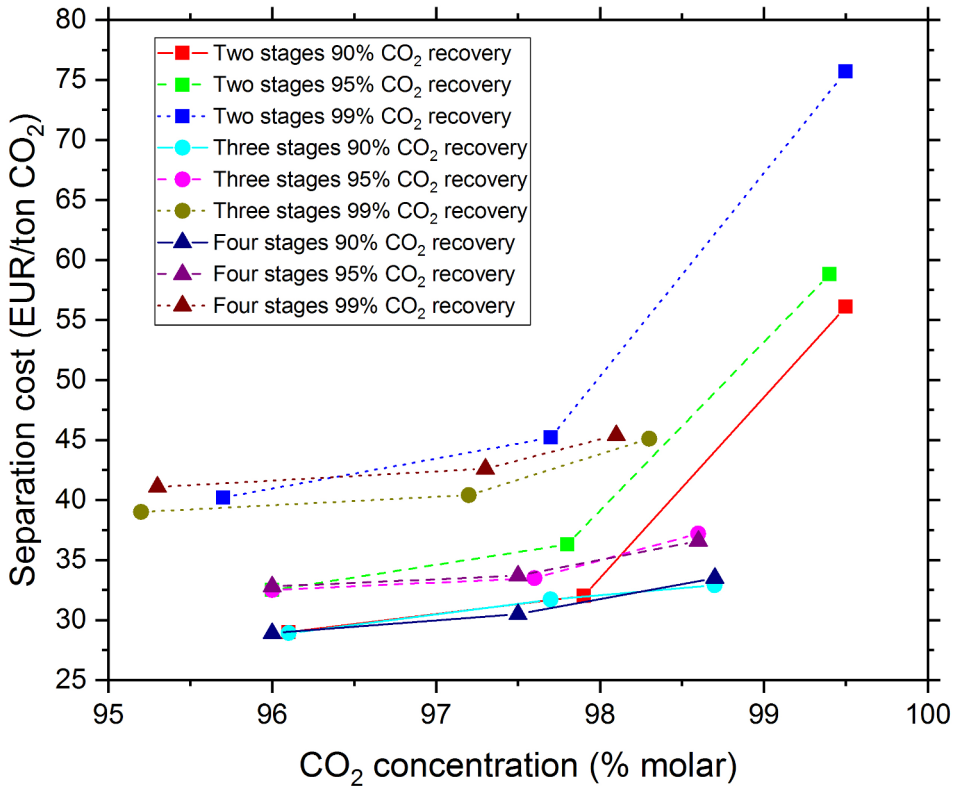

Figure 3.7: Separation cost vs CO_2 product purity for the optimal configurations with two, three and four stages. Data from left to right on each series correspond to N_2 residual contents of 1%, 0.5% and 0.1% respectively. Straight lines are drawn between adjacent data for illustration purposes.

3.4 Sensitivity analysis of the process

The effect of imposing a uniform pressure ratio and lower values in the membrane permeance and CO_2 selectivity during the optimization procedure was evaluated for the production of a CO_2 product respecting a 99% recovery and 0.1% N_2 concentration. The uniform pressure ratio was achieved by using a uniform downstream pressure for all the membrane stages. So, upstream and downstream pressures are the same for all membrane stages. Resulting configurations are compared to the optimal case which corresponds to the three stage cascade presented in Figure 3.6 (i), for which a separation cost of 45.1 EUR/ton CO_2 was calculated.

3.4.1 Effect of uniform pressure ratio

The results of performing the process optimization under an uniform pressure ratio for all membrane stages on process configuration and separation cost is presented in Figure 3.8. The lowest separation cost possible was 51.3 EUR/ton CO_2, 13.7% higher than for the optimal case obtained considering variable pressure ratios. This corresponds to the configuration presented in Figure 3.8 a). It can be seen that the optimal process configuration suggested by the algorithm is no longer a three stage cascade but a two stage cascade where the third module is applied on the retentate from the first stage. Compared with the optimal case obtained with variable pressure ratios, a slightly lower upstream pressure is required, 3.25 vs. 3.43 bar, but the total membrane surface is higher, at 170 155 vs. 154 202 m^2. The second best configuration suggested by the algorithm corresponds to a three stage cascade as presented in Figure 3.8 b). Here similarly to case a), a lower upstream pressure of 3.07 bar is applied along with a higher total membrane surface of 191 474 m^2. In both a) and b) the highest vacuum allowed by the algorithm was applied (0.2 bar) leading to an increase of capital and energy expenditures related to vacuum operation. This and the increase in membrane related costs exceeded the small decrease in compression related costs product of the reduction in upstream membrane pressure, resulting in higher separation costs than the reference case with variable independent downstream pressure as shown in 3.8 c).

This illustrates the ability to design more cost-effective separation configurations when considering non-uniform pressure ratios. In the reference case, the highest vacuum is applied on the first stage, 0.2 bar, a higher downstream pressure of 0.6 bar is used on the second and no vacuum is used on the third and final stage. When considering the uniform pressure ratio, there is no longer the possibility to distribute more efficiently the driving force among the stages, which resulted in higher costs and the use of the highest vacuum levels in all stages increasing the energy consumption of the separation.

3.4.2 Effect of decrease in membrane permeance

The results of performing the process optimization considering a membrane with half the gas permeances from Table 3.1 on process configuration and separation cost is presented in Figure 3.9. Membrane selectivity remains unchanged, and only permeance is reduced. The lowest separation cost in this case was 49.7 EUR/ton CO_2, 10.2% higher than for the optimal case obtained considering pure-gas permeances. Process configuration is still a three stage cascade compared to the reference case with the ideal permeances, however upstream pressure, downstream pressure for the second stage and membrane surface for all stages are higher in comparison. The main responsible for the increase in separation cost are membrane related costs because of the reduction in permeance. The optimal configuration in this case operates at a higher upstream pressure which is interesting since this typically leads to a net increase in separation costs. Here; however, this increase helps to lower the additional membrane surface required to achieve the separation

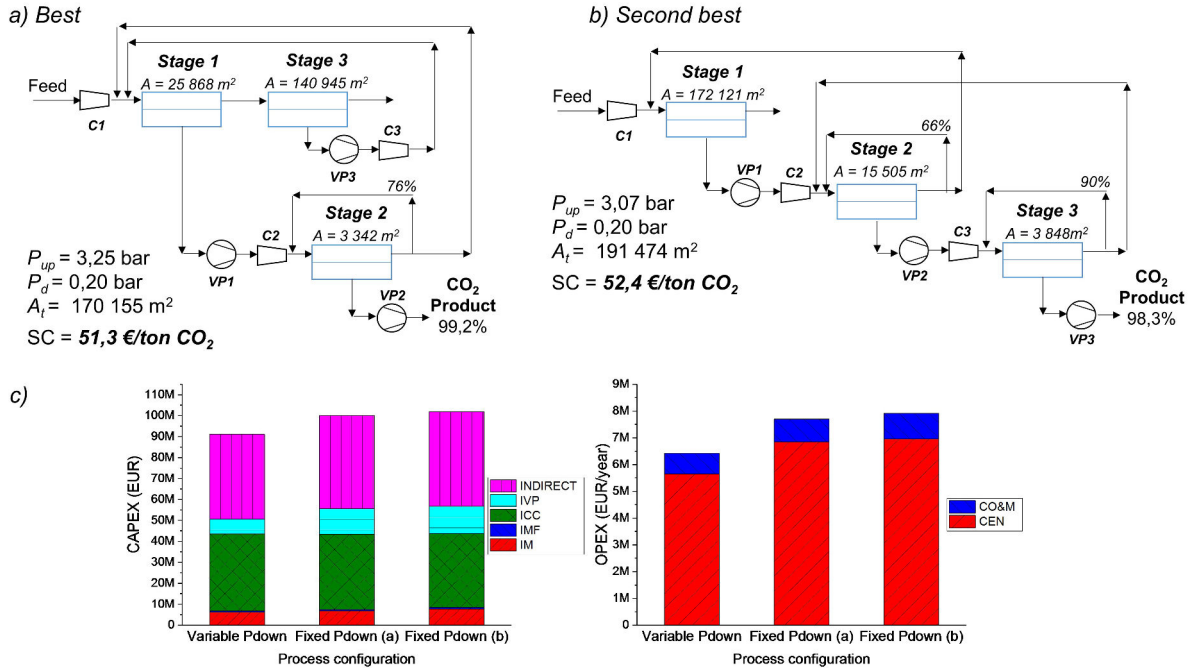

Figure 3.8: Effect of imposing an uniform pressure ratio on all stages on process configuration and separation cost. Best (a) and second best (b) process configurations, and CAPEX and OPEX (c) of the configurations compared to the reference case with independent pressure ratio for each stage. The number of membranes stages is set to three and separation constraints are 99% CO_2 recovery and 0.1 %N_2 content.

which is the main additional cost in the low permeance case. Sub-optimal solutions were obtained at lower upstream pressures, supporting the interest of this approach.

3.4.3 Effect of decrease in membrane selectivity

The results of performing the process optimization considering a membrane with half the CO_2 selectivity from Table 3.1 on process configuration and separation cost is presented in Figure 3.10. Only CO_2 permeance is reduced, leading to a decrease in CO_2 selectivity to all other gas components. The lowest separation cost in this case was 60.3 EUR/ton CO_2, 33.7% higher than for the optimal case obtained considering pure-gas permeances. The optimal configuration in this case is still a three stage cascade as in the reference case, albeit with the use of self-recycling in the third stage. The selectivity decrease leads to a small increase in upstream pressure, 3.93 bar vs. 3.43 bar, to the use of vacuum on the permeate side of all stages, and to an increase of total membrane surface. Energy related costs from additional compression and vacuum operation are the major responsibles for the increase in final separation cost. Suboptimal configurations included the use of higher upstream pressures and close versions of the configuration from Figure 3.10 all including one or more self recycles.

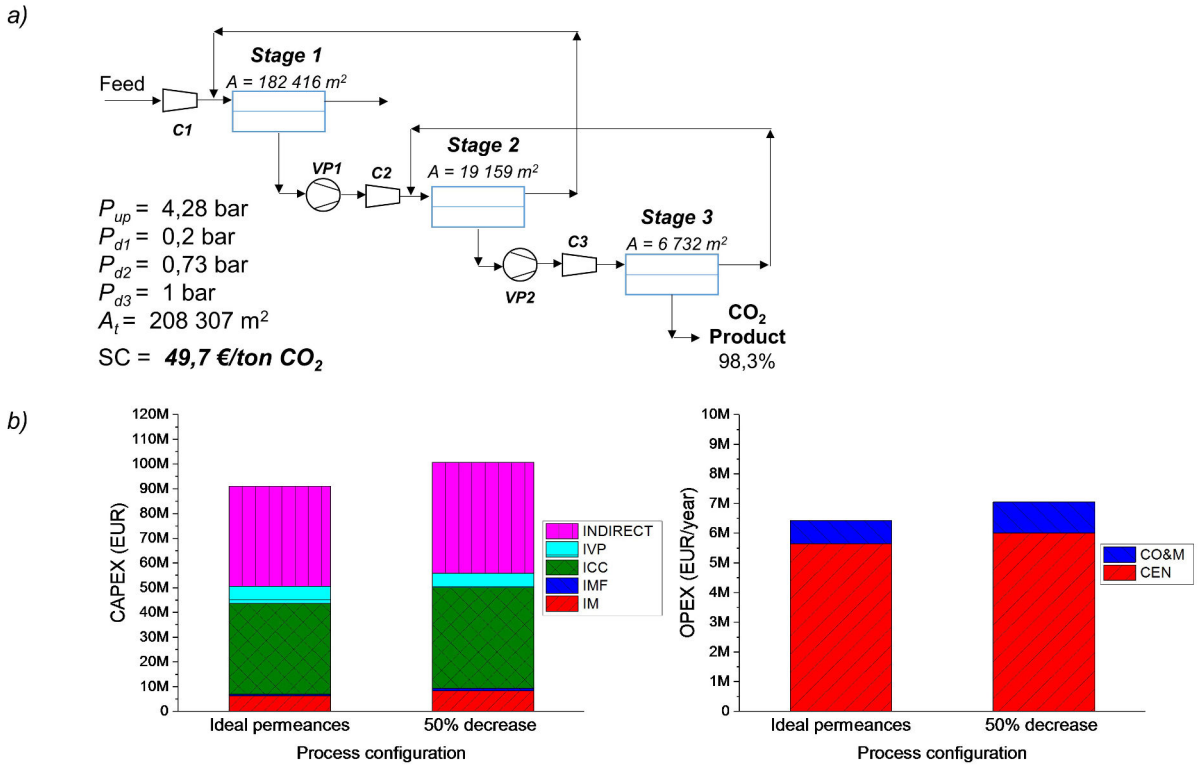

Figure 3.9: Effect of a 50% decrease in gas permeance of all components on process configuration and separation cost. Resulting process configuration (a), and CAPEX and OPEX (b) of the configuration compared to the reference case with permeances at pure gas values. The number of membranes stages is set to three and separation constraints are 99% CO_2 recovery and 0.1 %N_2 content.

3.5 Summary and conclusions

This chapter presented an application of validated global optimization approach for a Non Linear Programming (NLP) formulation based on a presented superstructure for the design and optimization of multistage membrane separation processes.

A mapping of optimal process configurations for CO_2 recovery from BFG was presented for separations including up to four membrane stages and with varying purity and recovery constraints, i.e. 90-99% CO_2 and 1-0.1% N_2 content. The optimal operation variables, upstream, downstream pressure and surface for each stage, are presented in each case. For two stage processes, two-stage cascades with full recycle of the retentate of the second stage were the optimal configuration for the conditions evaluated. Separation cost was in the range of 29 to 75.7 EUR/ton CO_2.

The use of three stage configurations allows to reduce separation cost when high recovery and/or purity is required. Separation costs in the range of 29 to 45.1 EUR/ton CO_2 were calculated in this case. For CO_2 recoveries of 95% to 99% and 0.5% N_2 content, the third stage is used to recover CO_2 from the retentate of the first stage of a two stage

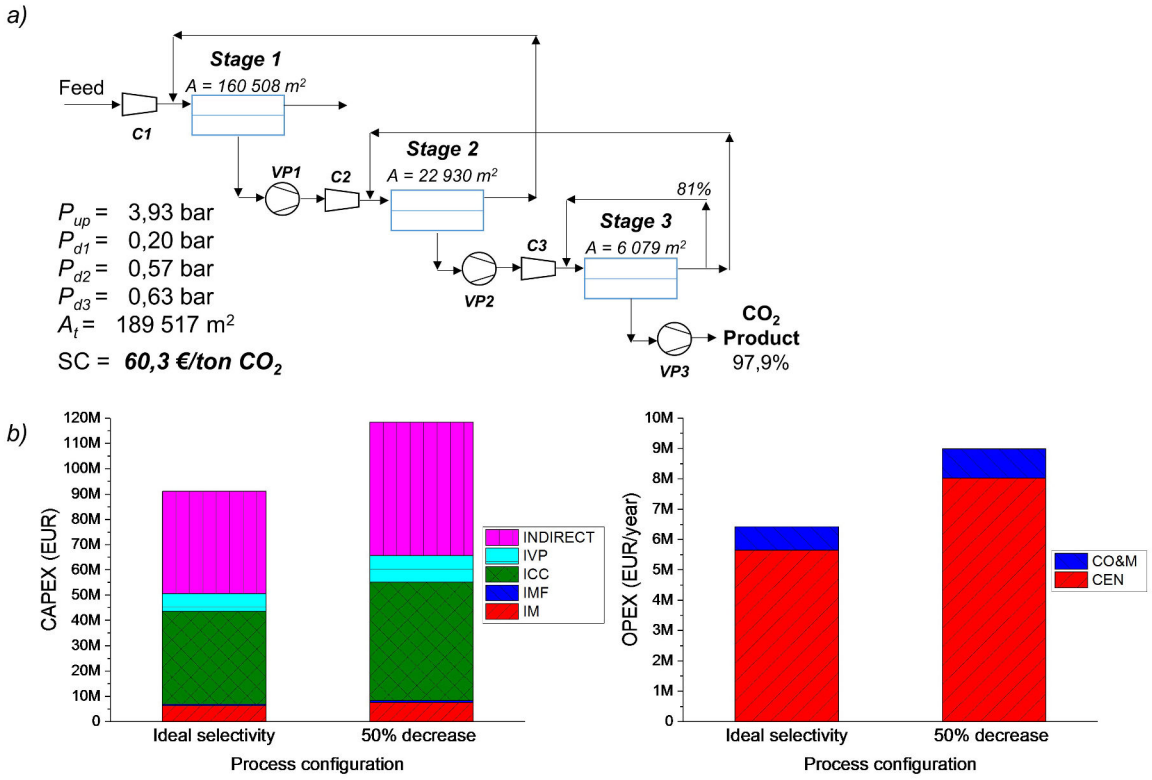

Figure 3.10: Effect of a 50% decrease in CO_2 selectivity on process configuration and separation cost. Resulting process configuration (a), and process CAPEX and OPEX (b) compared to the reference case with selectivity at pure gas value. The number of membranes stages is set to three and separation constraints are 99% CO_2 recovery and 0.1 %N_2 content.

cascade. For a 0.1% N_2 content, a three stage cascade was the preferred configuration in all the 90-99% recovery range. No marked improvements in separation cost were obtained for process configurations with four membrane stages. Small reductions of less than 1 EUR/ton CO_2 in some cases are not considered to be relevant enough to justify the increasing complexity when considering real-life operation.

The impact of process design and optimization under uniform pressure ratio for all stages was illustrated for one separation case with a CO_2 recovery of 99% and N_2 content of 0.1%. The optimization under independent pressure ratios allowed for a process with lower separation costs thanks to the possibility to distribute more efficiently the driving force among membrane stages. Furthermore, the impact of reductions in membrane permeance and selectivity that could occur under real operation conditions was explored supposing first a 50% decrease in membrane permeance of all species, and second by supposing a 50% decrease in CO_2 permeance only, to simulate a decrease in CO_2 selectivity. The 50% decrease in overall membrane permeance, caused a 10% increase in separation cost, while the 50% decrease in CO_2 selectivity caused a 34% increase. This suggests that particular efforts should be directed to ensure that membranes can retain expected selectivities under actual operation conditions. Decreases in membrane permeance only,

showed to have less of an impact in comparison for the optimal process configurations evaluated in this work. Because of the constraints emerging form the optimization approach, the cost model used in this work included only the main and most important cost elements affecting final separation cost. Care must be taken if the calculated costs are to be compared with other separation technologies since different cost parameters and additional cost elements may have been considered. The proposed configurations should be evaluated under the same cost framework as the competing technologies in such a case. In conclusion, it is important to stress the key issues of multistage membrane process optimization problems pointed out through this study. The quality of the membrane module simulation framework (i.e. no use of a simplified solution or analytical expression) and the efficiency of the global optimization algorithm obviously play a key role. The latter has been shown to offer significant improvements, as shown by the comparison to the reference case. Moreover, it is very important to generate all connections possibilities, including recycling loops and allow both the upstream and downstream pressure to vary for each stage. We notice that a large number of studies in this field do not fulfill these conditions (i.e. pressure ratio is fixed for all the stages in several studies, and no vacuum possibility is taken into account). Last but not least, the possibility to use different membranes for each stage, which is not achieved in this work, should offer interesting possibilities. This point remains largely unexplored and will be addressed in a forthcoming study.

Chapter 4

Nitrogen production from air: a process synthesis study

This chapter presents a membrane process synthesis of nitrogen production from the air by polymeric membranes. The impact of membrane performance on optimal process design while minimizing the product cost is evaluated at four different levels of N_2 purity (90, 95, 99, and 99.9%). Firstly, this effect is investigated in a process with commercial polymer membranes (PSF and PPO). In a second step membrane material is considered as a variable of the optimisation problem. Permeability and selectivity of the membrane can be chosen among the classical Robeson's trade-off representation. Two options are evaluated:

- the membrane can be freely chosen but will be the same for each membrane module of the cascade
- the membrane can be freely and independently chosen for each membrane module

Table 4.1 presents the decision variables and auxiliary equipment applied in Nitrogen Enriched Air (NEA) processes.

Table 4.1: Summary of decision variables and auxiliary equipment which are considered for optimization of NEA processes.

Industrial application	Feed compositions	Area	P_{up}	P_{down}	# of stages	PermSelectivity	Auxiliary equipment			
							C_p	Expander	V_p	Valve
N2 enrichment from air	$O_2 - N_2$	Var	Var & Uniform	Var & Ind.	up to three	Var and Ind.	✓	✗	✓	✗

4.1 A multistage system with different membrane performances

In 1991, Robeson published upper bound relations for permeabilitys/selectivity trade-off of many of gas pairs [27]. He improved his results and published new upper bound relationships for these trade-offs in 2008. Equation 4.1 demonstrates the Robeson bound correlation between permeability and selectivity of each gas pair.

$$P_i = k\ \alpha_{ij}^n \tag{4.1}$$

where P_i is the permeability of the fast gas, α_{ij} is the selectivity, k is the "front factor" and n is the slope of the log–log plot of the equation 4.1.

To the best of our knowledge, no generic method has proposed until now to achieve the optimal membrane performance (e.g. membrane permeability and selectivity) along the Robeson bound. They are often determined with test and trial method [36] for each stage along the Robeson bound. In the next section, we will explain how to adapt the mathematical optimization method (which is mentioned in 2.3) to this purpose.

4.1.1 Adapted optimization model

To obtain the optimal membrane performance in a membrane gas separation process, we increased the degree of freedom of the optimization model and considered both permeability and selectivity as decision variables. The optimal values of permeability and selectivity must satisfy the Robeson bound equation 4.1.

To increase the number of feasible solutions to the optimization problem, we limit the area below the Robeson bound and ignore the areas with less possibility for the optimal performances based on commercial performance values. As a consequence, the dashed area in figure 4.1 which is limited by Robeson's upper bound relationship is defined as the feasible region where the membrane performances are allowed to vary within it.

Two different cases are considered for the variable performances:

- Uniform performances variable: the solutions obtained in this case necessarily make use of the same, optimal membrane, for all the stages of the system.
- Independent performances variables: the solutions obtained in this case make use of a different optimal membrane to be selected for each stage when a multistage solution is investigated.

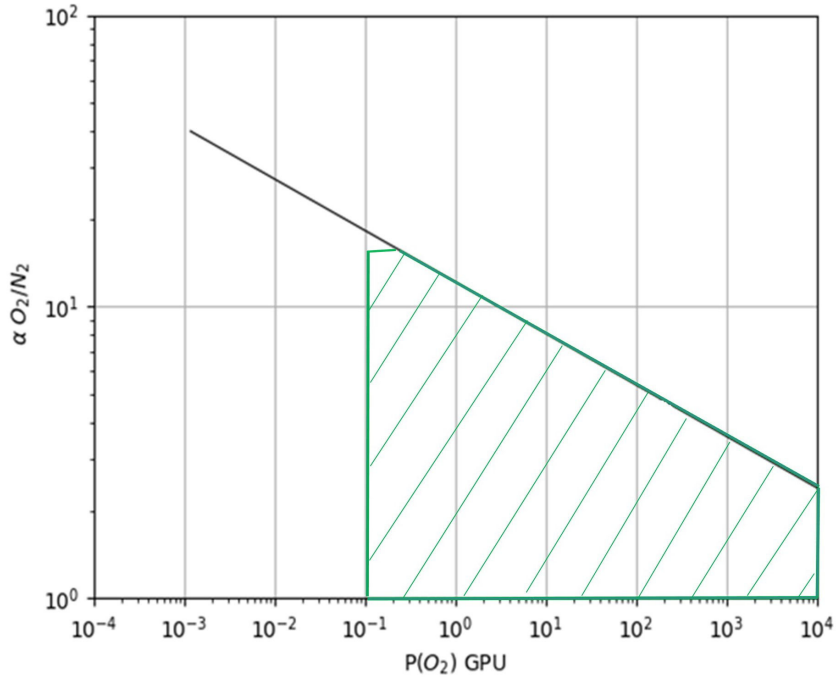

Figure 4.1: Dashed area shows the domain used for optimal membrane identification when performances are not fixed.

The optimization model is adapted by adding the following decision variables:

- $0.1 \leq \mathrm{P_{O_2}} \leq 10000$: Permeance of O_2 as fastest component[GPU]
- $0.0066 \leq \mathrm{P_{N_2}} \leq 6666.6$: Permeance of N_2 [GPU]
- $1.5 \leq \alpha \leq 15$: Selectivity

The lower and upper bound of each variable is determined based on the defined domain which is shown in figure 4.1.

Now, we describe the constraints that are added to the model for the uniform and independent case respectively.

In the case of uniform membrane performances, we have:

Robeson upper bound relationship:

$$P_{O_2} \leq k \cdot \alpha^n \tag{4.2}$$

The selectivity relation:

$$P_{O_2} \leq \alpha \cdot P_{N_2} + \epsilon \tag{4.3}$$

The relation between permeances of O_2 and N_2:

$$P_{O_2} \geq P_{N_2} + \epsilon \tag{4.4}$$

The equation 2.9 is adapted to the new mode. In case of uniform membrane performances we obtain:

$$g_{s,i}^{perm} y_{s,O_2,i}^{perm} = \frac{Acell_s}{\delta}(P_{O_2} P^{up} y_{s,O_2,i}^{ret} - P_{N_2} P_s^{down} y_{s,O_2,i}^{perm}) \quad \forall s \in \mathcal{S}, i \in \mathcal{C} \tag{4.5}$$

$$g_{s,i}^{perm} y_{s,N_2,i}^{perm} = \frac{Acell_s}{\delta}(P_{N_2} P^{up} y_{s,N_2,i}^{ret} - P_{N_2} P_s^{down} y_{s,N_2,i}^{perm}) \quad \forall s \in \mathcal{S}, i \in \mathcal{C} \tag{4.6}$$

In the case of independent membrane performances, we have:

Robeson upper bound relationship:

$$P_{s,O_2} \leq k \cdot \alpha^n \tag{4.7}$$

The selectivity relation:

$$P_{s,O_2} \leq \alpha \cdot P_{s,N_2} + \epsilon \tag{4.8}$$

The relation between permeances of O_2 and N_2:

$$P_{s,O_2} \geq P_{s,N_2} + \epsilon \tag{4.9}$$

Adapting equation 2.9 to new mode:

$$g_{s,i}^{perm} y_{s,O_2,i}^{perm} = \frac{Acell_s}{\delta}(P_{s,O_2} P^{up} y_{s,O_2,i}^{ret} - P_{s,N_2} P_s^{down} y_{s,O_2,i}^{perm}) \quad \forall s \in \mathcal{S}, i \in \mathcal{C} \tag{4.10}$$

$$g_{s,i}^{perm} y_{s,N_2,i}^{perm} = \frac{Acell_s}{\delta}(P_{s,O_2} P^{up} y_{s,N_2,i}^{ret} - P_{s,N_2} P_s^{down} y_{s,N_2,i}^{perm}) \quad \forall s \in \mathcal{S}, i \in \mathcal{C} \tag{4.11}$$

4.2 Optimal performance membrane materials

This section is presented in the form of a publication. The paper was published in the Journal of Chemical Engineering Science. This study intends to compare the performances of commercial membrane materials in air separation with optimal ones and demonstrate the importance of applying optimal performances membrane in minimizing the process cost [63].
A copy of the paper is presented in the following link:
https://www.sciencedirect.com/science/article/pii/S0009250919306013

Chemical Engineering Science 207 (2019) 1196–1213

Contents lists available at ScienceDirect

Chemical Engineering Science

journal homepage: www.elsevier.com/locate/ces

Polymeric membrane materials for nitrogen production from air: A process synthesis study

M. Bozorg [a,b,c], B. Addis [a], V. Piccialli [c], Álvaro A. Ramírez-Santos [b], C. Castel [b], I. Pinnau [d], E. Favre [b,*]

[a] Université de Lorraine, CNRS, LORIA, F-54000 Nancy, France
[b] Université de Lorraine, CNRS, LRGP, F-54000 Nancy, France
[c] Dipartimento di Ingegneria Civile e Ingegneria Informatica, Universitá degli Studi di Roma Tor Vergata, viale del Politecnico 1, 00133 Rome, Italy
[d] Advanced Membranes and Porous Materials Research Center, King Abdullah University of Science and Technology, Thuwal, Saudi Arabia

HIGHLIGHTS

- Increasing process complexity with target nitrogen purity.
- Similar design between industrial practice and process synthesis.
- Vacuum pumping generates lower costs.
- No interest to use different membranes in multistage units.
- Higher permeance better than higher selectivity.

GRAPHICAL ABSTRACT

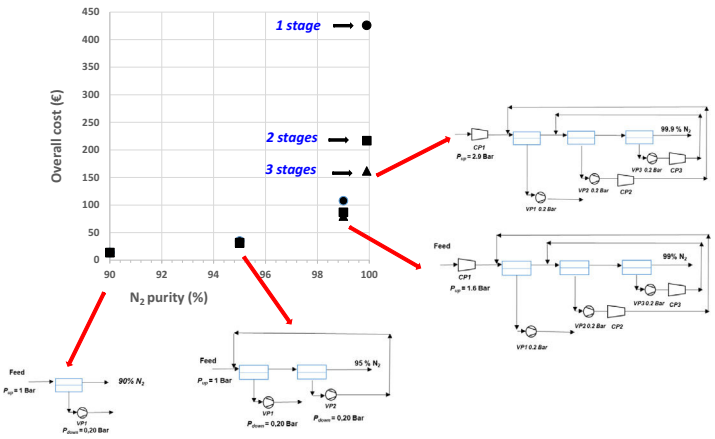

ARTICLE INFO

Article history:
Received 18 April 2019
Received in revised form 4 June 2019
Accepted 14 July 2019
Available online 16 July 2019

Keywords:
Nitrogen
Membrane
Process
Synthesis
Optimization
Materials
Cost

ABSTRACT

Nitrogen production from air by membrane gas separation processes is a mature technology which is applied in numerous industrial sectors (chemical, food, aeronautics, space..). Depending on the nitrogen purity requirements (typically between 90 and 99.9%), single stage or multistage membrane process configurations are used. A very large number of advanced membrane materials have been recently reported, showing increasing permeability and/or selectivity for air separation applications (i.e. trade-off limits of dense polymeric materials for the O_2/N_2 gas pair) compared to the commercially available membranes. The interest of these new materials in terms of nitrogen production cost and their impact in terms of process configuration are reported through a process synthesis study. Based on a tailor made optimization methodology and program, the production cost and associated optimal process configuration are first identified for two standard O_2/N_2 separation membranes at four different levels of N_2 purity (90, 95, 99, 99.9%). The same strategy is then performed with advanced trade-off membrane materials, with the possibility to combine different materials in multistaged systems. The impact in terms of nitrogen production cost for the different purities and the corresponding optimal membrane materials and process configurations are discussed. Surprisingly, a medium membrane selectivity combined to a high

* Corresponding author.
E-mail address: eric.favre@univ-lorraine.fr (E. Favre).

https://doi.org/10.1016/j.ces.2019.07.029

Nomenclature

Parameters

a	annuity coefficient for equipment [Dimensionless]
ICF	indirect cost factor [Dimensionless]
k	frontfactor of the log-log plot of the Robeson bound [Dimensionless]
K_{el}	electricity cost factor [EUR/kWh]
K_m	unit cost of membrane module [EUR/m^2]
K_{mf}	base frame cost [EUR]
K_{mr}	membrane replacement cost [EUR/m^2]
M_{N_2}	N_2 molar mass [kg/mol]
MDF_{cc}	compressor module factor [Dimensionless]
MF_{cc}	compressor material factor [Dimensionless]
n	slop of the log-log plot of the Robeson bound [Dimensionless]
R	ideal gas constant[J K^{-1} mol^{-1}]
T	temperature[K]
t_{op}	operation time per year [h/year]
UF_{2000}	update factor [Dimensionless]
γ	gas expansion coefficient [Dimensionless]
δ	thickness of the membrane layer [μm]
η	isentropic compressor efficiency [Dimensionless]
θ	stage cut of membrane separation[Dimensionless]
λ	isentropic vacuum pump efficiency [Dimensionless]
ν	membrane annual replacement rate [Dimensionless]
ϕ	mechanical efficiency [Dimensionless]

Variables

A_{m_s}	area of membrane [m^2]
A_T	total area of the membrane system [m^2]
CAPEX	capital expenditures [EUR]
C_{cap}	annual capital costs [EUR/year]
C_{en}	annual electricity cost [EUR/year]
C_{cc}	compressor cost [EUR]
$C_{O\&\ M}$	annual operation and maintenance investment cost [EUR/year]
C_{tot}	total annual costs [EUR/year]
C_{vp}	vacuum pump cost factor [EUR/kW]
F^{Ret}	system retentate flowrate [mol/s]
I_{cc_f}	feed compressor investment cost [EUR]
I_{cc_s}	membrane compressor investment cost [EUR]
I_{m_s}	membrane surface investment cost [EUR]
I_{mf_s}	membrane permanent frame investment cost [EUR]
I_{vp_s}	vacuum pump investment cost [EUR]
$M_{N_2\ per\ year}$	annual separated N_2[Tons/year]
OPEX	operational expenditures [EUR/year]
p_{d_s}	down stream pressure of membrane s[bar]
p_{up}	up stream pressure of all membranes [bar]
P_j	permeance of component j[GPU]
SC_{N_2}	specific N_2 production cost [EUR/Ton N_2]
X_j^{Ret}	fraction of component j into the system retentate [Dimensionless]
W_{cp_f}	feed compression power consumption of membrane [kW]
W_{cp_s}	permeate compression power consumption of membrane into s_1[kW]
W_{tot}	total energy consumption [kW]
W_{vp_s}	vacuum power consumption of membrane [kW]
α	selectivity [Dimensionless]

permeability is shown to systematically offer the best set of performances, for mono or multistaged systems. Vacuum operation and recycling loops are shown to generate lower N_2 production costs.

1. Introduction

Membrane processes are one of the key technologies for gas separation applications (Heinz-Wolfgang, 2008; Seider et al., 2009). Hydrogen purification, natural gas treatment, Volatile Organic Compounds recovery, gas drying are increasingly applied into different industrial sectors thanks to membrane units (Favre, 2010), but the number one market of membrane gas separations remains nitrogen production from air (Nitrogen Enriched Air, NEA) (Baker, 2009). Starting form a nitrogen content in air of approximately 79%, a membrane gas separation unit indeed enables purity levels of 90% or more to be easily obtained. A membrane process is continuous (no regeneration step), it does not involve chemicals, does not generate waste, offers intensification possibilities, it is modular (ease of scale up) and does not imply complex operations (such as cycles) (Henis, 1994). These arguments are of major interest for on board systems (e.g. boats, planes, space applications). But membrane units are also used for large capacity industrial applications, such as blanketing for explosive environments (hydrocarbons and solvent storage), or generation of inert atmospheres (e.g. non oxidizing) for chemicals or materials production, among others (Heinz-Wolfgang, 2008). Nitrogen production by membranes is also favorable because the target compound is less permeable than the air compounds to be eliminated (O_2, H_2O, CO_2). As a consequence, a purified stream of nitrogen can be continuously produced on the retentate (i.e. high pressure) side. In a large number of situations, no additional purification or recompression step are needed.

Generally speaking, membrane processes are more interesting for moderate purity, and low to moderate capacity N_2 applications (Prasad et al., 1994). Cryogeny is the best available technology for high purity (e.g. >99.99%) high capacity (e.g. >200 ton per day) units. Adsorption processes are favored for intermediate purity and capacity (Castle, 2002). The improvements in membrane materials and process designs have enlarged the domain of application of membranes through the years. Commercial membrane materials remain almost exclusively based on dense polymers, which should ideally combine a high selectivity and high permeability (Spillman, 1989). Hundreds of structures have been investigated in order to maximize these two characteristics (Mahajan and Koros, 2000; Thomas et al., 2009; Park et al., 2017) but a trade-off limit, based on a concept suggested by Robeson (2008), exists between the two. Few membrane materials for nitrogen production applications are commercially available today (i.e. polysulfones, polyimides, polyphenylene oxide) (Baker, 2009). The level of performances of these materials is below the trade-off limits and the interest of advanced materials, with performances close to the trade-off limit, in terms of N_2 production cost, is logically a key question. To our knowledge, no study addressed so far the rigorous analysis of the impact of advanced membrane materials for

nitrogen production. Such a piece of work should ideally combine a large choice of membrane materials together with modern process design tools, in order to identify the most promising production strategies.

In this study, the production cost of NEA with inlet flowrate of 10 mol/s for four different levels of purity is analyzed (90, 95, 99, and 99.9%). In a first step, the minimal cost and optimal process configuration with currently commercially available membrane materials is identified thanks to a tailor made process synthesis package, recently developed for carbon capture applications (Ramírez-Santos et al., 2018). The optimal structure (number of stages, compression or vacuum operation, multistage configuration) and the associated nitrogen production costs are thus obtained and will correspond to the reference case. In a second step, the possibilities of advanced trade-off materials are explored thanks to a novel, generic approach: the minimal production cost for a given nitrogen purity is identified based on systematic screening of trade-off membrane performances and process configurations (including compression, vacuum pumping and recycling loops), with two options: same optimal trade-off membrane used for all membrane stages or possibility to use a different trade-off membrane material in each membrane stage.

The objectives of the study are to provide an answer to the following questions:

- How does nitrogen purity impact process configuration and cost with currently commercially available membranes?
- What are the best process configurations and the associated costs with advanced membrane materials (i.e. trade-off limit performances)?
- What is the best membrane material for each nitrogen purity level within the trade-off limits (i.e. high selectivity or high permeability)?
- Is there an interest to combine different membrane materials into multistaged units for nitrogen production?

This set of results is expected to provide clear guidelines for air separation membrane developments and also help to better evaluate the interplay between materials performances, process design and production cost.

2. Process synthesis methodology applied to membrane gas separations and NEA production

2.1. Process synthesis and membrane gas separations: overall methodology

The optimal process designs detailed hereafter are obtained by means of a tailor made computer program specifically designed for membrane gas separations. Starting from separation specifications (feed composition, permeate and/or retentate composition), the optimal process flow-sheet and the associated operating conditions are identified thanks to a global optimization algorithm with an objective cost function. The overall process synthesis framework is summarized in Fig. 1.

The program makes use of a rigorous set of equations for membrane module simulation, extendable to multi-component mixtures (Bounaceur et al., 2017). All the possibilities of connections are explored for a system with one, two or three stages, including recycling loops from one stage to another or self recycling loops.

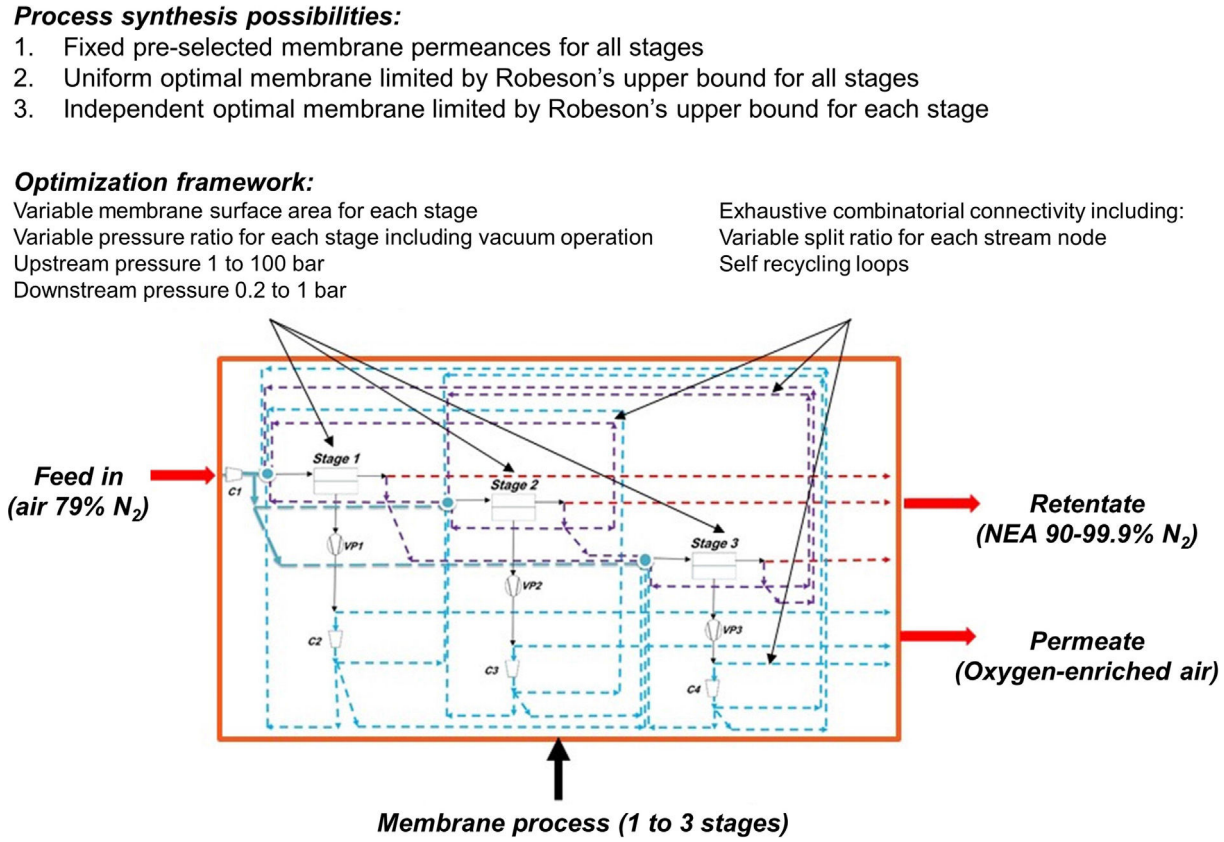

Fig. 1. Overall process synthesis framework used for this study. A membrane separation process including up to 3 stages with compressors and/or vacuum pumps and multiple connection possibilities including recycling loops is applied to nitrogen production from air with four different target purities. The different configuration possibilities and operating variables are taken into account in order to achieve the lowest production cost (i.e. objective function, detailed in Tables 1 and 2).

One specificity of the program, compared to most of the approaches in this domain, is to allow a variable pressure ratio in each stage with vacuum pumping as one possibility. A given range is applied to the operating conditions, in order to take into account technological limitations (typically upstream pressure is limited to 100 bar and vacuum limited to 0.2 bar). Compressors or vacuum pumps are included in the recycling loops when pressure changes exist at the boundaries of the connection. The overall cost function, taken as the objective function, takes into account capital expenses (CAPEX) such as compressors, vacuum pumps, membrane modules and operating costs (OPEX), such as energy requirement, membrane replacement and operation and maintenance cost. The cost function used for NEA production is detailed in Table 1. The detailed mathematical framework and associated optimization strategy can be found in Ramírez-Santos et al. (2018).

It is important to stress that the cost parameters and cost function listed in Tables 1 and 2 can vary from one study to the other. More precisely, membrane cost, membrane lifetime and the Indirect Cost Factor (ICF) can effectively differ among membrane processes technico-economical studies. For instance, membrane costs can range from 20 to 200 EUR per square meter, and membrane lifetime from 5 to 10 years. Separation cost used in this study is based on a model used in a previous work, following NETL guidelines (Ramírez-Santos et al., 2018). Capital cost includes membrane area and membrane frame, compressors and vacuum pumps. Heat exchangers represent a relatively small part of total final costs and are not considered here for simplification purposes. Total capital investment (CAPEX) is calculated from the investment cost of the equipment supposing an indirect cost factor of 80 percent. Operational costs include electricity costs related to compression and vacuum equipment, membrane replacement, and operation and maintenance cost. Operation and maintenance costs have been simplified and are estimated at 3 percent of capital expenditures plus membrane replacement costs. Membrane replacement costs have been set at 25 EUR/m^2, a more conservative value than the 10 EUR/m^2 used in a previous work and closer to the 40 EUR/m^2 used for capital cost estimation. Only one annualization factor is used for all equipment including membranes. The annualization factor was calculated considering a period of 23 years and an interest rate of 7.4 percent. Total annual costs are divided per unit of product NEA per year to express final specific separation costs. For membrane gas separation processes, the impact of membrane cost and membrane lifetime is limited, due to the fact that capital cost is largely dominated by compressor cost (Prasad et al., 1994; Baker, 2009). It will be shown afterwards that the nitrogen market production cost by commercial membranes is correctly estimated thanks to the cost function detailed in Tables 1 and 2. This suggests that, even though a different cost function obviously would generate a slightly different production cost, the incidence in terms of process design and cost evaluation is limited.

Three different strategies have been used in the study:

- As a first step, membrane separation characteristics are fixed (i.e. membrane oxygen and nitrogen permeance), and the optimal process design and operating conditions is obtained for one, two and three membrane stages, for the four levels of target nitrogen purity (90, 95, 99 and 99.9%). Benchmark gas permeances for commercially available membranes are used.
- As a second step, the membrane characteristics are allowed to vary within a defined domain, limited by trade-off performances represented by Robeson's upper bound relationship and a single set of membrane permeances is allowed. As a consequence, the solutions obtained in this case necessarily make use of the same, optimal membrane, for all the stages of the system.

Table 2
Cost parameters used in Table 1.

Capital cost parameters		
C_{cc}	1×10^6	EUR_{2000}
C_{vp}	1500	EUR/kW
K_m	40	EUR/m^2
K_{mf}	286×10^3	EUR
MDF_{cc}	2.72	–
MF_{cc}	1.4	–
UF_{2000}	1.42	–
ICF	1.8	–
T	308.15	K
R	8.314	J K^{-1} mol^{-1}
η	0.85	–
ϕ	0.95	–
γ	1.36	–
λ	0.85	–
Annual cost parameters		
ν	0.2	–
K_{mr}	25	EUR/m^2
t_{op}	8322	h/year
K_{el}	0.044	EUR/kWh
a	0.0854	–
M_{N_2}	28.01	g/mol

Table 1
Cost equations used to determine product gas separation cost.

Equation		
$I_{m_s} = A_{m_s} \cdot K_m$	(1)	Membrane cost
$I_{mf_s} = (A_{m_s}/2000)^{0.7} \cdot K_{mf} \cdot (p^{up}/55)^{0.875}$	(2)	Membrane frame cost
$I_{cc_s} = C_{cc} \cdot (W_{cp_s}/10^3)^{0.7} \cdot MF_{cc} \cdot MDF_{cc} \cdot UF_{2000}$	(3)	Stage compressor cost
$I_{cc_f} = C_{cc} \cdot (W_{cp_f}/10^3)^{0.7} \cdot MF_{cc} \cdot MDF_{cc} \cdot UF_{2000}$	(4)	Feed compressor cost
$I_{vp_s} = C_{vp} \cdot (W_{vp_s})$	(5)	Vacuum pump cost
Capital expenditures		
$CAPEX = (I_{cc_f} + \sum_{s \in \mathscr{S}} (I_{m_s} + I_{mf_s} + I_{cc_s} + I_{vp_s})) \cdot ICF$	(6)	Total capital cost
Operational expenditures		
$C_{O\&M} = \sum_{s \in \mathscr{S}} A_{m_s} \cdot \nu \cdot K_{mr} + 0.03 \cdot CAPEX$	(7)	Operation and maintenance cost
$C_{en} = t_{op} \cdot W_{tot} \cdot K_{el}$	(8)	Energy cost
$OPEX = C_{en} + C_{O\&M}$	(9)	Total operational expeditures
Annual and specific separation costs		
$C_{cap} = CAPEX \cdot a$	(10)	Annual capital costs
$C_{tot} = C_{cap} + OPEX$	(11)	Total annual costs
$M_{N_2\ per\ year} = F^{Ret} \cdot X_{N_2}^{Ret} \cdot M_{N_2} \cdot 10^{-6} \cdot 3600 \cdot t_{op}$	(12)	Annual separated N_2
$SC_{N_2} = C_{tot}/M_{N_2\ per\ year}$	(13)	Specific N_2 separation cost

- As a final step, membrane permeances for each individual stage are allowed to vary within the same domain as in the previous step. This allows a different optimal membrane to be selected for each stage, when a multistage solution is investigated.

Nitrogen ranks among the top ten chemicals in terms of production capacity (ca 100 million tons per year), with a large portfolio of applications (inerting in chemical industries, food protection, steel manufacturing, light bulbs, cryopreservation) (Bounaceur et al., 2017). Production technologies systematically use air as a feedstock (i.e. 0.79 volume fraction nitrogen content). Depending on the nitrogen purity and unit capacity, cryogeny, adsorption based processes, Pressure Swing Adsorption (PSA) or membranes are used (Smith and Klosek, 2001). Membrane separations for NEA (Nitrogen Enriched Air) production correspond to the most recent production technology and compete with cryogeny and PSA when a moderate purity (typically below 99) and moderate capacity are required (Prasad et al., 1994). As already explained, Nitrogen production from air is today the biggest market of membrane gas separation processes, with more than 100,000 units installed through the world (Baker, 2009). From a membrane material point of view, dense polymers are exclusively used (Baker and Low, 2014). Oxygen, water and carbon dioxide are faster permeants than nitrogen into polymers. As a consequence, NEA is recovered dry and purified on the retentate (i.e. high pressure) outlet of the membrane modules. Different polymers have been developed for industrial scale application, with a classical selectivity/productivity trade-off to be tackled. Polysulfone (PSf), Polyimides (PI) and Poly-phenylene-oxide (PPO) dense skin membranes are commercially available (Seider et al., 2009). The two major performance characteristics of a given dense skin membrane are the separation performance, expressed through the O_2/N_2 selectivity(α^*), and the effective membrane productivity, usually expressed in GPU (Gas Permeation Unit). The selectivity/permeability trade-off curve for different polymers for the O_2/N_2 pair gas is shown on Fig. 2a. It can be noticed that oxygen is systematically faster than nitrogen (α>1). In order to translate the intrinsic polymer permeability into a process productivity variable (i.e. permeance, in GPU), a dense skin of 1 µm thickness is often assumed (Lin et al., 2013). The corresponding graph is shown on Fig. 2b (1 Barrer corresponds to 1 GPU in that case). The current level of performances of two classical commercially available air separation membranes (PSf and PPO), which will be used in this study,is indicated.

Besides the membrane material selection question, a process design analysis has also to be performed. The goal is to identify the most effective process structure and operating conditions, which reaches the specifications (nitrogen purity and production capacity) with the lowest cost. Surprisingly, this point is poorly documented in the open literature, despite the important market of nitrogen membrane production units. Fig. 3 summarizes three main configurations reported from industrial practice, which correspond to increasing levels of nitrogen purity (Prasad et al., 1994). An increasing number of membrane stages is needed when increasing the target nitrogen purity. The maximum number of stages is limited to three, because of the strong impact of multiple compressors in the overall cost (Heinz-Wolfgang, 2008; Seider et al., 2009; Baker, 2009). The increasing complexity of the process when a larger purity is aimed is noticeable (multiple stages with recycling loops). The process configurations reported on Fig. 3 correspond to the current state of the art of the most effective structures obtained with commercially available polymeric air separation membrane materials. Nevertheless, due to the very large nitrogen market, tremendous efforts have been made the last decades in order to push the limits of polymer performances. It is thus important to explore the impact of high performances membrane materials both in terms of nitrogen production costs and optimal process configurations.

2.2. NEA production: high performance materials

A series of high performance membrane materials covering a broad range of selectivity/permeability trade-off is detailed in Table 3. The different possibilities can be expressed through a generic trade-off equation, such as suggested by Robeson (2008). For the specific oxygen/nitrogen pair gas, the trade-off limit can be expressed as:

$$P_{O_2} = k\alpha^n \tag{1}$$

where $k = 1396000$ *Barrer* and $n = -5.666$.

This generic equation will be used to evaluate the interest of different high performance materials in the process synthesis study reported hereafter.

3. Results and discussion

3.1. Nitrogen production by commercially available membrane materials

In a first step, the minimal nitrogen production cost with current commercial membrane materials is explored. Two different membranes, summarized in Table 4, have been selected and the corresponding minimal production cost and optimal process configuration were evaluated. The two materials detailed in Table 4 correspond to two major families of polymers used for air separation applications. Polysulfone shows an increased selectivity, at the expense of a lower permeance. PPO shows the highest oxygen permeance, with a slightly lower selectivity. The objective of this first part of the study is to define the reference production costs and process configurations for these two membranes. The sensitivity of selectivity versus permeance, in terms of production cost and possible process configuration differences is also of interest.

The results obtained for PSF and PPO membranes are summarized Figs. 4 and 5 respectively.

Generally speaking, Figs. 4 and 5 confirm general statements and guidelines of membrane gas separation processes presented in Fig. 3:

- An increased target purity, increases the nitrogen production cost through a non linear quasi exponential dependence
- An increased nitrogen purity translates into an increasing number of stages and increasing process complexity (e.g. multiple recycling loops, combined compression and vacuum operation...).

A single stage process with no recycling loop systematically offers the best performances for 90 percent purity. Interestingly, no solution with 2 or 3 stages can be obtained by the computer program for this purity level. A series of 2 or 3 modules is generated, without recycling loop, without any recompression step; this is then equivalent to a single, segmented module. A two stage configuration with recycling loop is the best process for moderate (95 percent) nitrogen purity. Three stages, including two recycling loops, are needed for larger purity levels (99 and 99.9 percent). It is likely that nitrogen production cost is not competitive at this purity level. The competitive window for nitrogen production by membranes is effectively often mentioned to range from 90 to 99 percent (Prasad et al., 1994).

The general structures obtained through the process synthesis study perfectly fit the structures reported up to now (Fig. 3). The number of stages for the different purity levels, the number and

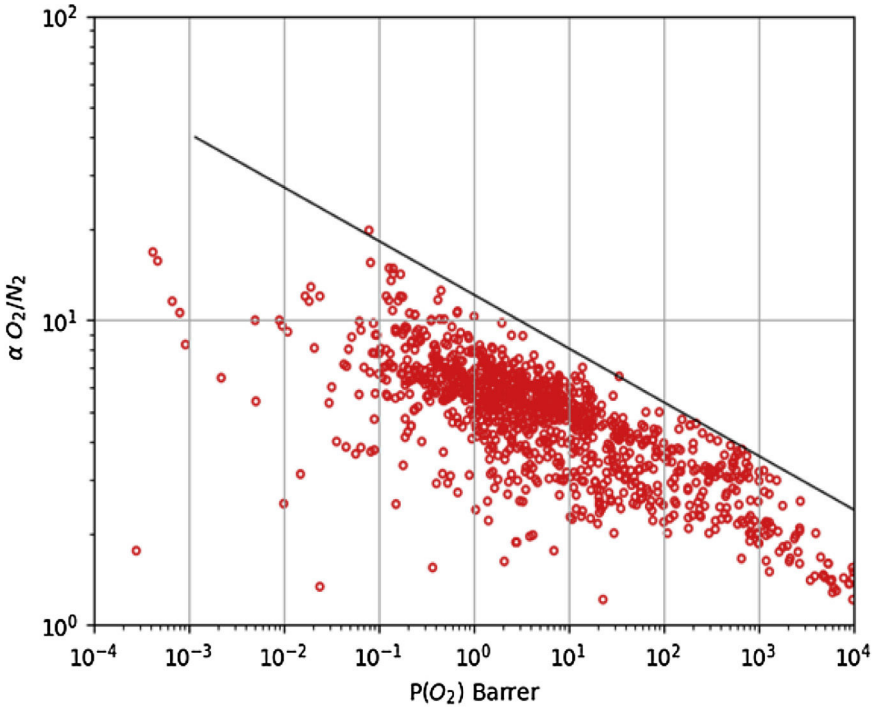

(a) O_2/N_2 polymeric materials trade-off curve [12]

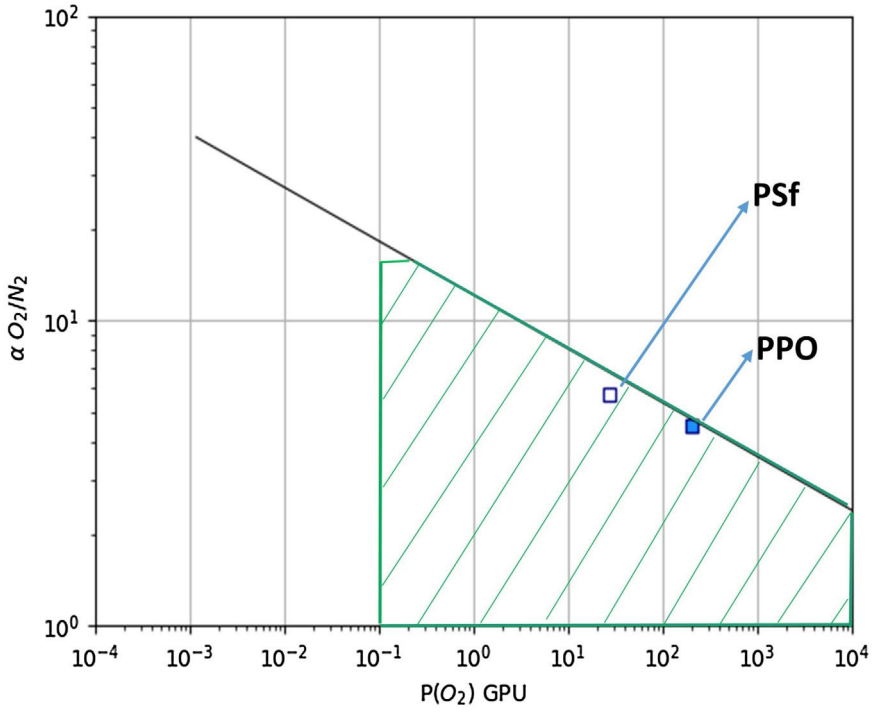

(b) Selectivity / permeance trade-off curve based on a 1 μm skin layer thickness and performances of two commercially available membrane materials (PSf and PPO). Dashed area corresponds to the domain used for optimal membrane identification when performances are not fixed

Fig. 2. Polymeric materials (a) and membrane (b) trade-off curves.

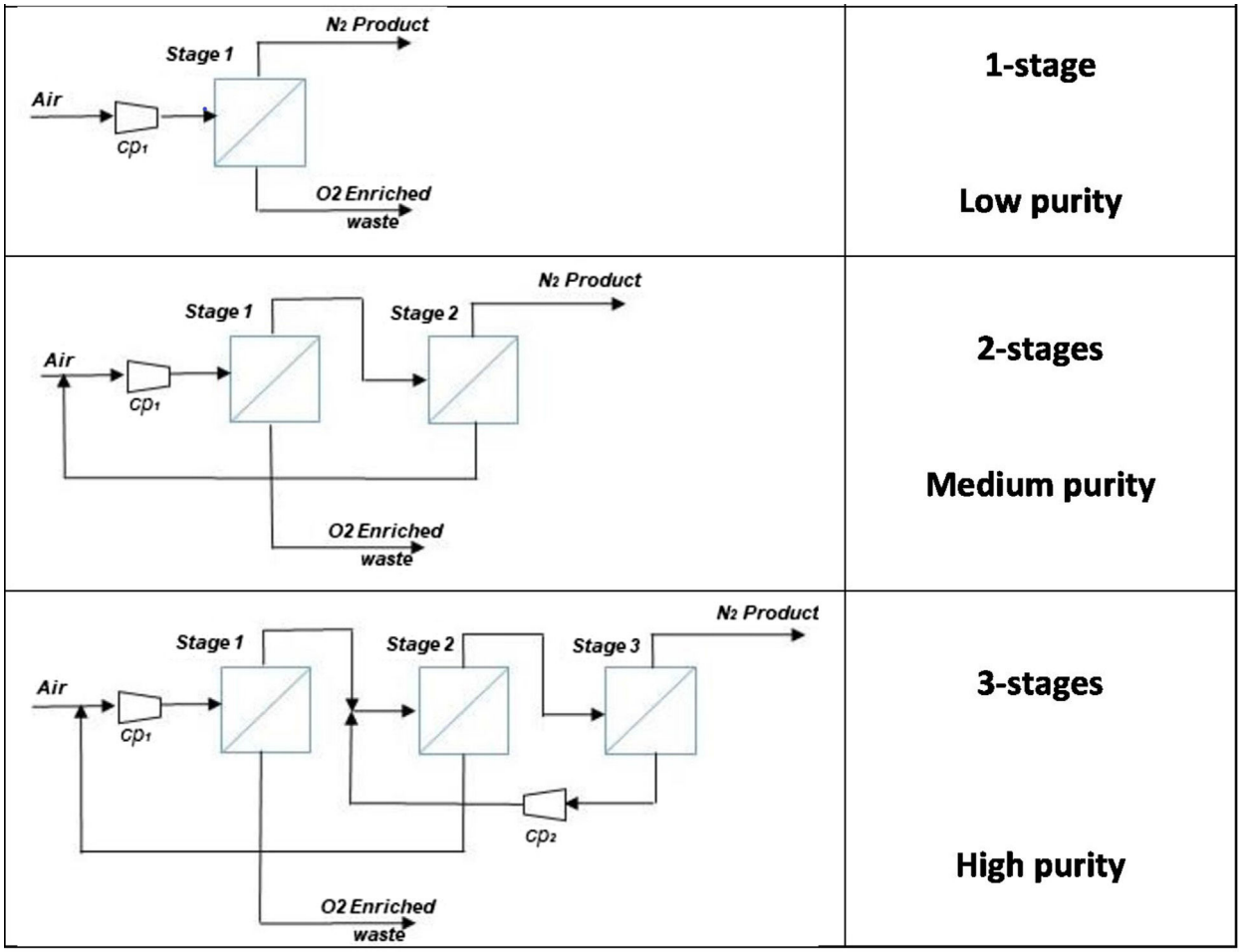

Fig. 3. Membrane process configurations for three different levels of nitrogen purity, adapted from Prasad et al. (1994).

Table 3
Examples of advanced membrane materials (not commercially available today), close to the Robeson trade-off limit, for air separation applications (from Robeson (2008)).

Polymer	Permeability O_2 (Barrer)	α O_2/N_2
Polyimide (BPDA-ODA)	0.079	19.8
Polyimide (BTDA-ODA)	0.170	14.2
Polyetherimide	0.90	11.2
Polypyrrolone (6FDA/PMDA(25/75)-TAB)	1.01	10.03
PPO sulfonated (32.9%) and brominated (60%)	12.6	7.4
PPO sulfonated (20.2%) and brominated (60%)	14.0	7.0
Polyimide (BADBSBF-BTDA)	18.0	9.0
Poly[1-phenyl-2-p-(trimethylsilyl) phenylacetylene]	1550	2.98
PIM-1	370	4.0
PIM-7	190	4.5

location of the recycling loops for multistage processes are exactly the same as the one detailed in Fig. 3. This point is remarkable and provides a good proof of the efficiency and relevance of the simulation/optimization program when applied to existing membrane materials. Moreover, a nitrogen production cost around 30 Euros per ton is obtained for a 95 percent purity, which matches the cost reported in a recent study (Schmidt and Clayton, 2013).

Furthermore, besides the confirmation of the three different process flow-sheets detailed in Figs. 4 and 5, the optimal structures and operating conditions obtained with commercial PSF and PPO membranes lead to additional insights, which are of interest:

- Vacuum operation is of major interest in order to generate the lowest production cost. This option is rarely taken into account by membrane process synthesis softwares. This operation possibility is included in our tailor made program and seems to be important for cost minimization. It has to be stressed that vacuum operation is most often discarded for industrial units, because of the large footprint of vacuum pumps, low energy efficiency and problems generated by leaks. Vacuum operation in membrane gas separations is effectively limited to VOC

Table 4
Characteristics of the two commercially available membranes used for NEA production in this work.

Polymer	O_2 permeance (GPU)	N_2 permeance (GPU)	α O_2/N_2 (–)	Reference
Polysulfone (PSF)[a]	27	4.7	5.7	Ettouney et al. (1998)
Polyphenyleneoxide (PPO)[b]	200	44	4.5	McConnell (2010)

[a] Example of membrane suppliers: AirProducts (Prism), AirLiquide.
[b] Example of membrane suppliers: Parker Hannifin.

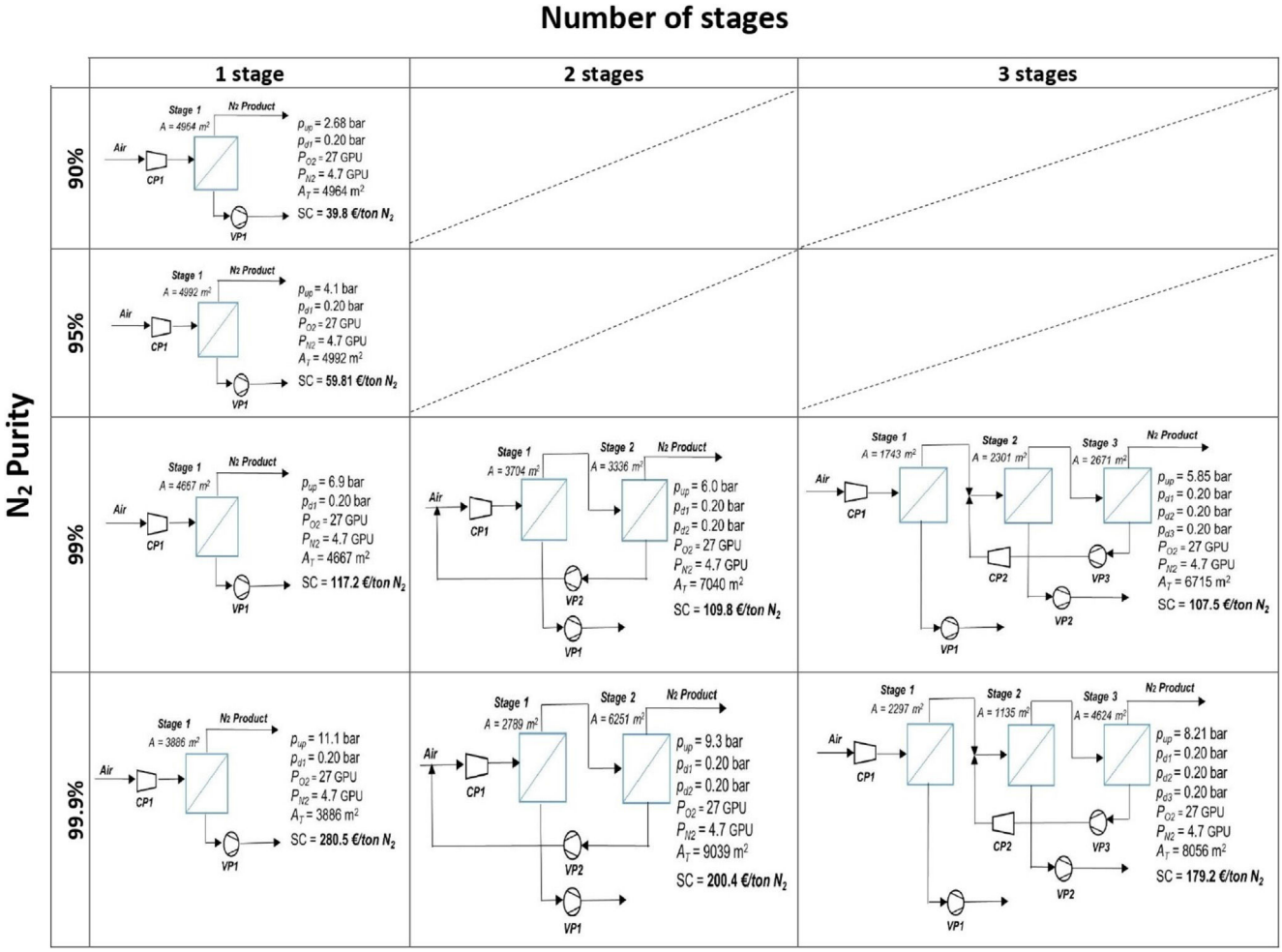

Fig. 4. Summary of the best NEA process configurations obtained with PSF membrane for up to three membrane stages and different nitrogen purity levels.

recovery, oxygen enriched air or carbon capture (Baker, 2009). These serious limitations have to be taken into account for NEA production. The optimal flow-sheets reported in Figs. 4 and 5 suggest however that the use of vacuum in place of or complementary to feed compression should be investigated. Feed compression is operated only for high purity levels, when too large membrane surface areas are needed. Vacuum pumping seems to offer a very useful solution when membrane surface area and energy requirement have to be balanced.

- Nitrogen production costs with PPO are systematically lower than with PSF. This suggests that a larger permeance such as offered by PPO is more interesting than a higher selectivity (offered by PSf).

The reference case obtained through this first process synthesis study confirms the rules and guidelines reported for nitrogen production by membranes. The impact of novel, high performance materials, such as those detailed in Table 3 and corresponding to trade-off limits, on these guidelines and conclusion are analyzed in the next section.

3.2. Nitrogen production by high performance membrane materials

In the second part of this study, the minimal nitrogen production cost with high performances membrane materials, within the trade-off limits, is explored. In that case, membrane performances (i.e. oxygen and nitrogen permeances) are not fixed (such as in the previous step) but these two variables are free within the trade-off limits shown on Fig. 2b (dashed area). Two different strategies have been compared:

- Membrane permeances are allowed to vary within the trade-off limits but the same membrane is used for all stages. One set of permeances is considered as in the previous section, but instead of being input values, the optimal pair of gas permeances are determined along with process configuration and operation parameters for each level of nitrogen purity by the optimization program.
- Membrane performances are allowed to vary within the trade-off limits but a different membrane can be selected for each stage. A set of optimal membrane permeances will be determined for each stage and nitrogen purity level. To our knowledge, this possibility has never been explored up to now for NEA production. The results of the optimization (process synthesis) are expected to generate useful guidelines for membrane material development: is it better to push selectivity or permeance in order to decrease NEA production cost? Is it interesting to combine different membranes in a multistaged unit, in order to achieve lower production costs?

The results of the two strategies (optimal membrane for all stages and optimal membrane for each stage) for NEA production study with four levels of nitrogen purity and for 1 to 3 stage units are detailed in the appendix A.12 and A.13. The optimal selectivity/

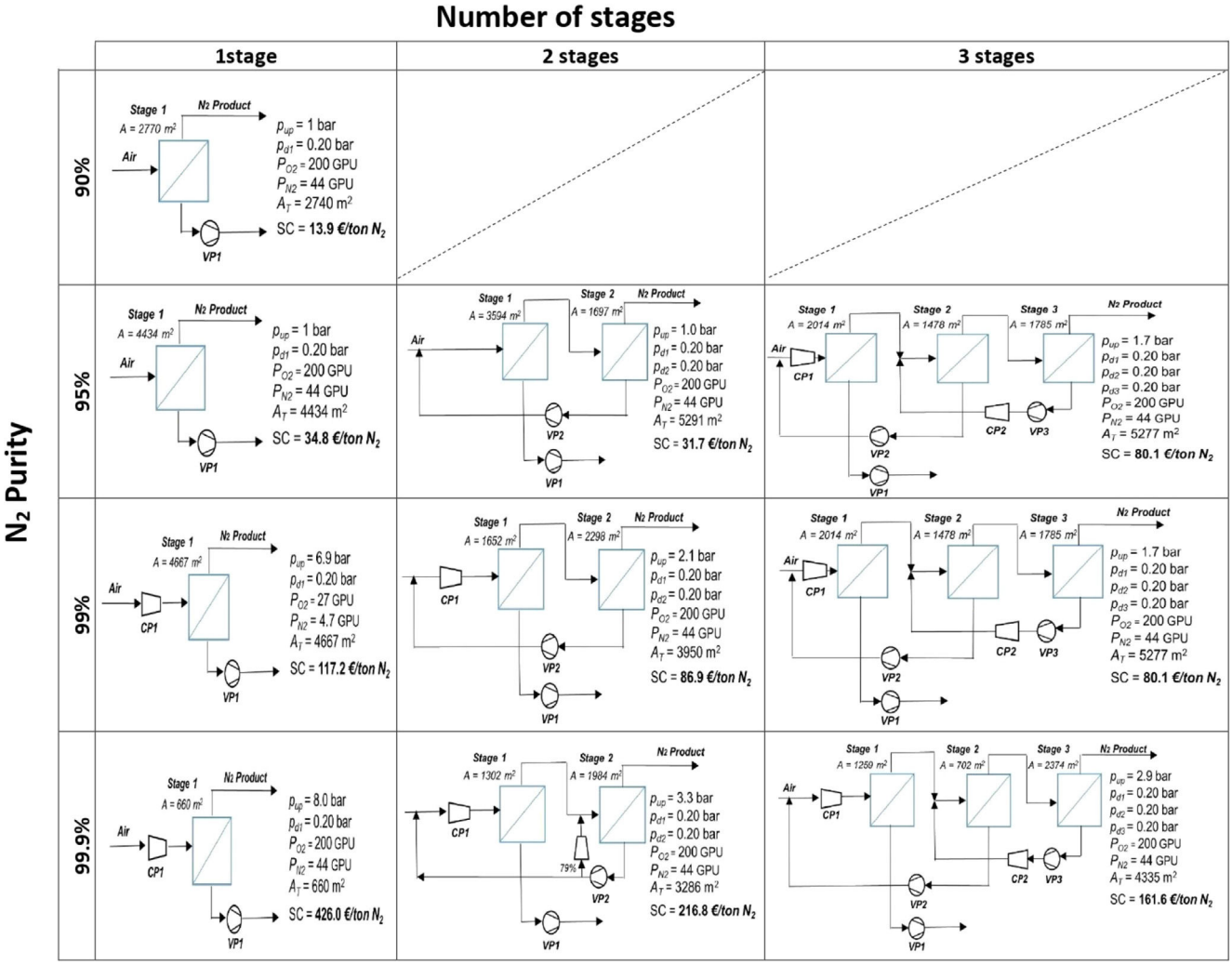

Fig. 5. Summary of the best NEA process configurations obtained with PPO membrane for up to three membrane stages and different nitrogen purity levels.

permeance for both strategies (considering membrane performance as uniform and independent variable in the system) are summarized in Fig. 6. Except for the 99.9 percent purity case, most optimal membrane performances are very close together. An increased permeance is favored, at the expense of a slight decrease in selectivity. Surprisingly, the variable permeability option (Fig. 6b) does not offer interesting performances. Indeed, the different membrane performances for the optimal membranes per stage case are very close and located in the same place as the optimal membrane for all stages case. This result is somewhat unexpected and it is of interest for NEA production.

The optimal flowsheets and operating conditions are summarized in Fig. 7 for both strategies.

From a production cost point of view, the high performance materials generate a significant decrease. A comparison between Fig. 4,5 and Fig. 7 shows the impact of improved membrane materials for the minimization of NEA production costs. The cost difference between having a uniform optimal membrane or having independent optimal membranes for each stage is negligible. This clearly results from the fact that the latter approach ends up to similar membrane performances than those generated by just considering one optimal membrane performance for all stages.

Since the results presented above highlight the interest of permeance over selectivity for NEA production, it is tempting to explore the incidence of thinner layers (i.e. larger permeance). Thin dense layers down to 50 nm are effectively achievable for some gas separation membranes (Favre, 2010). A 0.1 μm thickness could thus be possibly obtained with the trade-off materials listed in Table 3. This point will be analysed in the next section.

3.3. Nitrogen production by high performance membrane materials and ultra thin dense layer membranes

An optimization study of trade-off membrane materials showing a ten fold increase in permeance has been undertaken. This new case study corresponds to 0.1 μm thick layer membranes, in place of the standard 1 μm assumption taken in the previous sections. The best configurations, operating conditions and membrane performances for the four nitrogen purity levels are summarized in Fig. 8.

The optimal membrane performances for uniform and independent membrane performances are shown on the trade off curves presented in the Fig. 9.

The two strategies show, again, very close results. This confirms that for NEA production, the association of different membranes into multistage units is of low interest. A very narrow domain is obtained for optimal membrane performances for the different nitrogen purity levels. This result is surprising and also interesting because it suggests that a single optimal membrane development could possibly fit the requirements for a broad range of nitrogen

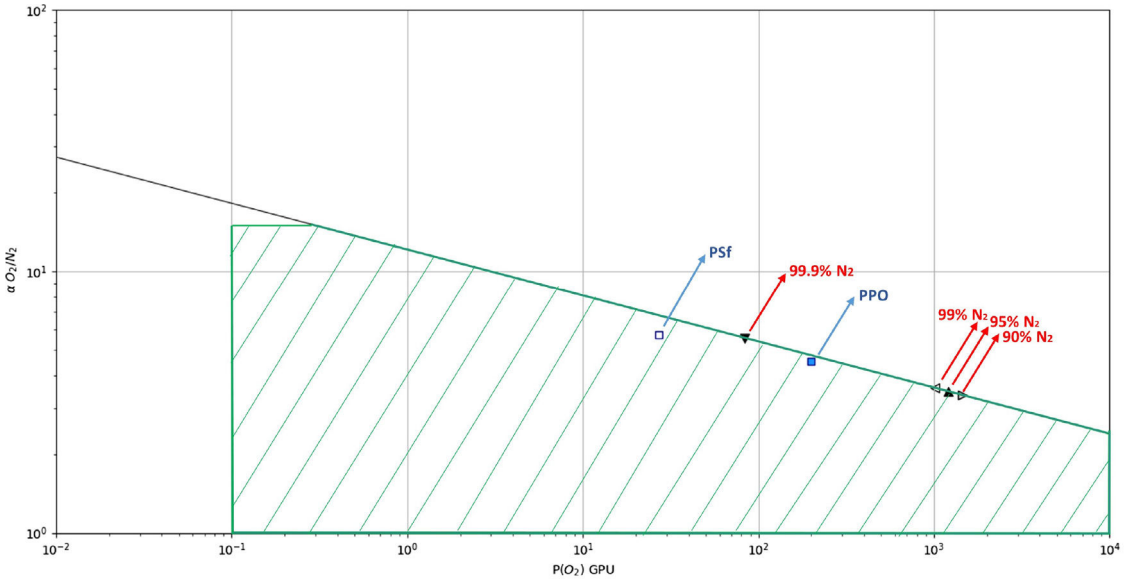

(a) Optimal membrane performances for the different nitrogen purity levels when the same membrane is used in all stages.

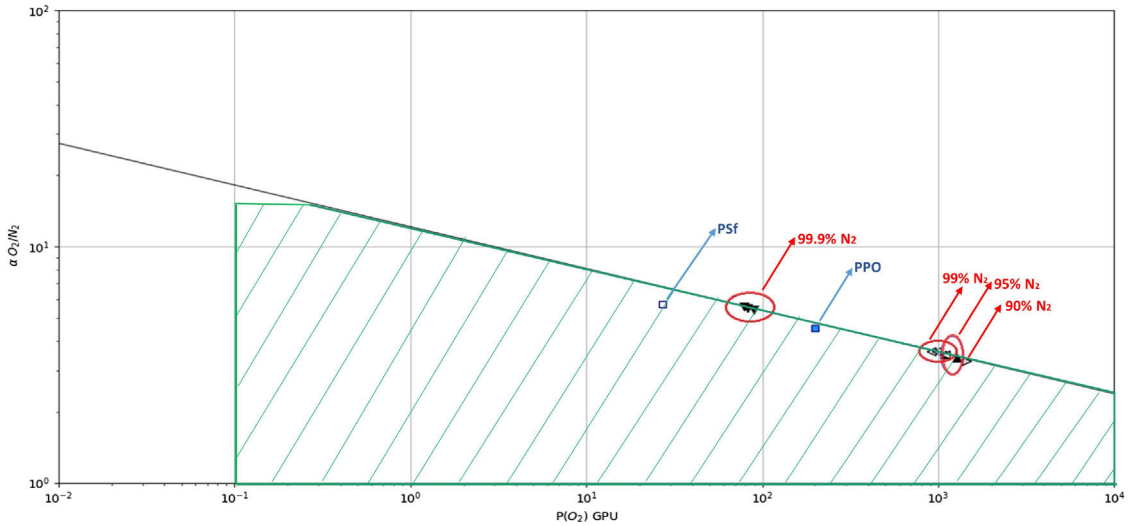

(b) Optimal membrane performances for the different nitrogen purity levels when a different membrane is used in each stage. PSF and PPO membranes are included for reference.

Fig. 6. Result of the membrane optimization study (red arrows) compared to the existing commercial membrane performances (blue arrows).

purities. In terms of selectivity/permeance trade-off, the optimal membrane characteristics clearly shift towards larger permeances, without large increase in selectivity. This unexpected result corresponds to a generic guideline for membrane materials development for NEA production: permeance has to be favored. The performances of recently reported materials such as PIM, with ultra-high permeabilities (Thomas et al., 2009), are of major interest in that perspective. It is worth to note that with high permeance membranes, the process configurations remain unchanged for each purity level, but the specific cost is largely decreased (typically around 40 percent). This highlights the potential of thin, highly permeable membrane materials for nitrogen production.

3.4. Synopsis

In the last part of this study, the different case studies are summarized in Table 5, in order to enable an overview of the key results. The optimal conditions for the four purity levels are presented for the current membrane materials (represented by PPO results), trade-off materials and ultra-high permeance materials (limited to the one optimal membrane for all stages case, the differences with the optimal membrane for each stage case being very small).

The overall set of results which are detailed in Table 5 can be summarized as follows:

- A higher nitrogen purity logically generates higher (non linear) production costs. This logical statement applies to both the current commercially available membranes and advanced prospective materials.
- Trade-off membrane materials offer promising performances in terms of production cost, with a two to three fold decrease compared to the current production cost. It is important to note that the average cost of 30 Euros per ton, obtained with commercial

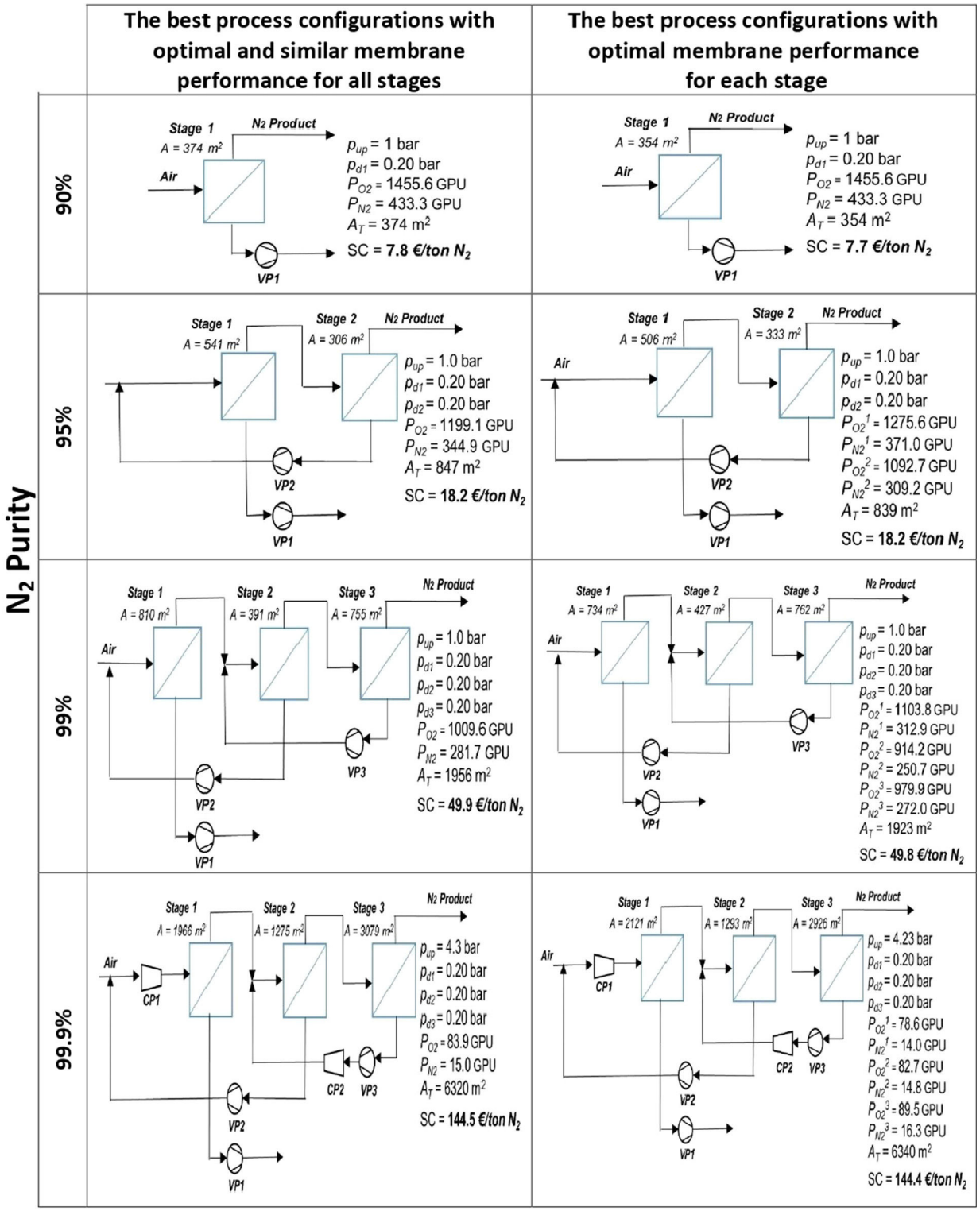

Fig. 7. Overall best process configurations with up to three membrane stages for different nitrogen purity levels including optimal membrane permeances when the same membrane is used in all stages (left) and when a different membrane is used in each stage (right).

PPO gas separation membranes for 95 percent purity, is in excellent agreement with a recent study (Schmidt and Clayton, 2013).

- A single stage process is the most economical for the lowest purity level (90% N_2), whatever the membrane type. Similarly, two and three stages processes with recycling loops offer better performances for higher nitrogen purity specifications, independently of the membrane characteristics. This shows the robustness of the process flowsheets, generated through engineering studies in the 80s. The three types of configurations, selected as target nitrogen purity only (Fig. 3) for decades, are indeed confirmed throughout the different case studies explored in this paper.

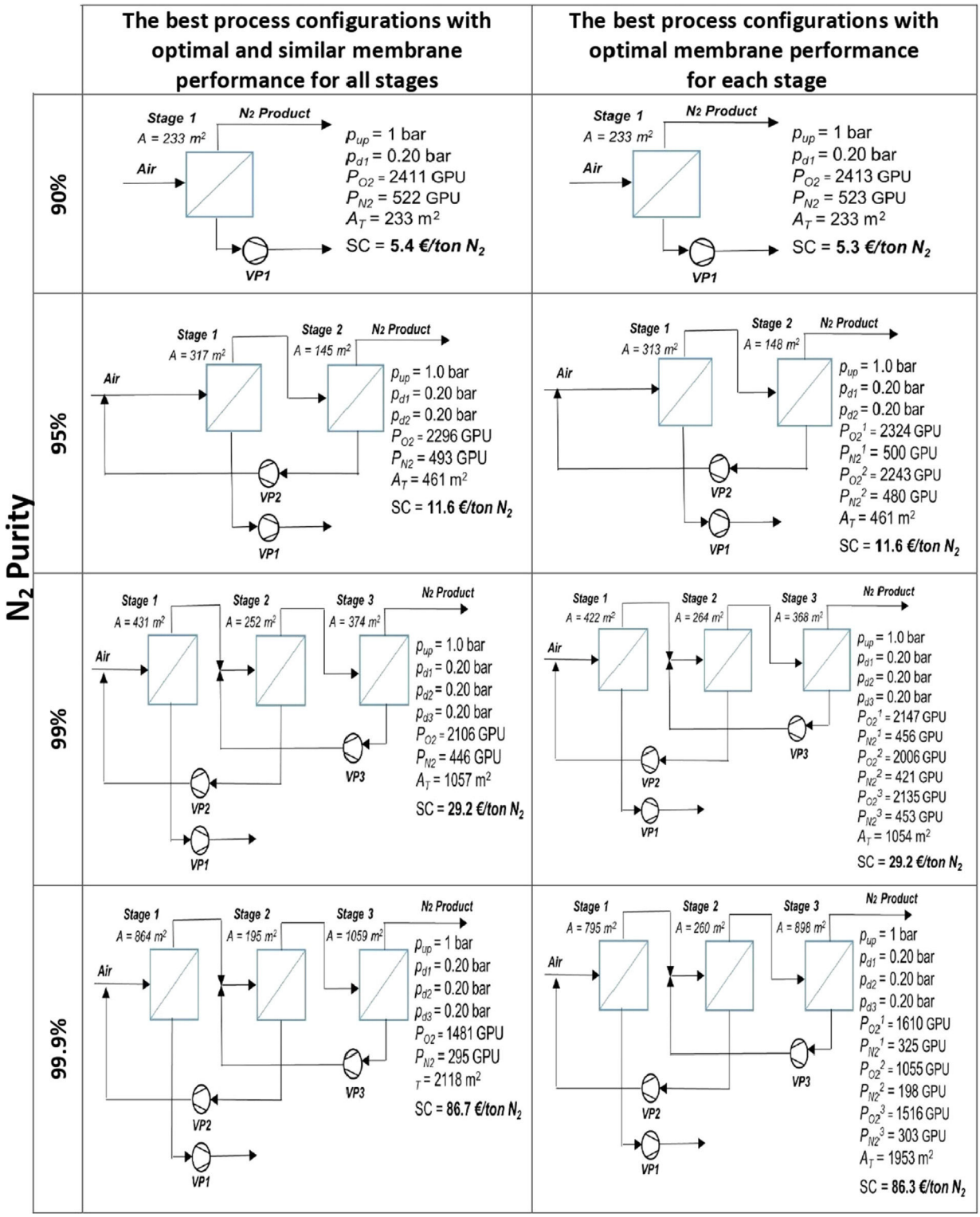

Fig. 8. Overall best process configurations with up to three membrane stages at different nitrogen purity levels including optimal membrane permeances when the same membrane is used in all stages (left) and when a different membrane is used in each stage (right). Membrane thickness used to calculate membrane permeance from permeability values is taken as 0.1 μm.

- In contrast to current practice, the optimal configurations obtained with high performance membrane materials make use of vacuum operation. Except for the high purity target, compression is not the best retained technology for the optimal configuration. This result shows the interest to combine materials and engineering for process design studies, and also the interest to systematically explore the vacuum option in membrane process synthesis studies. It has to be stressed that vacuum operation is often rejected for industrial applications due to the drawbacks of vacuum pumps (risk of leaks, large footprint,

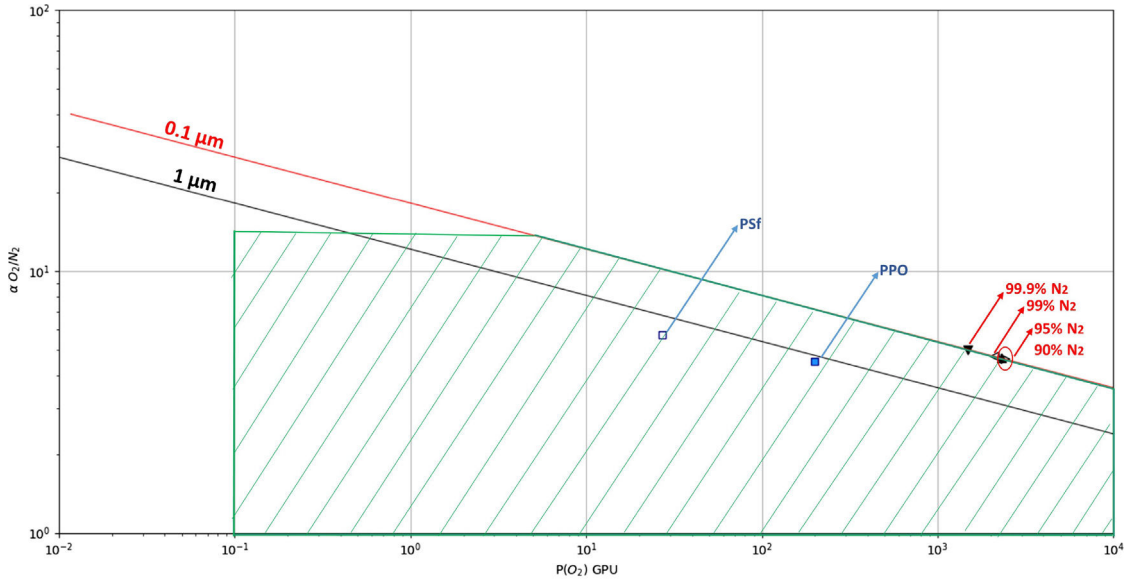

(a) Optimal membrane performances for the different nitrogen purity levels when the same membrane is used in all stages

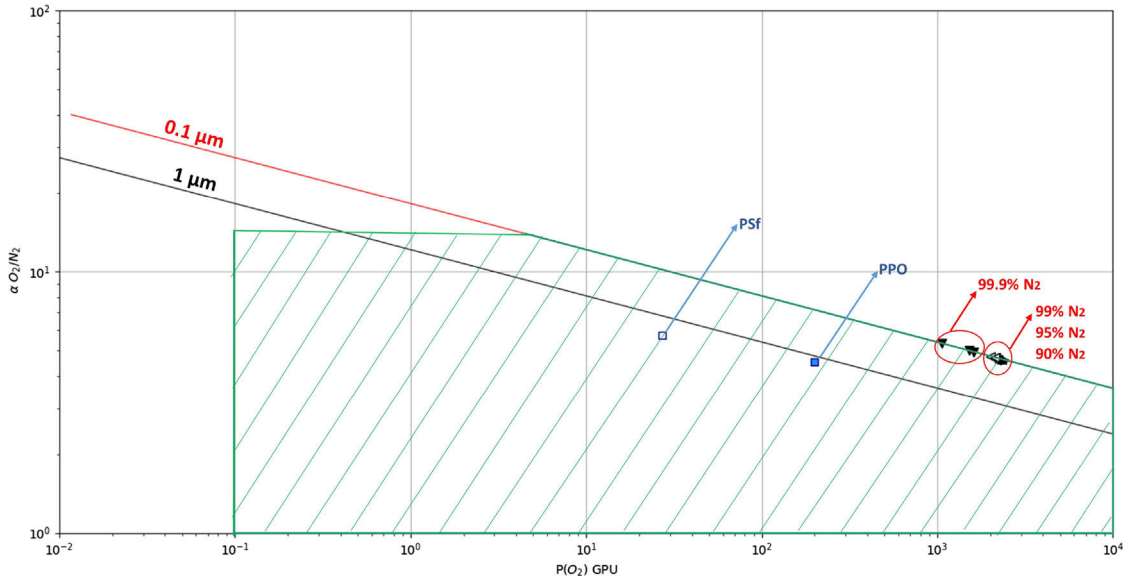

(b) Optimal membrane performances for the different nitrogen purity levels when a different membrane is used in each stage. PSF and PPO membranes are included for reference.

Fig. 9. Result of the membrane optimization study (red arrows) with high permeance membranes compared to the existing commercial membrane performances (blue arrows).

low energy efficiency, higher capital costs). The optimal results shown on Figs. 7 and 8 thus address a key question in terms of process selection.

- The overall stage cut (i.e. ratio of the total permeate over total feed flowrate) ranges between 0.4 and 0.85. This is typical of industrial membrane units (Favre, 2010). Thus, the fact that air is considered as free for NEA production does not generate very low stage cut values. Generally speaking, a larger stage cut is obtained when nitrogen purity increases, in order to achieve a much intense oxygen removal (oxygen being faster than nitrogen).
- The energy requirement has been also calculated and it is detailed in the last column of Table 5. Interestingly, the overall energy requirement (classically expressed in kWh per unit feed flowrate (Heinz-Wolfgang, 2008)) is comparable to previously reported data for NEA production (typically 0.26–0.45 kWh per standard cubic meter nitrogen at 98–99 percent (Heinz-Wolfgang, 2008)). Energy requirement for the optimal configuration seems to depend on nitrogen purity only, with a ten fold increase from 90 to 99.9 percent.
- One of the most striking and unexpected result of the study concerns the optimal membrane performances. First, a moderate selectivity is systematically obtained as the optimal one, whatever the nitrogen purity level. This point is counterintuitive. It is often stated that for high purity, a larger selectivity helps. Several studies in membrane materials science stress the importance of improved selectivities in order to extend the economic region of membrane separations (Mahajan and

Table 5
Summary of the best process configurations for NEA production with commercial membrane (PPO) and trade-off membrane materials with uniform permeability and 1 and 0.1 μm membrane layer thickness.

	N_2 purity	Cost (EUR/ton N_2)	Number of stages	α	P_{O_2} (GPU)	V_p/ C_p	θ	Energy (kWh/Nm^3)
Commercial membrane	90%	13.9	1	4.54	200	V_p	0.44	0.07
	95%	31.7	2	4.54	200	V_p	0.57	0.16
	99%	80.1	3	4.54	200	V_p & C_p	0.59	0.36
	99.9%	161.6	3	4.54	200	V_p & C_p	0.67	0.79
Optimal membrane performance	90%	7.8	1	3.4	1455.6	V_p	0.54	0.1
	95%	18.2	2	3.5	1199.1	V_p	0.64	0.22
	99%	49.9	3	3.6	1009.6	V_p	0.76	0.56
for all stages	99.9%	144.5	3	5.6	83.9	V_p & C_p	0.57	0.59
Optimal membrane performance	90%	5.4	1	4.6	2411	V_p	0.45	0.07
	95%	11.6	2	4.6	2296	V_p	0.57	0.15
	99%	29.2	3	4.7	2106	V_p	0.68	0.37
for all stages	99.9%	86.7	3	5	1481	V_p	0.85	0.98

Koros, 2000). The subtle interplay between permeance (surface area) and selectivity (separation performances) in multistage configurations including recycling loops suggests however, according to the results shown in Figs. 7 and 8 that a moderate selectivity associated to a trade-off permeance (i.e a much larger permeance compared to commercial membranes) is the best solution. To some extent, this conclusion is of great interest for the recent generation of high permeability polymers (TRP, PIM, superglassy) (Mahajan and Koros, 2000; Thomas et al., 2009; Park et al., 2017). Thus, it could be suggested to materials developers to promote permeability increase, rather than trying to develop super selective materials.

- Finally, the most puzzling results comes from the possibility to combine different membrane materials into multistage units. This option is almost unexplored in membrane science and has never been investigated for NEA production. The possibility to combine nitrogen selective and carbon dioxide selective membrane has been shown to offer very attractive performances for carbon capture applications (Yuan et al., 2014). It might be expected that for NEA production, the same conclusion could be drawn. It is often stated that different membrane selectivities may be optimum for different portions of an industrial plant (Baker and Low, 2014). Our study shows that the situation is completely different. The optimal multistaged processes shown on Fig. A.13 make use of approximately the same membrane (a moderate selectivity around 3.6–4.6, a permeance level at the trade-off limit). It is obvious that this statement does not systematically hold and should be reconsidered from case to case depending on the separation targets and feed mixture. For the set of parameters tested in our NEA study, it seems that the use of different membranes in a multistage system does not offer attractive improvement possibilities.

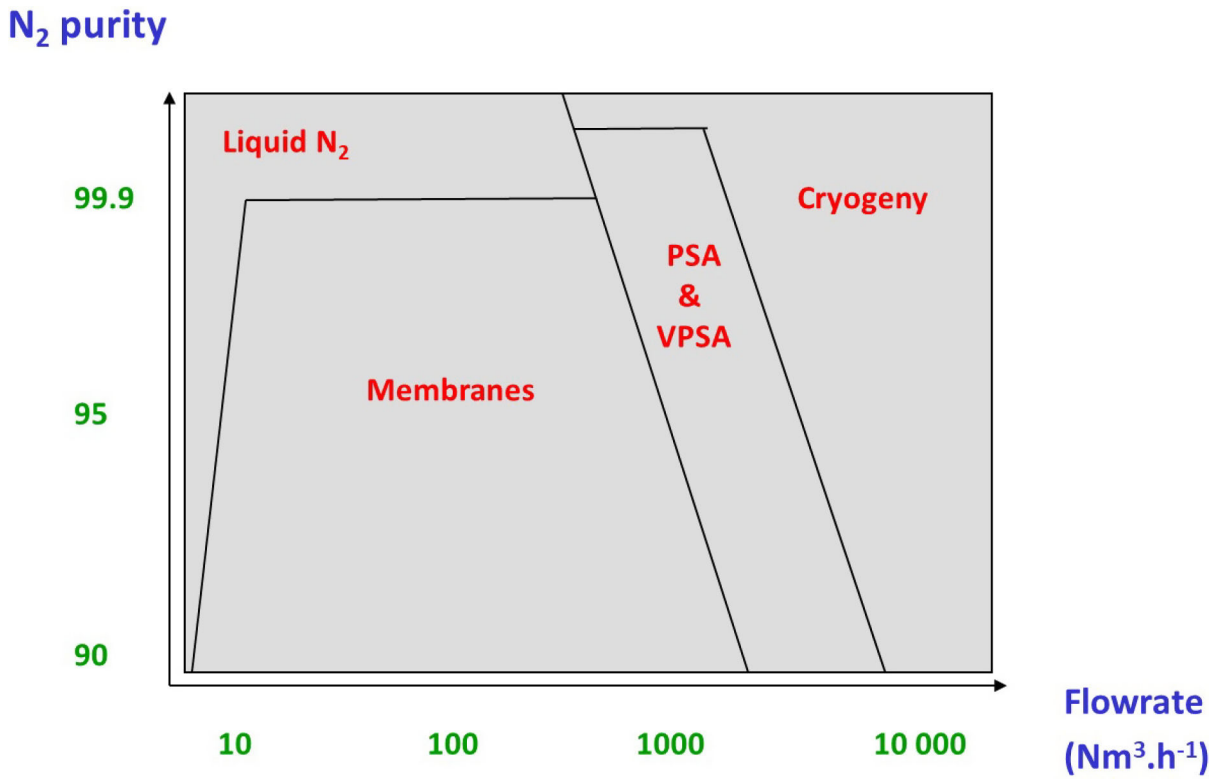

Fig. 10. Economic NEA production technologies as a function of nitrogen purity and production capacity. Adapted from Prasad et al. (1994) and Baker (2012).

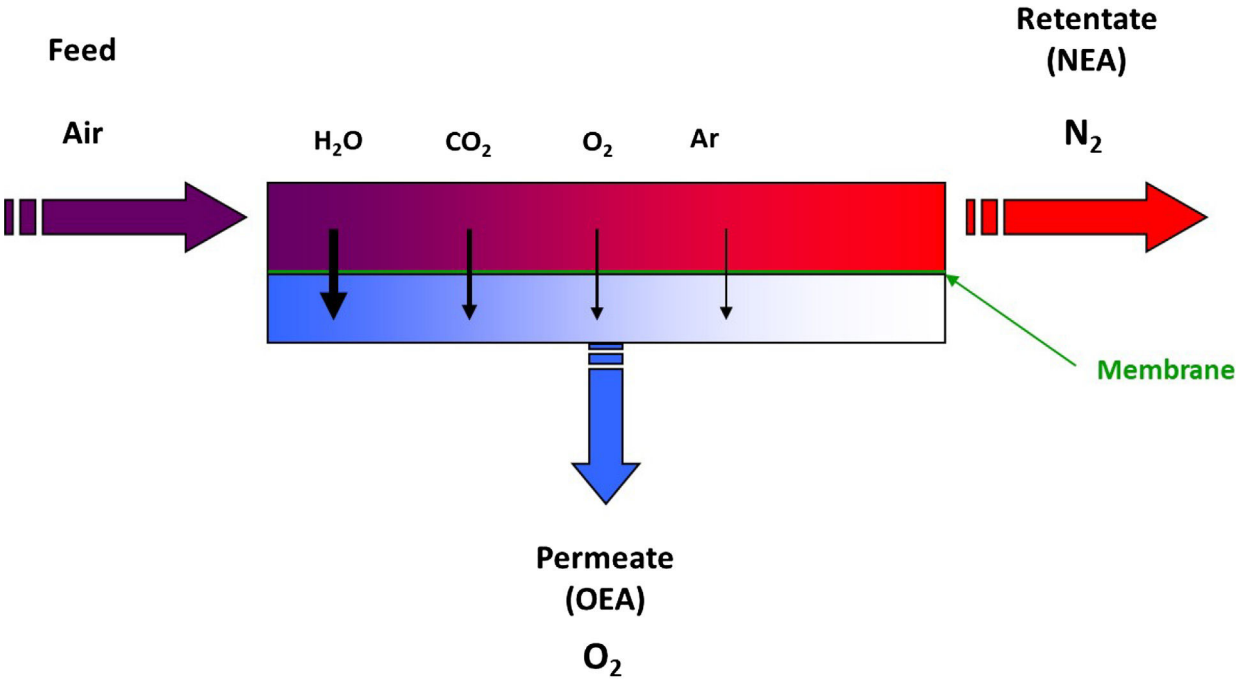

Fig. 11. Overview of air separation by polymeric membrane processes.

More generally, the domain of usage of membranes have gradually extended through the years towards other separation technologies for NEA production, thanks to improvements in materials and process design (Fig. 10). It is expected that the lower production costs based on improved membrane materials which have been identified in this study further extend the membrane domain. However, a rigorous technico-economical study of the different technologies is needed in order to evaluate the new process selection map. It has been shown that high nitrogen purities (i.e. >99 percent) remain expensive and require complex membrane production schemes. It is thus likely that improved, high permeance materials increase the application range of membranes for larger production capacities rather than larger purities.

Finally, it is important to recall that, similarly to any technico-economical study, the impact of the cost function on the results is a key question. The detailed cost contributions and overall objective function may indeed vary from one study to the other. For membrane separations however, CAPEX are always dominated by compressor costs, and OPEX always correspond to electricity costs. Consequently, while a different cost function obviously will generate different overall production costs, the optimal process design and associated optimal operating conditions usually are robust. The fact that the same process designs have been obtained through process synthesis as the one used in industry for decades shows that the methodology and objective function are relevant.

4. Conclusions and perspectives

Nitrogen Enriched Air (NEA) is the main application of membrane gas separations today. Nevertheless, few studies have been reported on either process (Prasad et al., 1994; Ajhar et al., 2008; Bozhenko and Bozhenko, 1995) or techno-economical analyses for this important application (Schell, 1985; Jain, 1989). The situation is quite different for Oxygen Enriched Air (OEA), which has been more extensively investigated (Rigby and Watson, 1994; Bhide and Stern, 1991; Gollan and Kleper, 1984; Haider et al., 2018). Numerous innovative NEA concepts have been explored, including adsorption, hybrid systems or membrane column processes (Zhu et al., 2008; Purnomo and Alpay, 2000; Agrawal, 1996). This study intended to achieve a rigorous optimization study of membrane gas separations units with up to three stages.

For the specific case of polymeric membranes, it has been shown that a large progress is achievable for the production cost point of view for low purity NEA (i.e. 90 and 95%), compared to the existing commercially available membrane materials. In principle, a very large cost decrease is also possible for higher purities (i.e. >95%), but the comparison to alternative technologies, such as PSA, is needed in that case.

More specifically, the process synthesis study performed on air separation has shown that:

- Process synthesis converges to the same process configurations as the ones developed by gas producers for a long time (same number of stages and recycling loops as a function of N_2 purity),
- Trade-off limit membrane materials do not impact the process configuration
- From a membrane materials point of view, a high permeance, combined to a moderate selectivity, offers the best performances, whatever the N_2 purity target. This result is of great importance for membrane material development because it suggests to promote highly permeable structures rather than very selective materials.
- The possibility to use different membranes into multistage units does not provide a significant improvement for NEA.
- Vacuum operation is a major interest (even though the practical use of vacuum pumps is not favored in industry due to large footprint and leaks complications).

It has to be stressed that the above conclusions are by no means generic, but limited to the NEA application with polymeric membranes. Future work on high performance materials, showing performances far beyond the trade-off limits (Koros and Zhang, 2017)

is currently in progress, in order to better understand the interplay between materials performances and process engineering. It might be that the conclusions obtained for polymeric membrane materials are completely different when ultrapermeable and/or ultraselective materials are used.

A similar study for Oxygen Enriched Air (OEA) production would also be of interest. It has been stated in the introduction that OEA production by membranes has been more intensively investigated than NEA. It is also important to take into account that OEA production by membrane processes is less favourable than NEA. For OEA indeed, the target mixture is recovered on the low pressure side (permeate) and is likely to be contaminated by fast compounds present in the feed mixture (air). Water, carbon dioxide, oxygen and argon being faster permeants than nitrogen (Favre, 2010), Fig. 11, an OEA study should ideally take into account the multicomponent separation problem. NEA production is thus a very favourable situation because the target compound is recovered under high pressure and all other compounds of the feed mixture (including argon) are removed because they are faster permeants into polymers (Haraya and Hwang, 1992).

Finally, the extension of the methodology to other gas separations applications (e.g. natural gas treatment, hydrogen purification) is obviously also of interest.

Acknowledgements

Research reported in this publication was supported by King Abdullah University of Science and Technology (KAUST # OSR-2016-CPF-2910).

Appendix A. The best process configurations for uniform and independent membrane performances

Figs. A.12 and A.13.

References

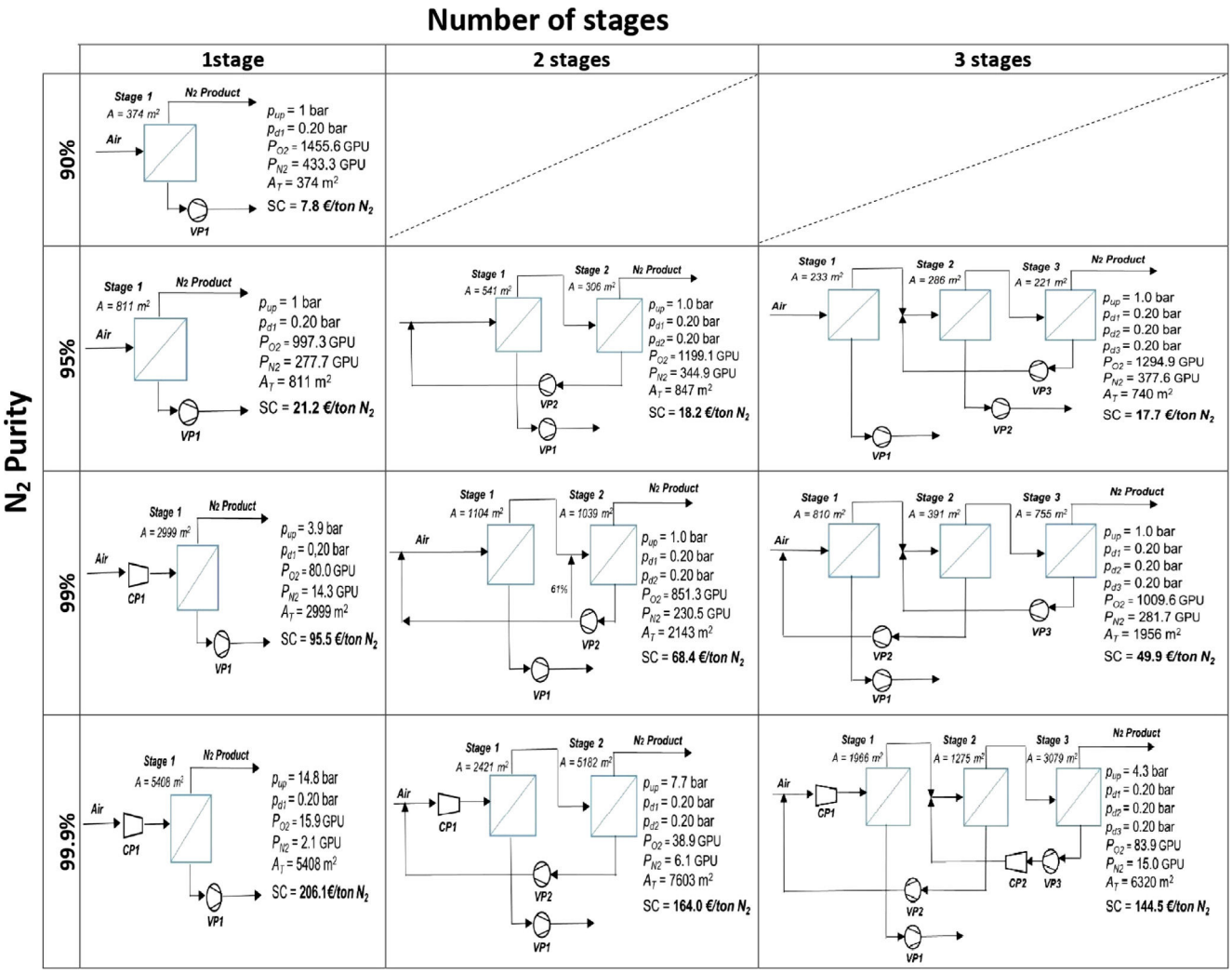

Fig. A.12. Summary of the best process configurations obtained when the optimal membrane is used in all stages. A membrane process with up to three stages and different nitrogen purity levels has been considered.

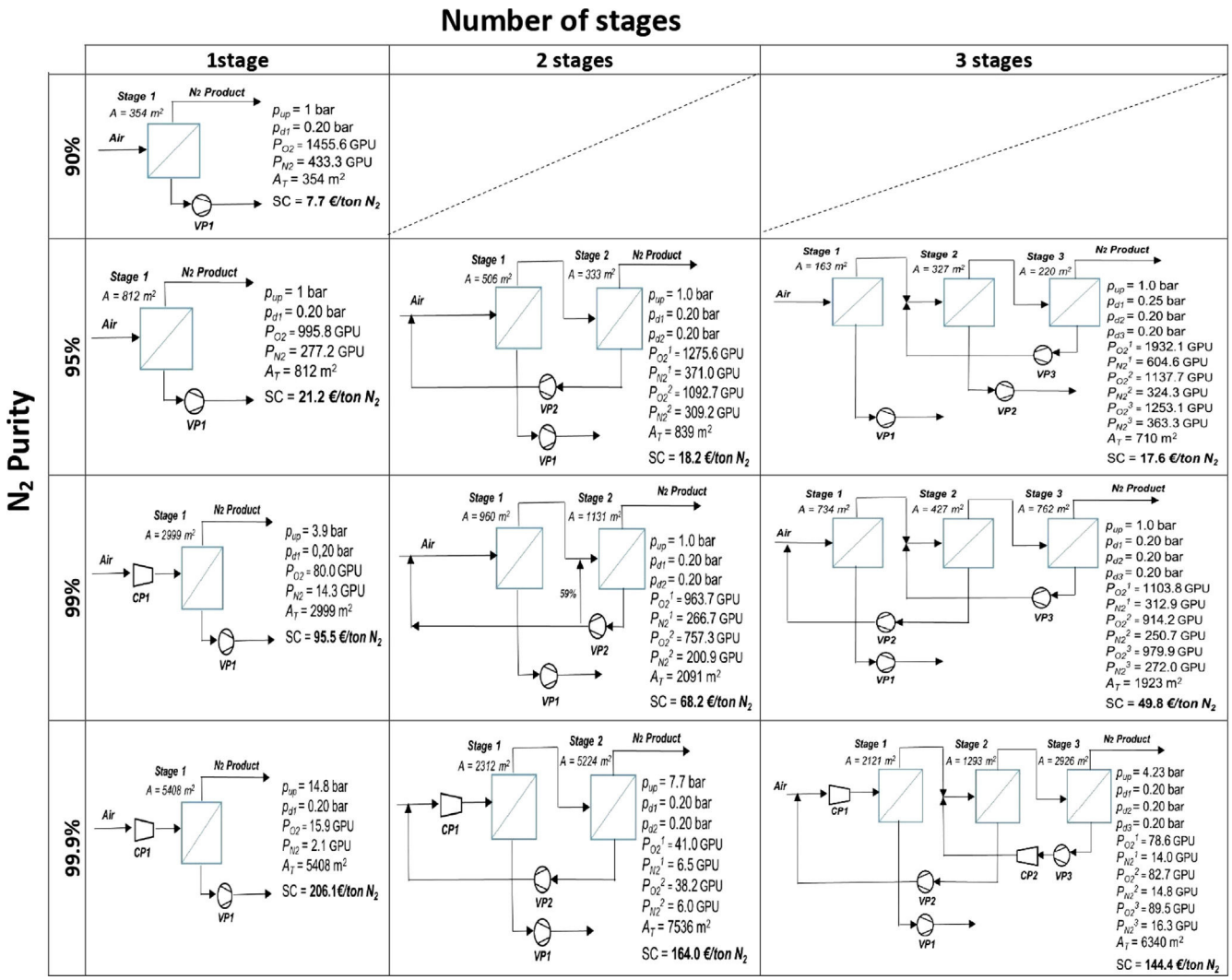

Fig. A.13. Summary of the best process configurations obtained with optimal membrane performance when a different optimal membrane is considered in each stage. A membrane process with up to three stages and different nitrogen purity levels has been considered.

Agrawal, R., 1996. Membrane cascade schemes for multicomponent gas separation. Indust. Eng. Chem. Res. 35, 3607–3617.

Ajhar, M., Follmann, M., Matthias, C., Melin, T., 2008. Membranes producing nitrogen-enriched combustion air in diesel engines: assessment via dimensionless numbers. J. Membr. Sci. 323, 105–112.

Baker, R.W., 2009. Future directions of membrane gas separation technology. Ind. Eng. Chem. Res. 41, 1393–1411.

Baker, R.W., 2012. Membrane Technology and Applications. John Wiley & Sons.

Baker, R.W., Low, B.T., 2014. Gas separation membrane materials: a perspective. Macromolecules 47, 6999–7013.

Bhide, B., Stern, S., 1991. A new evaluation of membrane processes for the oxygen-enrichment of air. II. Effects of economic parameters and membrane properties. J. Membr. Sci. 62, 37–58.

Bounaceur, R., Berger, E., Pfister, M., Santos, A.A.R., Favre, E., 2017. Rigorous variable permeability modelling and process simulation for the design of polymeric membrane gas separation units: memsic simulation tool. J. Membr. Sci. 523, 77–91.

Bozhenko, E., Bozhenko, S., 1995. Computer optimization of a membrane device producing N2 of 98% purity for preserving museum relics in the hermitage. Gas Sep. Purif. 9, 31–33.

Castle, W.F., 2002. Air separation and liquefaction: recent development and prospects for the beginning of the new millennium. Int. J. Refrig. 25, 158–172.

Ettouney, H.M., El-Dessouky, H.T., Abou Waar, W., 1998. Separation characteristics of air by polysulfone hollow fiber membranes in series. J. Membr. Sci. 148, 105–117.

Favre, E., 2010. Polymeric membranes for gas separation. In: Drioli, E., Giorno, L. (Eds.), Comprehensive Membrane Science and Technology. Elsevier, Oxford, pp. 155–212.

Gollan, A., Kleper, M., 1984. The economics of oxygen enriched air production via membranes. In: IETC - Industrial Energy Technology Conference (1984) Energy Systems Laboratory (http://esl. tamu.edu): Texas A & M University (<http://www.tamu.edu>).

Haider, S., Lindbråthen, A., Lie, J.A., Hägg, M.-B., 2018. Carbon membranes for oxygen enriched air–part ii: Techno-economic analysis. Sep. Purif. Technol. 205, 251–262.

Haraya, K., Hwang, S.-T., 1992. Permeation of oxygen, argon and nitrogen through polymer membranes. J. Membr. Sci. 71, 13–27.

Heinz-Wolfgang, H., 2008. Industrial Gases Processing. Wiley-VCH Verlag GmbH & Co, KGaA.

Henis, J.M., 1994. Commercial and practical aspects of gas separation membranes. In: Paul, D.R., Yampolskii, Y.P. (Eds.), Polymeric Gas Separation Membranes. CRC Press, Boca Raton, FL.

Jain, R., 1989. Method for economic evaluation of membrane-based air separation. Gas Sep. Purif. 3, 123–127.

Koros, W.J., Zhang, C., 2017. Materials for next-generation molecularly selective synthetic membranes. Nature materials 16, 289.

Lin, H., Zhou, M., Ly, J., Vu, J., Wijmans, J.G., Merkel, T.C., Jin, J., Haldeman, A., Wagener, E.H., Rue, D., 2013. Membrane-based oxygen-enriched combustion. Indust. Eng. Chem. Res. 52, 10820–10834.

Mahajan, R., Koros, W.J., 2000. Factors controlling successful formation of mixed-matrix gas separation materials. Indust. Eng. Chem. Res. 39, 2692–2696.

McConnell, S., 2010. Heavy-duty diesel engine nox reduction with nitrogen-enriched combustion air, Argonne National Laboratory # 02-VTCE-GS-009.

Park, H.B., Kamcev, J., Robeson, L.M., Elimelech, M., Freeman, B.D., 2017. Maximizing the right stuff: the trade-off between membrane permeability and selectivity. Science 356.

Prasad, R., Notaro, F., Thompson, D., 1994. Evolution of membranes in commercial air separation. J. Membr. Sci. 94, 225–248.

Prasad, R., Shaner, R.L., Doshi, K.J., 1994. Comparison of membranes with other gas separation technologies. In: Paul, D.R., Yampolskii, Y.P. (Eds.), Polymeric Gas Separation Membranes. CRC Press, Boca Raton, FL, pp. 531–614.
Purnomo, I., Alpay, E., 2000. Membrane column optimisation for the bulk separation of air. Chem. Eng. Sci. 55, 3599–3610.
Ramírez-Santos, Á.A., Bozorg, M., Addis, B., Piccialli, V., Castel, C., Favre, E., 2018. Optimization of multistage membrane gas separation processes. Example of application to CO2 capture from blast furnace gas. J. Membr. Sci. 566, 346–366.
Rigby, G.R., Watson, H.C., 1994. Application of membrane gas separation to oxygen enrichment of diesel engines. J. Membr. Sci. 87, 159–169.
Robeson, L.M., 2008. The upper bound revisited. J. Membr. Sci. 320, 390–400.
Schell, W., 1985. Commercial applications for gas permeation membrane systems. J. Membr. Sci. 22, 217–224.
Schmidt, S., Clayton, R., 2013. Dynamic design of a cryogenic air separation unit, Lehigh University, p. 41.
Seider, W.D., Seader, J.D., Lewin, D.R., 2009. Product & Process Design Principles: Synthesis. John Wiley & Sons, Analysis and Evaluation.
Smith, A., Klosek, J., 2001. A review of air separation technologies and their integration with energy conversion processes. Fuel Process. Technol. 70, 115–134.
Spillman, R.W., 1989. Economics of gas separation membranes. Chem. Eng. Prog. 85, 41–62.
Thomas, S., Pinnau, I., Du, N., Guiver, M.D., 2009. Pure- and mixed-gas permeation properties of a microporous spirobisindane-based ladder polymer (PIM-1). J. Membr. Sci. 333, 125–131.
Yuan, M., Narakornpijit, K., Haghpanah, R., Wilcox, J., 2014. Consideration of a nitrogen-selective membrane for postcombustion carbon capture through process modeling and optimization. J. Membr. Sci. 465, 177–184.
Zhu, X., Sun, S., He, Y., Cong, Y., Yang, W., 2008. New concept on air separation. J. Membr. Sci. 323, 221–224.

Errata list

Table 4.2: Erratum list of the paper [63].

Page/Figure/case study	Original figure	Corrected figure
1204/5/3 stages 95% N_2	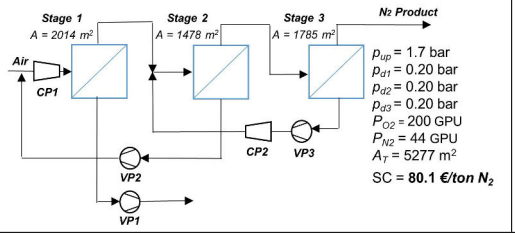	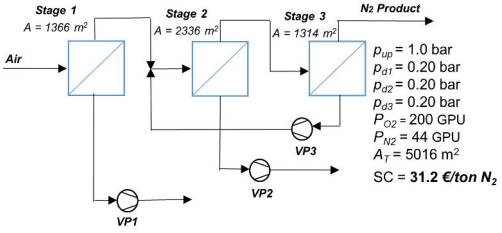

4.3 Effects of vacuum pump on membrane gas separation process

Vacuum operation has a major influence to decrease the production cost; however, it is rarely taken into account by membrane process synthesis software. The goal of this study is to evaluate the effects of vacuum pump on minimal process cost, optimal process configuration and operating conditions (maximum purity and recovery). To have a generic investigation, we consider six critical among those previously studied and presented in this work. Table 4.3 shows all considering cases.

It should be mentioned that for CO_2 capture from BFG and NEA cases, the objective functions that are presented in tables 3.2 and 1 in the paper "Polymeric membrane materials for nitrogen production from the air: a process synthesis study" in chapter 4 are applied respectively.

Table 4.3: Investigation of vacuum pump effects on different case studies

Case studies	
CO_2 **capture from BFG**	2 stages with 99% CO_2 recovery and 1% N_2 residual content 3 stages with 99% CO_2 recovery and 0.1% N_2 residual content
NEA with PPO membrane	2 stages with 99% N_2 product 3 stages with 99% N_2 product
NEA with PSf membrane	2 stages with 99% N_2 product 3 stages with 99% N_2 product

For each case, four sets of operating conditions were evaluated:

(i) Vacuum pump efficiency is fixed and equal to 0.85, value used in a lot of academic papers and works.

(ii) To be more realistic, vacuum pump efficiency is variable and equal to equation 4.12. Two vacuum levels are evaluated: 0.2 and 0.05 bar limitations

$$\eta_{vp} = 0.1058 \cdot ln(\frac{p_{down_s}}{p_{feed}}) + 0.8746 \tag{4.12}$$

(iii) The possibility of vacuum operation is not considered

4.3.1 Results and discussion

For PPO membrane, in both two and three stage process, the state with 0.05 vacuum limitation offers the best product cost value. The product cost increases approximately 25% from 0.05 to 0.2 vacuum limitation (both fix and variable vacuum efficiency cases). The maximum product cost happened in the state of a system without vacuum pump, which is 66% greater than the state of 0.05 vacuum limitation.

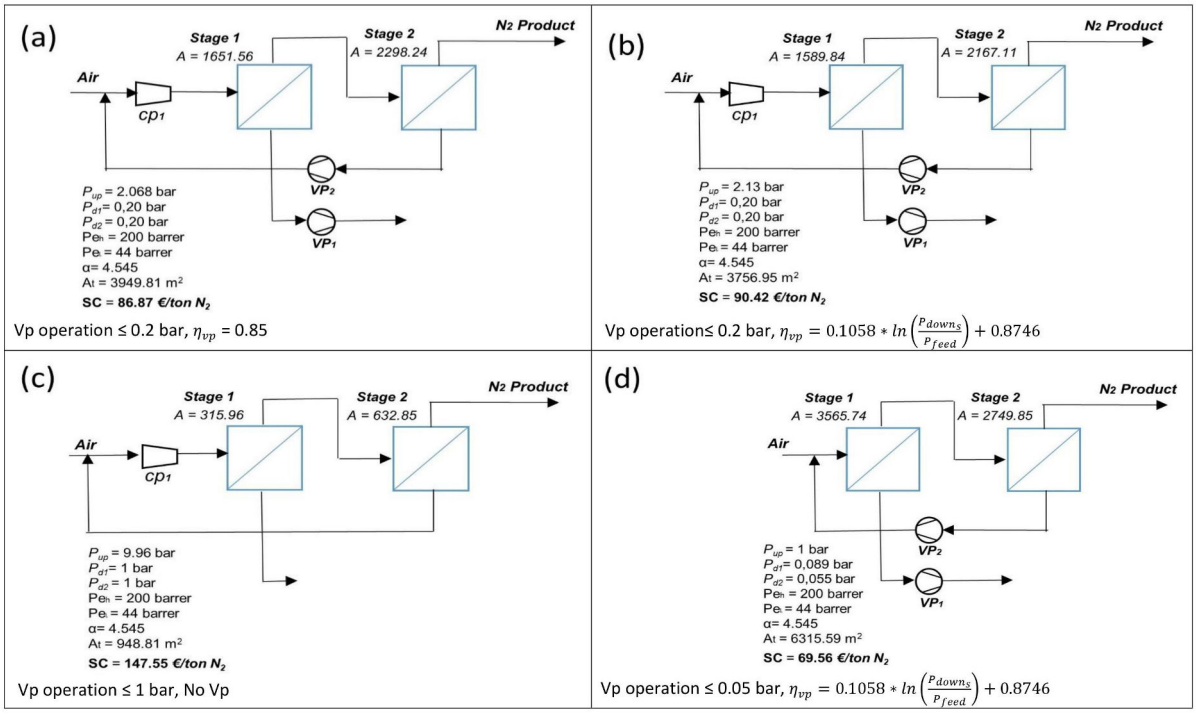

Figure 4.2: Investigating the vacuum pump effects by comparing optimal configurations (for two stages PPO membrane process with 99% N_2 production) with different vacuum efficiency.

In both cases (two and three stages) of PSf membrane and CO2 capture from BFG, the product cost of three states, 0.2 vacuum limitations (fixed and variable vacuum efficiency) and 0.05 vacuum limitation have slightly difference. The maximum product cost is concerning to the state of system without vacuum pump, which is 33% more than the case of 0.05 vacuum pump limitation.

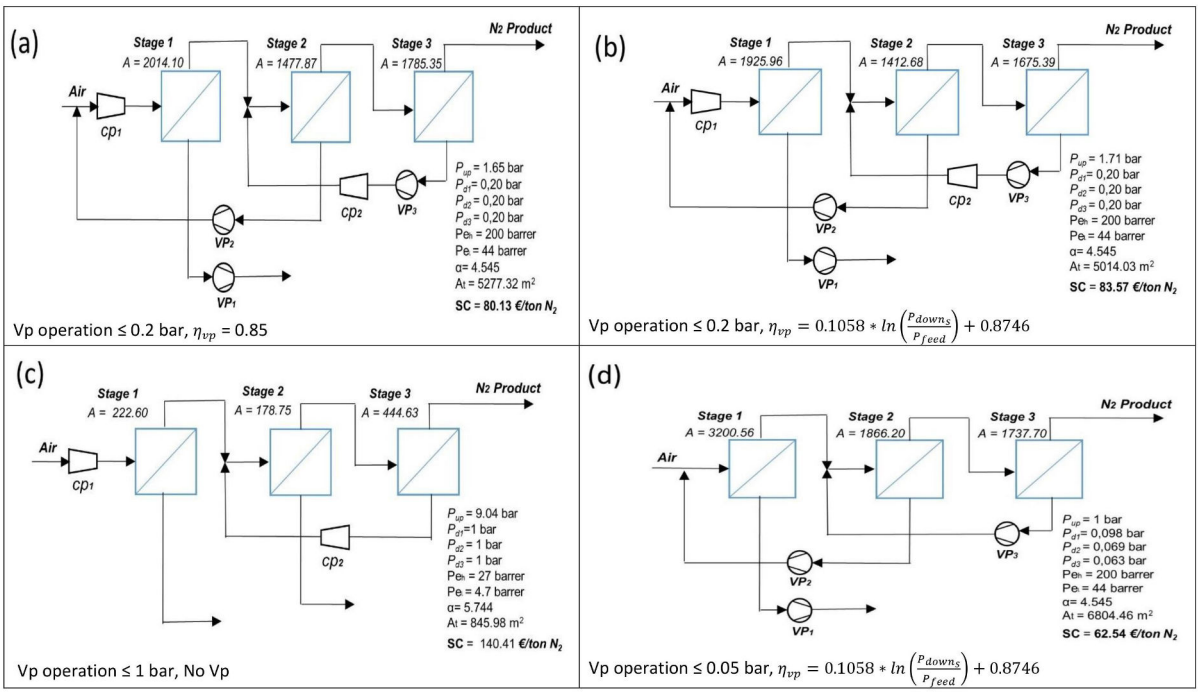

Figure 4.3: Investigating the vacuum pump effects by comparing optimal configurations (for three stages PPO membrane process with 99% N_2 production) with different vacuum efficiency.

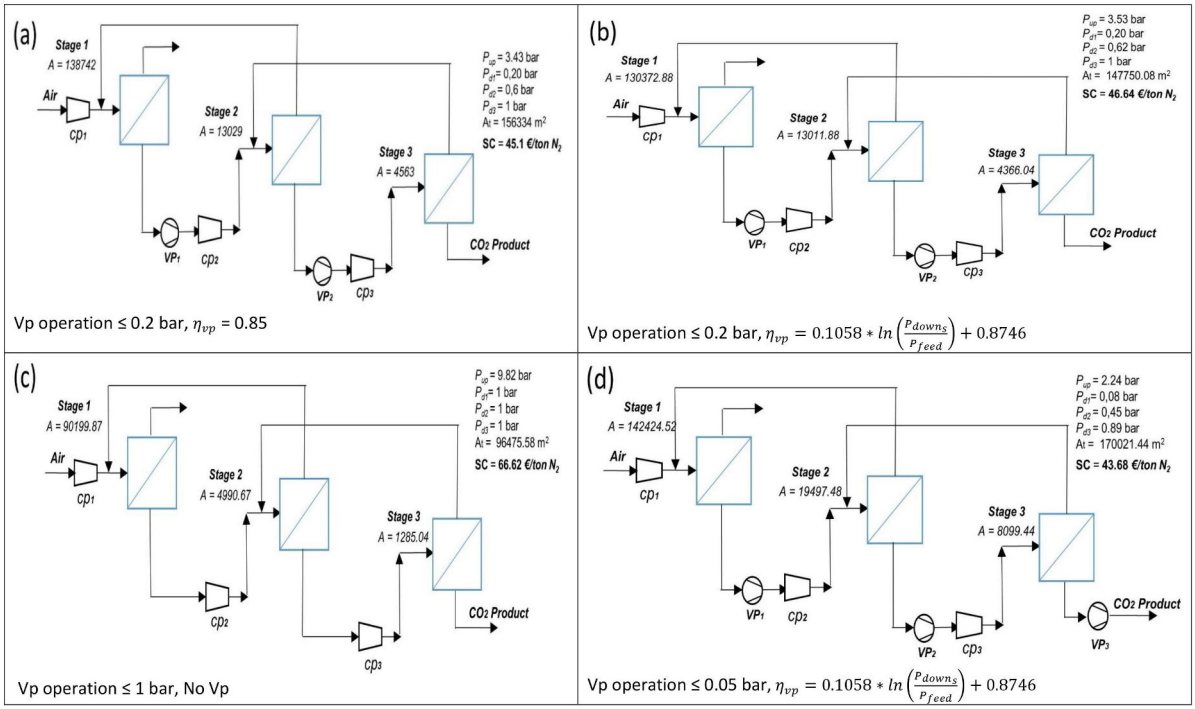

Figure 4.7: Investigating the vacuum pump effects by comparing optimal configurations (for CO_2 recovery from BFG in three stages membrane process with 99% CO_2 recovery and 0.1% N_2 residual content) with different vacuum efficiency.

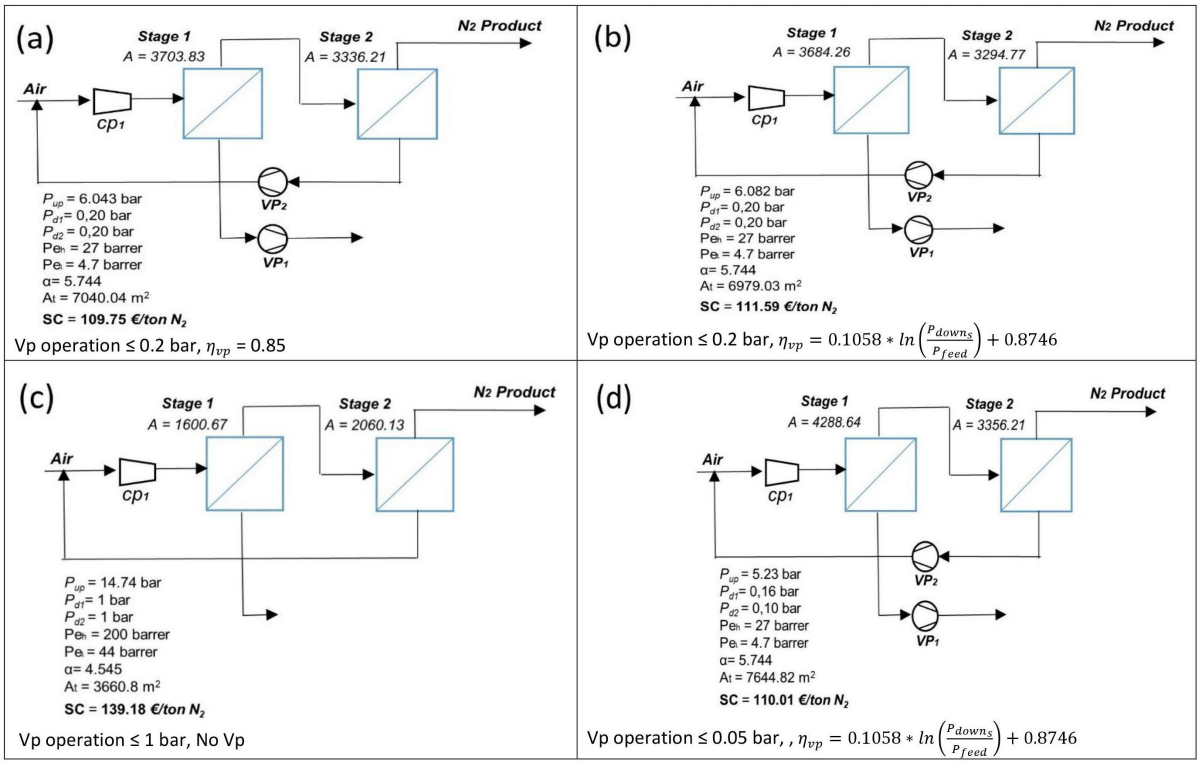

Figure 4.4: Investigating the vacuum pump effects by comparing optimal configurations (for two stages PSf membrane process with 99% N_2 production) with different vacuum efficiency.

In general speaking, for each case, all states have the same process configuration. As expected, the product cost significantly increases in the state of no vacuum pump in the system. Although in all cases, we have the maximum product cost in the state of not considering vacuum operating, the difference between 0.05 vacuum operating limitation and no vacuum pump operating in PPO case is much more PSf and CO_2 capture from BFG cases.

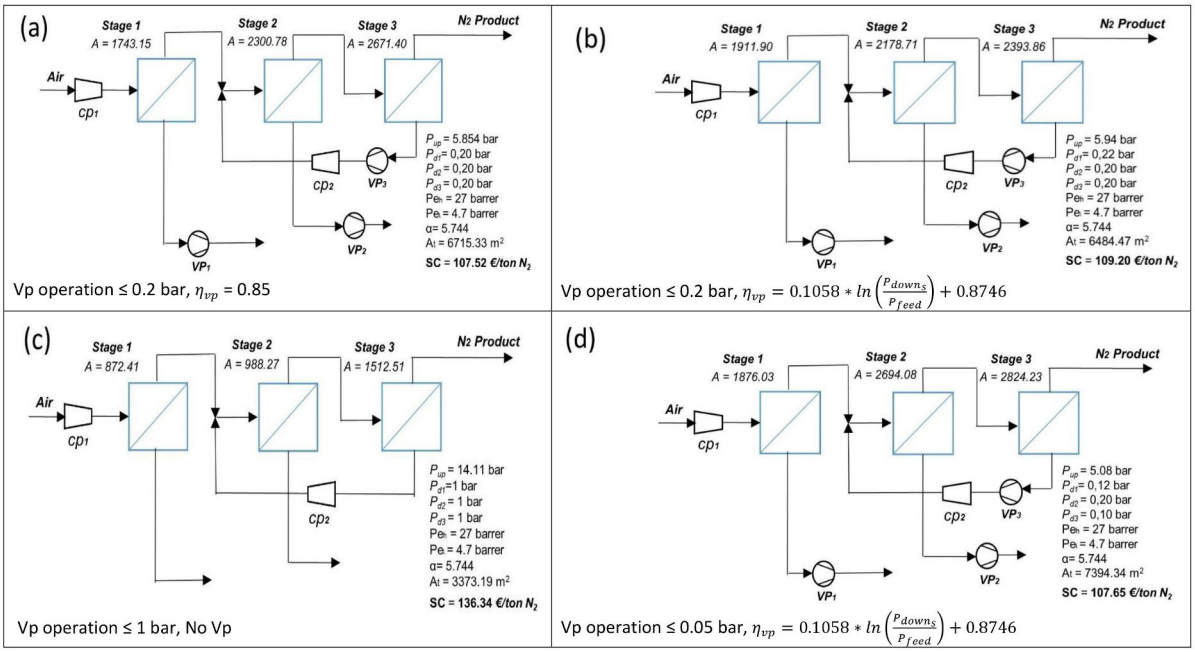

Figure 4.5: Investigating the vacuum pump effects by comparing optimal configurations (for three stages PSf membrane process with 99% N_2 production) with different vacuum efficiency.

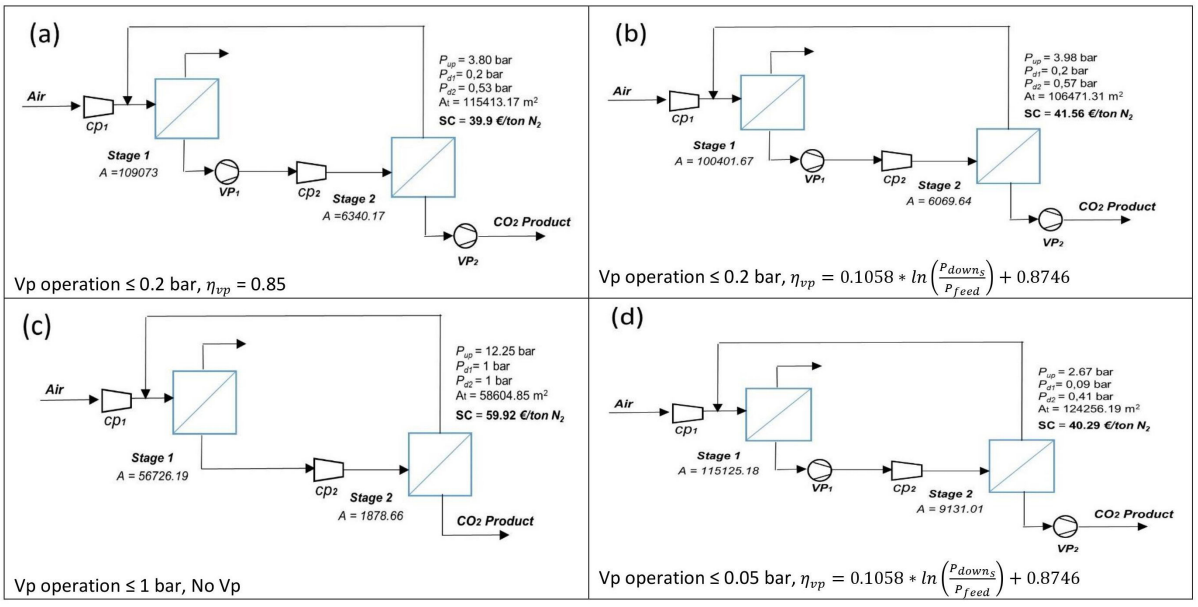

Figure 4.6: Investigating the vacuum pump effects by comparing optimal configurations (for CO_2 recovery from BFG in two stages membrane process with 99% CO_2 recovery and 1% N_2 residual content) with different vacuum efficiency.

4.4 Summary and conclusions

This chapter investigated systematically the effects of membrane performances on air separation process design.

The optimization method is adapted by adding new constraints concerning the performances variables. A generic and robust optimization model is presented to achieve the optimal membrane process design in terms of product cost and operating conditions.

The optimal membrane performance results demonstrates the importance of high permeable membrane rather than high selective one in NEA with polymeric membranes, regardless the N_2 purity target. In addition, the possibility of applying different membranes in a multistage process does not improve as much as expected the NEA results.

Although the practical use of vacuum pumps is not favored in industry for operability reasons, vacuum operation is of major interest. The effects of vacuum pump on membrane process design is studied, by comparing the optimal results of process with vacuum pump (and different efficiencies) or without vacuum pump. In order to have a general decision, this comparison has been done on the most critical cases of CO_2 capture form BFG and N_2 production from air with commercial membranes (PSf and PPO).

As expected, vacuum pump has a significant influence on a separation product cost. A 66% decrease of this cost is allowed by considering vacuum pump in the process.

Chapter 5

CO_2/CH_4 gas pair separation: Investigation on Biogas and Natural gas upgrading

This chapter presents a process synthesis study which aim is to identify the most efficient membrane materials (polymeric or high-performance ones) for the CO_2/CH_4 gas pair separation. The emphasize is done on two different case-studies: biogas and natural gas upgrading. A membrane process with up to three stages based on either polymer (cellulose acetate or polyimide) or high performance (zeolite) material has been considered. In the biogas upgrading case-study, three levels of outlet pressure (5, 10, and 15 bar) have been expected. Although the same components (CO_2 and CH_4) are considered for both case-studies, a main difference is represented by the value of the inlet stream pressures: 1 bar for the biogas upgrading and 60 bar for natural gas upgrading. Therefore, by considering the same membrane process, objective function, and optimization methodology the natural gas and biogas results are comparable in terms of CH_4 product cost and process configuration. Table 5.1 presents the decision variables and auxiliary equipment in CO_2/CH_4 gas pair separation.

The following of the chapter is organized as follows: in Section 5.1 the biogas purification case is reported, the material of this section is in the form of a publication (currently under revision), in section 5.2 an extension of this work, taking into account the possibility to set a different upstream pressure for each membranes is presented, and finally, in section 5.3 the natural upgrading case, will be studied extensively.

Table 5.1: Summary of decision variables and auxiliary equipment which are considered for optimization of CO_2/CH_4 *gas pair separation processes.*

Industrial application	Feed compositions	Area	P_{up}	P_{down}	# of stages	PermSelectivity	Auxiliary equipment			
							C_p	Expander	V_p	Valve
Biogas upgrading	$CO_2 - CH_4$	Var	Var & Uniform	Var & Ind.	up to three	fixed	✓	✓	✓	✓
Natural gas upgrading	$CO_2 - CH_4$	Var	Var & Ind.	Var & Ind.	up to three	Var and Ind.	✓	✗	✗	✓

5.1 Optimal membrane process design for biogas purification

This section is presented in the form of a publication. The paper has submitted in the Journal of Membrane Science and it is currently under revision. The impact of membrane performances and the outlet pressure on optimal membrane design and production cost is evaluated. This study demonstrates the importance of high performance membrane in minimizing the separation cost.

The proposed superstructure presented in Section 2.2, is adapted to this case study by considering the possibility of applying a compressor or an expander on outlet retentate stream to obtain the demanding outlet pressure. The mathematical optimization model is adapted by considering independently the two cases (compressor vs expander at the outlet) to keep the mathematical programming model continuous. Therefore for each case, the optimization algorithm is be executed twice (one for the compressor case and

one for the expander case) and then the two best solutions are analyzed and compared to obtain the overall best solution.

A new objective function is proposed to calculate the cost of the separation process. The difference of two states (application of compressor or expander) is implied in the objective function concerning the energy consumption calculation.

Optimal process design of biogas upgrading membrane systems: polymeric vs high performance inorganic membrane materials

M. Bozorg [a,b,c], Álvaro A. Ramírez-Santos [a], B.Addis [b], V. Piccialli [c], C. Castel [a], E. Favre [a,d]

[a] *Université de Lorraine, CNRS, LRGP, F-54000 Nancy, France*

[b] *Université de Lorraine, CNRS, LORIA, F-54000 Nancy, France*

[c] *Dipartimento di Ingegneria Civile e Ingegneria Informatica, Università degli Studi di Roma Tor Vergata, viale del Politecnico 1, 00133 Rome, Italy*

[d] *Corresponding author*

Abstract

Membrane separation is a key technology for biogas purification. Multistaged processes based on either cellulose acetate (CA) or polyimide (PI) materials are classically used for this application. In this study, a systematic process synthesis optimization is performed in order to identify the most cost effective solution for three different membrane materials (CA, PI, and zeolite) and three different outlet pressure levels (5, 10, and 15 Bar). It is shown that a costly (i.e. 2000 EUR per square meter vs 50 for CA and PI) but high performance membrane material such a zeolite offers the best cost effective solution compared to commercially available polymeric membranes. Increasing the outlet pressure increases the purification cost. Two stage processes with recycling loops offer the best balance between purity, recovery, complexity and cost, whatever the outlet pressure level. The use of vacuum pumping is shown to improve the process economy, while expander and extra feed compression do not show an interest.

Keywords: Membrane, Process, Synthesis, Biogas, Purification, Cost

5.1.1 Introduction

Biogas consists mainly of methane (CH_4) in a range of 50-70% and carbon dioxide (CO_2) at concentrations of 30-50%. Small amounts of other components are also present such as Nitrogen (N_2) at concentrations lower than 3%, water vapor up to saturation at the gas temperature, and oxygen (O_2) at concentrations lower than 1%; hydrogen sulfide (H_2S), ammonia (NH_3) and siloxanes can also be present in trace amounts depending of the biogas origin[64]. Biomethane is the term given to biogas that has been treated to remove all species besides methane and increase its concentration to meet transport and utilization specifications (equivalent to those of natural gas).

Biomethane can thus replace natural gas as a renewable, carbon neutral source since carbon present in biogas comes from sources having fixed that carbon from atmospheric CO_2. Any consumption of fossil fuels replaced by biomethane will lead to a net decrease of CO_2 emissions. Biogas treatment can be divided in a drying stage, where water is removed, a cleaning stage, where harmful or toxic compounds, mainly H_2S but also VOCs, siloxanes, CO and NH_3 are removed, and an upgrading stage where CH_4 concentration is increased mainly by the removal or existing CO_2. Water removal is done by a condenser and a demister or by adsorption technologies. Desulphurisation (H_2S removal) can be done by biological oxidation of the H_2S by aerobic sulphate oxidizing bacteria, by adding doses of iron hydroxide and/or iron salts during biomass digestion, by catalytic oxidation and adsorption with a material such as activated carbon or by caustic treatment with biological regeneration of the washing agent [65].

A number of technologies are available for biogas upgrading, these include: water scrubbing, physical scrubbing by organic solvents, chemical scrubbing by amine solutions, pressure swing adsorption, membrane separation and cryogenic separation [64]. All of these seek to separate the CO_2 in the biogas either by physical of chemical processes. New technologies under development include chemical hydrogenation processes and biological technologies seeking to produce either additional CH_4 from the available CO_2 or additional biomass that could be used for the extraction of high value added products or for biogas production in a circular economy[64].

Each of the available upgrading technologies has different advantages and disadvantages and they all aim to produce the highest CH_4 purity with the lowest CH_4 losses and energy consumption. Several reports exist in the literature reviewing the status and development perspectives of biogas upgrading technologies [64]–[69]. A summary of process metrics is presented in Table 5.2. There is not an overall better technology, and the best choice will depend on the specific, local conditions [65]. Additionally, total cost of ownership depends on the flowrate of raw biogas to be upgraded. For flowrates of up to around 1000 Nm^3/h of biogas, membrane upgrading has been cited as the cheapest technology, and a close alternative to water scrubbing at higher biogas flowrates [67], [70], [71]. Nevertheless confusion still exists as whether membrane upgrading is an overall expensive or inexpensive alternative as it is shown in Table 5.2. A more detailed information set on process comparison is shown in Apendix Table A.1.

Generally speaking, the main cost elements of membrane upgrading are the power consumption originating from the gas compressors/vacuum pumps (OPEX) and the compressors and membranes investment costs (CAPEX) [72]. To reach high CH_4 purities and recoveries, membrane upgrading is systematically based on multistage processes, for which the choice of the right membrane (or membranes), process architecture, and operating parameters are essential to reach the lowest cost possible. A few studies addressed cost analysis and process configuration analysis for biogas upgrading based on Process Systems Engineering approaches. For instance, two stage processes have been recently explored with cellulose acetate and carbon membranes [73], and polyimide two stage systems in another study [74]. A process synthesis study has been also performed with

a three stage process based on polyimide membranes, in order to achieve the maximal cost efficiency thanks to a process optimization methodology [35]. To our knowledge, no process synthesis study addressed a rigorous comparison of different membrane materials yet. More specifically, the key question of the potential interest of high performance (but often expensive) membrane materials for biogas (and natural gas) treatment, such as formulated by Baker [75], is thus unsolved.

In this paper, we present the application of a global optimization approach based on a NLP formulation of the optimization of membrane upgrading processes by means of a superstructure representation. This global optimization approach has been validated in a previous study [32]. Current upgrading membranes such as cellulose acetate and polyimide will be compared. In a second step, a high performance, inorganic membrane material will be explored. Among the different nanostructured materials which have been reported for biogas purification purpose (e.g. zeolites [76]–[78], silica [79], Carbon Molecular Sieves [80], [81], ...), we selected a commercially available zeolite membrane which has never been proposed for biogas applications. The aim is to evaluate from a process and cost perspective the impact of membrane performance. Moreover, the effect of the final pressure of the upgraded gas on the process cost and configuration is also considered since this has never been evaluated by Process Synthesis approaches. Biomethane injection pressure is indeed an important parameter for biogas infrastructure and pressure levels from 5 to 15 bar can be found depending on the location on the grid [73].

Table 5.2: Comparison between different methods of biogas upgrading

	Pressurized Water Absorption	Chemical absorption absorption	Pressure Swing Adsorption (PSA)	Membrane gas separation
CH_4 purity (%)	$\geq$ 98 %	$\geq$ 98 %	$\geq$ 97%	$\geq$ 98%
CH_4 Recovery (%)	$\geq$ 98 %	98-99 %	$\geq$ 92%	98-99%
Removed compounds	CO_2, VOC′s	CO_2, VOC′s	CO_2, VOC′s, O_2 N_2	CO_2, VOC′s, H_2O O_2
Energy requirement (kWh/Nm^3 raw biogas)	0.24-0.4	0.6-0.7	0.23-0.4	0.2-0.3
Cost efficiency	++	+/-	+/-	+++

5.1.2 Process synthesis methodology

5.1.2.1 Optimization method for membrane gas separation

In this study, a membrane process with up to three stage has been considered with the possibility of using a compressor or an expander for the product stream, with three

different product pressure levels (5, 10, or 15 bar). In order to achieve this target with a minimum process cost, the membrane process should be optimally designed. The optimal design of a membrane process means to determine the best possibility for the number of stage, the membrane material (polymer or inorganic), the elements included in the system (e.g. mixers, splitters, compressors, expanders, vacuum pumps and other necessary equipments; specially the compressor or expander on the product stream), their operating conditions and their connections. This requires a rigorous mathematical modeling approach in order to optimize the design of membrane separation systems. Process synthesis methods applied to membrane systems are intensively investigated, following the pioneering analysis of mass exchange networks by El-Hawagi in the 90's [32]. Numerous variants in terms of equipment, connection possibilities, set of constraints and objective function (i.e. overall cost function) can be found. While numerous process synthesis studies addressed the problem of carbon capture, hydrogen purification, Oxygen Enriched Air (OEA) and natural gas treatment, very few publications are reported for biogas purification. The most recent and detailed study has been performed by Scholz et al., with a structural optimization approach making use of GAMS software. A three stage process based on polyimide membranes is investigated, making use of a single compressor for an outlet pressure of 16 Bar. A parametric study shows that increased selectivities significantly improves the economy of the process. A limited set of connections (e.g. no self recycling loop), no vacuum pumping and a single outlet pressure are investigated.

In this study, a general and systematic optimization model for membrane process proposed in [32] is used, which takes into account all the mentioned possibilities as a degrees of freedom in a membrane system (vacuum pumping, self recycling loops). Moreover, three different outlet pressure levels are taken as constraints, for three different membrane materials. The overall target is to identify to what extent improved commercially available membrane materials, extended connection possibilities and supplementary equipment options (vacuum pump, expander) impact the biogas purification cost.

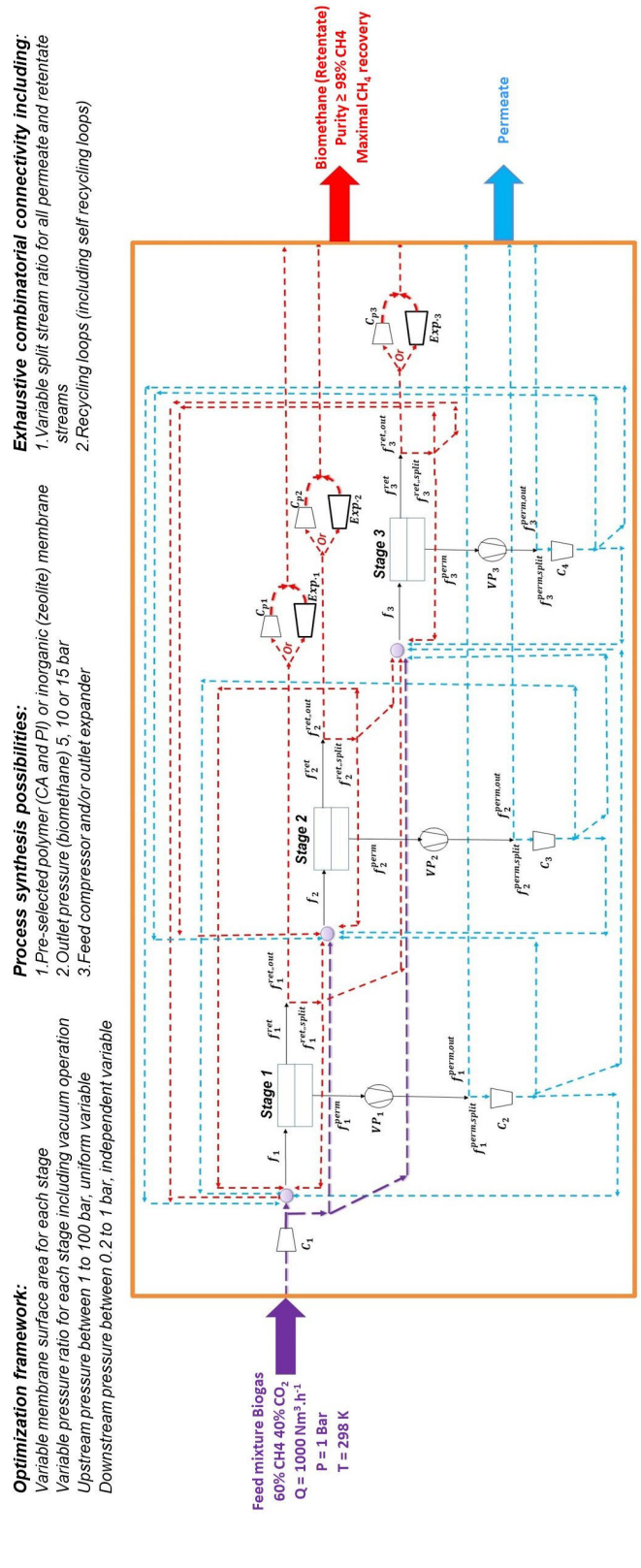

Figure 5.1: Overall process synthesis framework applied in this study. A membrane separation process including up to 3 stage with compressors and/or vacuum pumps and/or product compressor and/or expander is used. Multiple connection possibilities including recycling loops is applied to achieve biomethane with three levels of product pressures. The different configuration possibilities and operating variables are taken into account in order to achieve the lowest production cost (i.e. objective function, detailed in Tables 5.3 and 5.4).

More specifically, the overall process cost which is taken as the objective function of the optimization model, is the modification of [32] separation cost and [73] cost parameters. It takes into account the capital expenses (CAPEX) such as membrane area and membrane frame, vacuum pumps, compressors or expanders and the operating costs (OPEX), such as contract and material maintenance cost, local tax and insurance, labor overhead cost, energy requirement, membrane replacement and total operation. The cost function used for biogas upgrading and the parameters used in the objective function are detailed in Table 5.3 and Table 5.4 respectively. The energy requirement equations are explained in detail in 5.1.B.

Table 5.3: Cost equations used to determine product gas separation cost

Equipment cost		
$I_{m_s} = A_{m_s} \cdot K_m$	(5.1)	Membrane cost
$I_{mf_s} = (A_{m_s}/2000)^{0.7} \cdot K_{mf} \cdot (p^{up}/55)^{0.875}$	(5.2)	Membrane frame cost
$I_{c_s} = C_c \cdot (W_{cp_s}/74.6)^{0.77} \cdot (MPF_c + MF_c - 1) \cdot UF_{1968} \cdot K_{er}$	(5.3)	Stage compressor cost
$I_{c_f} = C_c \cdot (W_{cp_f}/74.6)^{0.77} \cdot (MPF_c + MF_c - 1) \cdot UF_{1968} \cdot K_{er}$	(5.4)	Feed compressor cost
$I_{c_{prod}} = C_c \cdot (W_{cp_{prod}}/74.6)^{0.77} \cdot (MPF_c + MF_c - 1) \cdot UF_{1968} \cdot K_{er}$	(5.5)	Retentate compressor cost
$I_{exp} = C_{exp} \cdot (W_{exp}/0.746)^{0.81} \cdot (MPF_c + MF_c - 1) \cdot UF_{2000} \cdot K_{er}$	(5.6)	Expander cost
$I_{vp_s} = C_{vp} \cdot (W_{vp_s})$	(5.7)	Vacuum pump cost
Capital expenditures		
$PFC = I_{c_f} + I_{c_{prod}}$ or $I_{exp} + \sum_{s \in \mathcal{S}} I_{m_s} + I_{mf_s} + I_{c_s} + I_{vp_s}$	(5.8)	Process facilities capital
$BPC = 1.12 \cdot PFC$	(5.9)	Contingency cost
$PC = 0.2 \cdot BPC$	(5.10)	Base plant cost project
$TFI = BPC + PC$	(5.11)	Total facility investment
$STC = 0.10 \cdot OPEX$	(5.12)	$Start - up$ cost
$CAPEX = TFI + STC$	(5.13)	Total capital cost
Operational expenditures		
$CMC = 0.05 \cdot TFI$	(5.14)	Contract and material maintenance cost
$LTI = 0.15 \cdot TFI$	(5.15)	Local taxes and insurance
$DL = 11 \cdot t_{op}$	(5.16)	Direct labor
$LOC = 1.15 \cdot DL$	(5.17)	Labor overhead cost
$EC = t_{op} \cdot W_{tot} \cdot K_{el}$	(5.18)	Energy cost
$MRC = \sum_{s \in \mathcal{S}} A_{m_s} \cdot \nu \cdot K_{mr}$	(5.19)	Membrane replacement cost
$OPEX = CMC + LTI + DL + LOC + EC + MRC$	(5.20)	Total operational expeditures
Annual and specific separation costs		
$APL = F^{PERM} \cdot 3600 \cdot 0.0224 \cdot K_{gp} \frac{X^{PERM}_{CH_4}}{X^{RET}_{CH_4}}$	(5.21)	Annual CH_4 losses
$TAC = CAPEX \cdot \frac{i \cdot (1+i)^{z-1}}{(1+i)^z - 1} + OPEX + APL$	(5.22)	Total annual costs
$SC_{CH_4} = TAC/(F^{RET} \cdot 3600 \cdot t_{op} \cdot 0.0224)$	(5.23)	Specific CH_4 separation cost

Table 5.4: Cost parameters used in Table 1

Capital cost parameters		
C_c	1×23000	USD_{1968}
C_{vp}	1000	EUR/kW
C_{exp}	420	USD_{2000}
K_m(polymer)	50	EUR/m^2
K_m(zeolite)	2000	EUR/m^2
K_{mf}	2.86×10^5	EUR
K_{er}	0.9	EUR/USD
MPF_c	2.9	-
MF_c	5.11	-
UF_{2000}	1.44	-
UF_{1968}	4.99	-
Operational and annual cost parameters		
ν	0.25	-
K_{mr}(polymer)	25	EUR/m^2
K_{mr}(zeolite)	2000	EUR/m^2
t_{op}	8322	h/year
K_{el}	0.08	EUR/kWh
K_{gp}	0.8	EUR/Nm^3
i	0.08	-
z	15	years
η_c	0.85	-
Φ	0.95	-
γ	1.36	-
R	8.314	$J/(K \cdot mol)$
T	293.15	K

The optimal process configuration and the associated operating conditions for the specific target (biomethane under product pressure) are achieved thanks to a a continuous global optimization algorithm presented in [32] to solve the proposed optimization model with the mentioned objective function.

5.1.2.2 Biogas purification process: Case study

A biogas with a flowrate of 12.393 mol/s, corresponding to around 1000 Nm^3/h is considered. Inlet gas pressure and temperature are 1 bar and 293.15°K respectively. A classical biogas composition, detailed in Table 5.5 is used [35]. Product purity is expressed in terms of CH_4 content in the outlet stream with the constraint of at least 98% CH_4, together to minimal methane losses in terms of optimization constraints (Figure 5.1).

Table 5.5: Biogas compositions

Gas component	Composition (%mol)
CH_4	60
CO_2	40

Process configurations up to three membrane stage are studied. The module pressure ratio is variable through a range of downstream and upstream pressure allowed for the optimization. Upstream pressure is the same for all the stages in the system. Technically, by considering vacuum pumping for each permeate stream in the system, the downstream pressure level is allowed to vary between 0.2-1 bar, while upstream pressure vary between 1-100 bar.

The goal of the study is to identify the most effective process structure and operating conditions, which reach the specifications (biomethane with target purity, maximal recovery and outlet pressure level) at the lowest cost. In order to achieve this aim, a system with polymeric membranes (cellulose acetate and polyimide) is first considered and the effects of the three different levels of biomethane pressure on process structure, operating conditions and process cost is studied. In a second step, the same scenario is performed on a process with inorganic (zeolite) membrane performances. Table 5.6 presents the performances of polymers and inorganic membranes used for the process synthesis study.

Table 5.6: Membranes characteristics used for the Process Synthesis study

Membrane material	P_{CO_2}(GPU)	P_{CH_4}(GPU)	Cost (EUR/m^2)	References	Comments
Cellulose Acetate (CA)	60	3	50	[35]	First commercialised membrane material for CO_2/CH_4 separation
Polyimide (PI)	60	1	50	[35]	Second generation polymeric membrane material (improved selectivity, close to trade-off limit)
Zeolite	3500	22	2000	[78]	High performance inorganic membrane material (breakthrough permeance and selectivity)

Figure 5.2a shows the permeability/selectivity trade-off for CO_2/CH_4 polymeric membrane materials [28]. The performances of the three membranes (CA, PI, and Zeolite) investigated in this study are reported in Figure 5.2b, where a one micron active layer thickness is used for the trade-off permeance calculation. The very large selectivity and permeance performances of the zeolite membrane, compared to existing polymeric membrane materials, is highlighted. This is however associated to a very high cost (Table 5.6). The balance between very high performances membrane material and very high cost will thus be analysed through this study.

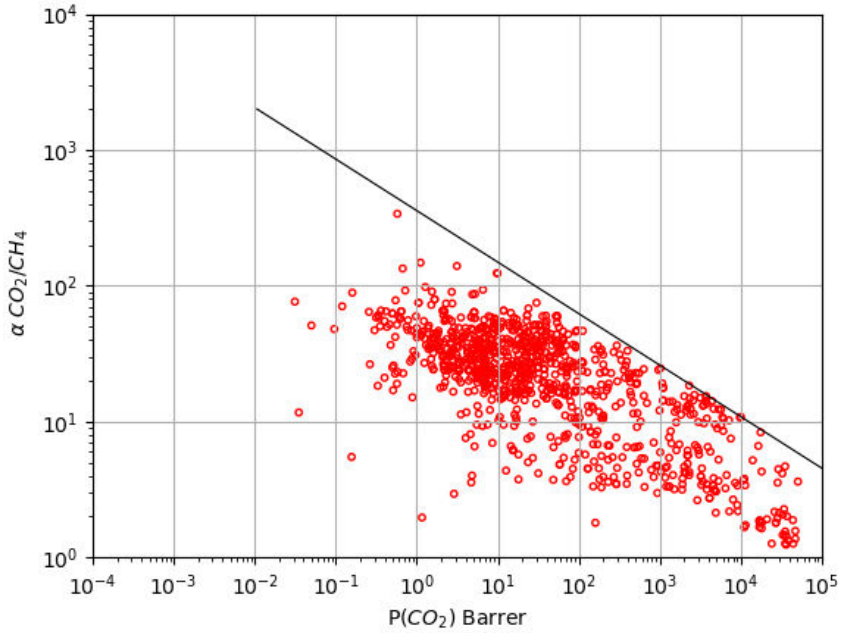

(a) CO_2/CH_4 selectivity / permeance trade-off curve of different commercial membranes [28]

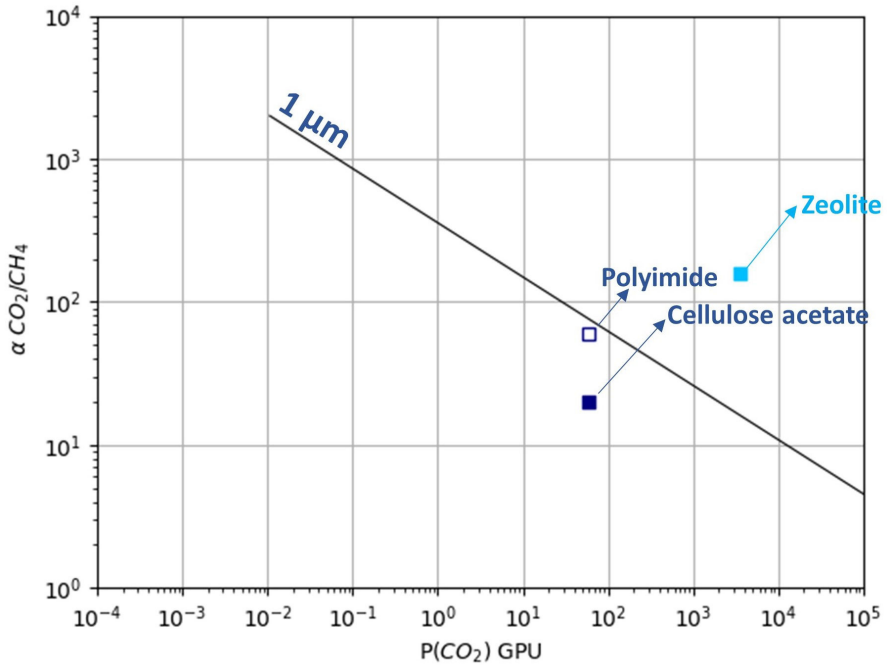

(b) Selectivity / permeance trade-off curve based on a 1 μm skin layer thickness and performances of two polymers (Polyimide and Cellulose acetate) and one inorganic (Zeolite) membrane materials.

Figure 5.2: Trade-off curves for CO_2/CH_4 gas pair based on permeability for different polymeric materials (a) and permeance for gas separation membranes (b)

In order to attain biomethane specifications, the possibility of using compressors and/or vacuum pumps and/or an expander on the product stream is investigated. In a first step, the upstream pressure is considered between one bar and the target outlet pressure. Then, the possibility of using/not using a compressor for the product stream is investigated. The product compressor cost (Equ. 5.5) and the corresponding the PFC (Equ. 5.8) are included in the objective function for that purpose. In a second step, the same senario is performed with a product stream pressure between the target pressure and 100 bar. The possibility of using/ not using an expander (i.e. an Energy Recovery System) for the product stream is thus explored. The expander cost (Equ. 5.6) and the associated PFC (Equ. 5.8) are then included in the objective function. The optimal process structure is finally obtained by comparing the results of these different steps for all cases (up to three stage, different membranes and different biomethane pressure levels).

The general methodology of the study is sketched in Figure 5.3. The idea is to provide, through Process Synthesis, a set of optimal solutions to the problem (upper part of the figure), so that the decision maker has an exhaustive view of the different possibilities in the process selection step (lower part of the figure).

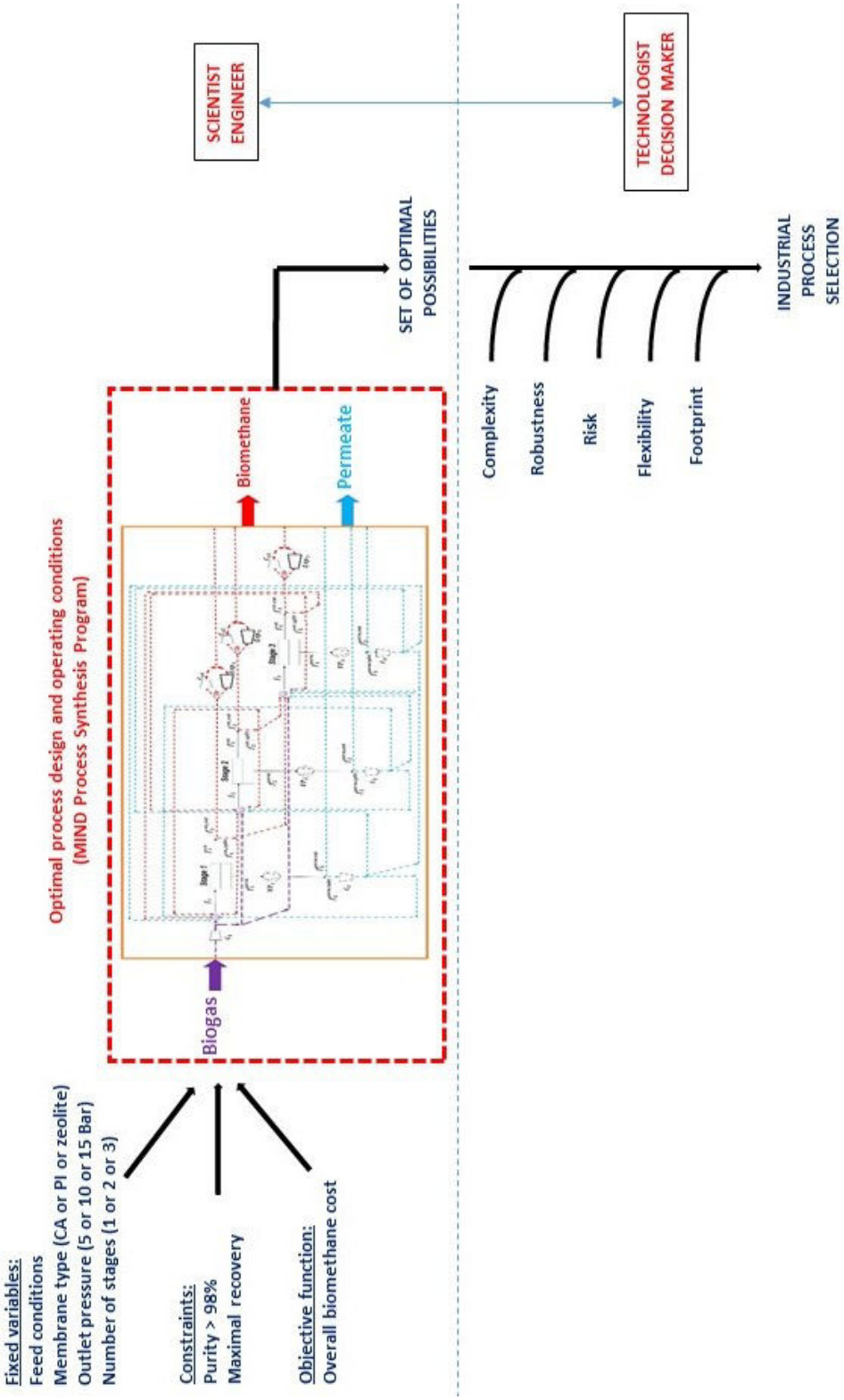

Figure 5.3: Generic representation of the different steps of a process selection strategy. Process synthesis in a first step proposes a portfolio of optimal solutions for different membranes, number of stages and operating conditions. A decision maker can then use this information set in order to select the best trade-off between cost, complexity, risk and flexibility

5.1.3 Results and discussion

5.1.3.1 Biogas purification by commercially available polymeric membrane materials

Polymeric membranes are classically used for gas separation applications [82], [83]. Polymers indeed offer low production cost, selective permeability, ease of processing and scaling up characteristics [69], [83], [84]. Cellulose acetate (CA) and Polyimide (PI) are preferred for biogas purification [72].

Figure 5.4 shows the optimal process configurations for biogas upgrading with three levels of biomethane pressure levels and for up to three membrane stage. Interestingly, the optimal process configuration is almost not impacted by the outlet pressure level. For one stage configurations, a recycling loop offers the best cost performances, whatever the outlet pressure. A significant cost decrease is obtained with two stage configuration. Again outlet pressure does not impact optimal configuration. Three stage processes generate a slightly lower purification cost compared to two stage. Two recycling loops are obtained in that case. This suggests two stage processes to be favored in place of three, when complexity is taken into account. This results corroborates classical industrial practice, where two stage processes are most often applied, be it for natural gas or biogas purification applications [72].

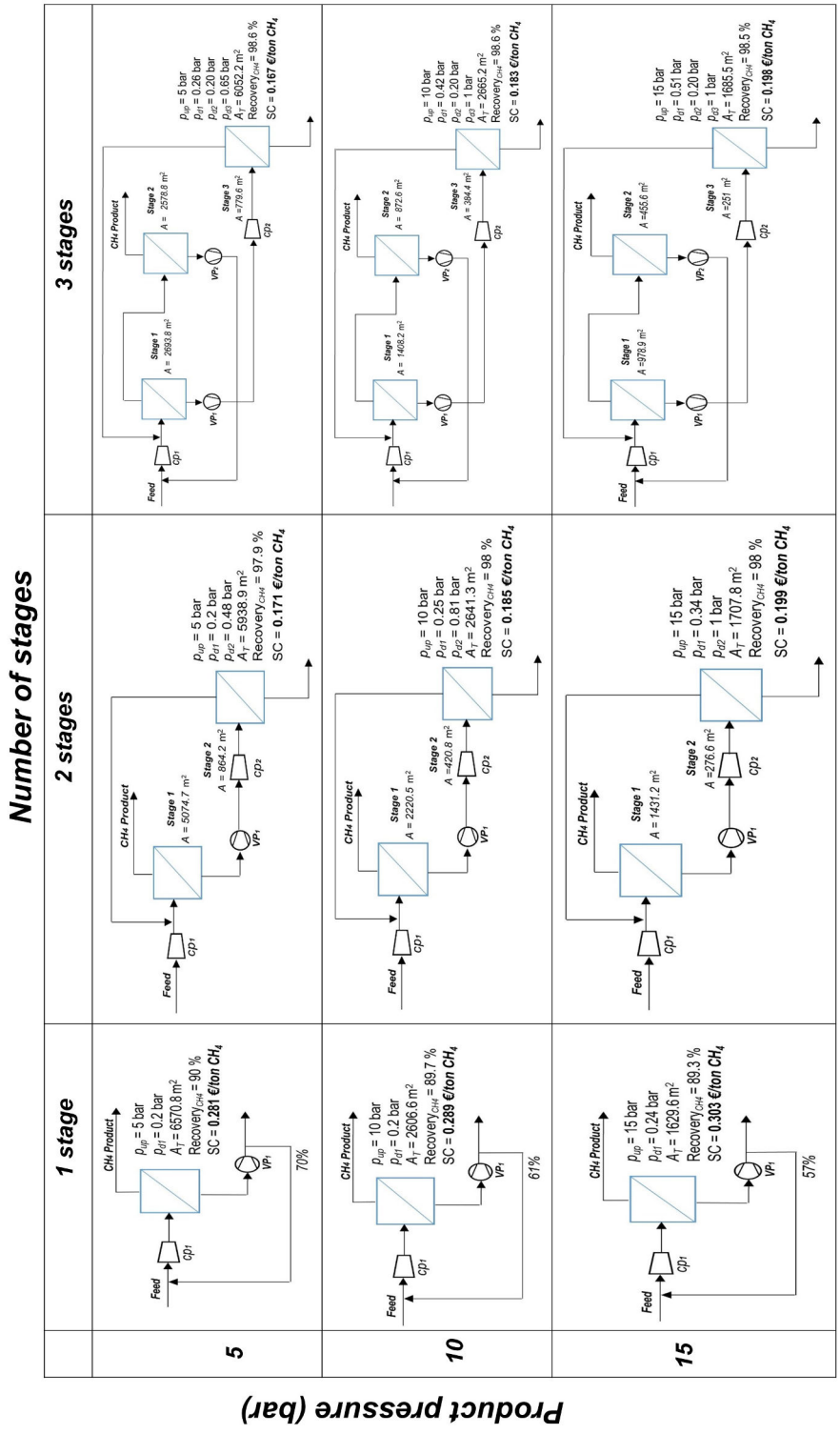

Figure 5.4: The best process configurations obtained with cellulose acetate membrane for up to three membrane stage and different levels of product pressure

Figure 5.5 shows the optimal process configurations for a polyimide (PI) membrane based process with up to three membrane stage and different product pressures.

PI is a second generation membrane material, which offers improved selectivity compared to CA (Table 5.6)[69], [83]. Globally speaking the results obtained with PI are close to those obtained with CA in terms of process structure and characteristics. The major difference comes from the lower purification cost obtained with PI membranes. Costs increase with outlet pressure level, decrease with the number of stages, but again with a very low difference between two and three stage. Expander and extra compression options are not interesting. A single stage process with a recycling loop is obtained for 5 bar pressure level, while a recycling loop is not included for 10 and 15 bar. Purification costs vary from 0.194 to 0.142 EUR/Nm^3 CH_4 depending on the outlet product pressure. With a single stage process, the separation cost is increased from 26.2% to 11.17% approximately in comparison to a two stage process.

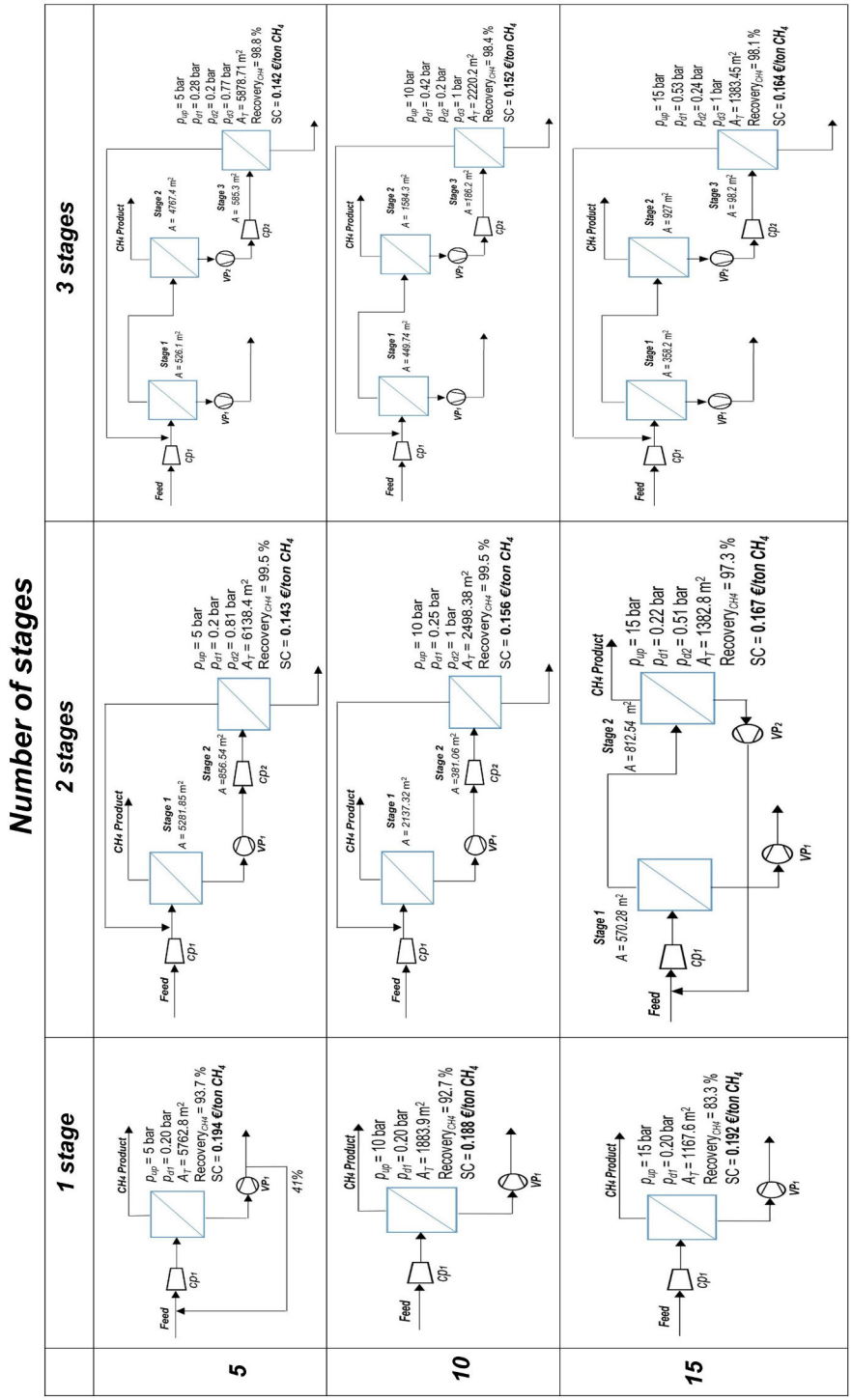

Figure 5.5: The best process configurations obtained with polyimide membrane for up to three membrane stage and different levels of product pressure

5.1.3.2 Biogas purification by high performance inorganic zeolite membrane

In the last part of the study, an inorganic zeolite membrane, showing breakthrough gas separation performances (beyond the Robeson upper bound) which is investigated in Figure 5.2b).

The optimal process configurations with up to three stage and three outlet pressure levels are shown in figure 5.6.

Globally speaking, the trends obtained with CA and PI are similar: purification costs decrease with the number of stages, a large improvement is obtained between one and two stage, a small cost improvement is obtained with three stage compared to two. Increased outlet pressure levels increase the purification costs. Extra compression and/or expander are not useful. Two stage configurations make use of one recycling loop, while three stage make use of two.

But, the most significant result of the zeolite membrane use is the large decrease in purification cost compared to CA and PI. The key question of the balance between high performances at the expense of a high cost is thus answered. Other aspects and limitations of zeolite membranes obviously have to be taken into account (few suppliers, lower compacity, mechanical resistance, sensitivity to water...). Coming back to the questions indicated in the introductory part, it can be stated that high performance zeolite membranes offer very attractive potentialities for biogas upgrading applications; the optimal process design are similar to PI processes. The very high permeance logically generates impressive decrease of the membrane surface area, while the high selectivity improves the energy efficiency.

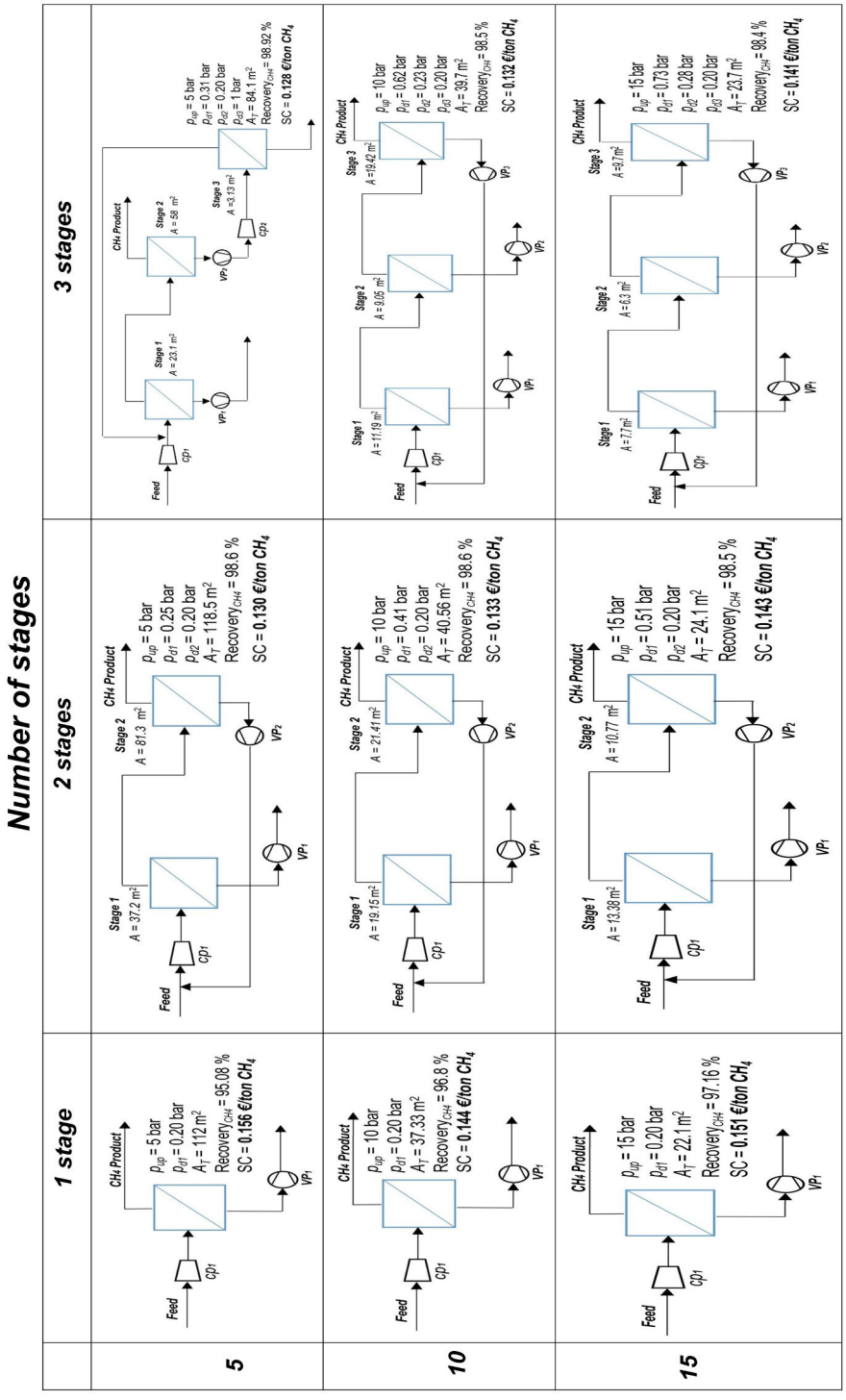

Figure 5.6: The best process configurations obtained with zeolite membrane for up to three membrane stage and different levels of product pressure

Figure 5.7 displays the overall separation cost of the optimal process configurations presented in the Figures 5.5, 5.4, and 5.6 regards to the range of the target product pressures for process with one, two, and three stage. Figure 5.7 shows that although the separation cost of a single stage process with all of mentioned membranes is dramatically more than two and three stage process, the separation cost of two and three stage process are quite close.

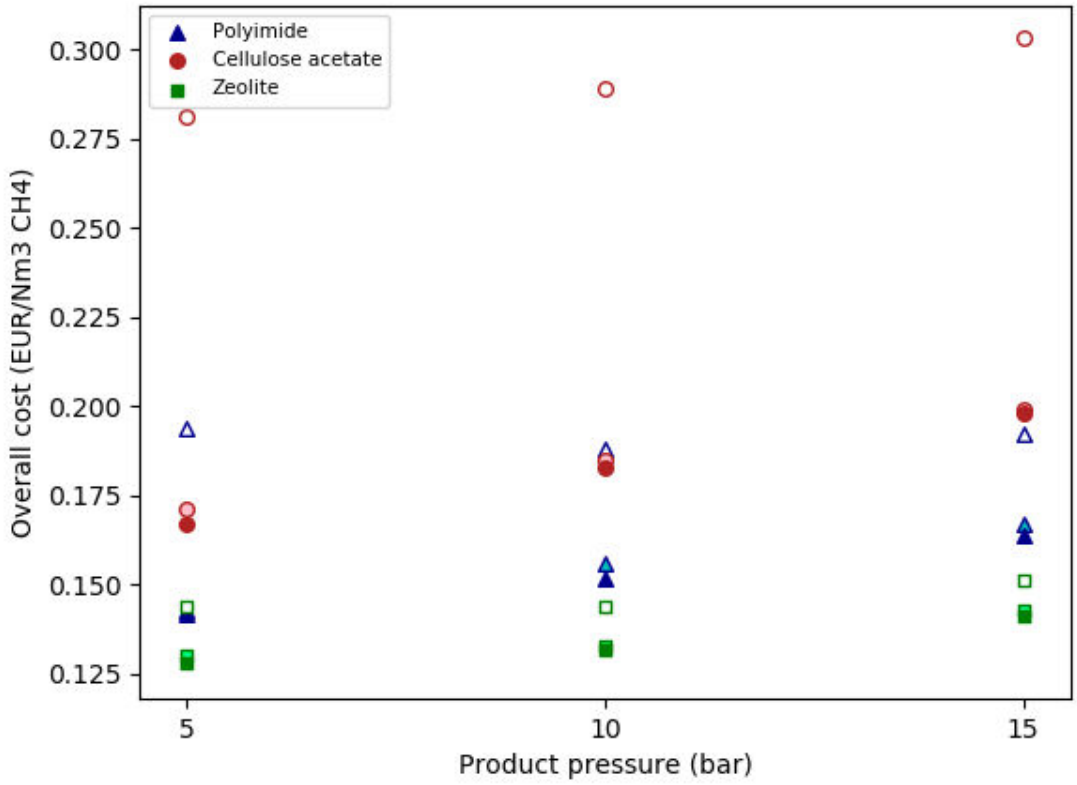

Figure 5.7: Overall separation cost vs product pressure for the optimal configurations obtained with different membranes. Open, light and dark symbols correspond to one, two and three stage processes respectively.

Minimal biogas purification costs as a function of a target product pressure are presented for the three different membranes and different number of stages in Figure 5.8. The benefits of PI vs CA and zeolite vs polymeric membrane materials is clear. The very small difference between two and three stage, whatever the membrane type is also noticeable.

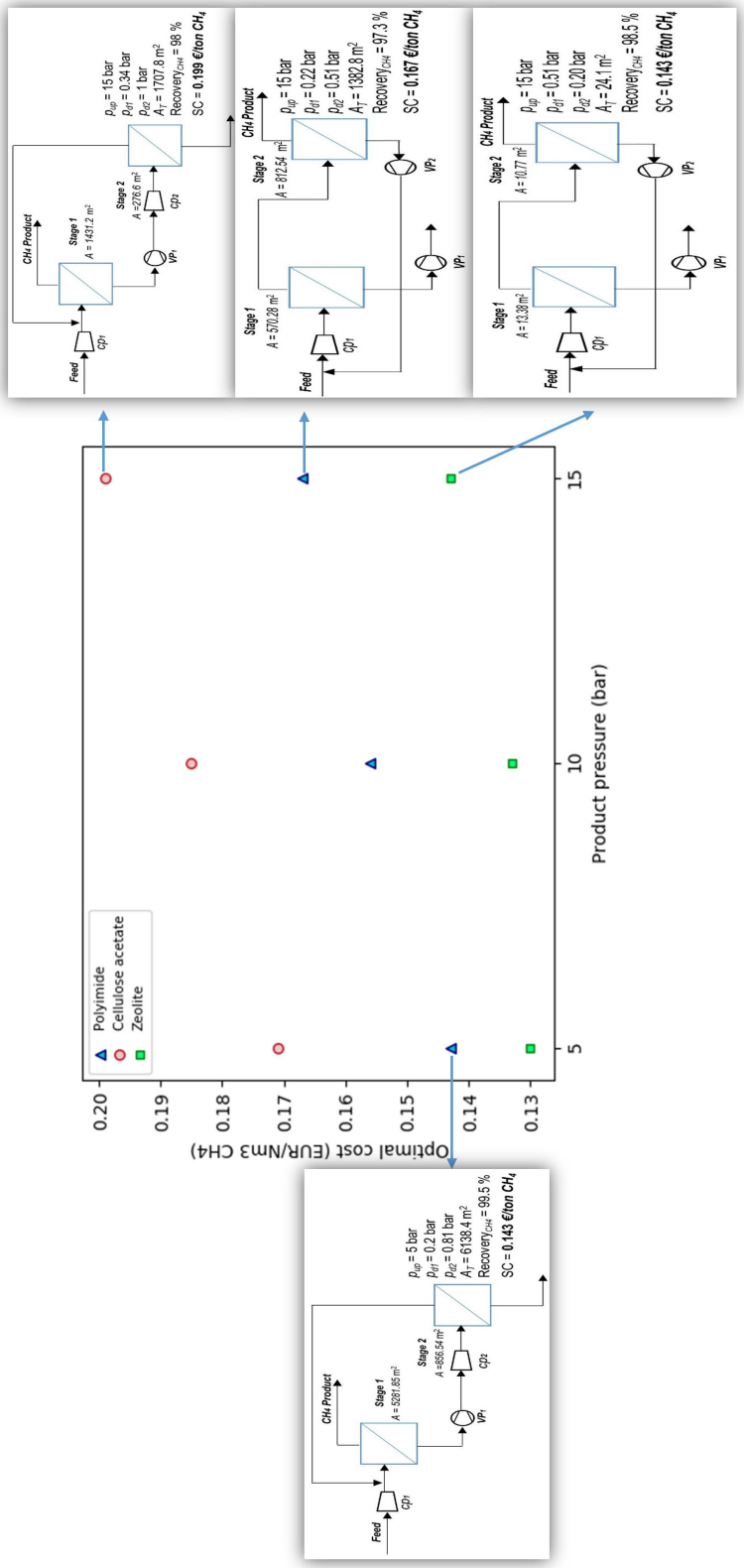

Figure 5.8: Minimal separation cost vs outlet product pressure for the different optimal two stage configurations obtained with the three different membranes.

5.1.3.3 Synopsis

A synopsis of the process configuration results generated through the process synthesis study is shown in Table 5.7. Taking the two stage optimal solution as the best balance between efficiency, cost and complexity, it can be seen that only two types of configurations are finally obtained. Interestingly, these two configurations, namely retentate recycle (left side of Figure 5.8) and permeate recycle (right side of Figure 5.8) have been already used by previous authors for biogas purification process studies. The retentate recycle option has been used for technico-economical studies [73] or process design studies [85], [86]. Alternatively, some authors only explore the performances of the permeate recycle configuration, either with two stage [74] or three stage [35], [42].

A larger outlet pressure generates a larger cost, which is significantly decreased with a zeolite membrane; in that latter case, the very high permeance of the membrane largely decreases the membrane surface area. The OPEX/CAPEX share ratio is roughly the same, whatever the membrane type and outlet pressure. The energy efficiency is in the range reported for membrane biogas upgrading units (Table 5.2).

Table 5.7: Summary of the best process configurations for biogas purification with polymer membrane (PI) and inorganic membrane (Zeolite).

	Polyimide membrane (PI)			Zeolite membrane		
Target product pressure (bar)	5	10	15	5	10	15
Number of stages	2	2	2	2	2	2
Process configuration	Retentate Recycle	Retentate Recycle	Permeate Recycle	Permeate Recycle	Permeate Recycle	Permeate Recycle
Overall cost (EUR/ Nm^3CH_4)	0.143	0.156	0.167	0.130	0.133	0.143
CAPEX(%)	81.7	81.8	82.5	77.9	80.1	81.8
OPEX(%)	18.3	18.2	17.5	22.1	19.9	18.9
Biomethane purity(%)	98	98	98	98	98	98
Biomethane recovery(%)	99.5	99.5	97.3	98.6	98.6	98.5
Overall membrane surface area(m^2)	6138.4	2498.4	1382.8	118.5	40.56	24.1
Stage cut	0.39	0.39	0.40	0.39	0.40	0.40
Energy efficiency (kWh/Nm^3)	0.27	0.29	0.33	0.21	0.26	0.30

The results summarized in Table 5.7 address a key question concerning the set of conditions which lead to either the retentate or permeate recycle option for a two stage process. To our knowledge, no systematic explanation of the criteria which induce the selection of one or the other of these two possibilities is available. Table 5.7 suggests that for a highly selective membrane and/or a high pressure, the permeate recycle configuration is the best choice.

We report in Table 5.8 a qualitative analysis of the conditions which will make one or the other of these two possibilities the best option. The key indicator is the extent of methane losses on the permeate outlet in the first stage. For a low selectivity membrane material, and/or low pressure difference, and/or high stage cut, the methane losses will be important [75] and it is logical to recover the permeate stream of the first stage and

recycle the methane from the retentate of the second stage. On the contrary, for a very selective membrane, and/or a high pressure difference, and/or a low stage cut, methane losses in the first stage will be low. In that case, it is more interesting to further increase the methane purity in a second stage, and recover the methane losses from the permeate of the second stage.

Table 5.8: Analyzing the optimal process results of polymer and zeolite membranes in biogas upgrading

Materials: Membrane selectivity	Low	High
Driving force: Transmembrane Pressure	Low	High
Productivity: Stage cut	High	Low
Process type	Low process selectivity of the first stage (Methane permeate flux maximal in first stage)	High process selectivity of the first stage (Methane permeate flux minimal in first stage)
Optimal configuration (2 stage example)	First stage permeate recovery and second stage retentate recycle to feed	Second stage permeate recycle to feed
	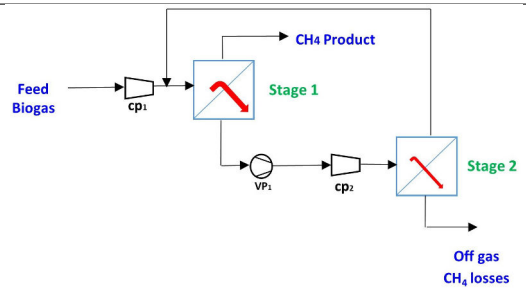	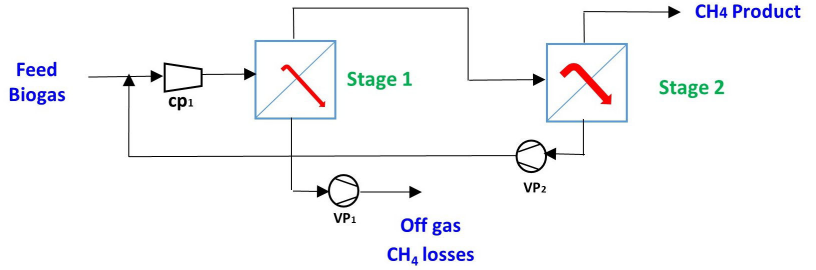
Equipment	2 compressors 1 vacuum pump	1 compressor 2 vacuum pumps
Examples	Low selectivity (e.g. CA) membrane and/or low transmembrane pressure (Biogas)	High selectivity (e.g. PI, zeolite) membrane and/or high transmembrane pressure (natural gas)
References	[73], [85], [86]	[35], [42], [74], [85]

5.1.4 Conclusions and perspectives

The objective of this study was to investigate the impact of high performance membrane materials, extended equipment and process connection possibilities and outlet pressure levels on biogas purification costs.

The results can be summarized as follows:

- A high performance, very expensive (e.g. 2000 EUR per square meter) membrane material offers promising perspectives in terms of biogas purification cost. This result confirms the attractiveness of high performance, costly materials, such as generally suggested by Baker, for the specific case of biogas purification. It can be linked to the fact that for membrane gas separations, capital expenses are by far dominated by compressor costs, while membrane cost have a limited impact. In terms of materials performances, the interest of increased selectivity can be seen from the comparison between cellulose acetate and polyimide; the interest of both improved selectivity and permeance is shown by the zeolite membrane decreased costs.

- Optimal process designs are only slightly affected by membrane performances. Generally speaking, a two stage process with either a retentate or permeate recycling loop is expected to offer the best balance in terms of purity / recovery / process complexity and cost. This conclusion corroborates heuristics in CO_2/CH_4 membrane separation processes, such as classically used for natural gas treatment. It also shows that such a design is robust, whatever the membrane type or outlet pressure level.

- An increased outlet pressure logically generates higher purification costs; extra compression (i.e. feed compression above the outlet pressure level) or an expander do not improve the process economy

- Vacuum pumping is systematically applied for optimal process, whatever the outlet pressure level and number of stages. A moderate vacuum pumping is obtained through optimization (typically 0.2 to 0.5 Bar). This result is noticeable and suggests a more detailed analysis and evaluation for this option. Vacuum pumping is indeed almost systematically discarded for membrane gas separations, because of leaks issues, low energy efficiency and large footprints. Carbon post combustion capture and Oxygen Enriched Air are exceptions for which vacuum pumping is suggested. To our knowledge, vacuum pumping has never been applied for biogas purification, neither investigated for process synthesis studies for this application.

Finally, this study could be extended to more complex systems such as multicomponent feeds (impact of water or nitrogen), multimembrane systems (is there any interest to combine different membranes into multistaged units?) or multitarget applications (e.g. combined biogas purification and carbon capture objective).

The improvements suggested by this study logically remain to be evaluated within a technological and industrial constrained context. For instance, the use of vacuum pumps cannot be accepted unless breakthrough cost savings are obtained and risk issues (i.e.

oxygen in permeate due to leaks) are solved. Process complexity is also a problem and simple designs with minimal compressors, vacuum pumps, and connections will clearly be favored. We think however that the rigorous and exhaustive set of optimal process designs and operating conditions reported in this study will be of interest for decision makers in order to push the economy of biogas purification applications.

5.1.A Detail table of biogas purification methods:

Table A.1: Comparison of commercial biogas upgrading technologies. [64]–[70]

	Water scrubbing	Physical organic scrubbing	Chemical absorption	Pressure swing adsorption	Cryogenic separation	Membrane separation
CH_4(%) in upgraded gas	95-98[69]; >97[66]; >98[70]; 90-99[65]	>96, <93-98[69]; >97[66]	>98[69], [70]; >99[65], [66]	>96-98[69]; 95-99[66];97[70]	99[69]; 98[66]; 99.9[65]	90-92,96[69]; ;>98[64], [70]
CH_4 recovery (%)	>98[66], [68]; 96-98[64]; 98[70]; 98-99.5[65]	>97[68]; 96-98[64];	>99[68]; 96-99[64]; 98-99[70]	95-98[68]; 96-98[64];	90-98[68]; 97-98[64];	>96[68];96-98[64]; 98-99.5[70]
Removed elements	CO_2, H_2S, COV	CO_2, H_2S, NH_3, HCN, H_2O	CO_2, H_2S, COV	CO_2, COV, O_2, N_2	CO_2, H_2S, O_2, N_2	CO_2, H_2S, COV, O_2, H_2O
Energy consumption (kWh/Nm^3 upgraded)	0.2-0.5[69]; 0.4-0.5[68]; 0.3-0.9[64]; 0.24-0.4*[70]; 0.2-0.3*[65]	0.10-0.33[69]; 0.21[68]; 0.4[64]; 0.23-0.33*[65]	0.05-0.25[69]; [64], [68] 0.56-0.7*[70]; 0.06-0.17*[65]	0.16-0.43[69]; 0.23-0.30[64]; 0.23-0.4*[70]; 0.15-0.35*[65]	0.2-0.79[69]; 0.76[64];	0.18-0.35[69]; 0.22[68]; 0.18-0.20[64]; 0.2-0.3*[70]; 0.18-0.33*[65]
Upgrading cost	Inexpensive[69]; Expensive[68]; Medium[64]; High[66]; Medium[70]	Expensive [66], [68], [69]; Medium[64];	High[64], [69] [66], [70]; Expensive[68];	Relatively inexpensive[69]; Expensive[68] Medium[64]; High[66], [70]	Expensive[68], [69]; High[64], [66];	Expensive[69]; High[64]; Low[66], [70]
Main advantages	No chemicals, scalable, easy operation	Co-removal of impurities, low CH_4 losses, smaller footprint	High CH_4 purity, very low CH_4 losses, low power requirement	No chemicals, scalable, compact	High CH_4 purity, very low CH_4 losses, no chemicals	No chemicals, scalable, easy operation
Main drawbacks	Water demand, bacterial clogging, H_2S related corrosion	Difficult operation, heat required for solvent handling	High investment, Heat required for regeneration, solvent handling	High CH_4 losses, valve operation control, fouling by biogas impurities	High investment, high energy consumption, low temperature operation	Energy consumption can be high, membrane fouling

*per Nm^3 raw biogas

5.1.B Energy consumption calculations: Equation 5.24 implies the power required for compressing the fresh Feed. Note that if the upstream pressure of a membrane is equal to the fresh Feed pressure, W_{cp_f} equals to zero.

$$W_{cp_f} = \frac{Feed \times 10^{-3}}{\eta_c} \cdot \frac{\gamma \cdot R \cdot T}{\gamma - 1} \cdot [(\frac{P^{up}}{P_{in}})^{\frac{(\gamma-1)}{\gamma}} - 1] \tag{5.24}$$

Equation 5.25 implies the power required for compressing the permeate stream of stage s that does not go out of the system (enters to another stage in the system). It assumed that the compressor is preceded by a vacuum pump so, P_{in} equals to 1 bar.

$$W_{cp_s} = \frac{(f_s^{perm} - f_s^{perm,out}) \times 10^{-3}}{\eta_c} \cdot \frac{\gamma \cdot R \cdot T}{\gamma - 1} \cdot [(\frac{P^{up}}{P_{in}})^{\frac{(\gamma-1)}{\gamma}} - 1] \tag{5.25}$$

Equation 5.26 implies the vacuum pump energy consumption. Vacuum pump is used for the permeate stream of each stage "s" to increase the driving force in the system. For a membrane s, if the down stream pressure be equal to the atmospheric pressure, then this term equals to zero.

$$W_{vp_s} = \frac{f_s^{perm} \times 10^{-3}}{\eta_{vp}} \cdot \frac{\gamma \cdot R \cdot T}{\gamma - 1} \cdot [(\frac{P_{in}}{P_s^{down}})^{\frac{(\gamma-1)}{\gamma}} - 1] \tag{5.26}$$

where equation 5.27 presents η_{vp}.

$$\eta_{vp} = 0.1058 \cdot \ln(\frac{P_s^{down}}{P_{in}}) + 0.8746 \tag{5.27}$$

There is the possibility of using compressor or expander for the product stream to achieve a product with specific pressure. Equations 5.28 and 5.29 imply compressor and expander energy consumption required for the product stream respectively. If the upstream pressure is greater than the product pressure, we would use expander to obtain the determined target and vice versa. Therefore, the absolute value of the W_{exp} has been considered because the W_{exp} becomes negative based on 5.29 equation.

$$W_{cp_{prod}} = \frac{F^{Ret} \times 10^{-3}}{\eta_c} \cdot \frac{\gamma \cdot R \cdot T}{\gamma - 1} \cdot [(\frac{P^{prod}}{P^{up}})^{\frac{(\gamma-1)}{\gamma}} - 1] \tag{5.28}$$

$$W_{exp} = \left| \frac{F^{Ret} \times 10^{-3}}{\eta_c} \cdot \frac{\gamma \cdot R \cdot T}{\gamma - 1} \cdot [(\frac{P^{prod}}{P^{up}})^{\frac{(\gamma-1)}{\gamma}} - 1] \right| \tag{5.29}$$

Finally, the total power consumption of the system is the sum of the total compressing power (W_{cp_s} for each stage and W_{cpf} for the feed), the total vacuum pump power (W_{vp_s} for each stage) and product compressing if the product compressor used or subtraction of the expander power if the expander used in the system divided by the mechanical efficiency ϕ:

$$W_{tot} = \frac{W_{cp_f} + W_{cp_{prod}} + \sum_{s \in \mathcal{S}} (W_{cp_s} + W_{vp_s})}{\phi}, \qquad \text{Using compressor for } F^{Prod} \tag{5.30}$$

$$W_{tot} = \frac{W_{cp_f} + \sum_{s \in \mathcal{S}} (W_{cp_s} + W_{vp_s})}{\phi} - \phi \cdot W_{exp}, \qquad \text{Using expander for } F^{Prod} \quad (5.31)$$

5.2 Effects of independent upstream pressure in three stage biogas upgrading process

In what follows, we study the impact of allowing to chose independent values of upstream pressures for each stage in a biogas upgrading process. As a reference to our study, we considered the work presented in [35]. For this reason, before presenting our results, as we did for the case study presented in Section 2.6.1 ([10]), we would discuss briefly about the three stage optimal configuration presented in [35].

5.2.1 Break down the calculation of optimal three stage process in [35]

In [35], an optimization method for biogas upgrading is presented. Authors modelled the process synthesis as an MINLP problem and solved the problem using BARON solver through the GAMS software.

The inlet stream has the same composition (CO_2/CH_4) we considered in our work. The proposed superstructure includs compressors, vacuum pumps, and valves as auxiliary equipment. The upgraded gas is expected to be at a pipeline pressure of 16 bar. The important novelty of this paper is to consider both upstream and downstream pressures as independent variables in the system.

To have a better understanding of the presented results, we recalculate the cost of the three stage solution proposed in [35] based on the cost separation equations and parameters presented in the paper.

$$I_m = 585\ m^2 \cdot 55\ eur/m^2 = 32175\ eur \quad (5.32)$$

$$I_c = 4.91 \cdot 23000 \cdot ((\frac{26.76}{0.746})/100)^{0.77} \cdot (2.9 + 5.11 - 1) \cdot (1/1.2719) = 282638\ eur \quad (5.33)$$

$$EC = 26.76\ kW \cdot 8000\ h/year \cdot 0.08\ eur/kwh = 17126.4\ eur/year \quad (5.34)$$

$$TAC = 32175 \cdot 0.308669 + 282638 \cdot 0.180674 + 17126.4 = 78123.2\ eur/year \quad (5.35)$$

$$TAR = 4168\ mol/h \cdot 8.314 \cdot 273.15 \cdot 1e^{-5} \cdot 8000 \cdot 0.2 - 78123.2 = 73323.2\ eur/year \quad (5.36)$$

There is a small difference of 0.04% and 0.06 % in TAC and TAR calculations respectively. The differences are likely due to some rounding up before computing the TAC and TAR values.

If we recalculate the compressor power, using the given flows and pressures, we will detect a difference between the value presented in the paper (26.76 KW) and the recalculated value (29.26 KW). Both these value differ also from the values resulting from the calculations we obtain using our formulas (31 kW). These differences are not neglectful because of their significant impact on the TAC and the TAR values. Furthermore, simulation of the optimal configuration presented in [35] (as shown in Figure 5.9) performed with the ASPEN-MEMSIC simulator shows that the separation at each stage is about the same, except for the stage at 3.3 bar (254 m^2) where there is a significant difference in the purity of CH_4 lost at the permeate and the retentate flow (251 vs 419 mol/h). This gives a recovery of 99.3 instead of 99.6 as presented in the article.

Interestingly, the resulting optimal configuration matches the configuration of a three stage process previously patented by Evonik industry [42].

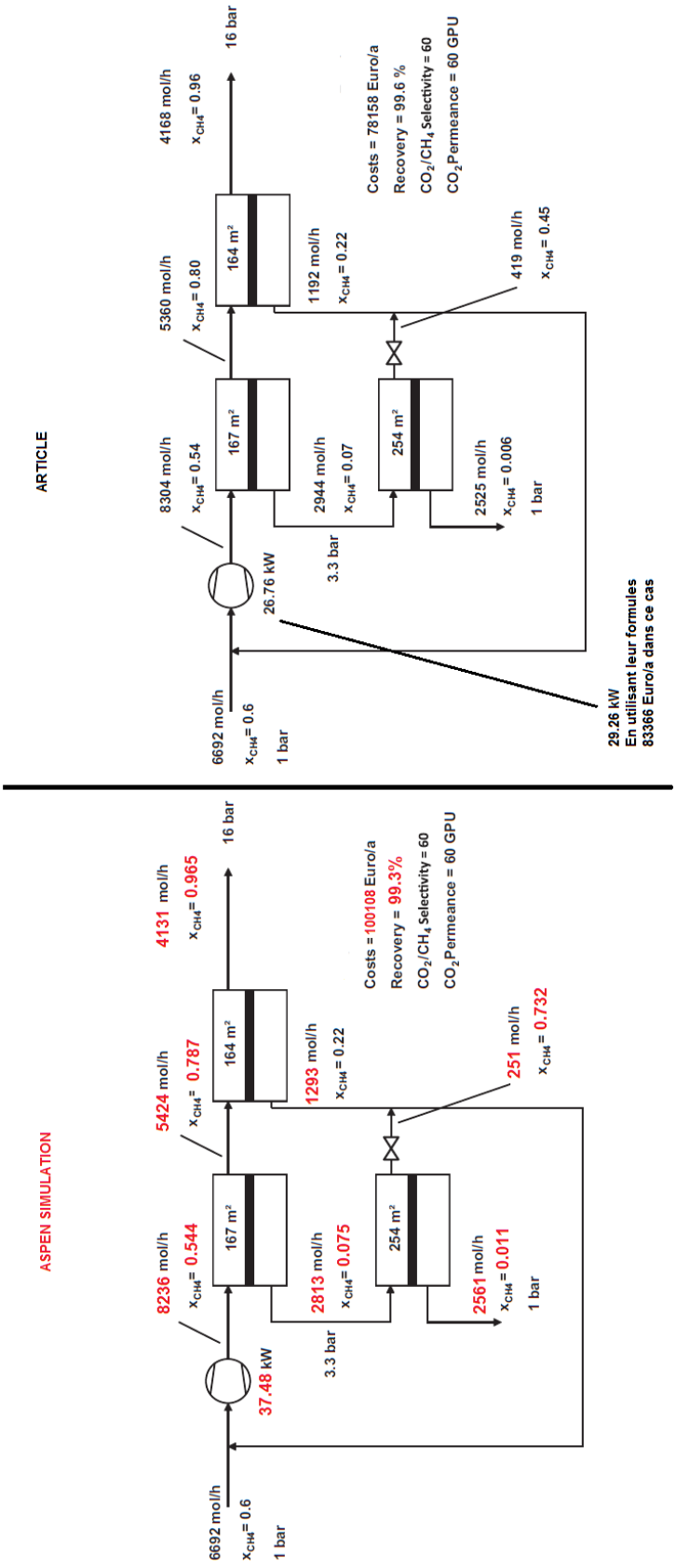

Figure 5.9: Comparison the three stage optimal result of [35] with its simulation result which is done with ASPEN

Since recalculation and simulation highlighted some differences in the presented optimal configuration in [35], we decided to compare our results with [42] patent and therefore, perform several tests using some of the assumptions presented in it. In what follows, we introduce the case study, the cost function and the results of our tests.

5.2.2 Effects of membrane performance

As [42], a biogas with a flowrate of 6692 mol/h, corresponding to around 1.858 mol/s is considered. Inlet gas pressure and temperature are 1 bar and 293.15°K respectively. A classical biogas composition is used, detailed in Table **??**. Product purity is expressed in terms of CH_4 content in the outlet stream with the constraint of at least 99.5% CH_4, together with a minimal methane losses as constraints.

Process configurations of three membrane stages is studied. The module pressure ratio is variable through a range of downstream and upstream pressure. Both upstream and downstream pressures are potentially different for all the stages in the system. The downstream pressure level is allowed to vary between 1-3 bar, while upstream pressure varies between 3-70 bar.

The goal of the study is to identify the most effective process structure and operating conditions, which reach the specifications (biomethane with target purity, maximal recovery and outlet pressure level) at the lowest cost.

Three sets of operating conditions were considered and evaluated through comparison, with increasing degrees of freedom:

(i) upstream and downstream pressures are independent variables and membrane material is fixed (applying PI membrane)

(ii) upstream and downstream pressures are independent variables and membrane material is variable but uniform

(iii) upstream and downstream pressures are independent variables and membrane material is variable and independent

5.2.3 Annual and specific separation costs

The overall process cost of the system (which is taken as the objective function of the optimization model) is the [35] separation and parameters cost. It takes into account the capital expenses (CAPEX) such as membrane area and membrane frame, vacuum pumps, compressors or expanders and the operating costs (OPEX), such as contract and material maintenance cost, local tax and insurance, labor overhead cost, energy requirement, membrane replacement, and total operation. The cost function and the parameters used in the objective function are detailed in Table A.2 and Table A.3 respectively.

Table A.2: Cost equations used to determine product gas separation cost

Equipment cost		
$I_{m_s} = A_{m_s} \cdot K_m$	(5.37)	Membrane cost
$I_{c_s} = C_c \cdot (W_{cp_s}/74.6)^{0.77} \cdot (MPF_c + MF_c - 1) \cdot UF_{1968} \cdot K_{er}$	(5.38)	Stage compressor cost
$I_{c_f} = C_c \cdot (W_{cp_f}/74.6)^{0.77} \cdot (MPF_c + MF_c - 1) \cdot UF_{1968} \cdot K_{er}$	(5.39)	Feed compressor cost
$I_{c_{prod}} = C_c \cdot (W_{cp_{prod}}/74.6)^{0.77} \cdot (MPF_c + MF_c - 1) \cdot UF_{1968} \cdot K_{er}$	(5.40)	Retentate compressor cost
$I_{exp} = C_{exp} \cdot (W_{exp}/0.746)^{0.81} \cdot (MPF_c + MF_c - 1) \cdot UF_{2001} \cdot K_{er}$	(5.41)	Expander cost
$I_{vp_s} = C_{vp} \cdot (W_{vp_s})$	(5.42)	Vacuum pump cost
Capital expenditures		
$CAPEX = I_{c_f} + I_{c_{prod}} \text{or } I_{exp} + \sum_{s \in \mathcal{S}} I_{c_s} + I_{m_s} + I_{vp_s}$	(5.43)	Total capital cost
Operational expenditures		
$EC = t_{op} \cdot W_{tot} \cdot K_{el}$	(5.44)	Energy cost
$OPEX = EC$	(5.45)	Total operational expeditures
Total annual cost		
$TAC = a_{equip} \cdot (I_{c_f} + I_{c_{prod}} \text{or } I_{exp} + \sum_{s \in \mathcal{S}} I_{c_s} + I_{vp_s}) + a_{mem} \cdot (\sum_{s \in \mathcal{S}} I_{m_s}) + OPEX$	(5.46)	Total annual costs
$SC_{CH_4} = TAC/(F^{RET} \cdot 3600 \cdot t_{op} \cdot 0.02271)$	(5.47)	Specific CH_4 separation cost
Total annual revenue		
$TAR = F^{RET} \cdot 3600 \cdot t_{op} \cdot 0.02271 \cdot K_{gp} - TAC$	(5.48)	Total annual revenue

Table A.3: Cost parameters used in Table 1

Capital cost parameters		
C_c	1×23000	USD_{1968}
C_{vp}	1000	EUR/kW
C_{exp}	420	USD_{2000}
K_m(polymer)	55	EUR/m^2
K_m(zeolite)	2000	EUR/m^2
K_{er}	0.786	EUR/USD
MPF_c	2.9	-
MF_c	5.11	-
UF_{2000}	1.44	-
UF_{1968}	4.91	-
a_{eqip}	0.180674	-
a_{mem}	0.308669	-
Operational and annual cost parameters		
t_{op}	8000	h/year
K_{el}	0.08	EUR/kWh
K_{gp}	0.2	EUR/Nm^3
η_c	0.72	-
γ	1.3	-
R	8.314	$J/(K \cdot mol)$
T	293.15	K

5.2.4 Energy consumption calculation

Here we explain in detail the energy consumption calculations respect to Table A.2.

Equation 5.49 implies the power required for compressing the fresh Feed. Note that if the upstream pressure of a membrane is equal to the fresh Feed pressure, W_{cp_f} equals to zero.

$$W_{cp_f} = \frac{Feed \times 10^{-3}}{\eta_c} \cdot \frac{\gamma \cdot R \cdot T}{\gamma - 1} \cdot [(\frac{P^{up}}{P_{in}})^{\frac{(\gamma-1)}{\gamma}} - 1] \tag{5.49}$$

Equation 5.50 implies the power required for compressing the permeate stream of stage s that does not go out of the system (enters to another stage in the system). It assumed that the compressor is preceded by a vacuum pump so, P_{in} equals to 1 bar.

$$W_{cp_s} = \frac{(f_s^{perm} - f_s^{perm,out}) \times 10^{-3}}{\eta_c} \cdot \frac{\gamma \cdot R \cdot T}{\gamma - 1} \cdot [(\frac{P^{up}}{P_{in}})^{\frac{(\gamma-1)}{\gamma}} - 1] \tag{5.50}$$

Vacuum pump is used for the permeate stream of each stage "s", to increase the driving force in the system. For a membrane s, if the down stream pressure be equal to the atmospheric pressure, then this term equals to zero.

$$W_{vp_s} = \frac{f_s^{perm} \times 10^{-3}}{\eta_{vp}} \cdot \frac{\gamma \cdot R \cdot T}{\gamma - 1} \cdot [(\frac{P_{in}}{P_s^{down}})^{\frac{(\gamma-1)}{\gamma}} - 1] \tag{5.51}$$

where $\eta_{vp} = 0.5$.

There is the possibility of using compressor or expander for the product stream to achieve a product with specific pressure. Equations 5.52 and 5.53 imply compressor and expander energy consumption required for the product stream respectively. If the upstream pressure is greater than the product pressure, we would use expander to obtain the determined target and vice versa. Therefore, the absolute value of the W_{exp} has been considered because the W_{exp} becomes negative based on 5.53 equation.

$$W_{cp_{prod}} = \frac{F^{Ret} \times 10^{-3}}{\eta_c} \cdot \frac{\gamma \cdot R \cdot T}{\gamma - 1} \cdot [(\frac{P^{prod}}{P^{up}})^{\frac{(\gamma-1)}{\gamma}} - 1] \tag{5.52}$$

$$W_{exp} = \left| \frac{F^{Ret} \times 10^{-3}}{\eta_c} \cdot \frac{\gamma \cdot R \cdot T}{\gamma - 1} \cdot [(\frac{P^{prod}}{P^{up}})^{\frac{(\gamma-1)}{\gamma}} - 1] \right| \tag{5.53}$$

Finally, the total power consumption of the system is the sum of the total compressing power (W_{cp_s} for each stage and W_{cpf} for the feed), the total vacuum pump power (W_{vp_s} for each stage) and product compressing if the product compressor used or subtraction of the expander power if the expander used in the system divided by the mechanical efficiency ϕ:

$$W_{tot} = W_{cp_f} + W_{cp_{prod}} + \sum_{s \in \mathcal{S}} (W_{cp_s} + W_{vp_s}), \qquad \text{Using compressor for } F^{Prod} \tag{5.54}$$

$$W_{tot} = W_{cp_f} + \sum_{s \in \mathcal{S}} (W_{cp_s} + W_{vp_s}) - W_{exp}, \qquad \text{Using expander for } F^{Prod} \tag{5.55}$$

5.2.5 Results and discussion

In a first step, we fix the membrane performances as polyimide membrane. The upstream pressure is allowed to vary and be different for each stage, having then upstream pressure as an independent variable. Figure 5.10 presents the result for the independent upstream pressure with Polyimide process. The same configuration as [42] is obtained.

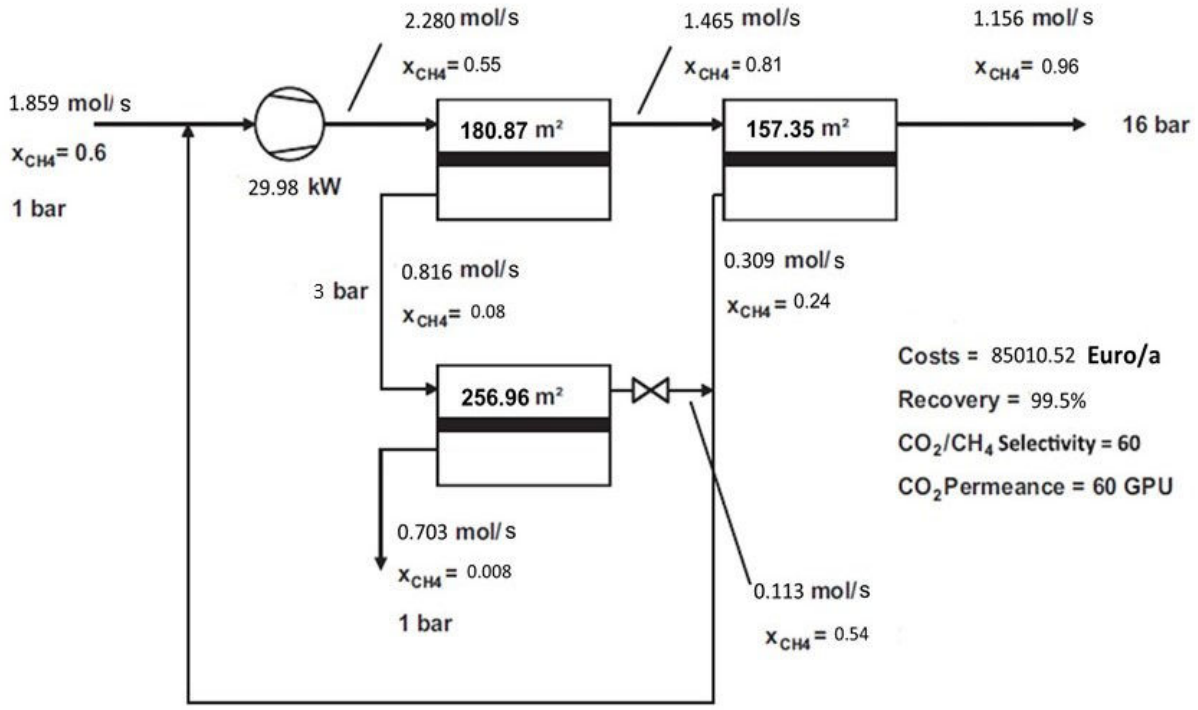

Figure 5.10: Optimal configuration for three stages membrane process with PI membrane and independent upstream pressure variable.

The next step is to keep upstream pressure as an independent variable while allowing performances (permeability/selectivity) to vary uniformly for all the membrane stages within the Robeson bound.

To increase the probability of finding a feasible solution, we limited the perm/selectivity region. This region is defined within the most probable perm/selectivity points. Following variables are added to the optimization model to determine the optimal membrane performance:

- $0.5 \leq \mathrm{P_{CO_2}} \leq 50000$: Permeance of CO_2 as fastest component [GPU]
- $0.33 \leq \mathrm{P_{CH_4}} \leq 333.33$: Permeance of CH_4 [GPU]
- $1.5 \leq \alpha \leq 150$: Selectivity

Figure 5.11a shows the CO_2/CH_4 trade- off curve. Figure 5.11b shows the defined feasible

region for permeability and selectivity variables based on the most probable domain for permeability/selectivity variables. Consequently, following constraints were imposed to the system.

Robeson upper bound relationship:

$$P_{CO_2} \leq k \cdot \alpha^n \tag{5.56}$$

where k = 5369140 and n = -2.636. The selectivity relation:

$$P_{CO_2} \leq \alpha \cdot P_{CH_4} + \epsilon \tag{5.57}$$

The relation between permeances of CO_2 and CH_4:

$$P_{CO_2} \geq P_{CH_4} + \epsilon \tag{5.58}$$

The equation 2.9 is adapted to the new model:

$$g_{s,i}^{perm} y_{s,CO_2,i}^{perm} = \frac{Acell_s}{\delta}(P_{CO_2} P^{up} y_{s,CO_2,i}^{ret} - P_{CH_4} P_s^{down} y_{s,CO_2,i}^{perm}) \quad \forall s \in \mathcal{S}, i \in \mathcal{C} \tag{5.59}$$

$$g_{s,i}^{perm} y_{s,CH_4,i}^{perm} = \frac{Acell_s}{\delta}(P_{CH_4} P^{up} y_{s,CO_2,i}^{ret} - P_{CH_4} P_s^{down} y_{s,CH_4,i}^{perm}) \quad \forall s \in \mathcal{S}, i \in \mathcal{C} \tag{5.60}$$

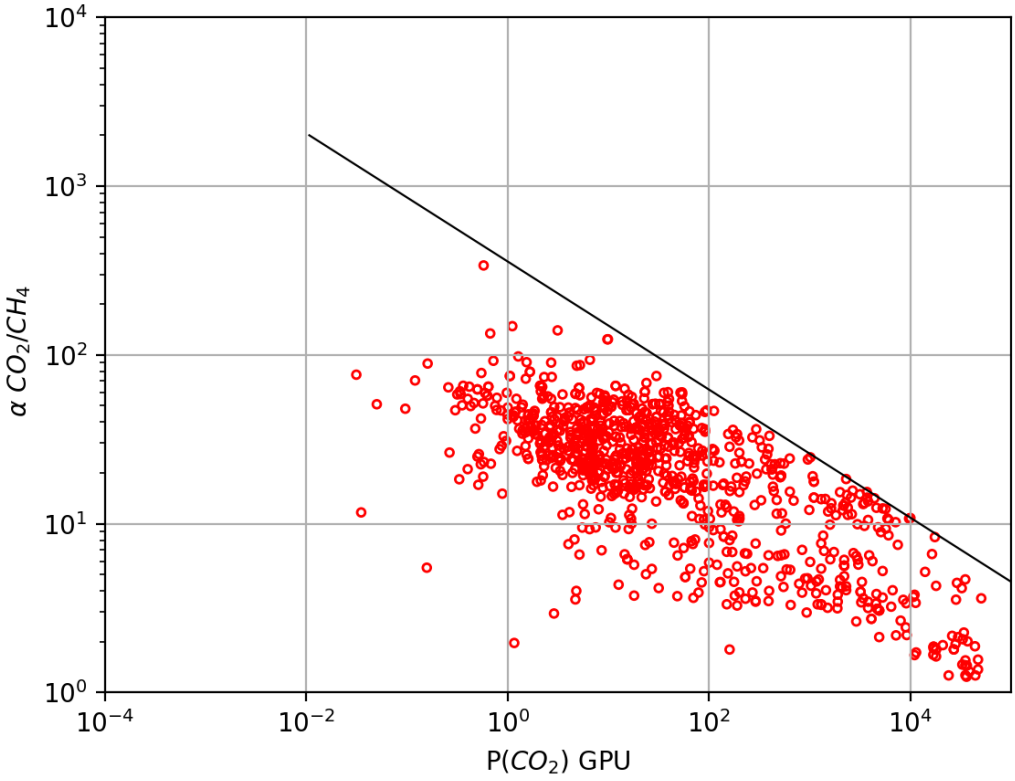

(a) CO_2/CH_4 polymeric materials trade-off curve [28]

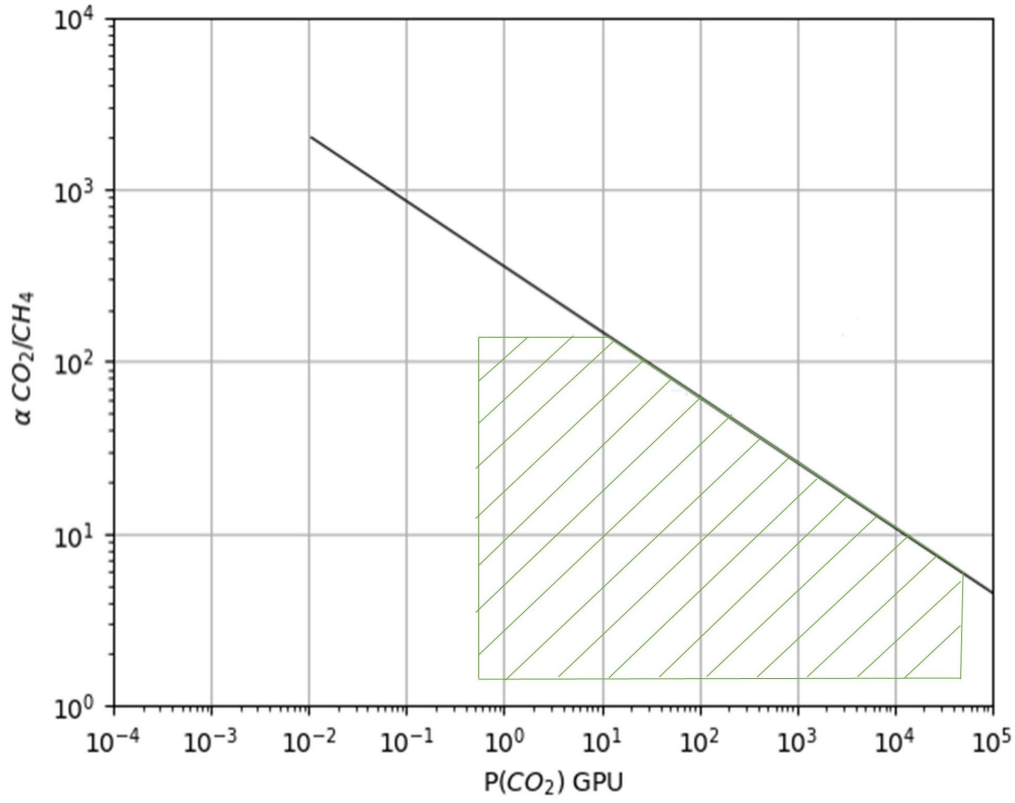

(b) Dashed area corresponds to the domain the domain used for optimal membrane identification when performances are not fixed

Figure 5.11: Selectivity / permeance trade-off curve based on a 1 µm skin layer thickness.

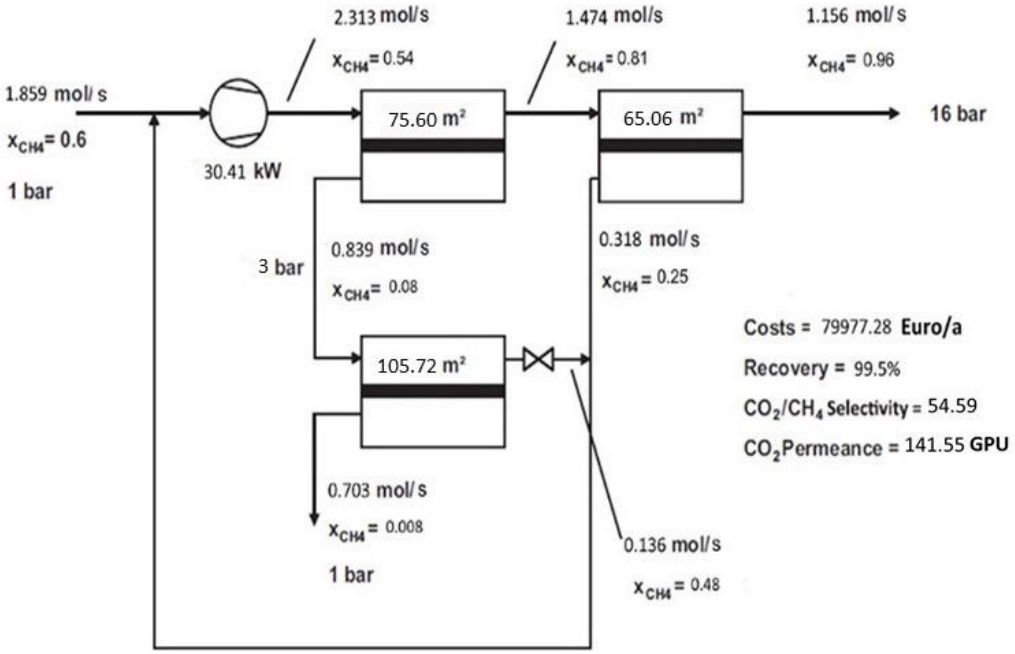

Figure 5.12: Optimal configuration for three stages membrane process with uniform membrane performances and independent upstream pressure variable.

Figure 5.12 presents the optimal process configuration with uniform Perm/Selectivity variable. As expected, by increasing the degrees of freedom better solutions are obtained. when compared to the optimal solution from the fixed performances membrane, this optimal solution leads to around 6% lower process cost. The optimal process calculated here and presented in Figure 5.12, has the same general configuration that the reference case presented in Figure 5.10.

As a further step, allowing both upstream pressure and performances (permeability/selectivity) to vary independently for all the membrane stages. Figure 5.13 shows the optimal process configuration.

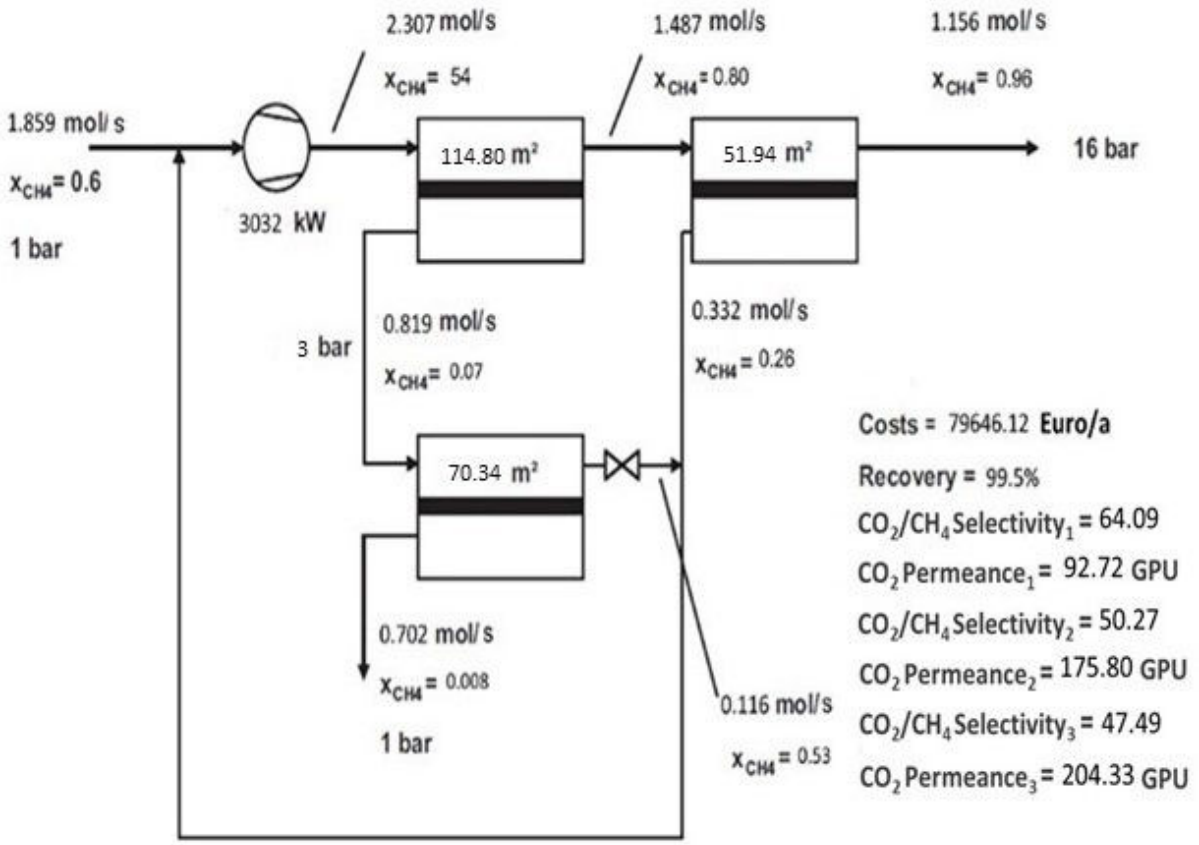

Figure 5.13: Optimal configuration for three stages membrane process with independent membrane performances and independent upstream pressure variable.

The process cost reduces around 7% (Table A.4) with the same general optimal configuration. Indeed, the optimal solution has always the same configuration, using the variable membrane performances decrease the product cost slightly.

Table A.4: Objective values of different tests on membrane performances

	Fixed performance(PI)	Variable performance	
		Uniform	Independent
Objective value (Euro/a)	85010.52	79977.28	79646.12

The general methodology of the study is to provide, through Process Synthesis, a set of optimal solutions to the problem, so that the decision maker has an exhaustive view of the different possibilities in the process selection step.

5.3 Natural gas upgrading

In the current context of the environmental crisis and the rising trend of energy consumption, alternatives in energy production methods are imperative. Finding a method to supply the high-energy demand and deal with environmental impacts such as global greenhouse gas at the same time is essential.

Natural gas with low emission through different natural resources becomes one of the most attractive, fastest and the growing fuel for generating electricity and heat of the world [87]. In addition to the importance of natural gas as a fuel, it is a source of hydrocarbons for petrochemical feeds. Natural gas can also contributes to the production of other potential products such as syngas and high purity hydrogen [88].

Natural gas, like other fossil fuels, is formed from the decomposition of living matters such as plants, animals, and micro-organisms that lived over millions of years ago and became a mixture of gases.

Although natural gas is considered as a clean fuel in comparison with other fossil fuels, the natural gas found in the reservoirs deposit is not necessarily "clean" and free of impurities. It consists of different range of compositions depending on its type, depth, and location of the underground reservoirs deposit and the geology of the area. Methane is the prevailing element of natural gas. Natural gas also consists of light and heavier hydrocarbons as well as contaminating compounds of CO_2, N_2, Hg, He, H_2S, etc. The impurities present in natural gas, need to be removed to natural gas meet the pipeline quality standard [88]–[90].

Carbon dioxide as one of the major contaminants of the natural gas must be removed in an optimal way to improve pipeline capacity and reduces compression horsepower. It affects the selling price of the natural gas as well as reduces the energy content of the gas. Besides, in the presence of water, it makes natural gas acidic which can damage the pipeline and the equipment of the system. Therefore, one of the vital stages in the natural gas purification is to remove carbon dioxide to improve the quality of natural gas product [91]–[93].

Membranes have been known as a mature technology that has been applied in natural gas upgrading. Currently, membranes are applied for carbon dioxide removal from natural gas at processing rates from million standard cubic feet per day (MMSCFD) to 250 MMSCFD. New units are also in design or construction stage to handle volumes up to 500 MMSCFD [94]–[97].

In this study, we consider membrane technology for natural gas purification. We evaluate, compare, and analyze the effects of different membrane performances to determine the best membrane performances that yield to achieve the optimal process design. The optimization method is applied to minimize the production cost while obtaining the product purity and maximum recovery.

5.3.1 Natural gas case studies

Natural gas with 10 mol/s flowrate, is considered. Inlet gas pressure and temperature are 60 bar and 293.15°K respectively. A classical natural gas composition, detailed in Table **??** is considered. Product purity is expressed in terms of CH_4 content in the outlet stream with the constraint of at least 98% CH_4, together to minimal methane losses in terms of optimization constraints.

Process configurations of up to three membrane stages are studied. Both upstream and downstream pressures are considered as independent variables. Technically, by considering upstream pressure as an independent variable the application of valve is practical, for some retentate stream depends on the case in the system. The downstream pressure level is allowed to vary between 1-60 bar, while upstream pressure varies between 60-100 bar. The vacuum pump is not applied in this system. Differently to the biogas case, there is no special constraint concerning the outlet pressure. It is expected to be 60 bar.

The goal of this study is to identify the most effective process structure and operating conditions, which reach the specifications (methane with target purity and maximal recovery) at the lowest cost. To this aim, a system with three membranes (cellulose acetate, polyimide, and zeolite) identical to the biogas case study is considered. The effects of applying different membrane materials with up to three stages on process structure, operating conditions, and process cost are studied.

5.3.2 Results and discussion

Figure 5.14 shows the optimal process configurations for natural gas upgrading with three membrane materials for up to three membrane stages.

For CA, one stage configuration with a recycling loop offers the best cost performances. A significant cost decrease is obtained with two stages configuration. Three stages processes generate a slightly lower purification cost compared to two stages. This suggests two stages processes to be favored in place of three, when complexity is taken into account. We stressed again that these results corroborate classical industrial practice, where two stages polymeric membrane processes are most often applied, for both natural gas or biogas purification applications [72].

Globally speaking, the results obtained with PI are close to those obtained with CA in three membrane stages and close to zeolite in one and two stages in terms of process configuration. The major difference between PI and CA comes from the lower purification cost obtained with PI membranes. In PI membrane, purification cost decreases from 0.121 to 0.101 EUR/Nm^3 CH_4 by going from one to two stages. Again there is a very low difference between two and three stages process cost.

Interestingly, the optimal product cost is almost not decreased by increasing the number of stages in a zeolite membrane. Therefore, one stage zeolite membrane is proposed as the optimal process configuration without any auxiliary equipment (compressor, expander,

and/or vacuum pump) for natural gas purification. Besides, the cost separation in zeolite case is dramatically less than PI and CA.

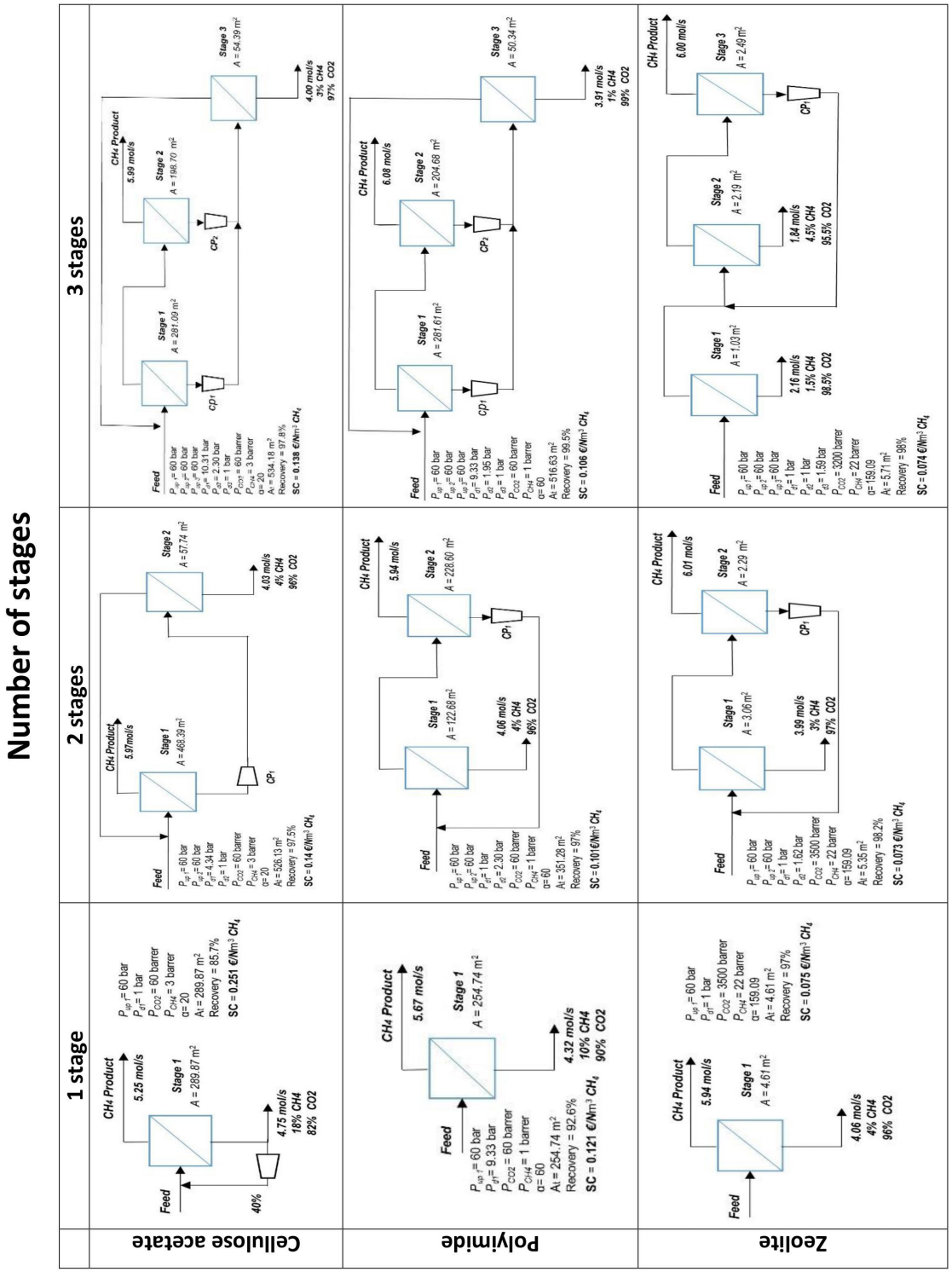

Figure 5.14: Best configurations for CA, PI, and Zeolite membranes with up to three stages in natural gas purification.

5.4 Summary and conclusions

Zeolite membrane with high-performance membrane material offers promising perspectives in terms of biogas purification cost. The comparison between optimal results of CA and PI shows in this case the interest of increased selectivity in terms of materials performances. Besides, the interest of both improved selectivity and permeance is shown by the zeolite membrane decreased costs.

Two stages process with either retentate or permeate recycling loop is offered as the optimal process design in terms of product cost and operating conditions (purity and recovery). The confirmation of this result in classically natural gas treatment shows the robustness of our method.

In biogas upgrading with uniform upstream pressure, vacuum pumping is systematically applied for optimal process. A moderate vacuum pumping is obtained through optimization (typically 0.2 to 0.5 Bar).

In the case of independent upstream pressure, the possibility of applying valve is added to the superstructure. The vacuum pump is not considered in this case. In the three stage process synthesis, the optimal process design is the same as [42] proposed design. In terms of optimal material performance, the interest of increased selectivity and permeance which vary for each stage is shown by decreased cost.

In natural gas upgrading, like the biogas upgrading, high performance and very expensive membrane material offer promising perspectives concerning the natural gas upgrading cost.

One stage high-performance membrane (zeolite), is offered as the optimal process design. In PI and CA, two stage process is designed offered the optimal process design like the biogas case.

Generally, in natural gas, the production cost for different membrane materials is lower than in the same cases in biogas upgrading. This shows the effects of the inlet stream pressure which is 60 times greater in natural gas upgrading than biogas upgrading.

Conclusion

Membrane processes are considered today as one of the key technology for gas separation applications, together with cryogenic and adsorption processes. Tremendous developments of this technology are expected based on the recent development of high-performance gas separation membranes (such as zeolites, carbon molecular sieves, graphenes, MOF...). Air separation, hydrogen purification, natural gas treatment, pollutant recovery, and carbon capture are, among others, classical challenges for which membrane processes already offer efficient solutions. Besides materials synthesis, process simulation is of major importance in order to identify the best design and set of operating conditions for a target application. This has been achieved first thanks to approximate analytical solutions in the 60's, numerical resolution methods in the 70's and Process Systems Engineering (PSE) methods in the 90's. Most membrane separation plants are designed today based on a systematic analysis of different process designs generated by process simulation tools.

A new approach of membrane process design has been more recently explored, through a Process Synthesis methodology. The objective is to identify the optimal design and operating conditions for a given set of constraints based on a systematic approach of all possible structures and range of operating variables. The major change compared to process simulation is that no process flowsheet is required; the optimal flowsheet is generated through a global optimization study, which makes use of all system components and process variables allowed by the designer. Membrane gas separations are one of the separation processes which is often selected for process synthesis studies. This results from the simplicity of the process for computation purposes:

- The system is under steady state conditions and is based on physical mechanisms (no time dependency, no chemical reactivity).
- The mass transfer resistance is located in the membrane; consequently, the separation performances are governed by ratios of transfer and contact time. There is no need to generate a specific geometry in order to compute mass transfer phenomena in fluids.
- The process is isothermal. No energy balance is needed.
- The transmembrane mass fluxes expressions are simple (no flux coupling, linear driving forces).

- Process designs are limited to 2 to 3 stages (because of the increasing cost of compressors when multistaged systems are used).
- The number of equipment devices is limited to compressors, vacuum pumps, valves, and membrane modules

Beyond the apparent simplicity of the problem, the state of the art analysis of Process Synthesis studies dedicated to membrane gas separation systems has shown several limitations and unexplored aspects:

- Rigorous module simulation approaches, extendable to multicomponent systems, are not always applied. Simple analytical expressions have been proposed by some authors, in order to decrease computational efforts. This strategy is risky, in that significant errors can result in the separation performance precision (i.e. criterion number one for a rigorous optimization study).
- Exhaustive connection possibilities, including self recycling loops and partial recycling connections, are not always taken into account.
- The number of equipment devices offered is sometimes incomplete. This applies more specifically to vacuum pumps, which are most often discarded in Process Synthesis programs.
- The range of operating conditions can be restricted to constant upstream pressure, constant pressure ratio or without vacuum conditions. This limitation can lead to design solutions that are far away from on optimum.
- A single membrane is used for the different membrane stages. The question of multi membrane systems in multistaged operations is almost never investigated.
- Finally, different optimization algorithms have been used by different authors and there is a lack of comparative studies among the various global optimization methods.

Based on the limitations which are listed above, a rigorous, systematic, multicomponent, multistage, multimembrane Process Synthesis program has been developed and used in this thesis. The most significant results, which have been obtained, can be summarized as follows:

A generic process superstructure with up to three stages has been considered. It consists of exhaustive connection layout including recycling loops, variable membrane surface, variable pressure ratio, variable membrane performances for each stage and the use of a different types of auxiliary equipment (compressor, vacuum pump, expander, and valve). The membrane process synthesis was expressed as a Non Linear Programming (NLP) optimization model based on the proposed superstructure. The resulting NLP model is a smooth, but highly non-convex continuous problem. This optimization problem was solved efficiently by means of a specialized global optimization approach: an adapted Monotonic Basin Hoping strategy.

The proposed approach was validated by comparing its optimal results in terms of configuration and separation cost with the solution presented in ([10] as a reference work. The method allowed to improve upon the existing solutions and, furthermore, to extend the analysis to process configurations with independent pressure ratios (thanks to the application of possibly different vacuum pressure in the downstream side of each membrane stage).

The proposed method was applied to optimize and analyze several well-known and important gas separation cases such as CO_2 recovery from BFG, N_2 production from the air, biogas upgrading, and natural gas upgrading. The degree of freedom of the optimization model increased case by case by considering more parameters as decision variables and optimizing the separation process design.

For recovery of CO_2 from BFG, a mapping of optimal process configurations was presented for two to four membrane stages (with 0.1-1% N_2 at 90-99% recovery). It presented, two and three stage cascades for "low" and "high" separation constraints respectively. Besides, a three stage configuration in which the additional stage is applied on the retentate of the first stage presented as an optimal configuration for "intermediate" separation constraints. It has been shown that there is no interest in using a four stages configuration, in fact, the higher complexity is not compensated by a significant reduction of the overall separation cost.

For this case study, an optimal process sensitivity analysis was performed in order to investigate the effects of uniform pressure ratio and decrease in membrane permeance and selectivity on the optimal process design.

The impact of membrane performances on optimal membrane process design, product cost, and the operational target is investigated systematically for NEA process. We increased the degrees of freedom of the optimization model by considering the possibility of applying different membrane performances for all (uniform) and each stage (independent). The optimization strategy has performed to investigate membrane gas separations units with up to three stages and different levels of nitrogen purity.

The optimal performance results have shown that a highly permeable material is preferable to a very selective material. Besides, it was shown that in a multistage NEA membrane process, the possibility of applying independent membrane performances does not allow to improve the NEA product cost.

Although the application of vacuum pressure is often denied in the industry, our results showed that it has a significant effect on reducing the separation cost of many processes. We have proven the generality of our claim by considering several critical case-studies and comparing results obtained with and without applying a vacuum pressure.

Finally, the optimization methodology was extended to CO_2/CH_4 separation on biogas and natural gas purification. The effects of high-performance membrane materials on an optimal membrane process and product cost was compared with polymeric membranes. Zeolite membrane, as an expensive membrane with high-performance material, offered

the most promising perspectives in terms of purification cost. The comparison between the optimal product cost results of cellulose acetate and polyimide membrane process showed the interest of increasing selectivity in material performances. However, the high-performance zeolite membrane conveyed the interest of both improved selectivity and permeance in decreasing the product cost. On the contrary, the membrane performance has a slight effect on the optimal process design.

An optimal two stages process configuration with either a retentate or permeate recycling loop was identified as the best balance in terms of purity, recovery, process complexity and separation cost. It implies the robustness of this result regardless of the membrane performances and outlet pressure level.

In addition to the membrane materials, in biogas upgrading, the effects of different levels of outlet pressures were investigated on product cost. As expected, by increasing the target pressure, the product cost was increased. There was no need for a product compressor or expander to obtain the target pressure.

This study was extended to a more complex system where an independent upstream pressure was considered. The optimal configuration converged to the configuration which was proposed for biogas purification with [42]. Surprisingly, the membrane performance has a negligible effect on the product cost and no effect on the optimal configuration.

In natural gas upgrading, one stage high-performance membrane with no auxiliary equipment was identified as the optimal result in terms of product cost and configuration. For the polymeric membranes (CA and PI), the two-stage configurations, as biogas upgrading, have shown the most promising optimal configuration.

Perspectives:

The main objective of this thesis was to explore the improvements that can be achieved in the field of Process Synthesis methods for membrane gas separation processes. It has been shown that the combination of rigorous module simulation, exhaustive connection possibilities, and efficient global optimization algorithm leads to novel results, compared to the state of the art. A lower cost has been generated for the blast furnace case, showing the interest of advanced optimization algorithms. Heuristics have been rediscovered for the nitrogen enriched air (NEA) study, showing the efficiency of the method, but, at the same time, novelties such as vacuum pumping have been shown to offer a significant cost decrease for NEA production. A dedicated study has shown that there is no interest to combine different membranes; a single optimal membrane has been identified for polymeric materials for the specific case of NEA production. These counterintuitive results shows the interest and potentialities of Process Synthesis for membrane developments. Finally, the interest of high performance, but expensive, inorganic membrane for biogas purification application has been demonstrated.

This first program achievement shows numerous perspectives for future developments:

- For membrane gas separations, a sweep gas option would be of great interest and

has never been explored. This possibility requires a reassessment of the connectivity rules because a two inlets / two outlets membrane box has to be taken into account. The impact of sweeping gas counterdiffusion should also be considered in the module simulation program. This achievement would be very interesting for multicomponent separation units and could lead to unexpected solutions in terms of module interconnections.

- An extension of the program to liquid separations is also of great interest, in order to investigated new applications (water treatment, drinking water production, biorefineries processes...). The main difficulty, in that case, is that liquid mass transfer resistance has to be taken into account (the membrane is no more the only resistance). A re-examination of the membrane module simulation program is thus necessary. The liquid mass transfer will likely be computed through correlations (with fluid velocity and physical properties as key variables). Additional design variables will thus result, extending the space of possibilities.

- Further developments could address the optimal design of hybrid systems, such as connecting a vapor separation membrane module to a distillation column. Several studies have been reported in this area, but it is likely that a rigorous, exhaustive program remains to be dedicated to these class of problems. The very large combinatorial set of hybrid membrane/distillation systems is a clear challenge in that case.

- This work can be enlarged to the application of different membrane performances on a multi-component gas separation process (this possibility has been explored for several gas pairs e.g. $O_2/N_2, CO_2/CH_4$).

- An exhaustive comparison between the proposed global optimization approach and evolutionary algorithm, which is proposed in [98] maybe yield to a hybrid method. It should be helpful to promote the efficiency of the optimization approach in the gas separation process.

- Furthermore, modifying the applied programming language (e.g. AMPL) for the optimization approach to another programming language which is much more closer to the machine language (e.g. Java or JuMP in Julia) to decrease the execution time will be helpful.

- Making a user-friendly application based on the optimization approach, to get the inlet values, auxiliary equipment, an objective function, and take the optimal process configuration like a simulator software, can be very practical for engineers in the industry.

- Finally, it would be very appealing to include reacting systems in the Process Synthesis program. The right combination of reactors and separators is indeed one of the most interesting and powerful problems for chemical engineers. The high complexity of chemical reactions in terms of numerical simulation and resolution (highly non linear behavior, stiff problems) is probably the reason why few re-

searchers address this challenge. The impressive development of computing and optimization methods opens however promising features in this domain.

In conclusion, the generic optimization approach plays a key role in achieving the optimal process configuration for each case. The obtained results demonstrate the efficiency of the optimization algorithm.

Résumé en français

Les technologies membranaires ont pris une importance croissante dans les applications industrielles au cours des dernières décennies. Elles sont devenues un procédé de référence dans l'industrie alimentaire, le traitement de l'eau et le dessalement. Elles prennent une place et un rôle de plus en plus importante dans d'autres secteurs tels que les soins de santé, la médecine et la pharmacie, l'énergie, le traitement du gaz et l'industrie pétrochimique. Les procédés membranaires bénéficient généralement d'un encombrement relativement petit et d'une réduction intéressante de la consommation d'énergie et de l'utilisation de produits chimiques (aucun solvant n'est nécessaire contrairement aux procédés classique gaz-liquide par exemple). La simplicité de fonctionnement et d'installation des systèmes à membrane, grâce à leur modularité, permet des changements d'échelle aisée en augmentant le nombre d'éléments et se traduit par une grande flexibilité. Le fonctionnement en régime permanent avec recyclage partiel ou complet du flux de rétentat/perméat est un autre avantage des systèmes à membrane [2], [3].

Il existe différents types de procédés membranaires, en fonction des applications visées, des conditions de fonctionnement et des phases (principalement gazeuses ou liquides) : perméation gazeuse, pervaporation, distillation membranaire, osmose inverse, ultrafiltration, microfiltration, dialyse et électrodialyse. De plus, divers procédés hybrides existent en raison du couplage des procédés membranaires avec d'autres procédés de séparation, notamment l'adsorption, l'absorption, l'évaporation, la cryogénie et la distillation. [4]. Les procédés de séparation par membrane peuvent être appliqués dans différents domaines de séparation tels que la séparation particules-liquide, la séparation liquide-liquide ainsi que la séparation des gaz. Cette thèse portera sur la l'optimisation de l'architecture des procédés (synthèse de procédé) de séparation des gaz par membrane.

Les procédés membranaires sont considérés aujourd'hui comme l'une des technologies clés pour les applications de séparation des gaz, avec les procédés cryogéniques et d'adsorption. D'énormes progrès de cette technologie sont attendus sur la base du développement récent de membranes de séparation des gaz à haute performance (telles que les zéolites, les tamis moléculaires carbonés, les graphènes, les MOF...). La séparation de l'air, la purification de l'hydrogène, le traitement du gaz naturel, la récupération des polluants et la capture du CO_2 sont, entre autres, des défis classiques pour lesquels les procédés membranaires offrent déjà des solutions efficaces.

Aujourd'hui, en raison des applications croissantes de la technologie de séparation des gaz

par membrane dans l'industrie, il est essentiel de développer une stratégie de conception précise, efficace et fiable. Pour concevoir un système efficace de séparation des gaz par membrane, différents aspects doivent être étudiés. La plupart des publications récentes sur la séparation des gaz par membrane se sont concentrées sur une série d'approches différentes pour promouvoir la conception d'un système de séparation par membrane (c'est-à-dire le matériau de la membrane, la conception du module de la membrane et la conception des procédés de séparation des gaz par membrane). Outre l'amélioration des matériaux et de la conception des modules membranaires, la conception efficace des procédés de séparation des gaz par membrane revêt une grande importance dans l'industrie.

La plupart des applications industrielles utilisant les procédés de séparation des gaz par membrane sont limitées à une seule étape. Cependant, en raison des limites inhérentes au mécanisme de séparation par solution-diffusion dans les membranes polymères, plusieurs étapes de séparation sont souvent nécessaires lorsque les applications exigent des niveaux élevés de récupération et de pureté d'un ou plusieurs composants, ou lorsque l'alimentation est pauvre en composants à récupérer ou les deux. En outre, une législation environnementale stricte et des contraintes de coûts d'investissement exigent l'utilisation de réseaux de membranes dans de nombreuses applications où le traitement partiel ou complet des flux de rétentat ou de perméat est soumis à de multiples étapes [8].

Plusieurs configurations de procédés sont possibles lorsque l'on considère une séparation membranaire à plusieurs étages (c'est-à-dire le nombre d'étages membranaires, la performance (perméabilité-sélectivité) et la surface de chaque étage, la pression en amont et en aval de chaque étage et les connexions de flux entre les étages). En dehors des membranes, le choix des options appropriées en tant que force motrice (c'est-à-dire les pompes à vide, les compresseurs, les turbines les vannes, etc.) conduit à des systèmes à membranes de plus en plus complexes. Les différentes combinaisons de ces modules donnent des résultats différents en ce qui concerne le pourcentage de gaz séparés. Cette tâche devient de plus en plus complexe à mesure que le nombre d'étapes de séparation augmente [9]. Ainsi, trouver la conception optimale pour le système de séparation des gaz devient le principal objectif de la conception du procédé.

En plus de la synthèse des matériaux, la simulation des procédés est d'une importance majeure afin d'identifier la meilleure configuration et la meilleure série de conditions d'opérationnelles pour une application spécifique. Ceci a été réalisé en premier lieu grâce à des solutions analytiques approximatives dans les années 60, des méthodes de résolution numérique dans les années 70 et des méthodes de génie des systèmes de procédés (PSE) dans les années 90. La plupart des usines de séparation par membrane sont aujourd'hui conçues sur la base d'une analyse systématique de différents modèles de procédés générée par des outils de simulation de procédés. Elles conduisent souvent à l'évaluation d'un nombre limité de configurations de processus basées sur les heuristiques du domaine et l'expérience. Ainsi, couvrir toutes les possibilités de configuration des procédés de séparation des gaz, en particulier dans les procédés membranaires multi-étapes, est fastidieux et prend du temps avec ces logiciels. Il est donc impératif d'adopter une approche précise,

efficace et fiable pour optimiser la conception de l'architecture des procédés de séparation des gaz par membrane.

À notre connaissance, très peu d'approches d'optimisation capables de concevoir avec succès le procédé de séparation des gaz par membrane ont été développées jusqu'à présent. En fait, en raison de la nature complexe des moduèes de flux à travers les membranes, les modèles unitaires existants dépendent de plusieurs hypothèses fixes. En conséquence, les outils numériques existants reposent souvent sur leur procédé et ne sont valables que dans une plage de fonctionnement limitée.

Une nouvelle approche d'optimisation des procédés membranaires a été explorée plus récemment, par le biais d'une méthodologie de synthèse des procédés. L'objectif est d'identifier la meilleure configuration et les conditions d'opérationnelles optimales pour un ensemble de contraintes données, sur la base d'une approche systématique de toutes les structures possibles et d'une série de variables opérationnelles. C'est une approche de rupture par rapport à la simulation de procédés car aucun schéma de procédé n'est nécessaire ; le schéma optimal est généré par une étude d'optimisation globale, qui utilise tous les composants du système et toutes les variables de procédé autorisées par le concepteur. La séparation des gaz par membrane est l'un des procédés de séparation qui est souvent choisi pour les études de synthèse des procédés. Cela résulte de la simplicité du procédé à des fins de calcul :

- Le système est en régime permanent et est basé sur des mécanismes physiques (pas de dépendance temporelle, pas de réactivité chimique).
- La résistance de transfert de masse est située dans la membrane ; par conséquent, les performances de séparation sont gouvernées par des rapports de transfert et de temps de contact. Il n'est pas nécessaire de générer une géométrie spécifique pour calculer les phénomènes de transfert de masse dans les fluides.
- Le procédé est isotherme. Aucun bilan énergétique n'est nécessaire.
- Les expressions des flux de masse transmembranaires sont simples (pas de couplage de flux, forces motrices linéaires).
- La conception des procédés est limitée à 2 ou 3 étages (en raison du coût croissant des compresseurs lorsque des systèmes à plusieurs étages sont utilisés).
- Le nombre de types d'équipements est limité aux compresseurs, pompes à vide, vannes et modules membranaires.

En plus de l'apparente simplicité du problème, l'analyse de l'état de l'art des études de synthèse des procédés consacrées aux systèmes de séparation des gaz par membrane a montré plusieurs limites et aspects inexplorés :

- Des approches rigoureuses de simulation de modules, extensibles aux systèmes à composants multiples, ne sont pas toujours appliquées. Des expressions analytiques simples ont été proposées par certains auteurs, afin de réduire les efforts de calcul.

Cette stratégie est risquée, dans la mesure où des erreurs significatives peuvent en résulter pour la précision des performances de séparation (c'est-à-dire le critère numéro un pour une étude d'optimisation rigoureuse).

- Les possibilités de connections exhaustives, y compris les boucles d'auto recyclage et les connections de recyclage partiel ne sont pas toujours prises en compte.
- Le nombre d'équipements proposés est parfois incomplet. Cela concerne plus particulièrement les pompes à vide, qui sont le plus souvent rejetées dans les études de synthèse de procédés.
- La gamme des conditions opérationnelles peut être limitée à une pression haute constante, un ratio de pression constant ou sans conditions de pompe à vide. Cette limitation peut conduire à des solutions de design qui sont loin d'être optimales.
- Une seule membrane est utilisée pour les différents stades de la membrane. La question des systèmes multimembranaires dans les opérations à plusieurs étages n'est presque jamais étudiée.
- Enfin, différents algorithmes d'optimisation ont été utilisés par différents auteurs et il y a un manque d'études comparatives entre les différentes méthodes d'optimisation globale.

Sur la base des limites énumérées ci-dessus, un programme de synthèse de procédés rigoureux, systématique, à plusieurs composants, à plusieurs étapes et à plusieurs membranes a été élaboré et utilisé dans le cadre de cette thèse. Les résultats les plus significatifs, qui ont été obtenus, peuvent être résumés comme suit :

Une superstructure de procédés générique comportant jusqu'à trois étapes a été envisagée. Elle consiste en un schéma de connexion exhaustif incluant des boucles de recyclage, une surface de membrane variable, un ratio de pression variable, des performances de membrane variables pour chaque étape et l'utilisation de différents types d'équipements auxiliaires (compresseur, pompe à vide, turbine et valve).

La synthèse du procédés membranaire a été exprimée comme un modèle d'optimisation de la programmation non linéaire (NLP) basé sur la superstructure proposée. Le modèle NLP qui en résulte est un problème continu lisse, mais fortement non convexe. Ce problème d'optimisation a été résolu efficacement au terme d'une approche d'optimisation globale spécialisée : une stratégie adaptée de la combinaison des Monotonic Basin Hoping (MBH) et Multi-start algorithms, afin de couvrir efficacement l'espace de recherche et de l'intensifier à travers lui pour trouver la solution globale optimale.

Dans l'approche proposée, nous avons principalement travaillé sur la partie de génération aléatoire, pour permettre de satisfaire les principales contraintes dans les points générés. En effet, si cette partie n'est pas effectuée avec soin, la procédure de recherche locale pourrait ne pas être en mesure de trouver un point faisable, ou trouver un point (très éloigné) de celui d'origine, rendant la recherche "complètement aléatoire" et perdant ainsi la capacité de recherche dans le voisinage typique du MBH.

L'approche proposée a été validée en comparant ses résultats optimaux en termes de configuration et de coût de séparation avec la solution présentée dans ([10] comme référence. La méthode a permis d'améliorer les solutions existantes et, en outre, d'étendre l'analyse à des configurations de traitement avec des rapports de pression indépendants (grâce à l'application d'une pression de vide éventuellement différente dans la pression base de chaque étage membranaire).

La méthode proposée a été appliquée pour optimiser et analyser plusieurs cas de séparation de gaz bien connus et importants, tels que la récupération de CO_2 à partir de BFG, la production de N_2 à partir de l'air, la valorisation du biogaz et la valorisation du gaz naturel. Le degré de liberté du modèle d'optimisation a évolué au cas par cas en considérant plus de paramètres comme variables de décision et en optimisant la configuration du procédé de séparation.

Pour la récupération de CO_2 de BFG, une cartographie des configurations optimales du procédé a été présentée pour deux à quatre étages de la membrane (avec 0,1-1% N_2 à 90-99% de récupération). Elle a présenté des cascades de deux et trois étages pour les procédés "faibles". et des contraintes de séparation "élevées" respectivement. En outre, une configuration à trois étages dans laquelle l'étage supplémentaire est appliqué sur le rétentat du premier étage est présentée comme une configuration optimale pour les contraintes de séparation "intermédiaires". Il a été démontré qu'il n'y a aucun intérêt à utiliser une configuration à quatre étages. La complexité plus élevée n'est pas compensée par une réduction significative du coût global de la séparation.

Pour cette étude de cas, une analyse de la sensibilité optimale du procédé a été réalisée afin d'étudier les effets du ratio de pression uniforme et de la diminution de la perméance et de la sélectivité de la membrane sur la conception optimale du procédé.

L'impact des performances des membranes sur la conception optimale du procédé, le coût du produit et la finalité opérationnelle est étudié systématiquement pour le procédé NEA. Nous avons augmenté les degrés de liberté du modèle d'optimisation en considérant la possibilité d'appliquer des performances membranaires différentes pour tous (uniformes) et pour chaque étape (indépendantes). La stratégie d'optimisation a permis d'étudier des unités de séparation des gaz par membrane comportant jusqu'à trois étapes et différents niveaux de pureté d'azote.

Les résultats des performances optimales ont montré qu'un matériau très perméable est préférable à un matériau très sélectif. En outre, il a été démontré que dans un procédé de membrane NEA à plusieurs étapes, la possibilité d'appliquer des performances de membrane indépendantes ne permet pas d'améliorer le coût du produit NEA.

Bien que l'application de la pression sous vide soit souvent refusée dans l'industrie, nos résultats ont montré qu'elle a un effet significatif sur la réduction du coût de séparation de nombreux procédés. Nous avons prouvé la généralité de notre affirmation en examinant plusieurs études de cas critiques et en comparant les résultats obtenus avec et sans application d'une pression sous vide.

Enfin, la méthodologie d'optimisation a été étendue à la séparation CO_2/CH_4 pour la purification du biogaz et du gaz naturel. Les effets des matériaux membranaires à haute performance sur un procédé membranaire optimal et le coût du produit ont été comparés à ceux des membranes polymères. La membrane en zéolite, en tant que membrane coûteuse avec un matériau à haute performance, offrait les perspectives les plus intéressantes en termes de coût de purification. La comparaison entre les résultats du coût optimal du produit du procédé de membrane en acétate de cellulose et en polyimide a montré l'intérêt d'augmenter la sélectivité des performances des matériaux. Cependant, la membrane en zéolite à haute performance a montré l'intérêt d'une sélectivité et d'une perméance améliorées pour réduire le coût du produit. Au contraire, la performance de la membrane a un léger effet sur la conception optimale du procédé.

Une configuration optimale du procédés en deux étapes avec une boucle de recyclage du rétentat ou du perméat a été identifiée comme le meilleur compromis en termes de pureté, de récupération, de complexité du procédé et de coût de séparation. e.

En plus des matériaux de la membrane, lors de la valorisation du biogaz, les effets de différents niveaux de pression de sortie ont été étudiés sur le coût du produit. Comme prévu, en augmentant la pression ciblée, le coût du produit a été augmenté. Il n'était pas nécessaire d'utiliser un compresseur ou une turbine de produit pour obtenir la pression cible.

Cette étude a été étendue à un système plus complexe où une pression haute indépendante a été prise en compte. La configuration optimale a convergé vers la configuration qui a été proposée pour la purification du biogaz avec [42]. Étonnamment, la performance de la membrane a un effet négligeable sur le coût du produit et aucun effet sur la configuration optimale.

Dans le domaine de la valorisation du gaz naturel, une membrane haute performance en une étape sans équipement auxiliaire a été identifiée comme le résultat optimal en termes de coût et de configuration du produit. Pour les membranes polymères (CA et PI), les configurations en deux étapes, comme la valorisation du biogaz, ont montré la configuration optimale la plus prometteuse.

L'objectif principal de cette thèse était d'explorer les améliorations qui peuvent être réalisées dans le domaine des méthodes de synthèse des procédés de séparation des gaz par membrane. Il a été démontré que la combinaison d'une simulation rigoureuse des modules, de possibilités de connexion exhaustives et d'un algorithme d'optimisation globale efficace conduit à des résultats inédits, par rapport à l'état de l'art. Un coût inférieur a été généré pour le cas des gaz de haut fourneau, ce qui montre l'intérêt des algorithmes d'optimisation avancés. L'heuristique a été redécouverte pour l'étude de la séparation des gaz de l'air (NEA), montrant l'efficacité de la méthode, mais, en même temps, des nouveautés telles que le pompage sous vide ont conduit une diminution significative des coûts pour la production de NEA. Une étude spécifique a montré qu'il n'y a pas d'intérêt à combiner différentes membranes ; une seule membrane optimale a été identifiée pour les matériaux polymères pour le cas spécifique de la production de NEA. Ces résultats

contre-intuitifs montrent l'intérêt et les potentialités de la synthèse des procédés pour le développement des membranes. Enfin, l'intérêt d'une membrane inorganique haute performance, mais coûteuse, pour l'application de purification du biogaz a été démontré.

Nomenclature

a	Annuity coefficient for equipment [Dimensionless]
A_s	Membrane area of membrane s [m^2]
A^{max}	Maximum allowed total area [m^2]
$Acell_s$	Area of a cell; in membrane s [m^2]
APL	Annual product losses [EUR/year]
BPC	Base plant cost [EUR]
C_{cap}	Annual capital costs [EUR/year]
C_{cc}	Compressor base cost [USD_{1968}]
C_{en}	Annual electricity cost [EUR/year]
C_{exp}	Expander base cost [EUR_{2000}]
$C_{O\&M}$	Annual operation and maintenance investment cost [EUR/year]
C_{tot}	Total annual costs [EUR/year]
C_{vp}	Vacuum pump cost factor [EUR/kW]
CAPEX	Capital expenditures [EUR]
CMC	Contract and material maintenance cost [EUR/year]
DL	Direct labor [EUR/year]
EC	Energy cost [EUR/year]

f_s^{perm}	Total permeate flowrate of membrane s [mol/s]
f_s	Feed flow rate entering into membrane s [mol/s]
F^{Perm}	System Permeate flowrate [mol/s]
$f_s^{perm,out}$	Permeate flowrate of membrane s going out of the system [mol/s]
$f_{s,s_1}^{perm,split}$	Permeate flowrate of membrane s entering into membrane s_1 [mol/s]
F^{Ret}	System Retentate flowrate [mol/s]
f_s^{ret}	Total retentate flowrate of membrane s [mol/s]
$f_s^{ret,out}$	Retentate flowrate of membrane s going out of the system [mol/s]
$f_{s,s_1}^{ret,split}$	Retentate flowrate of membrane s entering into membrane s_1 [mol/s]
f_s^{split}	Feed flow rate entering into membrane s [mol/s]
Feed	Feed gas flow rate enters into the system [mol/s]
$g_{s,i}$	Feed flowrate entering into cell i of membrane s [mol/s]
$g_{s,i}^{perm}$	Permeate flowrate of cell i of membrane s [mol/s]
$g_{s,i}^{ret}$	Retentate flowrate of cell i of membrane s [mol/s]
i	Interest rate [%]
I_{cc_f}	Feed Compressor investment cost [EUR]
I_{cc_s}	Membrane Compressor investment cost [EUR]
I_{m_s}	Membrane surface investment cost [EUR]
I_{mf_s}	Membrane permanentframe investment cost [EUR]
I_{vp_s}	Vacuum pump investment cost [EUR]
I_{exp}	Gas expander investment cost [EUR]
ICF	Indirect cost factor [Dimensionless]

k	Front factor of the log − log plot of the Robeson bound [Dimensionless]
K_{el}	Electricity cost factor [EUR/kWh]
K_{gp}	Upgraded biogas sales price [EUR/Nm^3]
K_m	Unit cost of membrane module [EUR/m^2]
K_{mf}	Base frame cost [EUR]
K_{mr}	Membrane replacement cost [EUR/m^2]
LOC	Labor overhead cost [EUR/year]
LTC	Local taxes and insurance [EUR/year]
$M_{product}$	Product Molar mass [kg/mol]
$M_{product\ per\ year}$	Annual separated product [Tons/year]
MDF_{cc}	Compressor module factor [Dimensionless]
MDF_{exp}	Module factor for expander [Dimensionless]
MF_{cc}	Compressor material factor [Dimensionless]
MF_{exp}	Material factor for expander[Dimensionless]
MPF_C	Material and pressure factor for compressor[Dimensionless]
MRC	Membrane replacement cost [EUR/year]
n	Slop of the log − log plot of the Robeson bound [Dimensionless]
OPEX	Operational expenditures [EUR/year]
P_{in}	Inlet stream pressure [bar]
P_{j_s}	Permeance of component j of membrane s[GPU]
P_s^{down}	Down stream pressure of membrane s [bar]
P_s^{up}	Up stream pressure of membrane s [bar]
PC	Project contingency cost [EUR]
PFC	Process facilities capital [EUR]

R	Ideal gas constant [$JK^{-1}mol^{-1}$]
$SC_{product}$	Specific product separation cost [EUR/Ton product]
STC	$Start - up$ cost [EUR]
T	Temperature [K]
t_{op}	Operation time per year [h/year]
TFI	Total facility investment [EUR]
TAC	Total annual costs [EUR/year]
UF_{1968}	Update factor [Dimensionless]
UF_{2000}	Update factor [Dimensionless]
W_{cp_f}	Feed compression power consumption of membrane s [kW]
W_{cp_s}	Permeate compression power consumption of membrane s into s_1 [kW]
$W_{c_{prod}}$	Upgraded gas compressor energy consumption [kW]
W_{exp}	Expander energy production [kW]
W_{tot}	Total energy consumption [kW]
W_{vp_s}	Vacuum power consumption of membrane s [kW]
$x_{s,j}$	Fraction of component j into the feed entering into stage s [Dimensionless]
$x_{s,j}^{perm}$	Fraction of component j of the permeate of stage s [Dimensionless]
X_j^{Perm}	Fraction of component j into the system permeate [Dimensionless]
$x_{s,j}^{ret}$	Fraction of component j of the retentate of stage s [Dimensionless]
X_j^{Ret}	Fraction of component j into the system retentate [Dimensionless]
$y_{s,i,j}$	Fraction of component j of the feed of cell i of stage s [Dimensionless]
$y_{s,i,j}^{ret}$	Fraction of component j of the retentate of cell i of stage s [Dimensionless]
$y_{s,i,j}^{perm}$	Fraction of component j of the permeate of cell i of stage s [Dimensionless]
Z	Project lifetime [years]

α	Selectivity [Dimensionless]
γ	Gas expansion coefficient [Dimensionless]
δ	Thickness of the membrane layer [μm]
η	Isentropic compressor efficiency [Dimensionless]
θ	Stage cut of membrane separation [Dimensionless]
λ	Isentropic vacuum pump efficiency [Dimensionless]
μ	Mutation rate in GA algorithm [Dimensionless]
ν	Membrane annual replacement rate [Dimensionless]
ϕ	Mechanical efficiency [Dimensionless]

Appendix A

Local vs. global optimal points

Generally, there are two types of solution which must be distinguished in optimization problems, local and global optimum solution. A global optimum is the best solution to the overall feasible region of an optimization problem. A local optimum, on the other hand, is optimal only with respect to feasible solutions close to that point. Points far from a local optimum play no role in its definition and may actually be preferred to the local optimum. In fact, we can define the local and global optimum as follow:
$x^* \in X$ is a local minimum point of the function f if:

$$\exists\, \epsilon > 0 \; \textit{such that} \; \forall x \in X \cap B(x^*, \epsilon); f(x^*) \leq f(x)$$

where $B(x^*, \epsilon) = \{x \in \mathbb{R}^n; ||x^* - x|| < \epsilon\}$
We can say that $x^* \in X$ is a global minimum solution for the function f if:

$$\forall x \in X; f(x^*) \leq f(x)$$

Figure 5.15: Local and global minimum of a non-linear function

Since some of nonlinear procedures cannot determine better than local maximum/minimum solution, the concept of a local maximum is extremely important from nonlinear programming point of view. Every global maximum is also a local maximum; hence the overall optimization problem can be viewed as seeking the best local maximum.

Convexity

A local minimum is known to be global if the function "curves upward" (convex function) and vice versa, a local maximum is global if the function is concave. For this reason the convexity of functions is very important in optimization problems. In convex problems any local optimum solution leads to global optimal solution; however, in a non-convex nonlinear optimization problem there is no guarantee that obtained local optimal solution is the global one in the feasible region. Optimization of separation of mixture gas is

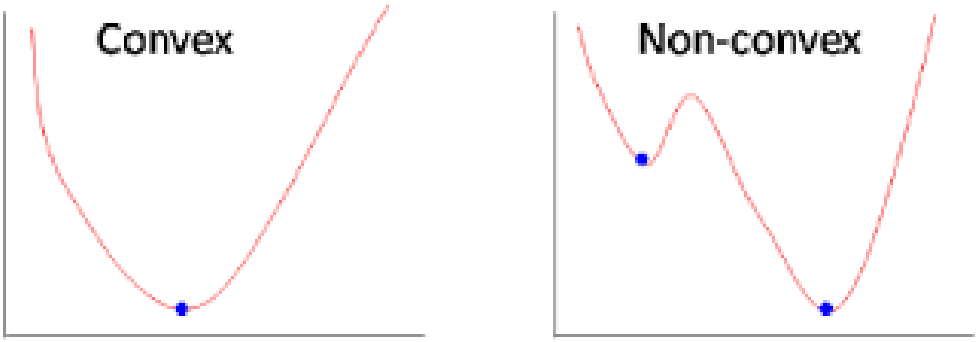

Figure 5.16: Convex v.s. non-convex function

modeled as a non-convex problem, so finding a local solution does not guarantee to have found the global one. Therefore, an efficient global optimization algorithm that seeks for to the best local optimum solution is essential.

Non-linear programming

A general optimization problem is to select a point x which is denoted as the vector of n decision variables, $x = (x_1, x_2, ..., x_n)$ from a given feasible region that is optimal (minimizes or maximizes) with respect of a given objective function f (x). The problem is called a nonlinear programming problem (NLP) if it includes at least one nonlinear function, which could be the objective function, or some or all of the constraints. Thus, in minimization form, the general nonlinear constrained programming problem is stated

as:

$$\begin{aligned} min \quad & f(x) \\ subject\ to \quad & g(x) \leq 0 \\ & h(x) = 0 \end{aligned}$$

where $f : \mathbb{R}^n \to \mathbb{R}$, $g : \mathbb{R}^n \to \mathbb{R}^m$, and $h : \mathbb{R}^n \to \mathbb{R}^p$ are all assumed to be twice continuously differentiable and real-valued.

A point $x \in \mathbb{R}^n$ is feasible, if all constraints of (2.22) are satisfied. The feasible region contains all feasible points

$$S := \{x \in \mathbb{R}^n |\ g_i(x) \leq 0, i = 1, ..., m \wedge h_j(x) = 0, j = 1, ..., p\}$$

The feasible region $S \subset \mathbb{R}^n$ is closed.
There are different algorithms for solving a nonlinear optimization problem e.g. Quassi-Newton, Trust region, conjugate gradient, SQP, interior point, and Branch-and-bound method. We do not explain about them for the sake of brevity.

Mixed integer non-linear programming

Mixed integer non-linear programming (MINLP) refers to optimization problems with continuous and discrete variables and non-linear functions in the objective function and/or the constraints. MINLPs arise in applications in a wide range of fields, including chemical engineering, finance, and manufacturing. The general form of a MINLP is:

$$\begin{aligned} min \quad & f(x, y) \\ subject\ to \quad & g(x, y) \leq 0 \\ & h(x, y) = 0 \\ & x \in X \\ & y \in Y\ integer \end{aligned}$$

where $f : \mathbb{R}^n \to \mathbb{R}$, $g : \mathbb{R}^n \to \mathbb{R}^m$, and $h : \mathbb{R}^n \to \mathbb{R}^p$ are all assumed to be twice continuously differentiable and real-valued.

Branch-and-bound, Outer Approximation and branch-and-cut are the three main algorithms for solving the MINLP optimization problems [99]–[101].

Generally, optimization of gas separation membrane system problem is classified as a MINLP problem which the objective or some of the constraints are not linear and there are both integer and continuous variables in the model. Although nonlinear programming problems are more complicated than linear programming problems, they are often crucial for representing real world application properly as a mathematical program, and this is the case for membrane systems.

Appendix B

Global optimization

A global constrained optimization problem can be defined as:

$$\begin{aligned} \min_{x \in \mathcal{S} \subset \mathbb{R}^{\backslash}} \quad & f(x) \\ \textit{subject to} \quad & g(x) \leq 0 \\ & h(x) = 0 \\ & a_i \leq x_i \leq b_i \end{aligned}$$

where $f : \mathbb{R}^n \to \mathbb{R}$, $g : \mathbb{R}^n \to \mathbb{R}^m$, and $h : \mathbb{R}^n \to \mathbb{R}^p$ are sufficiently smooth, $a_i, b_i \in \mathbb{R}$ are real bounds on the variable x_i, and $\mathcal{S} \subset \mathbb{R}^n$ is a compact set which (combined with the continuity or lower semi-continuity of f) guarantees the existence of the minimum value for f.

There is no algorithm able to find the solution of the global optimization problem in a finite number of steps. Hence, there is no guarantee to obtain the global optimal solution. Only a complete exploration of the feasible set can guarantee to find the global optimum. This is the particular structure of the global optimization problem [102].

Therefore, it is important to certify a good exploration of the feasible region to find as good as possible optimal point in a given amount of time [103].

Global optimization algorithms applied in gas separation

The aim of this section is not to give an overview of global optimization methods, but just to present the methods mostly utilized in optimization of membrane gas separation process.

Simulated Annealing Algorithm:

Simulated Annealing (SA) algorithm is an effective and general meta-heuristic method

for solving global optimization problems. "Annealing" is a physical process refers to an analogy with thermodynamics, specifically with the way that metal is slowly cool and anneal until its structure is eventually frozen at a minimum energy configuration. On the other words, in a liquid metal if the temperature is slowly decreased, the thermal mobility of the molecules is gradually lost and they can form a pure crystal with minimum energy. Simulated annealing put the objective function of an optimization problem instead of the energy of a material [104].

In a simple SA, starting from a starting point, at each iteration a next candidate point is randomly generated in a ball of given radius Δ with the center of current point x_k. The acceptance function guarantees all improvement steps are accepted [105]. For the case of not improving steps, the algorithm makes the move anyway with some probability less than 1 which is related to the temperature and the worsening in the objective with respect to the current point. The method has a decreasing probability to accept ascending steps with the decrease of the temperature.[104].

Algorithm 3 `Simulated Annealing`

procedure SIMPLE SIMULATED ANNEALING(Δ,T, N)
  $k = 0, t_k = T$
  $x_0 = x^*$ =random uniform point in $\mathcal{S}$
  while $k < N$ **do**
    y_k = random uniform point in $\mathcal{B}(x_k, \Delta)$
    p = random uniform point in [0,1]
    $A = \min\{1, exp(-\frac{f(y_{k+1})-f(x_k)}{t_k})\}$
    if $p \leq A$ **then**
      $x_{k+1} = y_{k+1}$
      if $f(x_{k+1}) < f(x^*)$ **then**
        $x^* = x_{k+1}$
    else
      $x_{k+1} = x_k$
    $t_{k+1} = U_z$
    $k = k + 1$
  return $x^*, f(x^*)$

The parameter t_k represents the temperature at iteration k, the set Z contains all the points observed up to the current iteration. The acceptance function $A(.)$, that has values in [0, 1], are used to determine the new point x_{k+1}. The next candidate point is generated and we decide whether to accept with probability A. The temperature is changed using a function $U(.)$ with non-negative values usually called cooling schedule [103].

SA is a descent algorithm modified by random ascent moves in order to escape local minima which are not global minima. Therefore, it is a general purpose, sequential algorithm

for finding a global minimum for a continuous function [106]. In fact, it can be applicable successfully when the barriers separating local minima are low with respect to the depth of valleys where such local minima lie. However, it seems that the time necessary to move uphill in order to escape from the attraction region of a local minimum is too high at least for hard GO problems, and might be more efficiently to use in restarting the search from scratch [107].

Genetic Algorithm:

Genetic algorithm (GA) is a stochastic optimization methods (like SA), inspired by natural evolution. A GA uses a highly abstract version of evolutionary processes to evolve solutions of a given problem [108]. It composed of two essential elements:

- Successive generations can differ from previous ones. Off springs generation inherit characteristics of their parents; however, the combining and mutating of these characteristics introduce variation from generation to generation
- Less fit off springs will be eliminated selectively[109]

GA operates on a population of artificial chromosomes which are strings in a finite alphabet (usually binary). Each chromosome represents a real number which is a measure of how good a solution it is to the particular problem. Starting with a randomly generated population of chromosomes, a GA carries out a process of fitness-based selection and recombination to produce a successor population, for the next generation. During recombination, parent chromosomes are selected using selection operator and crossover sites are chosen randomly. Their genetic material is recombined to produce child chromosomes. These then pass into the successor population. Latter in Mutation, random genes insert in offspring to maintain the diversity in population and avoid the premature convergence. As this process is iterated, a sequence of successive generations evolves and the average fitness of the chromosomes tends to increase until some stopping criterion is reached. In this way, a GA "evolves" a best solution to a given problem [110], [111].

In 4, the parameter m is the number of individuals in the population; parameter χ is the fraction of the population to be replaced by crossover in each iteration; and μ is donated the mutation rate.

Algorithm 4 `Simple Genetic Algorithm [109]`

procedure GENETIC ALGORITHM(χ, μ, N)
    // **Initialise generation 0:**
    $k = 0$
    P_k = a population of m randomly generated individuals
    // **Evaluate** P_k
    compute *fitness(i)* for each $i \in P_k$
    while $k < N$ or fitness of fittest individual in P_k is not high enough **do**
        //**Create generation** $k + 1$**:**
        //**1. Select parent from population:**
        Select $(1 - \chi) \times m$ members of P_k and insert into P_{k+1}
        //**2. Crossover:**
        select $\chi \times m$ members of P_k
        pair them up
        produce offspring
        insert the offspring into P_{k+1}
        //**3. Mutate:**
        select $\mu \times m$ members of P_{k+1}
        invert a randomly selected bit in each
        // **Evaluate** P_{k+1}**:**
        compute *fitness(i)* for each $i \in P_k$
        $k = k + 1$
    return the fittest individual from P_k

References

[1] I. Marriott, "Detailed mathematical modelling of membrane modules," *Computers and Chemical Engineering*, vol. 25, pp. 693–700, 2001.

[2] P. Bernardo and G. Clarizia, "30 years of membrane technology for gas separation," *Chemical Engineering*, vol. 32, pp. 1999–2004, 2013.

[3] S. Sridhar, S. Bee, and S. K. Bhargava, "Membrane-based gas separation: Principle, applications and future potential," *Chem. Eng. Dig*, pp. 1–25, 2014.

[4] J. A. Caballero, I. E. Grossmann, M. Keyvani, and E. S. Lenz, "Design of hybrid distillation- vapor membrane separation systems," *Industrial and Engineering Chemistry Research*, vol. 48, no. 20, pp. 9151–9162, 2009.

[5] J. K. Mitchell, "On the penetrativeness of fluids," *The Journal of the Royal Institution of Great Britain*, vol. 4, pp. 101–118, 1831.

[6] T. Graham, "On the absorption and dialytic separation of gases by colloid septa part i.—action of a septum of caoutchouc," *Journal of Membrane Science*, vol. 100, no. 1, pp. 27–31, 1995.

[7] R. W. Baker, "Future directions of membrane gas separation technology," *Industrial and Engineering Chemistry Research*, vol. 41, no. 6, pp. 1393–1411, 2002.

[8] R. Uppaluri, P. Linke, and A. Kokossis, "Synthesis and optimization of gas permeation membrane networks," *Industrial and Engineering Chemistry Research*, vol. 43, pp. 4305–4322, 2004.

[9] R. Spillman, "Economics of gas separation membrane processes," in *Membrane Separations Technology. Principles and Applications*, R. D. Noble and S. A. Stern, Eds., Amsterdam: Elsevier Science, 1995, pp. 589–667.

[10] R. Qi and M. A. Henson, "Membrane system design for multicomponent gas mixtures via mixed-integer nonlinear programming," *Computers and Chemical Engineering*, vol. 24, pp. 2719–2737, 2000.

[11] M. A. Norwell, *Handbook of compressed gases*, 4th ed. CGA Inc. Kluwer Academic Publishers, 1999.

[12] M. Carta, "Gas separation," in. Dec. 2015, pp. 852–855, ISBN: 978-3-642-40872-4. DOI: 10.1007/978-3-642-40872-4_261-1.

[13] D. M. Ruthven, S. Farooq, and K. S. Knaebel, *Pressure Swing Adsorption*. John Wiley & Sons Inc., 1993.

[14] J. D. Figueroa, T. Fout, S. Plasynski, H. McIlvried, and R. D. Srivastava, "Advances in CO_2 capture technology—the us department of energy's carbon sequestration program," *International Journal of Greenhouse Gas Control*, vol. 2, no. 1, pp. 9–20, 2008.

[15] D. Aaron and C. Tsouris, "Separation of CO_2 from flue gas: A review," *Separation Science and Technology*, vol. 40, no. 1–3, pp. 321–348, 2005.

[16] J. Mulder, *Basic principles of membrane technology*. Springer Science & Business Media, 2012.

[17] W. Ho and K. Sirkar, *Membrane handbook*. Springer Science & Business Media, 2012.

[18] P. M. Budd and N. B. McKeown, "Highly permeable polymers for gas separation membranes," *Polymer Chemistry*, vol. 1, no. 1, pp. 63–68, 2010.

[19] Y. Yampolskii, "Polymeric gas separation membranes," *Macromolecules*, vol. 45, no. 8, pp. 3298–3311, 2012.

[20] A. Fuertes and T. Centeno, "Preparation of supported carbon molecular sieve membranes," *Carbon*, vol. 37, no. 4, pp. 679–684, 1999.

[21] Z. Hong, F. Sun, D. Chen, C. Zhang, X. Gu, and N. Xu, "Improvement of hydrogen-separating performance by on-stream catalytic cracking of silane over hollow fiber mfi zeolite membrane," *International Journal of Hydrogen Energy*, vol. 38, no. 20, pp. 8409–8414, 2013.

[22] S. A. Rackley, *Carbon capture and storage*. Butterworth-Heinemann, 2017.

[23] P. M. Doran, *Bioprocess engineering principles*, 2nd ed. Elsevier, 2013.

[24] L.-Z. Zhang, *Conjugate heat and mass transfer in heat mass exchanger ducts*. Elsevier, 2013.

[25] J. G. Wijmans and R. W. Baker, "The solution-diffusion model: A review," *Journal of Membrane Science*, vol. 107, no. 1-2, pp. 1–21, 1995.

[26] S. Matteucci, Y. Yampolskii, B. D. Freeman, and I. Pinnau, "Chapter 1 in materials science of membranes for gas and vapor separation," in *Transport of gases and vapors in glassy and rubbery polymers*, Y. Yampolskii, I. Pinnau, and B. Freeman, Eds., Chichester, United Kingdom: Wiley & Sons, 2006, ISBN: 0-470-85345-X.

[27] L. M. Robeson, "Correlation of separation factor versus permeability for polymeric membranes," *Journal of Membrane Science*, vol. 62, no. 2, pp. 165–185, 1991.

[28] L. M. Robeson, "The upper bound revisited," *Journal of Membrane Science*, vol. 320, no. 1, pp. 390–400, 2008.

[29] E. Favre, "Chapter 2.08 in comprehensive membrane science and engineering," in *Polymeric membranes for gas separation*, E. Drioli and L. Giorno, Eds., vol. 2, Amesterdam: Elsevir, 2010, ISBN: 978-0-444-53204-6.

[30] Y. Shindo, T. Hakuta, H. Yoshitome, and H. Inoue, "Calculation methods for multicomponent gas separation by permeation," *Separation Science and Technology*, vol. 20, no. 5-6, pp. 445–459, 1985.

[31] R. W. Baker, *Membrane technology and applications*. John Wiley & Sons, 2012.

[32] Á. A. Ramirez-Santos, M. Bozorg, B. Addis, V. Piccialli, C. Castel, and E. Favre, "Optimization of multistage membrane gas separation processes. example of application to CO_2 capture from blast furnace gas," *Journal of Membrane Science*, vol. 566, pp. 346–366, 2018.

[33] E. Favre, "Comprehensive membrane science and engineering," in *Polymeric membranes for gas separations*, E. Drioli and L. Giorno, Eds., vol. 2, Amsterdam: Elsevier Science, 2010, ch. 10, pp. 155–211.

[34] R. Qi and M. A. Henson, "Optimization-based design of spiral-wound membrane systems for CO_2/CH_4 separations," *Separation and Purification Technology*, vol. 13, pp. 209–225, 1998a.

[35] M. Scholz, M. Alders, T. Lohaus, and M. Wessling, "Structural optimization of membrane-based biogas," *Journal of Membrane Science*, vol. 474, pp. 1–10, 2015.

[36] B. Ohs, J. Lohaus, and M. Wessling, "Optimization of membrane based nitrogen removal from natural gas," *Journal of Membrane Science*, vol. 498, pp. 291–301, 2016.

[37] P. Gabrielli, M. Gazzani, and M. Mazzotti, "On the optimal design of membrane-based gas separation processes," *Journal of Membrane Science*, vol. 526, pp. 118–130, 2017.

[38] A. M. Arias, M. C. Mussati, P. L. Mores, N. J. Scenna, J. A. Caballero, and S. F. Mussati, "Optimization of multi-stage membrane systems for CO_2 capture from flue gas," *International Journal of Greenhouse Gas Control*, vol. 53, pp. 371–390, 2016.

[39] R. Qi and M. A. Henson, "Optimal design of spiral-wound membrane networks for gas separations," *Journal of Membrane Science*, vol. 148, no. 1, pp. 71–89, 1998b.

[40] M. Yuan, K. Narakornpijit, R. Haghpanah, and J. Wilcox, "Consideration of a nitrogen-selective membrane for post combustion," *Journal of Membrane Science*, vol. 465, pp. 177–184, 2014.

[41] R. Uppaluri, R. Smith, P. Linke, and A. Kokossis, "On the simultaneous optmization of pressure and layout for gas permeation membrane systems," *Journal of Membrane Science*, vol. 280, pp. 832–848, 2006.

[42] M. Ungerank, B. Goetz, M. Priske, and H. Roegl, "Processs for separation of gases," US2013/0098242 (A1), Apr. 2013.

[43] A. Aliaga-Vicente, J. A. Caballero, and M. J. Fernandez-Torres, "Synthesis and optimization of membrane cascade for gas separation via mixed-integer nonlinear programming," *AIChE Journal*, vol. 63, no. 6, pp. 1989–2006, 2017.

[44] R. Agrawal and J. Xu, "Gas-separation membrane cascades utilizing limited numbers of compressors," *AIChE Journal*, vol. 42, no. 8, pp. 2141–2154, 1996.

[45] M. Faruque Hasan, R. C. Baliban, J. Elia, and C. Floudas, "Modeling, simulation, and optimization of postcombustion CO_2 capture for variable feed concentration and flow rate. 1. chemical absorption and membrane processes," *Industrial and Engineering Chemistry Research*, vol. 51(48), pp. 15 642–15 664, 2012.

[46] A. Shafiee, M. Nomvar, Z. Liu, and A. Abbas, "Automated process synthesis for optimal flowsheet design of a hybrid membrane cryogenic carbon capture process," *Journal of Cleaner Production*, vol. 150, pp. 309–323, 2017.

[47] C. A. Floudas, *Nonlinear and Mixed-Integer Optimization: Fundamentals and Applications*. New York: Oxford University Press, 1995, ISBN: 3257227892.

[48] R. Fourer, D. M. Gay, and B. W. Kernighan, "Ampl: A mathematical programming language," MANAGEMENT SCIENCE, Tech. Rep., 1989.

[49] R. H. Byrd, J. Nocedal, and R. A. Waltz, "Knitro: An integrated package for nonlinear optimization," in *Large-Scale Nonlinear Optimization*, G. Di Pillo and M. Roma, Eds. Boston, MA: Springer US, 2006, pp. 35–59.

[50] R. Bounaceur, E. Berger, M. Pfister, Á. A. Ramirez-Santos, and E. Favre, "Rigorous variable permeability modelling and process simulation for the design of polymeric membrane gas separation units: Memsic simulation tool," *Journal of Membrane Science*, vol. 523, pp. 77–91, 2017.

[51] H. Zhai and E. S. Rubin, "Techno-economic assessment of polymer membrane systems for postcombustion carbon capture at coal-fired power plants," *Environmental Science and Technology*, vol. 47, pp. 3006–3014, 2013.

[52] Á. A. Ramirez-Santos, C. Castel, and E. Favre, "Utilization of blast furnace flue gas: Opportunities and challenges for polymeric membrane gas separation processes," *Journal of Membrane Science*, vol. 526, pp. 191–204, 2017.

[53] A. A. Ramirez-Santos, C. Castel, and E. Favre, "A review of gas separation technologies within emission reduction programs in the iron and steel sector: Current application and development perspectives," *Separation and Purification Technology*, vol. 194, pp. 425–442, 2018.

[54] T. Merkel, H. Lin, X. Wei, and R. Baker, "Power plant post-combustion carbon dioxide capture: An opportunity for membranes," *Journal of Membrane Science*, vol. 359, pp. 126–139, 2010.

[55] T. Merkel, M. Zhou, and R. Baker, "Carbon dioxide capture with membranes at an igcc power plant," *Journal of Membrane Science*, vol. 389, pp. 441–450, 2012.

[56] T. Merkel and B. Freeman, *Membranes: An emerging CO_2 capture technology*, https://usea.org/sites/default/files/event-/MTRUSEAJune2017.pdf, (accessed 27 April, 2018), 2017.

[57] W. Luyben, "Design and control of gas-phase reactor/recycle processes with reversible exothermic reactions.," *Industrial Engineering CHemistry Research*, vol. 39, pp. 1529–1538, 2000.

[58] J. Ryans and M. J. Bays, "Run clean with dry vacuum pumps," *CEP Magazine*, vol. October, pp. 32–41, 2001.

[59] K. I. LTD, *Industrial vacuum system-products and packages*, https://http://kayblowers.com/wp-content/uploads/2016/02/Kay-Industrial-Vacuum-Pumps.pdf, (accessed 27 April, 2018), 2015.

[60] P. M. Follmann, C. Bayer, M. Wessling, and T. Melin., "Chapter 7: Membrane gas separation processes for post-combustion CO_2 capture," in *Membrane engineering for the treatment of gases Vol. 1*, E. Drioli and G. Barbieri, Eds., Cambridge, UK: RSC Publishing, 1995, pp. 196–214.

[61] A. Chauvel, G. Fournier, and R. Claude, *Manual of process economic evaluation*. Paris, FRANCE: Editions TECHNIP, 2003, ISBN: 1611972663, 9781611972665.

[62] V. Calabrò and A. Basile., "Chapter 4: Economic analysis of membrane use in industrial applications," in *Advanced membrane science and technology for sustainable energy and environmental applications*, E. Drioli and G. Barbieri, Eds., Cambridge, UK: Woodhead Publishing Limited, 2011, pp. 90–109.

[63] M. Bozorg, B. Addis, V. Piccialli, Á. A. Ramirez-Santos, C. Castel, I. Pinnau, and E. Favre, "Polymeric membrane materials for nitrogen production from air: A process synthesis study," *Chemical Engineering Science*, vol. 207, pp. 1196–1213, 2019.

[64] I. Angelidaki, L. Treu, P. Tsapekos, G. Luo, S. Campanaro, H. Wenzel, and P. Kougias, "Biogas upgrading and utilization: Current status and perspectives," *Biotechnology Advances*, vol. 36, pp. 452–466, 2018.

[65] D. Wilken, F. Strippel, F. Hofmann, M. Maciejczyk, L. Klinkmuller, L. Wagner, G. Bontempo, J. Munch, S. Scheidl, M. Conton, *et al.*, "Biogas to biomethane," *Fachverband Biogas e. V. Germany, Freising. ISSN*, 2017.

[66] I. Ullah Khan, M. H. D. Othman, H. Hashim, T. Matsuura, A. Ismail, M. Rezaei-DashtArzhandi, and I. Wan Azeele, "Biogas as a renewable energy fuel- a review of biogas upgrading, utilisation and storage," *Energy Conversion and Management*, vol. 150, pp. 277–294, 2017.

[67] M. Miltner, A. Makaruk, and M. Harasek, "Review on available biogas upgrading technologies and innovations towards advanced solutions," *Journal of Cleaner Production*, vol. 161, pp. 1329–1337, 2017.

[68] O. W. Awe, Y. Zhao, A. Nzihou, D. P. Minh, and N. Lyczko, "A review of biogas utilisation, purification and upgrading technologies," *Waste and Biomass Valorization*, vol. 8, no. 2, pp. 267–283, 2017.

[69] R. Kapoor, P. Ghosh, M. Kumar, and V. K. Vijay, "Evaluation of biogas upgrading technologies and future perspectives: A review," *Environmental Science and Pollution Research*, vol. 26, no. 12, pp. 11 631–11 661, 2019.

[70] Y. Rouaud, *From biogas to biomethane. air liquide sales presentation for biogas upgrading solutions.* 2013.

[71] F. Bauer, C. Hulteberg, T. Persson, and D. Tamm, *Biogas upgrading-review of commercial technologies. sgc rapport*, 2013.

[72] R. W. Baker, *Membrane technology and applications*. John Wiley & Sons, 2012.

[73] S. Haider, A. Lindbråthen, and M.-B. Hägg, "Techno-economical evaluation of membrane based biogas upgrading system: A comparison between polymeric membrane and carbon membrane technology," *Green Energy & Enviroment*, vol. 1, pp. 222–234, 2016.

[74] D. Havas and H. Lin, "Optimal membranes for biogas upgrade by removing co2: High permeance or high selectivity?" *Separation Science and Technology*, vol. 52, no. 2, pp. 186–196, 2017.

[75] R. W. Baker and B. T. Low, "Gas separation membrane materials: A perspective," *Macromolecules*, vol. 47, no. 20, pp. 6999–7013, 2014.

[76] J. Gascon, F. Kapteijn, B. Zornoza, V. Sebastian, C. Casado, and J. Coronas, "Practical approach to zeolitic membranes and coatings: State of the art, opportunities, barriers, and future perspectives," *Chemistry of Materials*, vol. 24, no. 15, pp. 2829–2844, 2012.

[77] Y. Chen, Y. Zhang, C. Zhang, J. Jiang, and X. Gu, "Fabrication of high-flux sapo-34 membrane on α-al2o3 four-channel hollow fibers for CO_2 capture from CH_4," *Journal of CO_2 Utilization*, vol. 18, pp. 30–40, 2017.

[78] K. Kida, Y. Maeta, and K. Yogo, "Pure silica cha-type zeolite membranes for dry and humidified CO_2/CH_4 mixtures separation," *Separation and Purification Technology*, vol. 197, pp. 116–121, 2018.

[79] N. Kosinov, C. Auffret, C. Gücüyener, B. M. Szyja, J. Gascon, F. Kapteijn, and E. J. Hensen, "High flux high-silica ssz-13 membrane for CO_2 separation," *Journal of Materials Chemistry A*, vol. 2, no. 32, pp. 13 083–13 092, 2014.

[80] C. Zhang and W. J. Koros, "Ultraselective carbon molecular sieve membranes with tailored synergistic sorption selective properties," *Advanced Materials*, vol. 29, no. 33, p. 1 701 631, 2017.

[81] W. J. Koros and C. Zhang, "Materials for next-generation molecularly selective synthetic membranes," *Nature materials*, vol. 16, no. 3, p. 289, 2017.

[82] S. Basu, A. L. Khan, A. Cano-Odena, C. Liu, and I. F. Vankelecom, "Membrane-based technologies for biogas separations," *Chemical Society Reviews*, vol. 39, no. 2, pp. 750–768, 2010.

[83] X. Y. Chen, H. Vinh-Thang, A. A. Ramirez, D. Rodrigue, and S. Kaliaguine, "Membrane gas separation technologies for biogas upgrading," *Rsc Advances*, vol. 5, no. 31, pp. 24 399–24 448, 2015.

[84] D. D. Iarikov and S. T. Oyama, "Review of CO_2/CH_4 separation membranes," in *Membrane Science and Technology*, vol. 14, Elsevier, 2011, pp. 91–115.

[85] Y. Alcheikhhamdon and M. Hoorfar, "Natural gas purification from acid gases using membranes: A review of the history, features, techno-commercial challenges, and process intensification of commercial membranes," *Chemical Engineering and Processing-Process Intensification*, vol. 120, pp. 105–113, 2017.

[86] R. W. Baker, "Future directions of membrane gas separation technology," *Industrial & engineering chemistry research*, vol. 41, no. 6, pp. 1393–1411, 2002.

[87] M. J. Economides and D. A. Wood, "The state of natural gas," *Journal of Natural Gas Science and Engineering*, vol. 1, no. 1-2, pp. 1–13, 2009.

[88] B. Shimekit and H. Mukhtar, "Natural gas purification technologies-major advances for CO_2 separation and future directions," in *Advances in natural gas technology*, IntechOpen, 2012.

[89] *Processing natural gas*, `http://naturalgas.org/naturalgas/processing-ng/`.

[90] *Definition of 'natural gas'*, `https://economictimes.indiatimes.com/definition/natural-gas`.

[91] D. Dortmundt and K. Doshi, "Recent developments in CO_2 removal membrane technology," *UOP LLC*, vol. 1, 1999.

[92] R. W. Baker and K. Lokhandwala, "Natural gas processing with membranes: An overview," *Industrial & Engineering Chemistry Research*, vol. 47, no. 7, pp. 2109–2121, 2008.

[93] *CO_2 removal from natural gas*, `https://www.mtrinc.com/our-business/natural-gas/co2-removal-from-natural-gas/`.

[94] S. Sridhar, B. Smitha, and T. Aminabhavi, "Separation of carbon dioxide from natural gas mixtures through polymeric membranes—a review," *Separation & Purification Reviews*, vol. 36, no. 2, pp. 113–174, 2007.

[95] S. Sridhar, R. Suryamurali, B. Smitha, and T. Aminabhavi, "Development of crosslinked poly (ether-block-amide) membrane for CO_2/CH_4 separation," *Colloids and Surfaces A: Physicochemical and Engineering Aspects*, vol. 297, no. 1-3, pp. 267–274, 2007.

[96] J. D. Wind, D. R. Paul, and W. J. Koros, "Natural gas permeation in polyimide membranes," *Journal of Membrane Science*, vol. 228, no. 2, pp. 227–236, 2004.

[97] H. Lin, L. S. White, K. Lokhandwala, and R. W. Baker, "Natural gas purification," *Encyclopedia of Membrane Science and Technology*, pp. 1–25, 2013.

[98] T. Neveux, "Ab-initio process synthesis using evolutionary programming," *Chemical Engineering Science*, vol. 185, pp. 209–221, 2018.

[99] O. K. Gupta and A. Ravindran, "Branch and bound experiments in convex nonlinear integer programming," *Management science*, vol. 31, no. 12, pp. 1533–1546, 1985.

[100] M. A. Duran and I. E. Grossmann, "An outer-approximation algorithm for a class of mixed-integer nonlinear programs," *Mathematical programming*, vol. 36, no. 3, pp. 307–339, 1986.

[101] I. Quesada and I. E. Grossmann, "An lp/nlp based branch and bound algorithm for convex minlp optimization problems," *Computers & chemical engineering*, vol. 16, no. 10-11, pp. 937–947, 1992.

[102] L. C. W. Dixon., "Global optima without convexity," *Technical Report, Numerical optimization*, 1978.

[103] B. Addis, E. Mosca, and F. Schoen, "Global optimization using local searches," PhD thesis, Global Optimization Laboratory, University of Florence, 2004.

[104] W. H. Press, S. A. Teukolsky, W. T. Vetterling, and B. P. Flannery, *Numerical recipes 3rd edition: The art of scientific computing*. Cambridge university press, 2007.

[105] S. Kirkpatrick, C. D. Gelatt, and M. P. Vecchi, "Optimization by simulated annealing," *science*, vol. 220, no. 4598, pp. 671–680, 1983.

[106] K.-L. Du and M. Swamy, "Search and optimization by metaheuristics," *Techniques and Algorithms Inspired by Nature; Birkhauser: Basel, Switzerland*, 2016.

[107] M. Locatelli and F. Schoen, *Global optimization: theory, algorithms, and applications*. Siam, 2013, vol. 15.

[108] P. A. Muñoz-Rojas, *Optimization of structures and components*. Springer, 2013.

[109] *Geneetic algorithms*, `http://www.cs.ucc.ie/~dgb/courses/tai/notes/handout12.pdf`.

[110] J. McCall, "Genetic algorithms for modelling and optimisation," *Journal of Computational and Applied Mathematics*, vol. 184, no. 1, pp. 205–222, 2005.

[111] J. Carlton, *Marine propellers and propulsion*. Butterworth-Heinemann, 2018.

Abstract

Optimization of membrane process architecture

Membrane separation is a well-known technology in gas purification, which is applicable in different aspects of the industry. Over the last decades, depending on the required separation performances, it became a viable alternative to several gas separation technologies (adsorption, cryogenics, gas/liquid contactors). To exploit at best this technology, nevertheless, tools to find cost-effective designs and operating conditions are necessary. While experimental optimization approaches applied to different case studies have been investigated extensively, a more generic optimization approach and its validation along different case studies are still missing. The work of this thesis starts with this key observation and tries to fill this gap.

The membrane process synthesis is modelled as a nonlinear and non-convex mathematical optimization problem based on a superstructure paradigm covering a wide range of possible units (membrane modules, compressors, and vacuum pumps) and connections as exhaustive as possible. Realistic and detailed cost functions are used as the objective in the optimization. A continues global optimization strategy, that can be considered as the composition of two algorithms: Multistart and Monotonic Basin Hopping (MBH); is presented to solve the aforementioned optimization problem.

The efficiency of this overall optimization approach is, first, validated by comparing its solution with the ones presented in the literature. Then, the proposed method is applied to the optimization of several important gas separation cases (CO_2 recovery from blast furnace gas, O_2/N_2 air separation, and biogas and natural gas purification) by increasing the membrane system degree of freedom step by step. Detailed analysis of the results is discussed in terms of process architecture and cost distribution (CAPEX, OPEX).

Keywords: Gas separation, Membrane process, Global optimization, MBH Algorithm

Résumé

Optimisation d'architecture de procédés membranaires

Les procédés de séparation membranaire sont une technologie bien connue et déjà largement utilisée dans le domaine de la purification des gaz. Ces procédés sont applicables à de nombreux secteurs d'activités industriels. Selon les performances de séparation recherchées, elles peuvent constituer une alternative intéressante aux technologies existantes de traitement des gaz (adsorption, cryogénie, contacteurs gaz/liquide). Pour exploiter au mieux cette technologie, le développement d'outils d'aide à la décision permettant d'identifier les procédés et les conditions opératoires économiquement avantageux est absolument nécessaire. Bien que les approches expérimentales d'optimisation appliquées à différentes études de cas conservent un intérêt certain, une approche générale et sa validation dans le cadre de différentes études de cas font toujours défaut. L'objectif principal de cette thèse est de développer un outil numérique le plus générique possible d'optimisation de procédés de séparation membranaire.

Dans ce travail, la synthèse du procédé membranaire est traitée et modélisée comme un problème d'optimisation mathématique non linéaire et non convexe basé sur un paradigme de superstructure couvrant une combinatoire d'unités (modules membranaires, compresseurs, pompes à vide) et de connexions la plus exhaustive possible. Des fonctions de coûts réalistes et détaillées sont utilisées comme fonction objectif dans l'optimisation. Une stratégie d'optimisation globale continue, qui peut se considérer comme la composition de deux algorithmes : Multistart et Monotonic Basin Hopping (MBH) ; est présentée pour résoudre le problème d'optimisation susmentionné.

L'efficacité de cette démarche d'optimisation est dans un premier temps validée en comparant sa solution à celles présentées dans la littérature. La méthode proposée est ensuite appliquée à l'optimisation de plusieurs cas emblématiques de la séparation de gaz (CO_2 de gaz de haut fourneaux, séparation O_2/N_2 de l'air, traitement du biogaz et du gaz naturel). Différents degrés de liberté du système sont permis et analysés selon les cas (pressions variables, type de membrane variable). L'analyse détaillée des résultats est discutée en termes d'architecture de procédés et de distribution des coûts (CAPEX, OPEX)

Mots clés : Séparation de gaz, Procédé membranaire, Optimisation globale, Algorithme MBH